

# Middlesex University Research Repository

An open access repository of

Middlesex University research

<http://eprints.mdx.ac.uk>

Luxton, William Booth (1997) The exposure and deterioration of granitic building stone. PhD thesis, Middlesex University. [Thesis]

This version is available at: <https://eprints.mdx.ac.uk/10167/>

## Copyright:

Middlesex University Research Repository makes the University's research available electronically.

Copyright and moral rights to this work are retained by the author and/or other copyright owners unless otherwise stated. The work is supplied on the understanding that any use for commercial gain is strictly forbidden. A copy may be downloaded for personal, non-commercial, research or study without prior permission and without charge.

Works, including theses and research projects, may not be reproduced in any format or medium, or extensive quotations taken from them, or their content changed in any way, without first obtaining permission in writing from the copyright holder(s). They may not be sold or exploited commercially in any format or medium without the prior written permission of the copyright holder(s).

Full bibliographic details must be given when referring to, or quoting from full items including the author's name, the title of the work, publication details where relevant (place, publisher, date), pagination, and for theses or dissertations the awarding institution, the degree type awarded, and the date of the award.

If you believe that any material held in the repository infringes copyright law, please contact the Repository Team at Middlesex University via the following email address:

[eprints@mdx.ac.uk](mailto:eprints@mdx.ac.uk)

The item will be removed from the repository while any claim is being investigated.

See also repository copyright: re-use policy: <http://eprints.mdx.ac.uk/policies.html#copy>

## **Middlesex University Research Repository:**

an open access repository of  
Middlesex University research

<http://eprints.mdx.ac.uk>

Luxton, William Booth, 1997.  
The exposure and deterioration of granitic building stone.  
Available from Middlesex University's Research Repository.

---

### **Copyright:**

Middlesex University Research Repository makes the University's research available electronically.

Copyright and moral rights to this thesis/research project are retained by the author and/or other copyright owners. The work is supplied on the understanding that any use for commercial gain is strictly forbidden. A copy may be downloaded for personal, non-commercial, research or study without prior permission and without charge. Any use of the thesis/research project for private study or research must be properly acknowledged with reference to the work's full bibliographic details.

This thesis/research project may not be reproduced in any format or medium, or extensive quotations taken from it, or its content changed in any way, without first obtaining permission in writing from the copyright holder(s).

If you believe that any material held in the repository infringes copyright law, please contact the Repository Team at Middlesex University via the following email address:  
[eprints@mdx.ac.uk](mailto:eprints@mdx.ac.uk)

The item will be removed from the repository while any claim is being investigated.

# The Exposure and Deterioration of Granitic Building Stone

William Booth Luxton

Urban Pollution Research Centre  
Middlesex University

Submitted in partial fulfilment of the requirements of  
Middlesex University for the degree of Doctor of Philosophy

February 1997

## Abstract

The study of building stone decay is a field of increasing importance. Many previous studies have focused on limestone, and recently on sandstone. These studies can provide information on the spatial and temporal distribution of weathering forms and the degree of impact of polluted urban atmospheres. Several of these schemes rely on subjective visual appraisal by the examiner, which is unreliable and prone to measurement error. To counter these problems, and address the relative paucity of studies on granitic building stone, a novel semi-quantitative measure of rock quality was created.

The creation of the Stone Deterioration Index (SDI) allowed the evaluation of long-term granitic building stone decay, while the short-term response of fresh granite to atmospheric exposure was examined through the use of microcatchment units (MCU's). The measurement of run-off water and the physical response of fresh granite over a 91 week exposure period at three sites of varying pollution concentrations, allowed an assessment of the relative importance of surface roughness, composition and, dry & total deposition on deterioration rates. The exposure programme used MCU's containing granodiorite slabs with different degrees of surface roughness (finish) to collect run-off. This was measured for volume, pH, conductivity, and selected anion and metal concentrations. Run-off concentrations were measured by a Dionex 2000i ion chromatograph and a Perkin-Elmer ICP 40 inductively coupled plasma spectrometer respectively.

Site was the most important factor in determining run-off concentrations showing significant variations between the urban and rural sites. Surprisingly, MCU composition and surface roughness variations had little influence on component concentrations, and there were no systematic significant inter-finish variations. The MCU slabs showed no significant changes in weight, surface roughness or composition as a result of exposure.

Granitic carousel tablets of varying composition, designed to assess the relative influence of dry and total deposition on granitic deterioration, also showed no systematic effects from exposure. The lack of significant variation between the pre- and post-exposure characteristics of the MCU slabs and carousel tablets could indicate that exposure length was not sufficient to generate measurable decay features.

The assessment of long-term decay rates by the SDI, which was non-destructive and applied *in situ*, involved the measurement and rating of four parameters (surface strength, surface roughness, surface coatings and discolouration), to form a semi-quantifiable measure of rock quality. Eleven churches in Dartmoor, built between 1430AD-1896AD, were assessed by the SDI to provide a measure of long-term deterioration rates.

Cross-church comparisons revealed no consistent effects on deterioration rates with increasing stone height. Aspect, however, did play a major role in influencing deterioration rates. The south facing walls (mean: 60 SDI points) showed the least amount of decay and had the slowest deterioration rate, while west (mean: 56 SDI) and north facing walls (mean: 53 SDI) deteriorated 6% and 14% faster than south facing walls respectively. Results suggest biological weathering was the major process in granite building stone deterioration in the Dartmoor region. These findings correspond to research by Robinson and Williams (1996) on sandstone churches. They ranked aspect by weathering scores derived from visual assessment of individual stone block, and found deterioration features were strongly affected by aspect, in the order; East>North>West>South.

Although there is convergence in the decay pattern between aspects for the two stone types, the SDI index was formulated for coarse-grained igneous rocks, where it shows a strong statistical relationship between building age and rock quality ( $r=0.74$ ). This allowed the formulation of an average linear deterioration rate for granite buildings in a clean, rural environment of 4.59 SDI points per hundred years.



## CONTENTS

	Page Number
Chapter titles . . . . .	i
Figures . . . . .	v
Tables . . . . .	viii
Plates . . . . .	x
Acknowledgements . . . . .	xi

## CHAPTER TITLES

### CHAPTER 1. Introduction

1.1 INTRODUCTION . . . . .	1
1.2 AIMS . . . . .	1
1.3 OUTLINE OF THESIS . . . . .	2
1.4 ASSOCIATED PUBLICATIONS AND CONFERENCES . . . . .	3

### CHAPTER 2. The Nature and Weathering of Granite

2.1 INTRODUCTION . . . . .	4
2.2 FORMATION AND PLACEMENT OF GRANITE . . . . .	4
2.2.1 The Cornubian Batholith . . . . .	5
2.3 GRANITE TYPES . . . . .	6
2.3.1 Alkaligranites . . . . .	8
2.3.2 Ademellites . . . . .	9
2.3.3 Granodiorites . . . . .	9
2.3.4 Dartmoor and Bodmin Moor Granites . . . . .	10
2.4 GENERAL ASPECTS OF WEATHERING . . . . .	13
2.5 ALTERATION OF GRANITE . . . . .	15
2.6 LATE AND POST SOLIDIFICATION/CRYSTALLISATION ALTERATION . . . . .	16
2.6.1 Deuteric Alteration . . . . .	16
2.6.2 Hydrothermal Alteration . . . . .	17
2.6.3 Pneumatolysis . . . . .	17
2.7 SHALLOW-DEPTH AND SUB-AERIAL ALTERATIONS . . . . .	18
2.7.1 Mechanical weathering . . . . .	18
Unloading/Dilation Joints . . . . .	19
Thermal weathering . . . . .	20
Frost action . . . . .	21
Salt Weathering . . . . .	22
Abrasion . . . . .	25
Alternate Wetting and Drying . . . . .	25
2.7.2 Chemical Weathering . . . . .	26

Solution . . . . .	27
Oxidation/Reduction . . . . .	28
Hydration/Hydrolysis . . . . .	28
Rain Action . . . . .	30
Fog and Condensation . . . . .	32
Mineral Alteration . . . . .	33
<b>2.7.3 Biological Weathering</b> . . . . .	34
Ion Exchange and Uptake . . . . .	35
Mineral Acid Production . . . . .	36
Organic Acid Production . . . . .	37
Physical Disruption . . . . .	38
Increased Time of Wetness . . . . .	38
<b>2.8. STONE DECAY THRESHOLDS</b> . . . . .	39

## CHAPTER 3. Air Pollution in the UK

<b>3.1 INTRODUCTION</b> . . . . .	42
<b>3.2 GASEOUS POLLUTANTS</b> . . . . .	43
<b>3.2.1 Oxides of Carbon</b> . . . . .	44
<b>3.2.2 Nitrogen Oxides</b> . . . . .	44
<b>3.2.3 Sulphur Oxides</b> . . . . .	49
<b>3.2.4 Ozone</b> . . . . .	50
<b>3.2.5 Ammonia</b> . . . . .	51
<b>3.3 PARTICULATES</b> . . . . .	52
<b>3.3.1 Nitrate and Sulphate Aerosols</b> . . . . .	53
<b>3.3.2 Chloride</b> . . . . .	54
<b>3.3.3 Carbonaceous Particles</b> . . . . .	54
3.3.3.1 Oil Derived Carbonaceous Particles . . . . .	55
3.3.3.2 Coal Derived Carbonaceous Particles . . . . .	55
3.3.3.3 Vehicle Derived Particulates . . . . .	56
<b>3.3.4 Black/Brown Crusts and Iron-Rich Patinas</b> . . . . .	57
<b>3.4 DEPOSITED IONS</b> . . . . .	59
<b>3.5 DEPOSITION MECHANISMS</b> . . . . .	62
<b>3.5.1 Dry Deposition</b> . . . . .	63
<b>3.5.2 Wet Deposition</b> . . . . .	63
<b>3.6 ACID RAIN</b> . . . . .	65

## CHAPTER 4. Sample Exposure Studies

<b>4.1 SAMPLE EXPOSURE INTRODUCTION</b> . . . . .	67
<b>4.2 SAMPLE SELECTION</b> . . . . .	67
<b>4.2.1 Carousel Tablets</b> . . . . .	69
<b>4.2.2 Micro-Catchment Units</b> . . . . .	69
<b>4.3 SAMPLE PREPARATION</b> . . . . .	70
<b>4.3.1 Carousel Tablets</b> . . . . .	70
<b>4.3.2 Micro-Catchment Units</b> . . . . .	71
<b>4.4 SAMPLE SITES</b> . . . . .	72
<b>4.4.1 London, St. Paul's Cathedral</b> . . . . .	72

4.4.2	Birmingham, Five-Ways House	73
4.4.3	Dartmoor, Yarnier Wood	74
4.5	SAMPLE EXPOSURE	74
4.5.1	Exposure Carousels	75
4.5.2	Micro-Catchment Units	76
4.6	SAMPLE ANALYSIS	78
4.6.1	Exposure Carousels	78
4.6.1.1	Weight Loss and Gain.	78
4.6.2	Micro-Catchment Units	78
4.6.2.1	Weight Loss and Gain.	78
4.6.2.2	Collection of Run-Off Water	79
4.6.2.3	Surface Roughness Analysis	80
4.6.2.4	End Analysis	81
4.7	ANALYTICAL METHODS	81
4.7.1	Ion Chromatography	81
4.7.1.1	Determination of Anions	82
4.7.2	Inductively Coupled Plasma - Atomic Emission Spectrophotometry	82
4.7.2.1	Determination of Cations	83
4.7.3	Surface Roughness Measurements	83
4.7.4	S.E.M. and E.D.X Analysis	84

## CHAPTER 5. Sample Exposure Results

5.1	INTRODUCTION	87
5.2	RUN-OFF ANALYSIS	87
5.2.1	Run-Off Characteristics	90
5.2.1.1	Volume	90
5.2.1.2	pH	91
5.2.1.3	Conductivity	93
5.2.2	Anions	95
5.2.2.1	Chloride	95
5.2.2.2	Nitrate	100
5.2.2.3	Phosphate	103
5.2.2.4	Sulphate	105
5.2.3	Metals	108
5.2.3.1	Aluminium	109
5.2.3.2	Calcium	113
5.2.3.3	Magnesium	117
5.2.3.4	Iron	121
5.2.4	Site Effects on Run-off Characteristics	125
5.2.5	Roughness Effects on Run-off Characteristics	126
5.3	CAROUSEL TABLET ANALYSIS	127
5.3.1	Upper Suite Weight Changes	128
5.3.2	Lower Suite Weight Changes	131
5.3.3	Site and Suite Variations	133
5.3.4	Stone Type Variations	136
5.4	MICRO-CATCHMENT STONES ANALYSIS	137

5.4.1	Weight Changes	137
5.4.2	Slab Roughness Variation	140
5.4.3	SEM/EDX Analysis	144
5.5	CONCLUSIONS	146

## CHAPTER 6. *In Situ* Building Deterioration Assessment Study: SDI Scheme

6.1	INTRODUCTION	150
6.2	ROCK CLASSIFICATION SCHEMES IN ENGINEERING GEOLOGY	152
6.2.1	Engineering Rock Mass Rating Schemes	153
6.2.2	Weathering Grade Classifications	155
6.2.3	Rock Index Classifications For Engineering	156
6.3	STONE DETERIORATION INDEX	158
6.3.1	Building Decay Parameters and Class Boundaries	160
6.3.1.1	Pilot Study	166
6.3.2	Surface Strength	167
6.3.3	Surface Roughness	171
6.3.4	Surface Coatings	174
6.3.5	Surface Discolouration	176

## CHAPTER 7. Results of the Dartmoor Churches Study

7.1	INTRODUCTION	180
7.2	CHURCH DETERIORATION RATING	180
7.2.1	Luesdon Cross	182
7.2.2	Lydford	185
7.2.3	Mary Tavy	189
7.2.4	Moretonhampstead	195
7.2.5	Peter Tavy	200
7.2.6	Postbridge	203
7.2.7	Princetown	206
7.2.8	Shaugh Prior	209
7.2.9	Sheepstor	212
7.2.10	Widcombe in the Moor	216
7.3	COURSE AND ASPECT RATING VARIATION	220
7.3.1	South Facing Walls	221
7.3.2	West Facing Walls	224
7.3.3	North Facing Walls	227
7.3.4	Interior Walls	229
7.3.5	Exterior Course Averages	233
7.3.6	Medieval and 19 <sup>th</sup> century Church Aspect Differences	237
7.4	AGE - RATING COMPARISONS	239
7.5	CONCLUSIONS	250

## CHAPTER 8. Discussion and Conclusions

<b>8.1 INTRODUCTION</b>	253
<b>8.2 GRANITE EXPOSURE STUDIES</b>	254
<b>8.3 STONE DETERIORATION INDEX RESULTS</b>	263
<b>8.4 CONCLUSIONS</b>	271
<b>8.5 AREAS FOR FUTURE RESEARCH.</b>	273
<b>8.5.1 Granite Exposure Studies</b>	273
<b>8.5.2 Stone Deterioration Index Development</b>	274
 <b>REFERENCES</b>	 277
 <b>APPENDIX.</b>	 297
 <b>GLOSSARY OF TERMS.</b>	 312

## FIGURES

### CHAPTER 2

Figure 2.1	Principal granite outcrops of south-western England	6
Figure 2.2	Compositional curves of the igneous continuum	8
Figure 2.3	Granite distribution on Dartmoor and Bodmin Moor	11
Figure 2.4	The stone decay system	13
Figure 2.5	The deterioration factors that can affect stone quality	16
Figure 2.6	Cross-section of stone, showing salt efflorescence and subflorescence	23
Figure 2.7	Possible patterns in stone decay rates	39
Figure 2.8	Mass loss from stonework during weathering	40

### CHAPTER 3

Figure 3.1	SO <sub>2</sub> levels in Belfast and London over time	42
Figure 3.2	Changes in NO <sub>x</sub> end user emissions between 1970 and 1994	45
Figure 3.3	NO <sub>2</sub> distribution in the UK during 87-90	46
Figure 3.4	The atmospheric NO <sub>x</sub> cycle	47
Figure 3.5	NO release rates as a function of time and stone mass	48
Figure 3.6	Changes in SO <sub>2</sub> emissions by end users between 1970-1994	50
Figure 3.7	The atmospheric SO <sub>x</sub> cycle	50
Figure 3.8	Mean daily O <sub>3</sub> and SO <sub>4</sub> aerosol concentrations in London	51
Figure 3.9	The cycle of NH <sub>3</sub> compounds in the atmosphere	52
Figure 3.10	Diesel derived particulate composition	56
Figure 3.11	Some of the effects of carbonaceous particle deposition on a stone surface	58
Figure 3.12	The possible actions of calcium and sulphates on granite	61
Figure 3.13	Characteristic ion concentrations as a function of drop radius	65

### CHAPTER 4

Figure 4.1	The carousel tablets and steel fixtures	70
Figure 4.2	Street plan of London, showing St. Paul's Cathedral	72

Figure 4.3	The location of exposure racks on the roof of St. Paul's	73
Figure 4.4	The location of exposure racks on the roof of Five-Ways House, Birmingham	73
Figure 4.5	The location of the Dartmoor exposure site	74
Figure 4.6	Diagram showing exposure carousel details	75
Figure 4.7	Micro-catchment unit and exposure rack dimensions	76
Figure 4.8	1 <sup>st</sup> and 2 <sup>nd</sup> order roughness measurements	84
Figure 4.9	EDX elemental analysis of an orthoclase feldspar	86

## CHAPTER 5

Figure 5.1	Frequency distributions for $\text{SO}_4^{2-}$ , $\text{Cl}^-$ and conductivity measurements at different sites and finishes	87
Figure 5.2	Weekly chloride, $\text{SO}_2$ and $\text{NO}_x$ distribution for London	97
Figure 5.3	Weekly chloride, $\text{SO}_2$ and $\text{NO}_x$ distribution for Birmingham	98
Figure 5.4	Weekly chloride and $\text{SO}_2$ distribution for Dartmoor	99
Figure 5.5	Weekly nitrate, $\text{SO}_2$ and $\text{NO}_x$ distribution for London	101
Figure 5.6	Weekly nitrate, $\text{SO}_2$ and $\text{NO}_x$ distribution for Birmingham	102
Figure 5.7	Average weekly nitrate distribution for Dartmoor	103
Figure 5.8	Average weekly phosphate concentrations	104
Figure 5.9	Weekly sulphate, $\text{SO}_2$ and $\text{NO}_x$ distribution for London	106
Figure 5.10	Weekly sulphate, $\text{SO}_2$ and $\text{NO}_x$ distribution for Birmingham	107
Figure 5.11	Average weekly sulphate distribution for Dartmoor	108
Figure 5.12	London runoff average weekly aluminium distribution	110
Figure 5.13	Birmingham runoff weekly average aluminium distribution	111
Figure 5.14	Dartmoor runoff average weekly aluminium distribution	112
Figure 5.15	Weekly calcium runoff distribution, London	114
Figure 5.16	Weekly calcium runoff distribution, Birmingham	115
Figure 5.17	Weekly calcium runoff distribution, Dartmoor	116
Figure 5.18	Weekly magnesium runoff distribution, London	119
Figure 5.19	Weekly magnesium runoff distribution, Birmingham	120
Figure 5.20	Weekly magnesium runoff distribution, Dartmoor	120
Figure 5.21	Weekly iron runoff distribution, London	123
Figure 5.22	Weekly iron runoff distribution, Birmingham	123
Figure 5.23	Weekly iron runoff distribution, Dartmoor	124
Figure 5.24	Mean carousel tablet weight changes; upper suite	128
Figure 5.25	Upper suite weight changes from initial condition	130
Figure 5.26	Mean carousel tablet weight changes; lower suite	131
Figure 5.27	Lower suite weight changes from initial condition	132
Figure 5.28	Upper and lower suite weight change	134
Figure 5.29	Changes from initial slab weight between exposure sites	138
Figure 5.30	M.C.U slab weight changes, by finish	139
Figure 5.31	Control and sample slab roughness comparisons	142
Figure 5.32	Polished exposure slab transect	143
Figure 5.33	Cut exposure slab transect	143
Figure 5.34	Flame exposure slab transect	144
Figure 5.35	Detail of the London flame-dressed transect, showing a orthoclase mineral	145
Figure 5.36	Incremental depth composition spectra, plagioclase mineral	146

## CHAPTER 6

Figure 6.1	Aspects of stone deterioration . . . . .	162
Figure 6.2	The relationship between Schmidt Hammer rebound and different measures of rock surface weathering . . . . .	168
Figure 6.3	Surface variability measurement . . . . .	172
Figure 6.4	Surface roughness rating point distribution . . . . .	174

## CHAPTER 7

Figure 7.1	Church and monument locations around Dartmoor . . . . .	191
Figure 7.2	Generic tower and course position within churches . . . . .	182
Figure 7.3	Orientation, position and dimensions of Luesdon cross . . . . .	183
Figure 7.4	Sketch plan of Luesdon Cross . . . . .	183
Figure 7.5	Luesdon cross course rating distribution . . . . .	185
Figure 7.6	Plan view of Lydford church and interior . . . . .	186
Figure 7.7	Sketch plan for Lydford church, south facing wall . . . . .	187
Figure 7.8	Lydford course rating distribution . . . . .	188
Figure 7.9	Site plan of Mary Tavy, the tower and vestry . . . . .	189
Figure 7.10	Sketch plan of Mary Tavy Church, south facing wall . . . . .	190
Figure 7.11	Sketch plan of Mary Tavy Vestry . . . . .	191
Figure 7.12	Mary Tavy course rating distribution . . . . .	192
Figure 7.13	Mary Tavy Vestry course rating distribution . . . . .	194
Figure 7.14	Site plan of Moretonhampstead church and interior . . . . .	195
Figure 7.15	Sketch of Moretonhampstead Church, South wall . . . . .	196
Figure 7.16	Moretonhampstead course rating distribution . . . . .	199
Figure 7.17	Site plan of Peter Tavy church and interior doorway . . . . .	200
Figure 7.18	Sketch plan of Peter Tavy Church, West facing wall . . . . .	201
Figure 7.19	Peter Tavy course rating distribution . . . . .	202
Figure 7.20	Site plan of Postbridge church . . . . .	203
Figure 7.21	Sketch plan of Postbridge church, north facing wall . . . . .	204
Figure 7.22	Site plan and measurement site distribution of Princetown church . . . . .	206
Figure 7.23	Sketch plan of Princetown Church, east end average values . . . . .	207
Figure 7.24	Princetown course rating distribution . . . . .	208
Figure 7.25	Site plan of Shaugh Prior and interior . . . . .	209
Figure 7.26	Sketch plan of Shaugh Prior, south facing wall . . . . .	210
Figure 7.27	Shaugh Prior course rating distribution . . . . .	211
Figure 7.28	Site plan of Sheepstor church tower . . . . .	213
Figure 7.29	Site plan of Sheepstor church and interior details . . . . .	213
Figure 7.30	Sketch plan of Sheepstor Church, west facing wall . . . . .	214
Figure 7.31	Sheepstor course rating distribution . . . . .	216
Figure 7.32	Plan view of Widecombe Church and interior . . . . .	217
Figure 7.33	Sketch plan of Widecombe-in-the-Moor, north facing wall . . . . .	218
Figure 7.34	Widecombe Church course rating distribution . . . . .	219
Figure 7.35	Data distribution for south facing courses . . . . .	222
Figure 7.36	Data distribution of west facing courses . . . . .	226
Figure 7.37	Data distribution of north facing courses . . . . .	229
Figure 7.38	Data distribution of interior courses . . . . .	232

Figure 7.39	Mean course values, across all aspects . . . . .	234
Figure 7.40	External aspect course profiles . . . . .	236
Figure 7.41	Mean aspect distribution for C19 <sup>th</sup> and medieval churches	237
Figure 7.42	South aspect SDI deterioration rates . . . . .	242
Figure 7.43	Possible weathering pattern over time . . . . .	243
Figure 7.44	West aspect SDI deterioration rates . . . . .	244
Figure 7.45	North aspect SDI deterioration rates . . . . .	245
Figure 4.46	Average external SDI deterioration rates . . . . .	246
Figure 7.47	Exponential and linear deterioration estimations . . . . .	248

## CHAPTER 8

Figure 8.1	Control and exposed finish roughness variation . . . . .	259
Figure 8.2	Carousel tablet weight changes, by site and suite . . . . .	260
Figure 8.3	Limestone tablet weight changes at St. Marylebone . . . . .	262
Figure 8.4	Mean weathering scores for churches of different ages	267
Figure 8.5	Mean sandstone building weathering scores, plus two standard deviations . . . . .	268
Figure 8.6	Possible weathering patterns over time . . . . .	269
Figure 8.7	Average external SDI deterioration rates . . . . .	271

## TABLES

### CHAPTER 2

Table 2.1	The petrographic classification of acid igneous rock classes	7
Table 2.2	Chemical analysis of two samples of granodiorite from Mountsorrel quarry . . . . .	10
Table 2.3	A petrographic summary of main Dartmoor granite types	12
Table 2.4	Cumulative ion loss ( $\mu\text{eq cm}^{-2}$ ) in typical run-off samples	14
Table 2.5	Crystallisation pressures for some common salts . . . . .	23
Table 2.6	The possible alteration products from primary minerals	33
Table 2.7	Organic acids produced by organisms involved in biodeterioration . . . . .	37

### CHAPTER 3

Table 3.1	Table showing mean pollution concentrations in rural and urban exposure sites . . . . .	43
Table 3.2	Increases in estimated UK transport emissions 1980-1990	44
Table 3.3	Estimated emissions of $\text{NO}_x$ by end users: 1970 - 1994	45
Table 3.4	Estimated emissions of $\text{SO}_2$ by end users: 1970 - 1994	49
Table 3.5	Composition of particles gathered from Leeds in 1982 - 83	53
Table 3.6	The physiochemical properties of carbonaceous particles	55
Table 3.7	Table showing typical scavenging ratios . . . . .	64

### CHAPTER 4

Table 4.1	Type, location and use of granites in exposure programme	68
Table 4.2	Granite type and approximate modal composition . . . . .	68
Table 4.3	Mean air pollution levels during the exposure period	72
Table 4.4	Properties of the ionic exchange column . . . . .	81
Table 4.5	Ion chromatograph operating conditions . . . . .	82



## CHAPTER 5

Table 5.1	Run-off volume means and standard error, by finish and site	91
Table 5.2	Mean finish and site pH and standard error	92
Table 5.3	Mean conductivity measurements, by finish and site	94
Table 5.4	Average site anion concentration, across blank and finish	95
Table 5.5	Chloride means and standard error, by finish and site	96
Table 5.6	Nitrate means and standard error, by finish and site	100
Table 5.7	Phosphate means and standard error, by finish and site	104
Table 5.8	Sulphate means and standard error, by finish and site	106
Table 5.9	$\text{Al}^{3+}$ runoff means and standard error, by finish and site	109
Table 5.10	$\text{Ca}^{++}$ runoff means and standard error, by finish and site	113
Table 5.11	$\text{Mg}^{++}$ runoff means and standard error, by finish and site	118
Table 5.12	$\text{Fe}^{++}$ runoff means and standard error, by finish and site	122
Table 5.13	Mean percentage change from initial carousel tablet weight	127
Table 5.14	Upper suite percentage change from initial dry weight	129
Table 5.15	Lower suite percentage change from initial dry weight	132
Table 5.16	Site and suite variation in weight changes	135
Table 5.17	Percentage change from initial weight, by finish and site	137
Table 5.18	Mean run-off concentrations, by site	141
Table 5.19	Roughness measurements from control and sample slabs	141

## CHAPTER 6

Table 6.1	The Price classification, based on rock parameters	154
Table 6.2	Rock weathering classifications for rock mass and material rating currently recommended for engineering purposes	155
Table 6.3	The RQD rock quality evaluation table	156
Table 6.4	Rock weathering classes and granite indices test values	157
Table 6.5	Physical tests used in rock quality assessment	161
Table 6.6	Minimum tests required to account for all weathering aspects	165
Table 6.7	Weathering grades with N-Type Schmidt Hammer values	169
Table 6.8	Surface strength assessment chart	170
Table 6.9	Surface roughness assessment chart	173
Table 6.10	Cross-church average coverage for different walls	175
Table 6.11	Surface coating/crustal coverage assessment chart	176
Table 6.12	Discolouration assessment chart	177
Table 6.13	Correlation between SDI parameters and building age	178
Table 6.14	The SDI rating table	179

## CHAPTER 7

Table 7.1	Average block ratings, by aspect, for Luesdon cross	184
Table 7.2	Average course ratings, by aspect, for Lydford	187
Table 7.3	Summary of the average course ratings for Mary Tavy	192
Table 7.4	The average block ratings for Mary Tavy Vestry	193
Table 7.5	Internal/external surface strength ratios of Moretonhampstead Church	197
Table 7.6	Average course values for Moretonhampstead church	197
Table 7.7	Average course rating for Peter Tavy church	201

Table 7.8	Total block ratings for Postbridge church . . . . .	205
Table 7.9	Average block rating values for Princetown church . . . . .	208
Table 7.10	Average course rating values for Shaugh Prior . . . . .	211
Table 7.11	Average course ratings for Sheepstor church . . . . .	215
Table 7.12	Average course ratings for Widecombe-in-the-moor church . . . . .	218
Table 7.13	Average block ratings by course, south facing walls . . . . .	221
Table 7.14	Average block ratings by course, west facing walls . . . . .	225
Table 7.15	Average block ratings by course, north facing walls . . . . .	227
Table 7.16	Average block ratings by course, interior walls . . . . .	230
Table 7.17	Exterior and interior wall averages and standard error across all churches . . . . .	232
Table 7.18	Average block ratings by course, average across all aspects . . . . .	233
Table 7.19	Aspect means and variation for C19 and medieval churches . . . . .	239
Table 7.20	Correlation between SDI parameters and building age . . . . .	240
Table 7.21	Average SDI values for interior and exterior church walls . . . . .	241
Table 7.22	Linear SDI deterioration rates between external aspects . . . . .	248
Table 7.23	Exponential SDI deterioration rates per century . . . . .	248

## CHAPTER 8

Table 8.1	Exposure site pollution averages . . . . .	255
Table 8.2	Finish means across components and sites . . . . .	256
Table 8.3	Correlation values between building age and individual index parameters and SDI block totals . . . . .	265
Table 8.4	Exterior and interior wall averages and standard error of the mean across all churches . . . . .	266
Table 8.5	Linear and exponential SDI deterioration rates . . . . .	270
Table 8.6	Age/aspect correlation values . . . . .	270

## PLATES

### CHAPTER 2

Plate 2.1	Burrator Quarry Dartmoor, with parallel dilation jointing . . . . .	20
-----------	---	----

### CHAPTER 4

Plate 4.1	Microcatchment and carousel exposure rig, Birmingham . . . . .	77
-----------	--	----

### CHAPTER 7

Plate 7.1	Luesdon Cross, south facing . . . . .	183
Plate 7.2	Lydford church, south facing wall, showing cleaned area . . . . .	186
Plate 7.3	Mary Tavy church, south facing wall . . . . .	190
Plate 7.4	Mary Tavy Vestry, south facing wall . . . . .	191
Plate 7.5	Moretonhampstead church, south facing wall . . . . .	196
Plate 7.6	Moretonhampstead church, north facing wall . . . . .	198
Plate 7.7	Peter Tavy church, west facing wall . . . . .	200
Plate 7.8	Postbridge church, north facing wall . . . . .	204
Plate 7.9	Princetown church, east end . . . . .	207
Plate 7.10	Shaugh Prior, south facing wall . . . . .	210
Plate 7.11	Sheepstor church, west facing wall . . . . .	214
Plate 7.12	Widecombe-in-the-Moor church, north facing wall . . . . .	217

## ACKNOWLEDGEMENTS

This project was supported by a SERC quota grant.

A number of people have been particularly helpful and supportive during the course of the PhD, especially Dr. Terry Hawkins, whose insight, enthusiasm and humour made a difficult task more bearable.

Others have had significant inputs, including Professor Ron Hamilton and Dr. Brian Shutes from Middlesex University, and John Houston from the Building Research Establishment. Paul Kershaw, John Schmitt and Alan La Grue were also extremely helpful in patching together temperamental and unreliable lab equipment when all seemed lost. I would like to thank Peter Künzli and Richard Luxton as well, for their staunch efforts in helping me collect data from Dartmoor churches in the middle of frequent rain, gales and snow storms.

Finally I dedicate this thesis to Lianne Older, who took up a PhD of her own to keep me company as I struggled with my work.

## CHAPTER 1. Introduction

### 1.1. INTRODUCTION

In Europe, building decay as a result of atmospheric and pollution processes has been recorded as early as the ancient Greeks, who referred to contaminants in the air and the removal of stone by water (Camuffo, 1992). Recently, the rate of building deterioration experienced by Europe's monuments and culturally important buildings has increased. Leysen *et al* (1989) state that the damage done to buildings in the last 50 years is as important as that of the former 500 years, even though current levels of SO<sub>2</sub> are lower than in the past (Brimblecombe, 1977).

Granite, which is perceived to be a hard and resistant rock, has been used in the construction of culturally important buildings for the past 5,000 years. Like other common building materials such as limestone, however, it is at risk from pollution-induced decay (Cooper *et al*, 1993), which reduces the strength of the material and its aesthetic appeal. However, unlike limestone (e.g. Jaynes and Cook, 1987), there have been relatively few examinations of the role pollution plays in the deterioration of granitic building stone, in both the short- and the long-term.

To address this, a short-term exposure programme was developed, coupled with a method to quantifiably evaluate stone deterioration non-destructively and *in situ*. Given the increases in building decay rates, it is important to be able to easily and accurately determine the condition of sensitive buildings for remedial and conservation purposes.

### 1.2. AIMS

The project was designed to examine building stone deterioration in 'clean' and polluted atmospheres. Two routes were chosen for this.

The first area of research was a two year exposure programme to evaluate the levels of deterioration granite experienced as a result of exposure to a polluted atmosphere. This was studied by analysing the composition of run-off collected from granite surfaces situated at three contrasting sites in England. Each site (London, Birmingham and Dartmoor) contained three granodiorite slabs with differing degrees of surface roughness and a glass blank. Weight changes associated

with dry and total deposition on carousel tablets at each of the sites were also evaluated.

The second and most significant area for study, was the formulation of a Stone Deterioration Index (SDI), which allows an accurate, *in situ* and non-destructive method of building decay assessment. The SDI scheme avoids process- and feature-led decay evaluation, by assessing the products of the total deterioration processes that affect the building stone condition. This is achieved through the measurement of selected near-surface characteristics of building stones (surface strength, surface roughness, biological/pollutant coatings and stone discolouration). This generic approach allows the comparison of buildings in different weathering regimes and pollution environments. The SDI classes were based on values derived from selected granitic churches located in the Dartmoor region, England..

### 1.3. OUTLINE OF THESIS

The thesis is comprised of eight chapters. Chapter 1 presents the aims and outline of the research programme. Chapter 2 provides an overview of the formation, placement and types of granite found in the Dartmoor region of south west England. Later sections cover the mechanical, chemical and biological mechanisms involved with stone deterioration. Chapter 3 examines the processes and impact of air pollution on building stone, while Chapter 4 details the exposure sites, the methods used in sample selection, and the run-off and slab analysis. In Chapter 5, the results of the micro-catchment unit run-off analyses are presented, followed by examinations of dry and total deposition rates on the carousel tablets. Analyses of the surface roughness and composition of the micro-catchment slabs are also examined. An overview of engineering geology rating and classification schemes, and the formulation of the Stone Deterioration Index is presented in Chapter 6. In Chapter 7, the results of the church studies are presented. These are broken down into individual church results, as well as collective studies on the impact of aspect, height above ground and age on the SDI values. Finally, Chapter 8 summarises and relates the findings of the two research programmes to each other, and identifies areas of future research.

## 1.4. ASSOCIATED PUBLICATIONS AND CONFERENCES

### Conferences and Seminars Attended

Granite Weathering and Conservation, University of Dublin, 16-17 September, 1993.

EC Environmental Research Workshop 'Degradation and Conservation in Granitic Rocks in Monuments', Santiago de Compostela, Spain. 28 - 30 November, 1994.

Symposium on the Environmental Impact of Transport. Royal Society of Chemistry, Industrial Division, 23 November, 1993.

Vehicle Emissions and Air Quality, Middlesex University, 28 March, 1994.

S.W.A.P.N.E.T (Stone Weathering and Air Pollution Network), Portsmouth University, November, 1994.

### Presentations

Granite Decay in Southwest England. Poster presentation in 'Granite Weathering and Conservation', University of Dublin, 1993.

Analysis of Granitic Run-off. Poster Presentation in 'Degradation and Conservation in Granitic Rocks in Monuments', Santiago de Compostela, Spain. 1994.

Pollution Induced Granite Weathering, at 'SWAPNET', Portsmouth University, November, 1994.

### Publications

Hamilton, R. S., Hawkins, T. R. W., and Luxton, W, 1996. Air Pollution and Damage to Building Stone. In *Degradation and Conservation of Granitic Rocks in Monuments. Proceedings of the EC Workshop Held in Santiago de Compostela (Spain) on 28-30 November 1994. Protection and Conservation of the European Cultural Heritage. Report No 5*, ed. M. A. Vincente, J. Delgado-Rodrigues & J. Acevedo, pp. 463-468. Brussels: European Commission.

Luxton, W. B, and Hawkins, T. R. W. A Deterioration Index for 'Granitic' Building Stone. In preparation.

## CHAPTER 2. The Nature and Weathering of Granite

### 2.1. INTRODUCTION

'Granite' is used widely by the public and professionals to denote an igneous rock that contains quartz, feldspars and micas. However, this is a generalisation because granite rocks belong to an extensive group that contains many sub-divisions, each based on the method of formation, type of intrusion, texture, and the varying chemical and mineralogical composition of the rock. The formation and intrusion of granite types will be discussed first, as these factors can strongly influence the mineralogical and petrographical characteristics of the rocks. Emphasis will be placed on the granites of SW England, and to a lesser extent, the Mountsorrel granodiorite - the rock types studied in the research. This will be followed by a summary of the physical and chemical weathering processes that can result in rock deterioration.

### 2.2. FORMATION AND PLACEMENT OF GRANITE

Granite is an igneous rock, and is generally conceived as being formed by the cooling and crystallisation of magma. The location and placement of granite is strongly influenced by its origin, in that it is a product of past tectonic or orogenic processes. Some granitic rocks, however are not intrusive and are formed through the permeation of country rock by hydrothermal fluids and volatiles.

Magmas are mobile fluid rocks below the earth's surface, which are divided into two classes; felsic (or acid) and mafic (or basic). Felsic magmas are lower density magmas, which result in the formation of 'acid' rock such as granites and granodiorites. Mafic (or basic) magmas, are of higher density and result in the formation of gabbros, dolerites and basalts. Through magma mixing or differentiation, intermediate rocks such as syenites and diorites are produced.

Granite magmas are the products of either partial melting or crystallisation differentiation. The partial melting of either sedimentary rocks and their metamorphic equivalents or igneous rocks of intermediate to basic composition, or the differentiation of basaltic or andesitic magma. No other source materials have

suitable compositions or exist in sufficient quantities to produce granite magma in the required amounts (Hall, 1987).

When batches of rising felsic magma cool and solidify they form masses up to tens of kilometres across called plutons. Where plutons coalesce they form even larger masses, up to many hundreds of kilometres in diameter known as batholiths. These are composite bodies, with no visible floor or roof, that can vary considerably in size, composition and time of emplacement, resulting in a heterogeneous rock mass, with varying physical properties (Moorhouse, 1964; Hughes, 1982). This may be due to differentiation or multiple injection of the magma (Barker, 1983). These characteristics determine the durability and weathering resistance of the rock; porosity, crystal-size, percentage pore space per unit volume and the rock composition.

### **2.2.1. The Cornubian Batholith**

The Cornubian batholith of west Devon and Cornwall is composed of many individual intrusions. Although a small batholith on global standards, with a length of about 250 km, it has undergone many late- and post-magmatic processes, including mineralization. The thickness of the granite varies from around 20 km thick in the east, to half that in the west, and is 40-60 km wide at its base (Floyd *et al*, 1993).

The granites in the south-west of England date from the Hercynian age, and outcrop in six major areas, Dartmoor (about 600 km<sup>2</sup>), Bodmin Moor (190 km<sup>2</sup>) St. Austell (85 km<sup>2</sup>), Carnmenellis (130 km<sup>2</sup>), Lands End (190 km<sup>2</sup>) and the Scilly isles. The exposed granite, which also includes outcrops of smaller size and area such as Kit Hill and Hingston Down, are all part of the same granite mass, being projecting outcrops on the top of the Cornubian granite batholith. Radiometric dating of the exposed biotite-bearing granites indicate that the main period of magmatism was between 290-289Ma BP - followed by a second phase 10Ma later (Jackson *et al*, 1982)

The outcrops of the protrusions at the top of the batholith are approximately cylindrical or conical in form, and were thought to be emplaced, like the main granite batholith, by large-scale block stopping and cauldron subsidence. There is evidence



for these methods of emplacement; little deformation of the projecting bosses, smaller scale stoped blocks in one of the bosses, xenoliths included in the granite fabric, and the intrusion of microgranite in Dartmoor. (Exley and Stone, 1982).

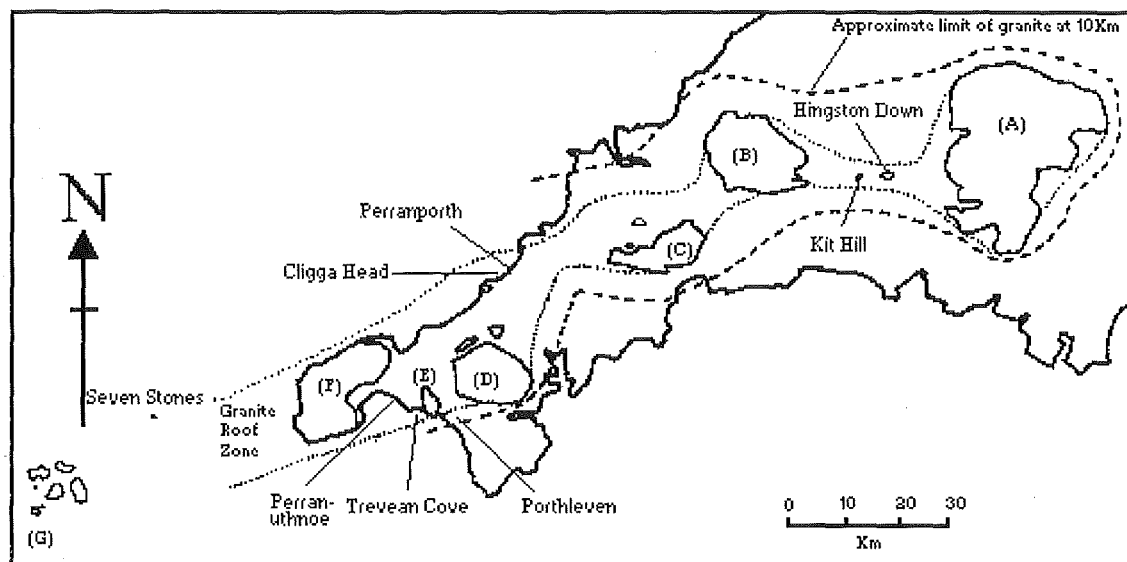


Figure 2.1. Principal granite outcrops of south-western England, and approximate form of the Cornubian batholith. A) Dartmoor; B) Bodmin Moor; C) St. Austell; D) Carnmenellis; E) Tregonning - Godolphin; F) Land's End; G) Scilly Isles (From Exley and Stone, 1982).

A second magmatic activity stage occurred around 270Ma BP, and resulted in the emplacement of a second magma, which crystallised to give rise to localised albite-zinnwaldite-topaz granite found at some exposed batholith sites. Circulating hydrothermal fluids led to decomposition of the granite through the development of clay minerals such as smectite and illite, by alteration of the felsic minerals. This was the result of pneumatolysis (see section 2.6.3) and other hydrothermal process (Palmer and Neilson, 1962; Floyd *et al*, 1993).

### 2.3. GRANITE TYPES

Granites are medium to coarsely crystalline acid igneous rocks that contain between 10-40% free quartz. Granite is the main igneous building stone, with an average crushing strength of sound granite ranging from  $135 \times 10^6$  to  $245 \times 10^6 \text{ N m}^{-2}$ .

and a specific gravity of 2.67 for alkali granite and 2.72 for granodiorite.

Classification of granite and other acid rocks (containing  $\geq 66\%$  free silica ( $\text{SiO}_2$ ) and over 10% free quartz) is based on two parameters, the rocks bulk chemistry and crystal size, both of which are influenced by the method of formation. Using bulk chemistry and texture it is possible to subdivide acid rocks into nine classes, shown in Table 2.1.

Crystal Size	Alkali-feldspar $< 2/3$	Alkali-feldspar & plagioclase each between $1/3$ and $2/3$	Plagioclase $> 2/3$
Coarse	Alkali-granites	Adamellites	Granodiorites
Medium	Alkali-microgranites	Micro-adamellites	Micro-granodiorites
Fine	Rhyolites	Rhyo-dacites	Dacites

Table 2.1. The petrographic classification of acid igneous rock classes (Hatch *et al*, 1972).

Individual granites are also usually referred to by the quantitatively dominant mineral, apart from feldspars and quartz. This leads to species of granite, e.g. tourmaline-granites and muscovite-biotite-granites.

Granites are part of an igneous rock series, and their position in the granite - granodiorite - diorite continuum is decided by their chemical composition. The differing composition of the continuum members can be illustrated by a variation diagram, is shown in Figure 2.2, which has been determined from the analysis of the percentage mineral compositions in typical igneous rocks. The curves show an increase in the magnesia, calcium and iron content of the series as it moves towards the more basic end of the continuum (Blyth and de Freitas, 1974).

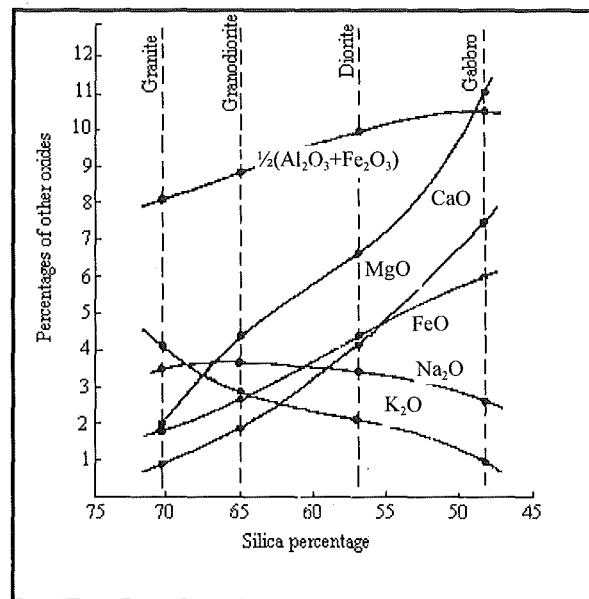


Figure 2.2. Compositional curves of the igneous continuum (Blyth and de Freitas, 1974).

### 2.3.1. Alkaligranites

Alkali-granites are the most common granites in the UK, and have a mineralogical composition where  $K_2O$  and  $Na_2O$  are present, and where K-feldspars exceed plagioclase feldspars. Within alkaligranites there are two main types of feldspar distribution; 1) A single feldspar type, an orthoclase-albite intergrowth (perthite), and 2) Two or more feldspar types, a K-feldspar and a Ca/Na plagioclase. It is the second type that is more common, the first being strongly associated with high level, sub-volcanic environments where cooling is rapid. The second two-feldspar type generally had a slower cooling rate, and this has resulted in the separation of the feldspathic constituents. Quartz is around 30% of the total rock by weight, and can be either institial or lobed into some of the feldspar crystals. A small amount of iron ore is also usually found in alkali granites.

Biotite mica and tourmaline are the only two mafic minerals likely to be found in alkali granites. Both micas (biotite and muscovite) can appear in the rock, with pleochroic haloes found in the biotite from the radioactive minerals zircon and xenotime. Rarely small amounts of other micas, e.g. lepidolite, may be present.

In alkali-granites, there is usually some mineral alteration, especially the conversion of biotite to chlorite and sericite along cleavage planes, and the kaolinization or sericitization of feldspars (Hatch *et al*, 1972).

### 2.3.2. Ademellites

These are the middle members of the coarse-grained Acid igneous rocks, and are also known as quartz-monzonites. The rocks in this group have plagioclase feldspar in almost equal proportion to alkali feldspars, and no one type of feldspar exceeds the total feldspar content of the rock by 60%. This means that it is possible to have a potentially significant source of calcium ions within the rock.

The essential quartz, alkali-feldspar and plagioclase are often accompanied by biotite, or biotite and hornblende. Therefore, as the definition of adamellite does not refer to the quantities of dark minerals that can be found in the rock, adamellite is often referred to as a biotite-granite, or biotite-hornblende-granite (Hatch *et al*, 1972).

### 2.3.3. Granodiorites

These are the most mafic members of the acid (or felsic) igneous rocks and tend towards an 'intermediate' composition. Plagioclase feldspars are dominant, making up at least 66% of the total feldspars. The felsic minerals are accompanied by varying proportions of coloured silicates, biotite and hornblende (Hatch *et al*, 1972). Granodiorite is quartz-rich but the sub-species, tonalite and quartz-mica diorite, only contain quartz as an accessory mineral.

Granodiorite has a higher calcium content than alkali granites and has been used in the exposure programme to compare these two granite types. The granodiorite was taken from Mountsorrel Quarries, located near Leicester, one of the largest road-stone producing granite quarries in England.

A petrographic and chemical x-ray analysis from Redland Aggregates on two samples of granodiorite taken from the Mountsorrel quarry, shown in Table 2.2, summarised the rocks as composed of un-strained quartz, plagioclase and zoned alkali feldspar phenocrysts and biotite mica with some chlorite alteration products. The rock type is categorised as granite/granodiorite.

Element	% Composition	% Composition
	Mountsorrel, 10mm crushed granite	Mountsorrel, quarry fines granite
Loss on Ignition (1000°C)	0.75	0.80
Fe <sub>2</sub> O <sub>3</sub>	2.29	1.99
SiO <sub>2</sub>	72.5	74.5
TiO <sub>2</sub>	0.36	0.34
CaO	2.66	1.54
K <sub>2</sub> O	3.70	3.89
Al <sub>2</sub> O <sub>3</sub>	13.5	12.9
MgO	1.09	1.13
Na <sub>2</sub> O	3.00	2.73
<b>Total</b>	<b>99.85</b>	<b>99.82</b>

Table 2.2. Chemical analysis of two samples of granodiorite from Mountsorrel quarry (analysis conducted by UK Analytical Ltd. for Redlands Aggregates, 1992).

#### 2.3.4. Dartmoor and Bodmin Moor Granites

Granites found on Dartmoor and Bodmin Moor are part of the exposed Cornubian batholith, which is composed mainly (90% - Hawkes and Dangerfield, 1978) of coarse megacrystic (or porphyritic) biotite granite (classed as Type B by Exley and Stone, 1982), which has a ground mass of crystals over 3mm. Less than 10% is fine grained biotite-granite (Type C), shown below in Figure 2.3. There are other types comprising a few percent by volume, such as the lithium-mica, topaz and fluorite granites, but these are seen as local variations of biotite granite (Exley *et al*, 1982). The compositional variations are shown below in Table 2.3.

The Dartmoor biotite granites have been subdivided into three main classes by Floyd *et al*, (1993), with the coarse-grained megacrystic biotite-granite (described by Fookes *et al*, (1971) as a medium-grained quartz-feldspar-biotite with scattered megacrysts of feldspar and quartz) labelled as Type B, and the fine-grained biotite-granite as Type C. There are also local variations on the major rock types, formed by slight differences in the rock forming environment, leading to differences in the crystal size, percentage phenocrysts etc. (Fookes *et al*, 1971; Exley *et al*, 1982). Only Type B and Type C granites will be covered in detail, although a summary of Dartmoor granite characteristics is shown in Table 2.3.

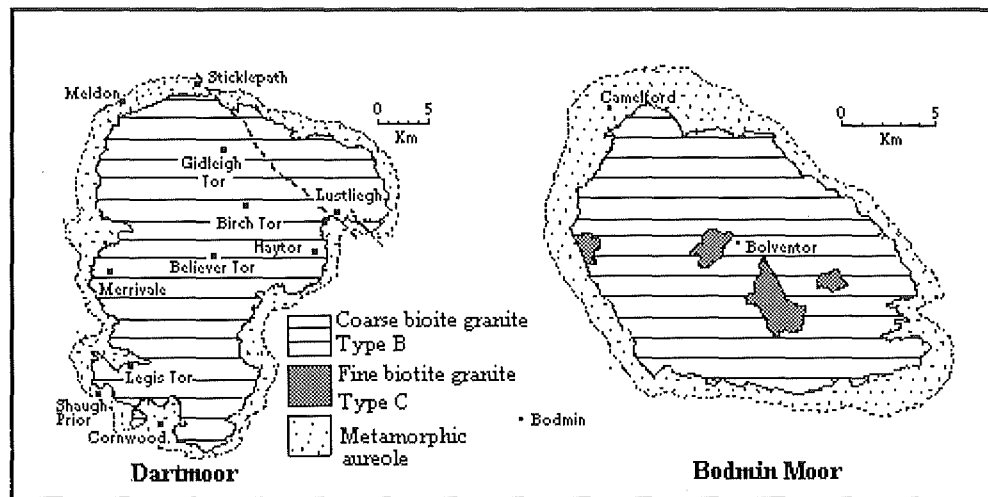


Figure 2.3. Granite distribution on Dartmoor and Bodmin Moor (From Exley and Stone, 1982).

**Type B**, Coarse-grained megacrystic biotite-granites: These rocks are medium- or coarse-grained, and often contain alkali feldspar megacrysts which can range in length from 1.7cm to 5cm (Floyd *et al*, 1993). The megacrysts are commonly euhedral or subhedral, with irregular edges. Microperthite is often found in the feldspar crystals (Exley *et al*, 1982), and a dark tourmaline (schorl) is locally common.

Granite Type B is found at Haytor, Dartmoor, in conjunction with a later intrusive fine grained granite sheet. The coarse-grained biotite-granite contains xenoliths, and also shows evidence of tourmalinization. The presence of the tourmaline veins, and nodular masses of tourmaline called 'suns', indicate Haytor rocks are relatively boron rich.

			Minerals (approximate mean modal amounts in parentheses)					
Type	Description	Texture	K-feldspar	Plagioclase	Quartz	Micas	Tourmaline	Others
A	Basic microgranite	Medium to fine; ophitic to hypidiomorphic	(Amounts vary)	Oligoclase-andesine (amount vary)	(Amounts vary)	Biotite predominant, some muscovite	Often present	Hornblende, apatite, zircon, garnet
B	Coarse-grained megacrystic biotite granite	Medium to coarse; megacrysts 5-17 cm maximum, mean about 2 cm. Hypidiomorphic, granular	Euhedral to subhedral; microperthitic (32%)	Euhedral to subhedral. Often zoned.	Irregular (34%)	Biotite, often in clusters (6%); muscovite (4%)	Euhedral to anhedral. Often zoned. 'Primary' (1%)	Zircon, ore, apatite, andalusite etc. (total 1%)
C	Fine-grained biotite granite	Medium to fine, sometimes megacrystic; hypidiomorphic to aplitic	Subhedral to anhedral; sometimes microperthitic (30%)	Euhedral to subhedral. Often zoned.	Irregular (33%)	Biotite 3% Muscovite (7%)	Euhedral to anhedral. 'Primary' (1%)	Ore, andalusite, fluorite (total <1%)
D	Megacrystic lithium-mica granite	Medium to coarse; megacrysts 1-8.5 cm, mean about 2 cm. Hypidiomorphic	Euhedral to subhedral; microperthitic (27%)	Euhedral to subhedral; unzoned (26%)	Irregular; some aggregates (36%)	Lithium-mica (6%)	Euhedral to anhedral. 'Primary' (4%)	Fluorite, ore apatite, topaz (total 0.5%)
E	Equigranular lithium-mica granite	Medium-grained; hypidiomorphic, granular	Anhedral to interstitial; microperthitic (24%)	Euhedral. Unzoned (32%)	Irregular; some aggregates (30%)	Lithium-mica (9%)	Euhedral to anhedral (1%)	Fluorite, apatite (total 2%); topaz (3%)
F	Fluorite granite	Medium-grained; hypidiomorphic, granular	Sub-anhedral; microperthitic (27%)	Euhedral. Unzoned (34%)	Irregular (30%)	Muscovite (6%)	Absent	Fluorite (2%), topaz (1%), apatite (<1%)

Table 2.3. A petrographic summary of main Dartmoor granite types (Floyd *et al.*, 1993).

**Type C, Fine-grained biotite-granites:** This granite group is present is most of the exposed batholithic bosses, and differs from Type B granites in texture. Although it can be megacrystic, its alkali feldspar megacrysts range in size from 1 - 2cm in length, with a ground mass crystal size of less than 1mm. The fine-grained granites are thought to have been intruded into the earlier megacrystic biotite-granites, because they are frequently seen to cut across veins of the megacrystic granite.

There is often a large amount of variation in the alkali/plagioclase feldspar and biotite/muscovite ratios. However, the composition of type C granites is similar to Type B granites, in that there is; 30% alkali feldspar, 26% plagioclase, 33% quartz, 3% biotite, 7% muscovite 1% tourmaline and <1% others. Some of the Type C granites contain pockets and veins of tourmaline, and these rocks have little or no biotite.

## 2.4 GENERAL ASPECTS OF WEATHERING

Weathering or stone decay is the result of the interactions between four variables: Material, form, process and environment (Smith, 1996), shown below in Figure 2.4.

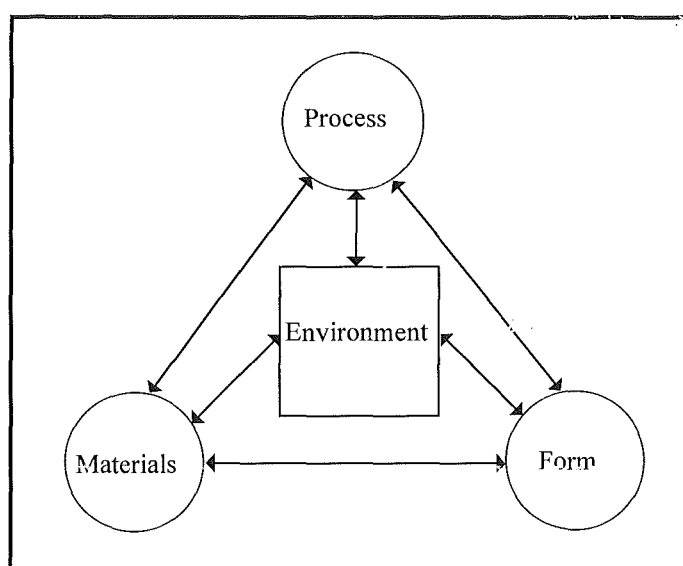


Figure 2.4. The stone decay system (Smith, 1996).



The material variable is an endogenous factor that covers a stone's properties, such as chemical, physical and mineralogical characteristics (Vicente, 1996). This can be very influential in determining the scale and type of weathering process which affect the monument, with monuments frequently showing highly diversified stone varieties, both in composition and performance (Delgado-Rodrigues, 1996).

The Form variable in Figure 2.4 refers to the surface morphology, from plaque formation; the detachment or spalling of large pieces of the stone surface, to sand disaggregation; the loss of small mineral grains. Process covers the agents of change, such as salt weathering. Processes are controlled by a combination of environmental and material properties.

Environment can be either dependant or independent of the other three variables, with the interactions changing with the scale of investigation. Although 'physical' and 'chemical' weathering processes occur and interact together, often with positive and negative feedback mechanisms (Smith, 1996), one may dominate according to specific environmental conditions. Physical weathering is usually the result of temperature change, mechanical and internal loads, while chemical weathering is mainly brought about by the action of water and other components transported in solution (hydrolysis and oxidation) (Delgado-Rodrigues, 1996). Therefore climate is an important component of the environmental conditions.

The importance of each of the individual variables is shown by weathering rate comparisons between granite, marble and sandstone. Under similar environmental conditions, and with similar sample (form) characteristics (sample height, surface roughness, surface area etc.), granite weathers considerably less than sandstone or marble. The most resistant rock in the group (the material variable), granite was exposed to the atmosphere by Sweevers and Van Grieken (1992) alongside sandstone and marble samples in micro-catchment units, with the run-off collected and analysed. The cumulative ion loss after 106 weeks of exposure is shown in table 2.4.

The extremely low level of ion exchange by granites in comparison to limestone, marble and sandstone has also been noted by Sweevers, Peeters and Van Grieken (1995), who found that the weathering of Leinster granite over 2-3 years was almost negligible.

	Blank	Mansfield sandstone	Pentelic marble	Leinster granite
Cl <sup>-</sup>	25.8	0.83	1.00	0.41
NO <sub>3</sub> <sup>-</sup>	5.59	-0.11	0.73	0.78
SO <sub>4</sub> <sup>2-</sup>	17.4	39.5	33.9	1.71
Na <sup>+</sup>	14.1	1.21	-0.60	-0.90
Ca <sup>++</sup>	13.5	40.6	87.7	1.21
Mg <sup>++</sup>	4.66	25.7	1.95	0.31

Table 2.4. Cumulative ion loss ( $\mu\text{eq cm}^{-2}$ ) in typical run-off samples after 106 weeks of exposure. Blank values are absolute concentrations, and stone values are corrected for the given blank value (Sweevers and Van Grieken, 1992).

A study by O'Brien, Bell, Orr and Cooper (1995) on the durability of limestone, marble and sandstone samples exposed at selected sites around Europe found that limestone was the least durable, followed by marble and sandstone, with loss rate for calcareous stone ranging between  $12.4 \text{ g m}^{-2}$  (Padua) to  $38.1 \text{ g m}^{-2}/\text{yr}$  (Manchester). The lower rate of stone loss for sandstone in comparison to limestone was supported by Halsey, Dews, Mitchell and Harris (1995), who found the weight loss rates for Hollington sandstone were approximately one eighth those experienced by Portland limestone in Dublin for the same duration. These values are still very high in comparison to granite, which experiences weight loss rates so small that are unreliable and difficult to interpret (Sweevers *et al*, 1995).

## 2.5 ALTERATION OF GRANITE

Stone deterioration is caused by interactions between rock minerals, pollutants, biota and the atmosphere, resulting in a reduction of the stone's strength, further weathering resistance and aesthetic value. Although there are numerous factors that directly affect a rock's material properties, shown in Figure 2.5, others act indirectly through synergistic and antagonistic reactions with other components of the deterioration system, i.e.: carbonaceous particles on stonework can result in a change in the structure of minerals around the particle through gypsum crystal initiation (Del Monte *et al*, 1984). The particles can also act as catalysts, increasing

the oxidation rate of  $\text{SO}_2$  to  $\text{H}_2\text{SO}_4$  in surface solutions (Madnawat *et al*, 1993), and therefore the amount of decay.

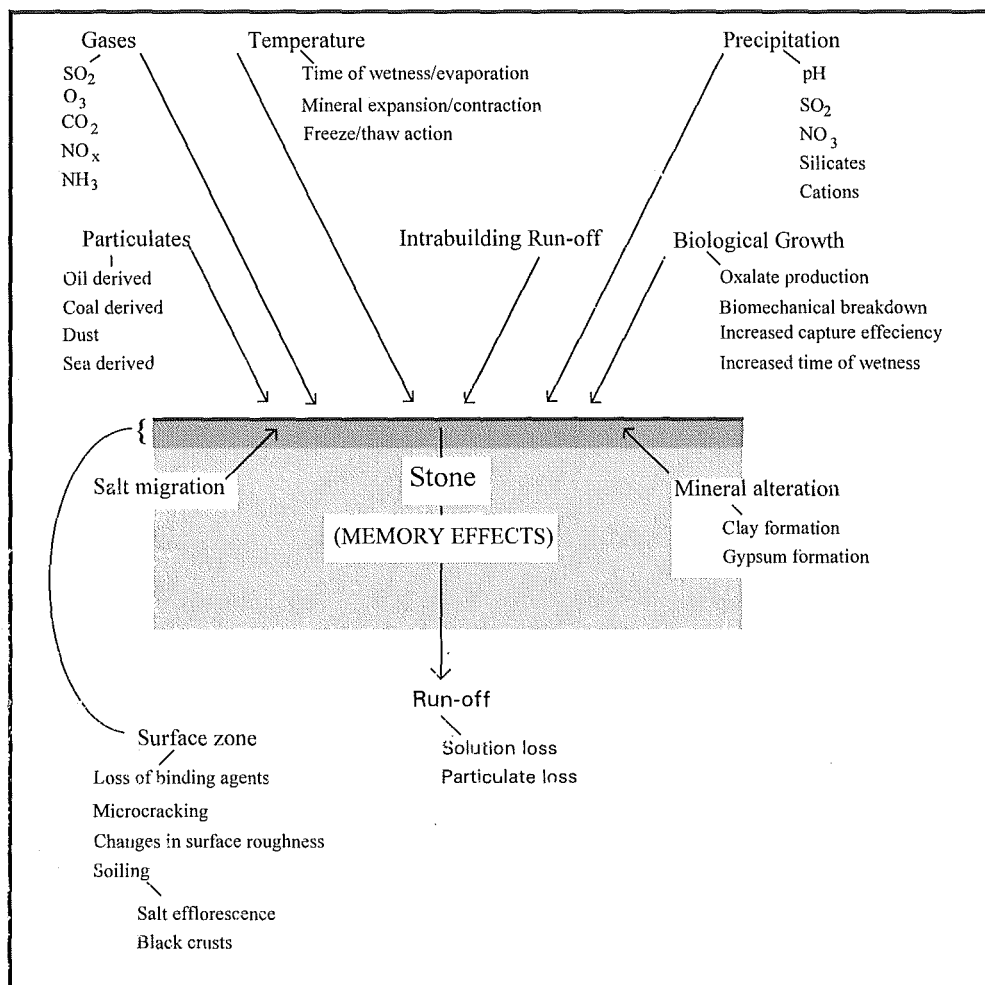


Figure 2.5. The deterioration factors that can affect stone quality (modified from Cooper, 1993).

Stone decay can also occur before the material has been even been quarried, with processes such as hydrothermal alteration and the formation of unloading (stress relief) joints. These processes will be considered first, and are followed by mechanical, chemical and biological methods of granite weathering.

## 2.6. LATE AND POST SOLIDIFICATION/CRYSTALLISATION ALTERATION

### 2.6.1. Deuteric Alteration

This is a metasomatic process, caused by the entrapment of late stage

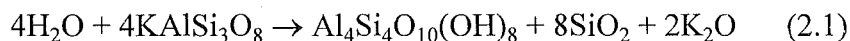
magmatic water in pre-solidification intrusive granites. Late stage metasomatic processes act on rocks below their solidus, however, and as component change occurs the solidus of the new mineral can be low enough to promote partial fusion (Barker, 1983).

The presence of water leads to the development of hydrous minerals in the established mineral fabric of the rock as chlorite replaces biotite, and plagioclase changes into a feldspar with a more albitic composition. This is usually accompanied with small amounts of epidote and zeolite minerals (Hughes, 1982).

### 2.6.2. Hydrothermal Alteration

Hydrothermal alteration is brought about by the action of hot solutions passing through post-crystallisation granite masses, usually at depth (up to hundreds of meters in tropical/sub-tropical areas of the world). The chemical and thermal imbalance causes an exchange of components across the contact zone. This process, also known as kaolinization, alters feldspars into fine, flaky aggregates of kaolinite.

H<sub>2</sub>O is the main causative agent of kaolinization, and it alters orthoclase feldspar (KAlSi<sub>3</sub>O<sub>8</sub>) to kaolinite (Al<sub>2</sub>Si<sub>2</sub>O<sub>5</sub>(OH)), shown in the following reaction.



Potassium that has been released by the reaction can combine with either CO<sub>2</sub>, forming soluble carbonates, or with other minerals to form sericite, a fine inter-crystalline muscovite mica (Hatch *et al*, 1972). Usually the silica and potassium are colloidal products, and are removed by leaching (Lumb, 1962). Extensive kaolinization, which only requires 6% of water by weight, will produce a completely rotted and very friable rock mass (Hughes, 1982).

### 2.6.3. Pneumatolysis

Pneumatolysis is another post-crystallisation alteration process. It occurs when a magmatic mass intrudes into already consolidated country rock, and volatile components from the magma pass into the country rocks along joints and fissures (Hatch *et al*, 1972). Escaping 'fugitive' constituents form a mixture of chemically

active elements in the gas and liquid phase at around 500°C, and can result in substantial physical and chemical changes to rock they pass through.

Pneumatolysis has two modes of occurrence, dependant on the composition of the residuum. The first is greisen, where greisen, an alteration product composed mostly of muscovite mica and quartz, is formed either at the margins of quartz and mineral-veins that are within 15cm of the contact surface, or in fractures within the rock mass. This produces numerous thin veins of white mica and quartz that penetrate the rock mass (Hatch *et al*, 1972).

The second mode is tourmalinization, the result of a boron-rich residuum altering both the granite and surrounding rock, and leading to the formation of tourmaline (Hughes, 1982; Deer *et al*, 1992). The presence of boron allows the formation of iron-rich tourmaline schorl at the expense of biotite. With increasing flux concentrations the tourmaline expands, gradually replacing the other granitic constituents, especially the feldspars (Hatch *et al*, 1987). This process can continue until all of the minerals, except quartz, have undergone pseudomorphic replacement.

## 2.7. SHALLOW-DEPTH AND SUB-AERIAL ALTERATIONS

Weathering affects rock throughout its whole lifetime, from influencing its formation to the breakdown of the rock into individual particles. Near-surface or sub-aerial weathering, i.e.; those processes that affect a rock mass as the overburden is removed, and the material is exposed to atmospheric processes and environmental change, can be divided into three main groups; mechanical, chemical and biological processes.

The main processes of each group will be examined for the role they can play in the deterioration of building stone. Although the decay mechanisms are examined individually, almost all weathering features are polygenetic in origin (Fookes *et al*, 1971; Smith *et al*, 1989), in that they are the result of more than one weathering process. Therefore, it is the interaction of the weathering processes that will produce rock decay, rather than any one individual mechanism.

### 2.7.1. Mechanical weathering

Physical processes result in the breakdown and disintegration of rock, leaving

chemically unchanged rock and minerals (Price, 1995). Physical weathering processes generally have the most aggressive effect on rock materials over engineering time (i.e. tens of years) (Fookes *et al*, 1988).

Casal Porto *et al* (1989) found that granite in Galicia, Spain, often shows weathering features similar to other rocks, such as sandstone and limestone. Differences in the weathering patterns were due to different crystal sizes and the varying mineralogical compositions of the granites. They also found that although plaque formation and alveolation on granite surfaces was reduced in comparison to other rock types in the same area, granular disintegration of the granites occurred at a much higher rate. They concluded that granular disintegration was the dominant weathering process in these environmental and climatic conditions.

### **Unloading/dilation Joints**

These cracks and joints are formed through a number of different processes as the rock moves towards equilibrium with the environment. The most common process is the release of energy which results in the development of fractures that lie parallel to the erosion surface (Price, 1995). These fractures can occur on both the material scale (microfractures), and the mass scale (joints) (Hencher and Martin, 1982).

There is a proportional relationship between rock strength and confining pressure. As the pressure acting on a rock is reduced, the result of overburden erosion, the amount of pressure, and therefore rock strength, decreases (Ollier, 1969). This reduces the rocks resistance to internal expansive forces created by a reduction in confining pressures, and it expands upwards (it is still confined laterally by other country rock). Expansion of the granite results in a series of joints that are formed parallel to the surface (Blyth and de Freitas, 1974), shown below in Plate 2.1, as well as the development of micro-dilation features formed by the differential expansion of constituent minerals. The micro-dilation features can lead to the development of inter-, intra-, and trans-granular microfracture networks within the stone (Smith and Magee, 1990; Delgado Rodrigues, 1996 ), which will increase the stone porosity and permeability.

Other joints in granite masses are thought to be of tectonic origin (Ollier, 1969), or the result of tensile stresses generated by confined or unequal forces of contraction within a rock mass. These forces can lead to the development of polygonal crack networks on the surface of the stones, although crack networks are not found on porphyritic granites such as the Dartmoor Type 'B' granites, perhaps because the rocks are insufficiently homogeneous (Williams and Robinson, 1989).

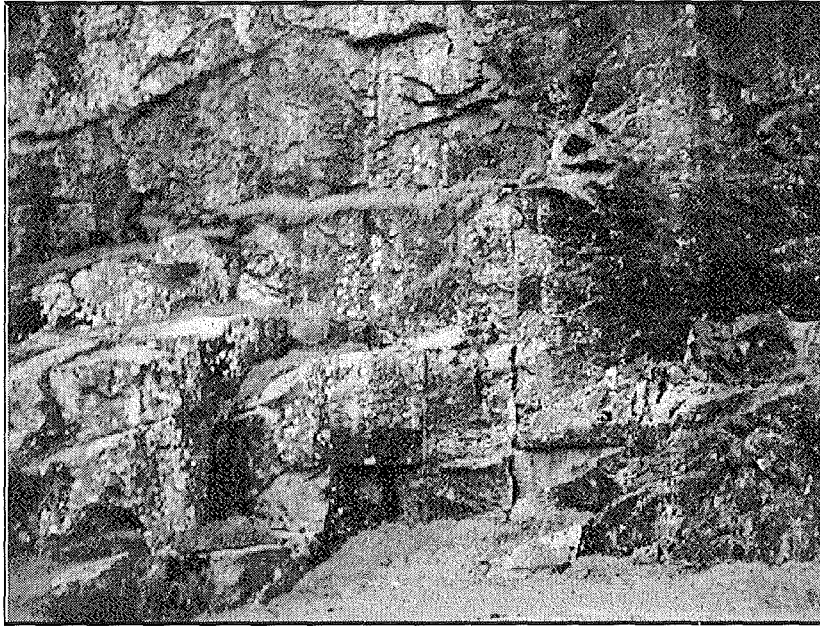


Plate 2.1. Burrator Quarry Dartmoor, with parallel dilation jointing (lower left).

### **Thermal Weathering**

Thermal weathering is caused by the mineral components of granite (quartz, feldspars and micas) possessing differing thermal expansion rates. The discrepancies between the rates produces strains in the rock, leading to microfractures and disaggregation of individual mineral crystals.

Repeated heating and cooling of rock in a diurnal cycle can often produce a surface temperature range of over 50°C, and leads to a cycle of mineral expansion and contraction, which weakens the rock and alters its physical properties. When the temperature on the outside of the rock causes the exterior to expand more rapidly than the interior, due to poor thermal conductivity, thermal gradients are formed that can alter rock performance. The expansion and contraction, caused by thermal

variations, can result in exfoliation of the stone as it adjusts to the environmental conditions. The strain energy can also lead to the initiation and expansion of microfractures and splits within the rock.

Weathered granites that contain alteration products in the fabric of the rock show less evidence of thermal weathering, due to the alteration products acting as dampers, absorbing the strains of differential thermal expansion of the minerals. This acts to lower the internal pressure in the rock, reducing the formation of decay features such as microfractures (Vincente *et al*, 1993).

The presence of water, however, dramatically accelerates the deterioration rate through the increased volumetric expansion of water over the surrounding rock. This is especially significant when water is trapped in capillaries, microfractures and pores within the rock (Selby, 1982), where freezing will cause spalling and further fracturing of the rock.

### **Frost Action**

Frost damage can be a significant process in the disintegration of building stone, where quick temperature changes around the freezing point can introduce rapid freeze-thaw cycles and damage stones in exposed areas. Water undergoes a volumetric expansion of around 9% on freezing at 0°C (Price, 1995), which can produce pressures upto a maximum of 212 N/mm<sup>2</sup> at -22 degrees. This can be particularly damaging to masonry and stones within the ground level splash water zone (Weber and Zinsmeister, 1991).

While the formation of ice crystals within rock pores has little effect when they are unconstrained by pore walls, disruption of the rock fabric can start to be initiated when 91% or more of the interior volume of the pore is filled (Weber and Zinsmeister, 1991). With the onset of low temperatures (around -5°C), rapid freezing of the surface of the water can occur, reducing expansion and acting as if the pore is a closed system (Ollier, 1969).

Even on low porosity rocks that are generally considered immune to freezing, frost action can still influence the disintegration of these rocks by prising individual grains and spalling rock plaques off the rock surface.



## Salt Weathering

Salts can be derived from a variety of sources in the environment; ground water, road de-icing salts, sea spray, unfavourable reactions between acid rain and masonry constituents and soluble particles contained in natural stone (Winkler, 1987). Salts can crystallise either on the surface as efflorescence, or within the stone as subflorescence, shown below in Figure 2.6. Efflorescence occurs when the supply of salt solutions transported from the inner core to the outer areas of stones by internal evaporation gradient exceeds the rate of evaporation, and leads to whitish crystalline salt deposits on masonry surfaces. Subflorescence occurs when the rate of evaporation is higher than the supply of salt-rich solutions, and crystallisation occurs below the stone surface, with newly formed salt crystals deposited between mineral grains and within capillaries. Warke and Smith (1994) found NaCl crystals had crystallised preferentially on pre-existing lines of weakness, such as microfractures and biotite mica cleavage planes. These salt deposits accumulate over time and can generate considerable internal pressures on the surrounding rock.

When salts have penetrated a rock mass, they can contribute to rock failure in three ways.

- 1) The growth of crystals from solution. Crystals are initiated in a rock pore or fracture, and larger crystals tend to grow at the expense of smaller crystals. The amount of pressure the crystal exerts on surrounding rock increases with crystal size, until the rock's tensile strength is exceeded and fracturing occurs (Selby, 1982).

- 2) Thermal expansion of crystals further increases pressure, with expansion rates of 1% per 54°C rise in temperature is not uncommon. This is considerably greater than granite (Cooke and Smalley, 1968). Stresses created by expansion of the crystals tend to concentrate at the inner extremity of the crack the salts are in, progressively enlarging the fissures (Selby, 1982).

- 3) Hydration of crystals, which will also produce further mineral expansion.

Some salts, such as halite, can retain considerable amounts of moisture when entrapped in stone, with the result that salt encrusted areas can remain moist for large parts of the year (Winkler, 1987). This can result in continual dissolution and precipitation around the efflorescence.

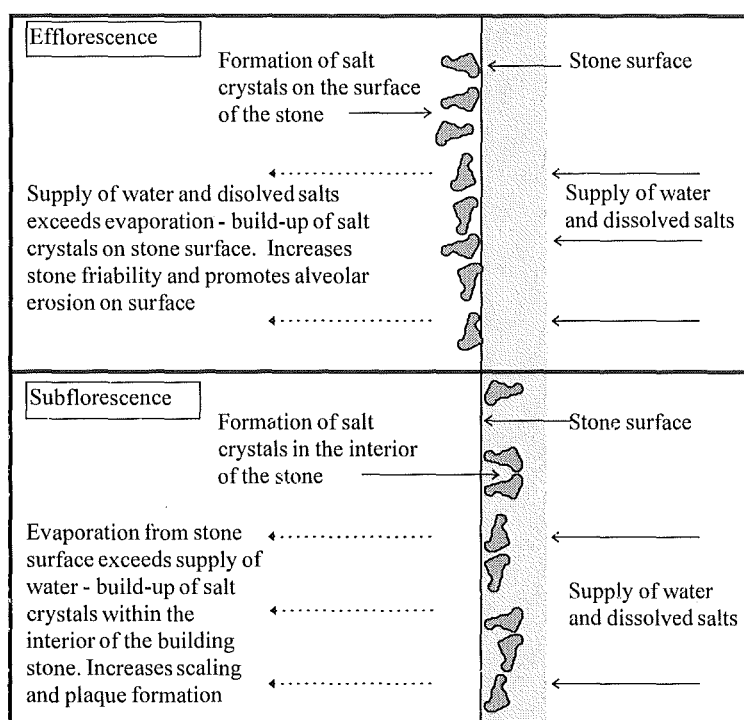


Figure 2.6. Cross-section of stone, showing salt efflorescence and subflorescence.

Crystallisation pressure is the causative agent for the majority of salt-induced weathering, and pressures for a variety of salts is shown below in Table 2.5.

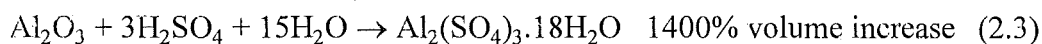
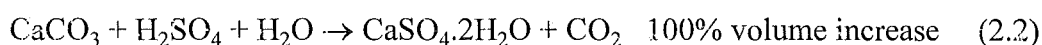
Salt	Chemical Formula	Crystallisation Pressure (atm)	
		0°C	50°C
SULPHATES			
Mirabilite	Na <sub>2</sub> SO <sub>4</sub> .10H <sub>2</sub> O	72	83
Epsomite	MgSO <sub>4</sub> .7H <sub>2</sub> O	102	125
Hexahydrite	MgSO <sub>4</sub> .6H <sub>2</sub> O	118	141
Gypsum	CaSO <sub>4</sub> .2H <sub>2</sub> O	282	334
Thenardite	MgSO <sub>4</sub>	292	345
CARBONATES			
Natron	Na <sub>2</sub> CO <sub>3</sub> .10H <sub>2</sub> O	78	92
CHLORIDES			
Bischofite	MgCl <sub>2</sub> .6H <sub>2</sub> O	119	142
Halite	NaCl	554	654

Table 2.5. Crystallisation pressures for some common salts (Winkler, 1987).

Casal Porto *et al*, (1989) suggested a three step process for disintegration of granite by soluble salts;

- 1) The slow accumulation of medium to low solubility salts, e.g. gypsum, near the stone surface reduces porosity and alters other physical properties.
- 2) The near-surface altered layer creates differences in the rocks thermal and hygrometric behaviour, leading to the production of sub-surface fissuring and plaque separation.
- 3) The final step is the continued build-up of mobile and active salts in the rock, which can result in the disaggregation of sand particles. This occurs as plaques are formed, and more intensely after they have detached. The disintegration processes that act after a plaque has fallen away usually prevents another forming in the same place.

The conversion of insoluble constituents of rock into soluble salts will result in a volume increase, and the reaction products have different molecular volumes i.e.:



Salt hydration is particularly effective in coastal areas, where salts are applied by sea spray, which then dries out. Subsequent re-wetting of the rock creates concentrated salt solutions that penetrate the rock then dry out, forming salt crystals. This cycle is repeated, with wetting and drying of the salts within the rock, producing angular rock fragments, formed by the wedging of salt crystals in microcracks.

Warke and Smith (1994), found that salt crystals preferentially exploited biotite mica in granite rocks. When the cleavage planes were orientated normal to the surface, the mineral showed extensive salt penetration and deposition, which was not found when the mineral was orientated parallel or sub-parallel to the surface.

Although normally associated with mechanical weathering processes, salts can also influence stone deterioration through chemical weathering. This is illustrated by cavernous weathering features, which have been attributed to mechanical rather than chemical processes. Studies on sandstones (Young, 1987)

and granites (Vicente, 1996) found that salts, particularly sodium chloride and sodium carbonate, increase the rate of stone deterioration by accelerating the rate of dissolution of silica through alkalinolysis under increasing pH (between 5 and 11). Young suggests that percolating salts increase the rate of granular disintegration of sandstone through the enhancement of the rate of silica solution, creating and enlarging voids in the rock fabric, rather than through crystallisation-hydration pressures.

The dissolution aspect of salt weathering is also demonstrated by rocks containing relatively insoluble minerals, which can migrate to the surface and form protective crusts. Ollier (1969) noted that manganese and iron oxides had formed a protective crust against salt weathering on granite blocks in Egypt.

### **Abrasion**

Abrasion, which is very rare in urban environments, is the effect of a mechanical force on a rock mass. It can be caused by friction and the impact of wind blown debris and water on a rock surface, which can dislodge mineral grains.

The energy of aeolian particle impact is linearly proportional to particle density, and while fine particles will be swept around a monument without impacting, coarser particles can overcome the viscosity of the wind and impact on the stone surface with great force (Camuffo, 1995).

As a result of the size of the particles needed to continue through the wind-stream viscosity around the surface of monuments, it usually particles that move by saltation (where sand grains are picked up and moved by a series of leaps though the air) that cause abrasion. This concentrates the erosion in the first metre of the monument above ground level (Camuffo, 1995).

### **Alternate Wetting and Drying**

This is an effective breakdown process for fine grained rocks. Water is attracted to a negatively charged surface of minerals by its positive hydrogen ions, and moves into the crystal lattice, producing a collapse of the crystal structure. When the crystal dries it then collapses to a smaller volume than before, ultimately leading to the disintegration of the rock (Selby, 1982).

The presence of clay and alteration minerals may also contribute to rock breakdown under alternate wet and dry conditions. Montmorillonite, for example, can expand up to 15 times its original volume on wetting, and if located in a pore or fracture, could exert considerable pressure on the surrounding rock.

Exfoliation is the usual process for the reduction of mineral expansion strain. In this process thin shells or disks of the altered material peel off from the rock mass, exposing a fresh surface, which then itself can undergo alteration into a secondary mineral (Ollier, 1969).

Casal Porto *et al* (1989) thought that granular disintegration and plaque formation on granite building stones in Galicia, Spain, were related to two factors. The amount of wetting and drying that the stone experienced, and the rate of salt build up in the rock. These two decay processes varied in intensity over the surface of the buildings, and produced differential weathering on the granite.

The formation of plaques usually occurred in areas of the building that retained moisture and stayed damp for long periods of time. The development of the plaques was mostly on fine- and medium-grained granites, being rare on coarse-grained granites.

### **2.7.2. Chemical Weathering**

Stone weathering is the result of complex interactions between material characteristics, environment and weathering processes, which can operate in conjunction, or sequentially, with other weathering mechanisms to produce weathering features (Smith *et al*, 1992). This means that although individual chemical decay processes are examined, they would invariably be acting on rock material with other physical and chemical processes.

Chemical weathering results in a change in the nature of the component minerals of a rock (Price, 1995), and contributes to the deterioration of building stones in a number of ways;

A) The formation of alteration minerals that occupy a larger volume than the original mineral. The volume changes result in pressure on the surrounding rock minerals and on the outer surface of the rock, promoting exfoliation and physical decay. The stresses generated by differential expansion of alteration minerals with

the rock matrix can also result in the development of microfracture networks within the stones (Smith and Magee, 1990).

B) The formation of solutions, which are then removed from the rock by run-off. Solution formation results in an increase in rock porosity, the result of microcrack and capillary network initiation (Baynes and Dearman, 1978). Changes in the rocks physical properties increase the rate and strength of future chemical and physical weathering processes.

C) The weathering and removal of minerals in granite, such as the feldspars and biotite mica, results in reduced mineral coherence at the surface of the stone, producing a rock that is more friable and susceptible to physical weathering.

Chemical decay processes require both water and heat to operate, and the rate of chemical action is determined by their quantities. Water acts as a carrier for the transport of aggressive chemical solutions that can be derived from the atmosphere, ground water and unfavourable reaction products from acid rain and masonry that can attack rock. These solutions can promote dissolution, leading to the formation of  $H^+$  and  $(OH)^-$  ions, which also react with rock minerals. Ambient air and rock temperature are also important in determining the rate of chemical weathering, as the rate of chemical reactions double with every  $10^\circ C$  rise. As a result, chemical reactions are several times faster in the tropics than in temperate areas, and there is a corresponding increase in the amount of chemical weathering a stone undergoes.

Rock decomposition is usually facilitated by mechanical weathering processes, which alter the condition of the rock and its minerals, rendering them more susceptible to chemical attack (Baynes and Dearman, 1978). The formation of irregularities on the surface of the rock minerals, such as microcracks and cleavage planes, can often act as an initiator for chemical attack (Dearman and Irfan, 1978; Brady, 1990).

Chemical weathering processes can result in the conversion of primary rock-forming minerals into new minerals, minerals that are often more soluble than the original components. The weathering rates can then be amplified by the dissolution and transport processes of the new minerals.

The physical resistance of the stone matrix will be reduced with the introduction of new minerals, and these can initiate the formation of voids and

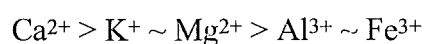
microfractures within the rock (Baynes and Dearman, 1978). These decay features create a larger surface area, and increase the porosity of a rock mass, further increasing the rate of rock weathering. There are three pathways for weathering elements to be introduced into the rock mass;

- 1) By water (rainwater, groundwater, seawater).
- 2) By aerosol (fog).
- 3) By diffusion (through gaseous particles such as SO<sub>2</sub>).

### **Solution**

Solution, along with oxidation/reduction, is one of the most important chemical decay methods for rock decomposition in engineering time (Fookes *et al*, 1988), and for siliceous rock over geological time (Saunders and Young, 1983). The rate of solution is dependant on temperature, flow velocity and pH. Hydrogen ions in solution are very mobile, and can replace cations in minerals that are in contact with the solution.

As hydrogen ions penetrate rock minerals along cleavage planes, they selectively remove ions from the crystal structure. This produces volume changes in the mineral, and results in the production of alteration minerals. There are numerous ions within a single mineral, and the order of elemental mobility for selected ions in granite is as follows (Haneef *et al*, 1993);



Ca<sup>++</sup> is the most mobile ion within granitic rocks, and it is also the ion that is involved in the most damaging decay process; gypsum formation through the sulphation of calcium. When Ca<sup>++</sup> is present within the granite rock mass as a minor constituent, it can also promote decay through dissolution and re-precipitation as calcite, increasing porosity, microfracture density and groundwater ingress (Kennan, 1973).

Despite the ion mobility order shown above, chemical discolouration of granite by iron-staining is common, as solubility is dependant on pH, with Fe<sup>3+</sup> 100, 000 times more soluble at pH 6 than pH 8.5 (Price, 1995). Fort González *et al*

(1993) found evidence for the reduction in  $\text{Fe}_2\text{O}_3$  and  $\text{SiO}_2$  quantities in rock, the result of plagioclase and biotite dissolution and decomposition.

Silica is generally insoluble at low pH, but this increases as pH rises. At pH levels of 9 or over there is a marked increase in the solubility of silica, resulting in the dissolution and migration of silica from building block interiors to the stone surface. This leads to the formation of a thin hardened crust with crumbling underneath (Winkler, 1987). Solubilization of silica on the surface of granitic rocks can be induced through interactions with deposited alkaline compounds. When the silica is reprecipitated it can form Si, Si-Al or Si-Al-Fe compounds (clays) (Schiavon, 1993).

Increasing salt concentrations can also increase the rate of silica dissolution, with increasing chloride and sulphate ion concentration increasing the rate of crystalline silica, and increasing sodium chloride and pH accelerating the rate of amorphous silica dissolution (Young, 1987).

### **Oxidation/Reduction**

Oxidation and reduction reactions involve the loss or gain of electrons from the product. Reduction occurs when electrons are gained as the result of a chemical reaction, and often occurs in waterlogged, anaerobic conditions.

Oxidation of silicate minerals is common, due to the cations that are present within the minerals crystal lattice. When these are converted into an oxidised state there is a change in the volume and net electrostatic charge of the mineral, which results in instability and susceptibility to further weathering reactions (Ollier, 1969).

### **Hydration/Hydrolysis**

Hydration occurs when dipolar water molecules are attracted to ions in the crystal lattice, resulting in the addition of water to the mineral. This is an important process in the formation of clay minerals, and can result in large volume changes as the mineral undergoes chemical change. Gypsum is a good example of hydration, with the formula  $\text{CaSO}_4 \cdot 2\text{H}_2\text{O}$ . With the addition of water to the crystal lattice there is a significant volume increase (100% on hydration), which can result in spalling and disaggregation of both limestones and granites.



At low temperatures and high relative humidities, hydration pressure developed by crystals against the pore walls can be very high, at the same order of magnitude as typical crystallisation pressures, up to  $219 \text{ N/mm}^2$  for gypsum at  $0^\circ\text{C}$  and a relative humidity of 100% (Weber and Zinsmeister, 1991). These pressures can produce microfractures and result in grain detachment.

Hydrolysis is the chemical reaction between ions in a mineral and the  $\text{H}^+$  and  $\text{OH}^-$  ions in water. The concentration of the  $\text{H}^+$  ions in a solution determines its pH, and can also contribute to the decay of a mineral. As hydrogen ion concentration increases, the solubility of  $\text{SiO}_2$  and  $\text{Al}_2\text{O}_3$  decreases, leading to the formation of clay minerals (Ollier, 1969). This is obviously important in either urban or acid rain affected areas, where the action of the rain water will lead preferentially to the formation of clay alteration minerals, rather than to the removal of the weathered primary minerals. The presence of the clay minerals either in, or on, the rock will lead to a further increased decay rate, and the products can be significant long after their creation by hydrolytic reactions.

Sequeira Braga *et al* (1993) looked at a granitic hospital in Spain, built at the turn of the nineteenth century. They found large proportions of secondary minerals in the granite, especially kaolinite and gibbsite. They felt these were present due to hydrolytic reactions occurring on the rock in the quarry. In studies of Konark Temple in India, Raymahashay and Sharma (1993) noted that the production of kaolinite and goethite from garnet in Khondalite rock increased porosity, promoting further damage to the temple.

## Rain Action

Precipitation is an effective method for transferring pollutants from the atmosphere to stone surfaces, through wet deposition processes. Although the pH of the incident rain is not the most significant factor in determining the surface moisture pH of a stone, it is influential. The principal ions present in acidified rain are the anions  $\text{SO}_4^{2-}$ ,  $\text{NO}_3^-$  and  $\text{Cl}^-$ , with  $\text{SO}_4^{2-}$  as the most significant contributor to low precipitation pH.

There are a number of parameters that influence the rate of pollutant uptake from the atmosphere, the rate of pollutant transfer to a surface and the amount of decay, both physical and chemical, that the precipitation event causes.

Drop size is important in the rate of pollutant dissolution and transfer. Large rain drops fall more quickly through the atmosphere than smaller ones, reducing the time available for gaseous oxidation and dissolution. The smaller drops have a lower velocity, increasing the time spent in the atmosphere. These differences in the residence time means that light rain has been found to have higher pollutant levels than heavy rain (Bächmann *et al*, 1995).

Rainfall intensity (precipitation volume over time) and duration are also important in determining the amount of decay that a stone experiences. Low intensity rainfall results in wetting the rock, without the subsequent surface flow of high intensity rain. Pollutant concentration within low intensity rain is also higher than high intensity rain, and the pollutant level, coupled with a lack of surface flow results in a greater amount of deterioration occurring than if there was heavy rain (Camuffo, 1995). High intensity rainfall results in surface flow on the stone, reducing the amount of time a pollutant can act on the rock before it is removed, along with any soluble reaction or alteration products.

Measurements of the chemical content of individual raindrops by Bächmann, Haag and Röder (1993) has shown that the duration of a rainfall event can have a significant influence on cation and anion concentrations. At the start of the rain event, raindrop pollution concentration increases with decreasing drop size, the result of small aerosol particle scavenging. Over time, this reaches a concentration maximum during the rain event, before concentration reduction occurs as aerosol particles are removed. This is supported by Conlan and Longhurst (1993) who reported that ion concentration in rain events measured at Manchester correlated significantly inversely with precipitation amount.

Namorado Rosa and Silva (1993), found water has a number of different processes that can lead to rock alteration or disintegration.

- 1) It has a larger thermal expansion coefficient than almost all the minerals found in granites. This can lead to the production of large internal pressures within the rocks as it expands in rock pores, especially on freezing.

2) The presence of water also results in the oscillation of the hygroscopic state of the external layers in the affected rock. This is due to changing humidity levels in the surrounding atmosphere, which produces moisture gradients within the rock, resulting in internal stresses and damage.

3) When there is water that is under pressure within a rock there are a further two paths for the alteration of the rock. A) Minerals can dissolve by pressure enhanced solubility, leading to diffusion and mass transport of the mineral solution. The presence of micas and clays offer sites for the dissolution of minerals within granites. B) Water can enlarge fractures when under pressure by purely physical methods, especially if there are cyclic loading rhythms, imposed by the atmosphere.

4) As rock starts to undergo alteration, the internal osmotic, crystallisation, hydration and thermal pressures within a rock will lead to an increased decay rate.

### **Fog And Condensation**

Fog can be important in the decay of rock. Consisting of small suspended water droplets that move in response to air currents around the stones surface, fog droplets usually have a higher sulphate content and lower pH than incident precipitation. This is due to lower deposition velocities, an increased residence time in the atmosphere (Bächmann *et al*, 1992), and a larger surface area/volume ratio (QUARG, 1993a).

As air reaches the dew point, water vapour becomes saturated at  $RH = 100\%$  and forms droplets of water. These can form in the free atmosphere, as condensation on a surface or inside internal pores (Weber and Zinsmeister, 1991). Surface water generated by fog and condensation can cause dissolution of the material matrix, the migration and precipitation of salt solutions within the stone through condensation/evaporation cycles and the increased deposition rate of airborne particles (Camuffo, 1995).

Fog deposition and condensation also results in wetting of the stone surface without the generation of run-off, and this produces a higher rate of stone decay than normal, as pollutant products are deposited in pores and microfractures found in the surface zone of the building stone. The products can then undergo hydration and

expansion, increasing the physical breakdown of the rock, without removal by surface flow.

### Mineral Alteration

Casal Porto *et al*, (1989) found that the only weathering products they could detect on granite monuments from Portugal and Galicia (NW Spain), were traces of Kaolinite and non-crystalline mixed Si-Al gels, which they viewed as alteration clays from granite weathering processes. These were found in similar quantities to those present on rocks from the original quarry, and Casal Porto *et al* felt this indicated that the majority of granite decay in the region is due to the effects of soluble salts.

Primary minerals within granites are physically and chemically changed by the alteration, addition and removal of ions from their crystal structure, through environmental processes such as solution and oxidation. The resulting alteration products depends on the original material, and the prevailing environmental conditions at the time of mineral alteration. Haneef *et al*, 1993, found that primary feldspar and biotite in Leinster granite under simulated decay conditions could produce several alteration products, as shown below in Table 2.6, depending on the original mineral and/or the prevailing environmental conditions.

Primary Minerals	Alteration Products
Feldspar (Orthoclase & microcline)	Sericite, Vermiculite, Kaolinite
Plagioclase	Biotite, Sericite (illite)
Biotite	Chlorite, Vermiculite, Kaolinite, Fe <sub>2</sub> O <sub>3</sub>

Table 2.6. The possible alteration products from primary minerals (Haneef *et al*, 1993).

Mineral alteration and clay mineral formation within the granite matrix is significant due to volume changes minerals can undergo on formation and wetting, increasing pressure on the surrounding rock grains. Biotite, for example, expands when it undergoes weathering; caused by the removal of K<sup>+</sup> ions from the crystal lattice, which promotes the splitting of biotite along cleavage planes. This increases

both the minerals surface area, and the rate of  $\text{Fe}^{2+}$  alteration by water-induced oxidation to  $\text{Fe}^{3+}$ .

$\text{Fe}^{3+}$  is removed from biotite by further water action, and redeposited on other areas of the granite. The Fe ions can then act as catalysts in the oxidation of  $\text{SO}_2$  into  $\text{SO}_3$  in the surface water layer, which leads to the formation of  $\text{H}_2\text{SO}_4$ . Clay minerals also have an increased cation exchange capacity over primary granite minerals, and can absorb  $\text{SO}_4$  ions, acting as nucleation sites for gypsum formation.

### 2.7.3. Biological Weathering

The presence of biological organisms on stone can result in weathering through a combination of mechanical and chemical processes. The growth of roots within confined spaces within the rock can result in mechanical failure of the stone, and organic acid secretions from lichens and from the roots of higher plants can produce the preferential solubilization of selected minerals, such as feldspar. Lichens that have colonised granite surfaces often use a combination of mineral dissolution and hyphae penetration to secure themselves to the rock substratum (Arino and Saiz-Jimenez, 1994).

The amount of biodeterioration a stone experiences is determined by a number of different factors (Rosual 1988). A) The dispersal of biological organisms on the rock surface, along cracks and in voids below the surface. B) The adhesive ability of organisms to stay on the surface. C) The environmental conditions affecting growth, e.g. water temperature and nutrient availability, and D) The production of mineral dissolving products by the organisms. Even with suitable conditions for growth, lithobiont numbers will be affected by temperature, pollutant concentration and substrate (Sorlini *et al*, 1982; Seaward and Giacobini, 1988).

A necessary precursor to biological growth is a nutrient medium, provided by moist masonry in shaded areas. This allows the colonisation of the stonework, in the order; Algae → fungi/Lichens → Mosses (Hawes, 1992), with later colonisers using the initial organisms as carbon sources (de la Torre *et al*, 1991). Indeed, algae and bacteria have been found growing in dissolution pits under lichens (Arino and Saiz-Jimenez, 1994).

Once established, the growth of moss, lichens and algae not only indicate high moisture levels, but the presence of the organisms generally prevents the complete drying of masonry, due to water retention by the organisms (Lal, 1985; Mulvin and Lewis, 1994). This increases the risk of frost damage and the rate of pollutant deposition from the atmosphere. This has been noted by Fobe, Sweevers, Vleugels and Van Grieken (1993) who found iron-rich patinas and gypsum crusts developing on natural sandstone under moss colonies, even in the absence of a recognised calcium source. They suggest the presence of the moss aids in the concentration and precipitation of  $\text{Ca}^{++}$  and  $\text{SO}_4^-$  from the atmosphere. This is supported by Ascaso, Vizcayno and García Gonzalez (1993) who found gypsum under lichen thalli growing on dolomitic limestone in Spain. Observations of gypsum and bacterial distributions suggested that bacterial colonies in the base of lichen thalli were scavenging sulphate ions from the atmosphere, and transforming the calcium carbonate into calcium sulphate.

Ion exchange, and the secretion of root acids by lichens and higher plants will also contribute to the decay of rock minerals - converting them into soil and clay components (Weber and Zinsmeister, 1991), and leaving a surface that is rough and pitted (Lal, 1985).

The growth of organisms on rock surfaces can result in the biodeterioration of constituent minerals, and although this was thought to only be significant over geological time, Seaward and Giacobini (1989) have found that it can also be significant over historical time (hundreds of years). There are several processes that can result in the decay of rock and its constituent minerals through the action of the colonising biological entities. The majority of the processes result either in the removal or loss of cations (usually metal cations) from the stone by solution, or incorporation into the organisms structure (McGee, 1989).

### **Ion exchange and Uptake**

Ion exchange between biological organisms and the stone substrate results in the replacement of small, negatively charged metal cations with  $\text{H}^+$  cations from the organism. Potassium, calcium, iron and phosphorous can be removed from the stone by the uptake of mineral ions by bacteria, fungi and lichens (Hawksworth and Rose,

1976). Some of the organisms that colonise rocks, especially crustose lichens like *Rhizocarpon geographicum*, accumulate the extracted minerals within their cell walls and use them as nutrients (Ascaso *et al*, 1990; Ascaso and Ollacarizqueta, 1991). Lichens are particularly efficient at the removal of cations from stone because they can initiate ion exchange along the length of their rhizomes (McGee, 1989).

Iron-rich patinas on the surface of granites are often found associated with areas of biological activity on the stone. The ion exchange activities of lithic organisms results in the solubilization and leaching of minerals from the substrate, particularly Fe, with precipitation of the minerals on the stone surface (Schiavon, 1993; Prieto Lamas *et al*, 1995).

The presence of the iron-rich patinas, which can also include K, Si and Al, increases the deposition rate for gaseous and particulate pollutants on the surface. This is due to the increased capture efficiency of the stone, caused by increases in the surface roughness and time-of-wetness. Higher pollutant concentrations on the stone surface result in the formation of additional acidic solutions, which further attack the stone, aiding the production of the iron-rich patina. Schiavon (1993) suggests that the role of iron-rich patinas in granite decay is not a passive one.

In addition to the biogenic iron-rich patinas, Fobe *et al* (1993) found gypsum crusts developing on natural sandstone outcrops. Although there was no obvious source for the Ca, they suggest that the presence of mosses aid in the concentration and precipitation of Ca and SO<sub>4</sub> ions.

### Mineral Acid Production

Bacteria, such as *Thiobacillus thiooxidans*, *Thiobacillus denitrificans*, *Thiobacillus thioparus*, *Nitrosomonas* and *Nitrobacter* can oxidise sulphur and nitrogen compounds (such as ammonia) to produce the mineral acids H<sub>2</sub>SO<sub>4</sub> and H<sub>2</sub>NO<sub>3</sub> (Sorlini *et al*, 1982; Bell *et al*, 1994). The production of mineral acids by chemolithotrophic nitrifiers has been linked to the production of NO from building stones through the oxidation of NH<sub>4</sub> by Baumgärtner *et al*, (1990), further fuelling the cycle of oxidation and acid production.

The production and action of these acids can act directly on rock substrate minerals, producing mineral volume changes, which will create and expand

microcrack networks. This increases the surface area, reducing the total time needed for dissolution to occur (McGee, 1989).

### Organic Acid Production

These acids are produced as a result of glucose dissimilation during cellular respiration, and are deposited on the outer surface of the fungal hyphae as crystals (Hawksworth and Rose, 1976). The volatile and semi-volatile organic acids, which include formic, acetic, butyric and lactic acids, can solubilize cations from granite minerals. The range of acids produced by organisms involved in biodeterioration is shown below in table 2.7.

Many micro-organisms take up iron from their substrate minerals - it is an essential trace element and is important in electron transfer reactions. The removal of iron from the minerals can result in the destruction and alteration of chlorite, vermiculite and biotite. Ascaso *et al*, (1990) found that under *Rhizocarpon geographicum* there were less feldspars than at other sites on the substrate rock. This is supported by Prieto Lamas *et al*, (1995), who found that there was less plagioclase feldspars at the surface of colonised rocks than in the interior.

Although similar in action to inorganic mineral acids, organic acids differ in that their action can be very concentrated and localised, due to the intimate contact between the stone substrate and the organism. The acids can produce increased stone solubility, salt migration and enlargement of the pores and capillaries.

Organism	Bacteria	Actinomycetes	Fungi	Algae	Lichens
<b>Organic Acid</b>	2-ketogluconic acid Lactic acid Formic acid Acetic Acid Butyric acid	Succinic acid	Oxalic acid Fumaric acid Citric acid Glycolic acid Gluconic acid Acetic acid Formic acid Succinic acid Malic acid	Humic acid Fulvic acid	Lichenic acid Fumarprotocetraric acid Squamatic acid

Table 2.7. Organic acids produced by organisms involved in biodeterioration (McGee, 1989; de la Torre *et al*, 1991).



The production of organic acids by colonising organisms can result in the chelation of the metal cations from the stone minerals. Chelation can be a significant biodeterioration process over a wide range of pH values (McGee, 1989), because organic acids can mobilise chemical elements from the minerals, and incorporate them in the cell walls of the organism. Ascaso and Ollacarizqueta (1991) have found Mn and Fe as the main component of cavity walls for lichens growing on a limestone substrate, with Si, Mg, Al and P also present in lesser proportions.

### **Physical Disruption**

The penetration of rhizines into the surface layers of the substrate stone can also promote physical destruction (rhizines are fungal hyphae bundles used by lichens for substrate attachment). Lichen hyphae have been found growing in biotite mica and feldspar crystal cleavage planes, promoting disaggregation of the minerals.

Lichens contain a large amount of water in their normal state, and can range from 100 - 300% of their dry weight when saturated. There is rapid thallus expansion upon wetting, and repeated extension and contraction of the thallus can result in the physical removal of individual mineral grains (Seaward and Giacobini, 1988; Bell *et al*, 1994). When minerals are detached by hyphae-induced disaggregation, some lichens i.e. *R. geographicum*, can grow around the mineral grains, incorporating them into the thallus (Ascaso *et al*, 1990; Prieto Lamas *et al*, 1995). This can occur on mica, quartz and feldspars.

### **Increased Time of Wetness**

Lithobionts, such as lichens and mosses, require a certain level of moisture for growth, and workers in Rome have found that their distribution is highly correlated to rainfall distribution (Caneva *et al*, 1992). This is supported by de la Torre *et al* (1991), who found extensive fungal growth on east and west facing walls, and less on north and south facing walls.

Given that the biological organisms will already favour moister areas for colonisation, the presence of lichens on stone work will further prolong the stones time of wetness - increasing the reaction times of dry deposition pollutants. The presence of lichens on the surface of building stones, and their subsequent effect on

time of wetness, can allow further biocolonisation of the stone by mosses and algae (Arino and Saiz-Jimenez, 1994).

Acting in conjunction with the increased time of wetness is the increased surface area of the wet lichen thallus, which will result in a greater rate of particulate matter entrapment. Lichens can increase wetness times by 2.5 times as long as that of uncolonized stone (Bell *et al*, 1994).

Overall, biological colonisation of building surfaces will promote the rates of decay and deterioration the stone experiences. The presence of hardy pioneer organisms will also aid in the further colonisation of the building, as nutrient and elemental (such as carbon) availability increases. Increased biological density on the stone surfaces will, in turn, increase the time of wetness and the rate of pollution capture of the stones, further increasing the decay rate.

## 2.8. STONE DECAY THRESHOLDS

Stone deterioration, which is the result of interactions between environmental, material, form and process factors, does not occur at a uniform rate over time (Smith, 1996). This is shown below in Figure 2.7, which illustrates possible decay rate changes over time: Line 1 represents no deterioration over time, while line 2 indicates a linear rate of deterioration. Line 3 shows stone quality decreasing asymptotically, and line 4 shows a steady rate of deterioration punctuated by a rapid period of decay (Turkington, 1996).

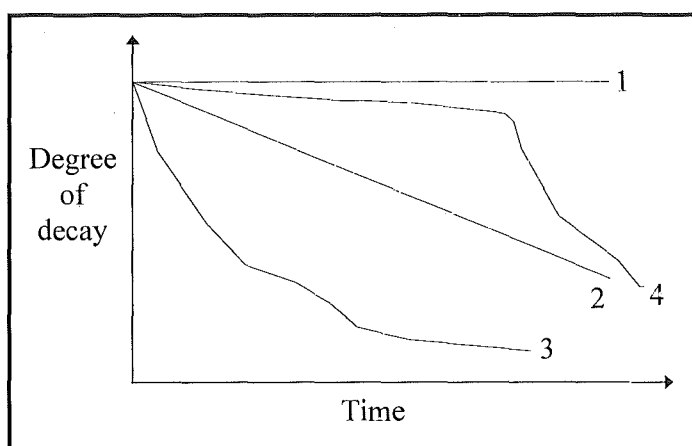


Figure 2.7. Possible patterns in stone decay rates (Turkington, 1996).

The episodic nature of stone decay has been explored by Smith, Whalley and Magee (1992), who report that weathering is not a constant process and is characterised by periods of relative quiescence interspersed with episodes of rapid change. This is typified by weathering processes such as spalling, which is discontinuous in time, and as the damage is a discrete time event it would plot as a step function of time (Livingston and Baer, 1988). Decay occurs, with mass loss from stonework shown in Figure 2.8, in a 'stepwise' or 'sporadic' fashion as stresses generated by the environment (i.e. frost action or vibration), internal stone constituents (i.e. salt precipitation or hydrating clay minerals) or human action (stone cleaning) exceed stone strength (Smith, Magee and Whalley, 1994). When stone strength is exceeded, catastrophic material loss can occur, such as scaling, spalling and plaque removal.

Helmi (1985) observed that granite in Egypt remained in a good condition for long periods of time, and then underwent rapid alteration and/or granular disintegration. Helmi suggests that the weathering of silicate rocks is exponential, very slow while the rock is fresh, but that it rapidly progresses once crystal lattice destruction has been instigated. This would follow line 4 in Figure 2.7.

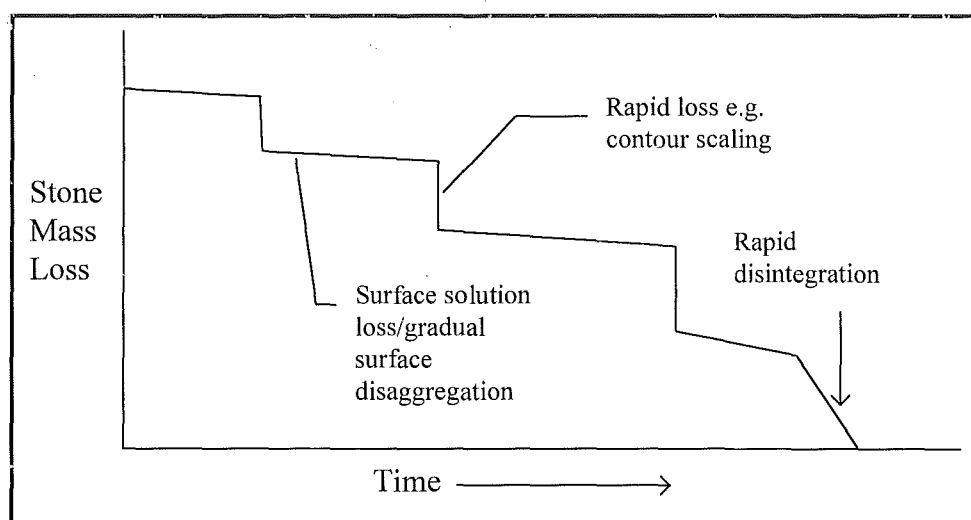


Figure 2.8. Mass loss from stonework during weathering (Smith *et al*, 1992).

Work by Selby (1982) on the 'dynamic equilibrium' of hillslopes led him to a similar model of threshold events and form adjustment, where exceeding the threshold stress initiates a step-wise, rapid change in the landform, followed by a period of relative stability and adjustment where there is virtually no change in the landform.

## CHAPTER 3. Air Pollution in the UK

### 3.1. INTRODUCTION

Air pollution has been a recurring problem in urban areas throughout the world since before the industrial revolution. After the age of mechanisation, however, the problems generated by increasing air pollution rose dramatically, and the deleterious effects they have on buildings similarly increased. Brimblecombe (1977) plotted  $\text{SO}_2$  levels (derived from coal imports to the London area) against time, and found they increased from 1600 to 1880, reaching a mean annual maximum of  $\sim 180 \mu\text{g m}^{-3}$ . The levels of estimated  $\text{SO}_2$  then decreased as a result of the growth in London's urban area and a reduction in the S content of imported coal.

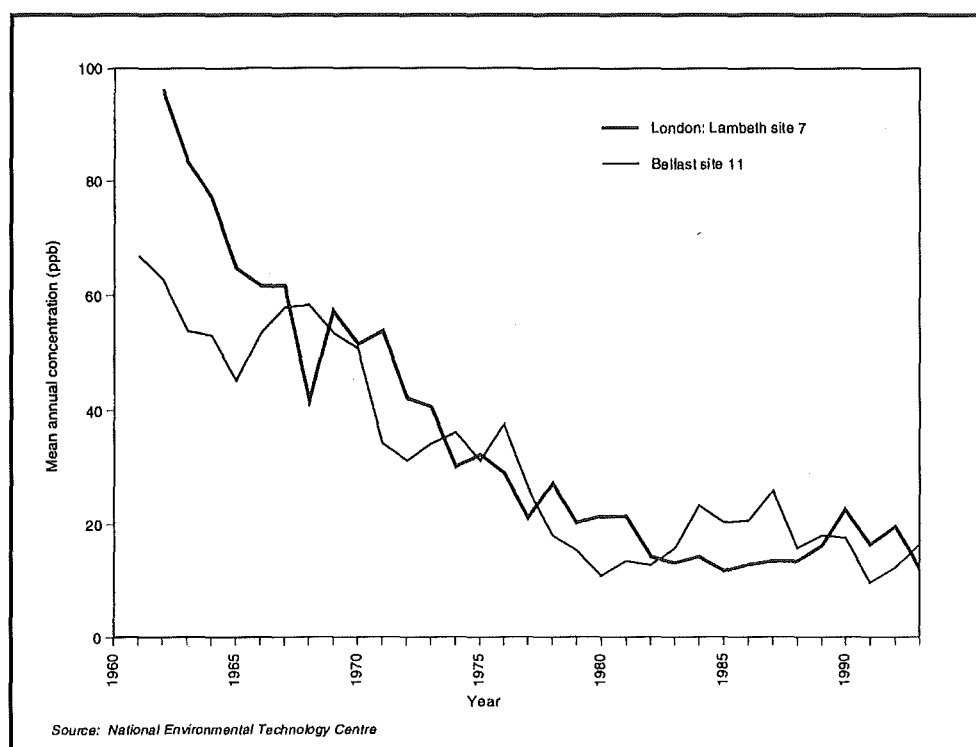


Figure 3.1.  $\text{SO}_2$  levels in Belfast and London over time (DOE, 1995b)

In response to the high levels of air pollution in urban centres, clean air laws and stricter emission controls were introduced in the fifties and sixties, and these also improved the quality of London's air (Brimblecombe, 1977), shown in Figure 3.1. Despite decreases in pollutant concentration, building stone decay rates have failed to

decline in line with pollutant reductions, especially in SO<sub>2</sub> concentrations (Bawden and Ferguson, 1987). This may partially be due to a 'memory effect' of the stone, which has been physically altered by exposure to high historic pollution levels. It could also be explained by the rise of other urban pollutants, such as NO<sub>x</sub> (which has doubled in concentration since the 1950's (BERG, 1989), although is now decreasing due to the introduction of catalytic converters, shown in Figure 3.2 on page 45) and hydrocarbons.

There are a multitude of effects anthropogenically generated pollutants can have on building stones, and below is a review of their effects, and the mechanisms by which they are transported to the surface.

### 3.2. GASEOUS POLLUTANTS

Gaseous pollutants, in urban areas, are generally the products of the internal combustion engine, although emissions from power stations can be significant on a national scale. This is shown by their contribution to SO<sub>2</sub> levels; although SO<sub>2</sub> emissions have decreased by 28% between 1992 - 94, power stations still contribute 65% of the total SO<sub>2</sub> emissions (DOE, 1996).

The concentrations of gaseous pollutants produced by combustion increase with increasing population density and automobile usage, as can be seen in the exposure period means of selected pollutants at the urban and rural measuring sites, shown in Table 3.1. While NO<sub>x</sub> and SO<sub>2</sub> are higher in urban areas (with power station emissions increasing in areas of high population), O<sub>3</sub> is predominantly a rural pollutant. The increasing importance of vehicle emissions to atmospheric quality is shown by the growth of UK transport emissions in Table 3.2.

	London		Birmingham		Dartmoor	
	8/94 - 4/95	5/95 - 4/96	8/94 - 4/95	5/95 - 4/96	9/94 - 4/95	5/95 - 4/96
SO <sub>2</sub> (ppb)	9.32	9.66	8.28	7.46	2.19	1.81
NO <sub>x</sub> (ppb)	76.63	83.49	47.97	50.67	8.8 - 12.7*	
PM <sub>10</sub> (µg m <sup>-3</sup> )	26.32	31.96	22.59	26.59	3.00 - 6.00**	

Table 3.1. Table showing mean pollution concentrations in rural and urban exposure sites. \* Background NO<sub>2</sub>. Values from Newton Abbot, 1994 NO<sub>x</sub> diffusion tube survey, AEA technology. \*\* Secondary particulate matter, estimated by HARM model (QUARG, 1996).

Pollutant	% Increase
Carbon Monoxide	46
Nitrogen Oxides	72
Volatile Organic Compounds	12
Black Smoke	75
Sulphur Dioxide	50
Carbon Dioxide	43

Table 3.2. Increases in estimated UK transport emissions, 1980-1990 (DOE, 1991).

As well as illustrating the growth in car numbers on the road network ( $\text{NO}_x$ ), the table also reflects the increase in diesel vehicles (black smoke) and the impact of catalytic converters ( $\text{CO}_2$ ).

### 3.2.1. Oxides of Carbon

There are two species of oxides of carbon; carbon dioxide and carbon monoxide. Only  $\text{CO}_2$ , however, has a significant influence on the rate of building decay. Both carbon dioxide and carbon monoxide are the product of combustion and organic respiration, and their concentrations in the urban atmosphere increased in-line with vehicle usage (see Table 3.3). This is shown by growth in CO total emissions, which increased 45% between 1970 and 1989 as a result of the doubling of emissions from road transport (DOE, 1995a). Since 1989, however, this has decreased from an end user emission level of 5,786 thousand tonnes to 4,346 thousand tonnes in 1994, a result of the introduction of catalytic converters (DOE, 1996), which convert CO to  $\text{CO}_2$ .

The main role of  $\text{CO}_2$  in stone deterioration is the acidification of rain water as it falls through the atmosphere. This produces precipitation with a theoretical pH of 5.6 when the amount of dissolved  $\text{CO}_2$  in raindrops reaches saturation, although precipitation has been found with a wide range of pH levels without containing anthropogenic pollutants (Butlin, 1991). Carbon monoxide, however, has little impact on stone decay rates, and is usually associated with health implications.

### 3.2.2. Nitrogen Oxides

Nitrogen is the most abundant gas in the atmosphere (78.09%), and is usually

an unreactive gas. It will, however, undergo chemical reaction under conditions of increased pressure or temperature, as found in combustion. This results in vehicles contributing up to 90% of  $\text{NO}_x$  concentrations in urban areas (QUARG, 1993a).

End User	1970	1980	1985	1987	1989	1991	1993	1994
Domestic	427	422	371	378	336	317	281	259
Commercial/ public service	97	117	110	106	94	96	73	70
Industry	734	569	475	507	487	437	383	368
Agriculture	25	22	20	19	17	15	13	12
Road transport	647	882	1060	1238	1419	1378	1231	1169
Other transport	238	193	187	171	192	198	191	187
Miscellaneous	126	153	159	171	170	147	125	114
Exports	7	14	12	17	18	22	30	28
other emissions	23	24	25	25	21	21	10	9
<b>Total</b>	<b>2324</b>	<b>2396</b>	<b>2419</b>	<b>2632</b>	<b>2754</b>	<b>2631</b>	<b>2337</b>	<b>2216</b>

Table 3.3. Estimated emissions of  $\text{NO}_x$  by end users: 1970 - 1994 (in thousands of tonnes) (DOE, 1996).

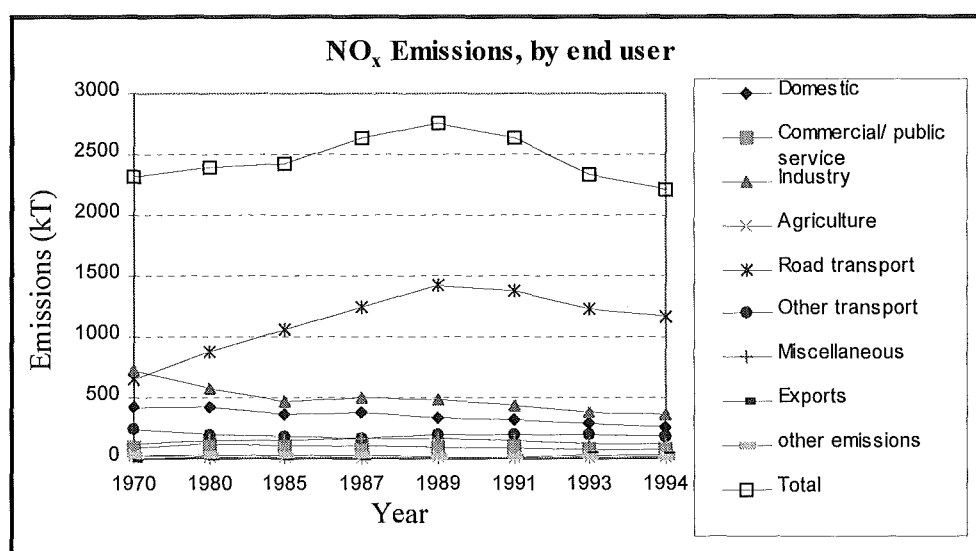


Figure 3.2. Changes in  $\text{NO}_x$  end user emissions between 1970 and 1994 (derived from DOE, 1996)

There are three main oxides of nitrogen; nitrous oxide,  $\text{N}_2\text{O}$ , nitric oxide,  $\text{NO}$  and nitrogen dioxide  $\text{NO}_2$ , and as their relative concentrations vary throughout the



diurnal cycle, the sum concentrations of NO and NO<sub>2</sub> are usually reported as oxides of nitrogen or NO<sub>x</sub> (Livingston, 1985). Although the emission rates for end users have been decreasing, shown below in Table 3.3 and Figure 3.2, transport emissions rose dramatically until 1989, when they started to decrease as a result of the introduction of catalytic converters.

Nitric oxide (NO) is produced by combustion processes, the action of soil bacteria and by lightning. The formation of NO<sub>x</sub> by combustion is the most common method in urban areas, where NO is oxidised to form nitrogen dioxide (NO<sub>2</sub>) (Amoroso and Fassina, 1983). This formation process is highlighted by Figure 3.3, which shows that average NO<sub>2</sub> concentrations between 1987-90 are highest around urban centres.

NO<sub>2</sub> can also be formed from NO by reaction with atmospheric oxidants, such as ozone. This is a rapid process, which also involves OH radicals, and occurs mainly in photochemical smogs. It can result in the oxidation of almost all of the atmospheric NO to NO<sub>2</sub>. Further oxidation and hydration of NO<sub>2</sub> on the surface of particulates and water droplets can lead to the formation of NHO<sub>3</sub> (Kirkitsos and Sikiotis, 1995).

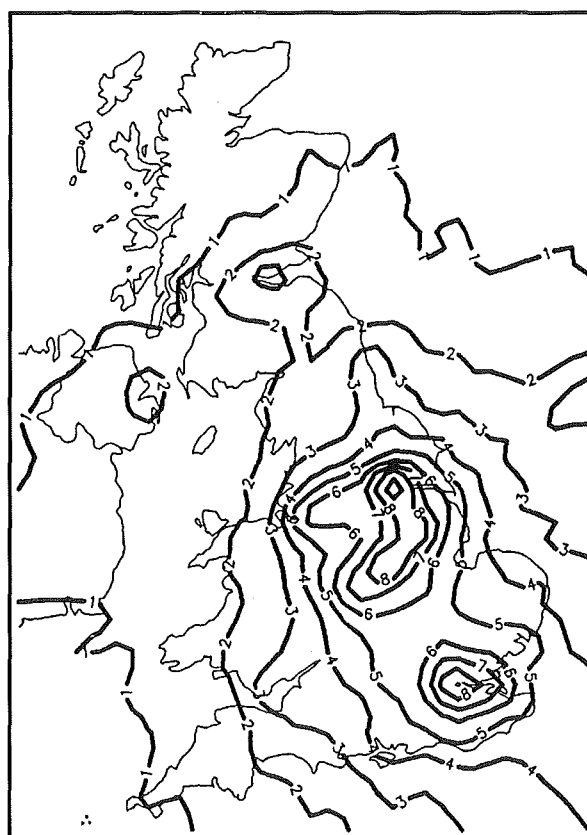


Figure 3.3. NO<sub>2</sub> distribution in the UK during 87-90 (Atkins and Lee, 1995).

This process is very dependant on OH radical concentration in the atmosphere, and the reaction rate drops off during the night when OH concentration drops markedly (Harrison, 1992). Atkins and Lee (1995) report that increased concentrations of  $\text{NO}_2$  during winter months are due to reductions in photochemical and dispersive activity. The reaction paths for  $\text{NO}_x$  are shown below in Figure 3.4.

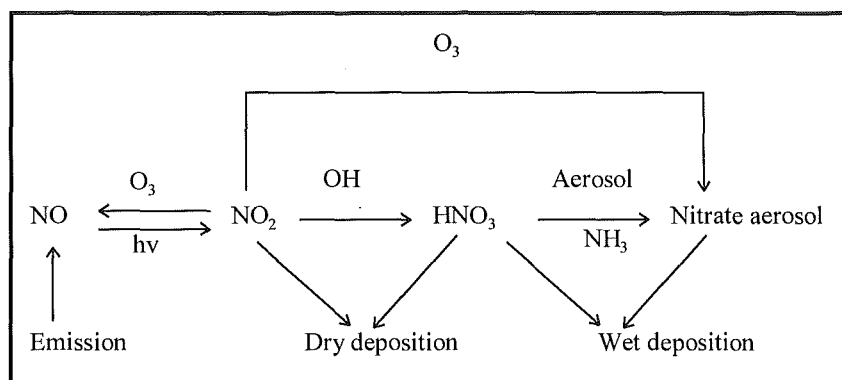


Figure 3.4. The atmospheric  $\text{NO}_x$  cycle (Metcalf *et al*, 1989).

The rate of  $\text{NO}_x$  oxidation is increased by the emission of NO and occasionally  $\text{N}_2\text{O}$  from building stones. This has been found by Baumgärtner *et al* (1990), who report that building stones (sandstones and concrete) can release NO in significant quantities for a prolonged period of time, at a rate proportional to the quantity of examined stone material, shown in Figure 3.5. They suggest that as building stone surfaces can be a source for atmospheric NO, rather than a sink, without showing increased deterioration,  $\text{NO}_x$  corrosion is due to the effects of  $\text{NO}_2$ .

The role of  $\text{NO}_x$  in stone deterioration is not fully understood at the moment, but it is thought that it has a more important function in the formation of atmospheric nitrates than in the formation of  $\text{HNO}_3$ . Although  $\text{NO}_x$  can undergo chemical changes to form  $\text{HNO}_3$ , it does so at approximately 10% per hour and so usually occurs downwind of the urban source (QUARG, 1993a).

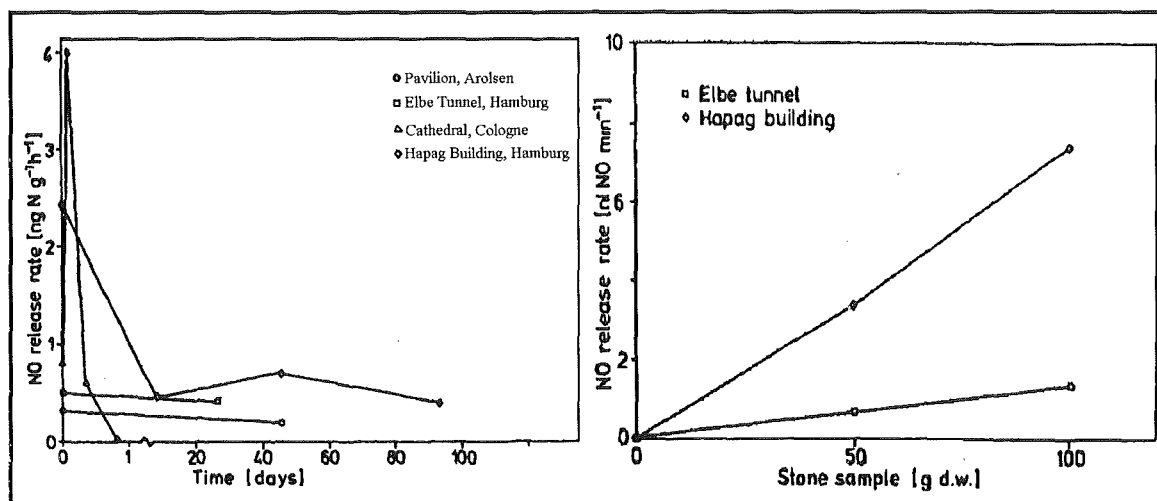


Figure 3.5. NO release rates as a function of time and stone mass (Baumgärtner *et al*, 1990).

Livingston (1985) concludes that although there is the formation of highly soluble nitrate deposits on stone surfaces, usually detected by water extraction of the soluble salts followed by wet chemical analysis or by non-quantitative XRD analysis, these are minor in comparison to sulphate products. The insignificance of deposited nitrates in stone decay is supported by Fobe *et al* (1993), who analysed anion leachates and petrographical thin sections from ferruginous sandstones in Belgium.

Livingston (1985) suggests that building surface nitrate concentrations are not purely a function of gaseous NO<sub>x</sub> concentrations, and that they are strongly influenced by the action of biological organisms on the stone surface. Micro-organisms and lithobionts, such as the lichens *Nitrosomonas* and *Nitrobacter*, can fix naturally occurring nitrogen and aid in the formation of nitrates and damaging acids on stone surfaces through the oxidation of ammonia, which can lead to the formation of HNO<sub>3</sub> (Bell *et al*, 1994). This will allow the colonisation of the substrate by further biological species, such as lichens and mosses.

Unlike sulphur oxides, the impact of NO<sub>x</sub> has little inhibitory effects on lichen growth (Hanksworth and Rose, 1976), and deposition of soluble nitrates, and the more insoluble sulphates, on stone surfaces by colonising bacterial species could aid the establishment of further biological species (Sorlini, Allievi, Sacchi and Ferrari, 1982).

### 3.2.3. Sulphur Oxides

Sulphur is present in the atmosphere in three main compounds: Sulphur dioxide ( $\text{SO}_2$ ), sulphur trioxide ( $\text{SO}_3$ ) and hydrogen sulphide ( $\text{H}_2\text{S}$ ) (Amoroso and Fassina, 1983). Although concentrations of  $\text{SO}_2$  have been declining, with industry reducing its emissions by 59% between 1970 - 1985, the contribution from road transport is increasing, from 3.1% in 1989 to 4.8% in 1994, shown in Table 3.4 and Figure 3.6. This is the result of an increasing percentage of diesel vehicles in the national fleet, and results in  $\text{SO}_2$  still being one of the most important gaseous pollutants in determining the rates of building stone deterioration.

End User	1970	1980	1985	1987	1989	1991	1993	1994
Domestic	1891	1459	1224	1217	1052	1021	865	719
Commercial/ public service	416	418	313	302	271	284	248	215
Industry	3175	2106	1401	1559	1563	1462	1305	1108
Agriculture	101	78	55	55	47	45	40	35
Road transport	101	129	90	95	115	113	131	130
Other transport	223	142	100	98	103	118	134	121
Miscellaneous	444	488	497	530	527	477	413	347
Exports	34	45	18	19	22	24	34	29
other emissions	43	38	30	26	26	21	16	15
<b>Total</b>	<b>6428</b>	<b>4903</b>	<b>3728</b>	<b>3901</b>	<b>3726</b>	<b>3565</b>	<b>3186</b>	<b>2719</b>

Table 3.4. Estimated emissions of  $\text{SO}_2$  by end users: 1970 - 1994 (in thousands of tonnes) (DOE, 1996)

Sulphur oxides are present in the atmosphere as a result of both natural events such as volcanoes, and anthropogenic activity such as power generation. The majority of  $\text{SO}_2$  concentrations in the UK is through the formation of sulphur oxides as a result of fossil fuels combustion, which all contain varying amounts of sulphur (QUARG, 1993a). When these are burnt, sulphur reacts with oxygen at a temperature determined rate to form  $\text{SO}_2$ . The oxidation rate of  $\text{SO}_2$  can be assisted by ozone and other atmospheric oxidants, i.e. hydrogen peroxide, and catalysts such as soot and smoke (Haneef *et al*, 1992; Amoroso and Fassina, 1983). The reaction paths for sulphur oxides is shown below in Figure 3.7.

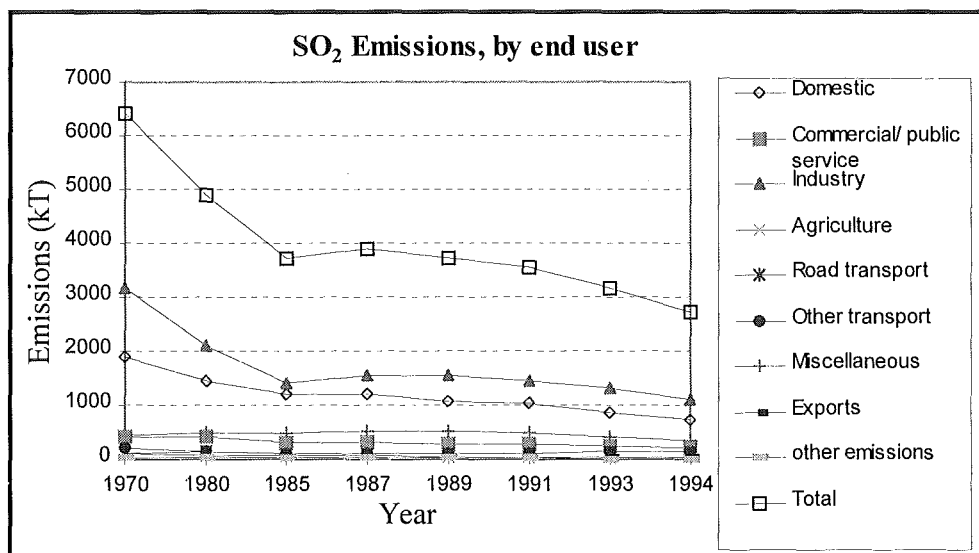


Figure 3.6. Changes in SO<sub>2</sub> emissions by end users between 1970 - 1994 (derived from DOE, 1996)

Although ozone assists in the oxidation of SO<sub>2</sub>, it does not significantly increase the rate of gaseous phase oxidation. When the oxidation is occurring in the surface moisture layer, however, the presence of ozone and metal catalysts can significantly increase the oxidation rate (Haneef *et al*, 1992).

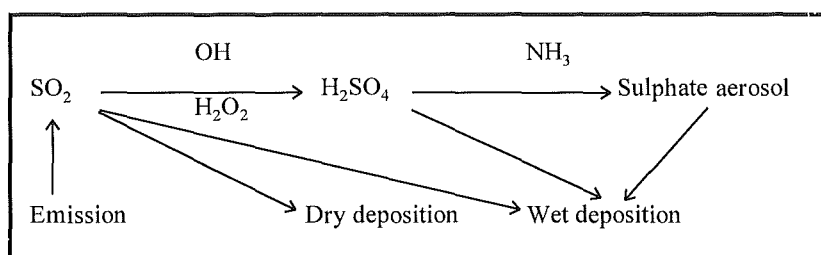


Figure 3.7. The atmospheric SO<sub>x</sub> cycle (Metcalf *et al*, 1989).

### 3.2.4. Ozone

A secondary pollutant, ozone is produced in two distinct regions of the atmosphere; in the upper atmosphere by the action of ultraviolet radiation on oxygen, and at ground level in urban environments by the action of sunlight on hydrocarbon 'smogs'.

A strong oxidant, ozone tends to be found at higher concentrations in rural areas ( $40 - 60 \mu\text{g m}^{-3}$ ) than urban areas ( $20 - 40 \mu\text{g m}^{-3}$ ) as urban concentrations are reduced by primary emissions of NO (BERG, 1989). With a UK mean of  $\sim 30$  ppb, concentrations are two to three times that of suggested pre-industrial levels of 10 -15 ppb of  $\text{O}_3$  near ground level (DOE, 1995a).

Ozone is also involved in the oxidation of  $\text{SO}_2$ , leading to the formation of sulphates and sulphuric acid, shown below in Figure 3.8 (QUARG, 1993a).

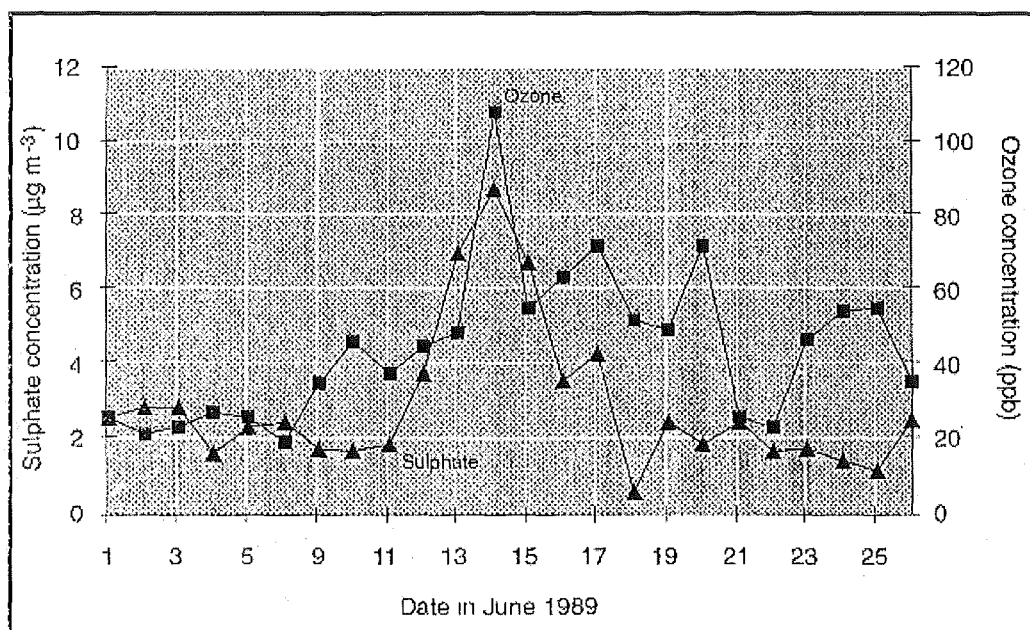


Figure 3.8. Mean daily  $\text{O}_3$  and  $\text{SO}_4$  aerosol concentrations in London (QUARG, 1993a). ■ = ozone concentrations, ▲ = sulphate concentrations.

### 3.2.5. Ammonia

Ammonia is the major neutralising gas in the atmosphere, with cattle waste as the largest source of ammonia in rural NW England, and humans as the second largest source (becoming the largest in urban environments) (Conlan and Longhurst, 1993).

Although it does not directly attack stone, ammonia is involved in the production of sulphuric acid, and the formation of ammonium salts. These are highly soluble salts that are carried in solution to the inside of stones, where they precipitate and contribute to stone decay through volumetric change.

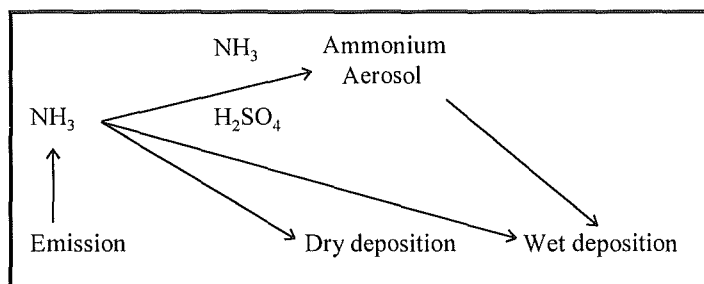


Figure 3.9. The cycle of  $\text{NH}_3$  compounds in the atmosphere (Metcalf *et al.*, 1989).

Ammonium can aid the formation of sulphuric acid by increasing the pH of water, which increases  $\text{SO}_2$  solubility. The rise in pH also increases the effects of catalysts on the oxidation of  $\text{SO}_2$  in solution, further increasing the rate of  $\text{H}_2\text{SO}_4$  production (Amoroso and Fassina, 1983). Both  $\text{H}_2\text{SO}_4$  and  $\text{HNO}_3$  can react with  $\text{NH}_3$  to produce ammonium salts, with Conlan and Longhurst (1993) measuring greater concentrations of  $\text{NH}_4^+$  and  $\text{SO}_4^{2-}$  in atmospheric precipitation in areas of high  $\text{NH}_3$  emissions.

### 3.3. PARTICULATES

Airborne particles have two sources of origin, primary and secondary. Primary particles are emitted from discrete sources such as motor vehicles, power stations and industrial sources, while secondary particles are formed in the atmosphere as a result of chemical reactions and condensation (QUARG, 1993a).

The main influence on particle behaviour in the atmosphere is the size or aerodynamic diameter of the particle. There are three modes of particle size; nucleation ( $< 0.2\mu\text{m}$  diameter), accumulation ( $0.2\text{--}2.0\mu\text{m}$  diameter) and coarse ( $> 2.0\mu\text{m}$  diameter) mode (QUARG, 1993). The composition of an urban particulate sample taken from Leeds in 1982 -1983 is shown in Table 3.5.

Secondary particulates (ammonium, nitrate and sulphate) are usually formed through the oxidation of  $\text{SO}_x$  and  $\text{NO}_x$  emitted by combustion sources (QUARG, 1996). These particles, along with carbonaceous particles, usually belong to the accumulation mode size fraction, which has the longest period of atmospheric residence (with a life-span of 7 - 10 days (QUARG, 1993b)). This means that the particles are not solely an urban phenomenon, but can be carried across a region.

QUARG (1996) reports that much or all of the summertime  $PM_{10}$  can be accounted for by the regional scale transport of photochemically oxidised sulphur compounds.

Component	Major Sources	% Total Mass of Particles
$NH_4^+$	Natural $NH_3$ emissions	6.8
$NO_3^-$	$NO_x$ emissions	4.2
$SO_4^{2-}$	$SO_2$ emissions	18
$Cl^-$	Sea salt, HCl from coal burning	5.5
$Na^+$ , $K^+$ , $Mg^{2+}$ , $Ca^{2+}$	Sea salt, dust	5
Carbonaceous material	Smoke emissions	39
Insoluble material	Wind-blown dust	21.5

Table 3.5. Composition of particles gathered from Leeds in 1982 - 83 (QUARG, 1993a).

### 3.3.1. Nitrate and Sulphate Aerosols

Aerosols are mixtures of air and small suspended particles that can be either solid or liquid. The majority of aerosols contain a mixture of both solid and liquid particles i.e. sea spray will contain solid salt crystals and water droplets.

There are a number of mechanisms that can result in the oxidation of  $SO_2$  to sulphate aerosols, and these can include homogeneous (direct and indirect photochemical reactions) and heterogeneous (catalytic or chemisorption) phase reactions (Cheng, 1983). The primary route, however, is the reaction of  $SO_2$  with OH radicals, which leads to the formation of  $H_2SO_4$  - one of the major components of secondary urban particulate material (QUARG, 1993a; QUARG, 1996). However, despite the contribution of sulphates to particulate levels, Hamilton *et al* (1995) report that the majority of sulphur dry deposition that occurred at three measured sites in the UK was due to deposition of gaseous sulphur, rather than particulate sulphur.

$NO_3^-$ , which is usually highly correlated with sulphate levels, has been increasing in concentration since the mid 1950's, without the recent decrease displayed by particulate sulphate (QUARG, 1996). Nitrate has also been reported to be increasing in concentration in the US, and Galloway and Likens (1981) ascribe the increases to three potential sources: increases in fossil fuel combustion; fertiliser application;  $NO_3^-$  production by lightning. Analyses of precipitation showed that while



the contribution to nitrate levels from lightning and fertiliser was negligible, increases were primarily due to fossil fuel combustion.

### 3.3.2. Chloride

Chloride levels in the atmosphere are usually a function of proximity to the coast-line. A primary particle, usually derived either from sea spray or road de-icing salts, where it is deposited as sodium chloride, chloride can also form from gaseous HCl (derived from pollution) and be deposited as ammonium chloride (QUARG, 1993a; QUARG, 1996). Its role in stone decay is usually small, however, and Fobe *et al* (1993) concluded that deposited chloride was insignificant in stone decay on ferruginous sandstones in Belgium.

### 3.3.3. Carbonaceous Particles

Carbonaceous particles, generated by diesel vehicles and power stations, are significant in stone decay, due to their abundance and distribution in urban environments, and their physical effects on stone. The carbonaceous particles affect the stone in a number of ways: 1) They are contributory sources of metals to the stone, with S, V and Fe concentration inversely proportional to particle size (Cheng, 1983). 2) They act as catalysts in the oxidation of SO<sub>2</sub> to SO<sub>3</sub> and H<sub>2</sub>SO<sub>4</sub>, and NO<sub>x</sub> to NO<sub>2</sub> and HNO<sub>3</sub>. 3) They can lead to the formation of black crusts on the surface of building stone, reducing a stone's resistance to weathering processes by changing the physical properties of the stone. The presence of crustal coverage will also cause a reduction in the buildings aesthetic value.

Carbonaceous particles, when present on a stone surface, can absorb sulphate from the atmosphere at a faster rate than surrounding stone (Hutchinson *et al*, 1992). The presence of a sulphate source on the stone can have implications for acidic solution generation and gypsum formation. Deposited particles will also increase the apparent surface roughness of the stone, which can lead to a higher rate of deposition, and a further increase in the capture efficiency of the stone.

There are three main types of carbon particulate source; oil-fired power plants, coal-fired power plants and vehicles. The source of origin affects the physical and chemical properties of the particles, and influences their role in stone decay.

### 3.3.3.1. Oil Derived Carbonaceous Particles

Oil-derived particles are spongy spheres with numerous pores on their surfaces that can contain a wide range of trace elements and pollutants. Particle analysis by Del Monte *et al* (1984) showed that these particles had a lower pH than coal-derived particles. This affected the stone decay rates measured around the particle deposition site.

The chemical composition of oil-derived particulates is complex, and particles can act as sources for the following elements: S, V, Al, Si, Na, Mg, K, Ca, Fe, Cu and Ni (Cheng, 1983; Del Monte *et al*, 1984; Sabbioni, 1995), shown in Table 3.6. The presence of both sulphur and calcium ions in oil-derived particles often results in the formation of gypsum crystals, utilising the particles as both source of calcium and sulphur and crystallisation nucleus (Del Monte *et al*, 1984).

### 3.3.3.2. Coal Derived Carbonaceous Particles

Coal-derived particles are smooth glassy spheres with few surface features, and they generally have a higher sulphur concentration than oil-derived particulates (2.9% for coal-derived particles against 1.9% for oil) (Cheng, 1983). Coal-derived particulates can also act as sources of Fe, Al, Si and S (Sabbioni, 1995), as seen in Table 3.6.

Description	Oil-derived	Coal-derived
Size distribution		
Less than 3 $\mu\text{m}$ , % by wt.	77.5	35.0
Mass median diameter, $\mu\text{m}$	0.38	4.9
Trace elements		
Major	V, Fe, Si, S, Ca	Fe, Ti, Si, S, K, Ca
Minor	Mg, Al, P, Ti, Cr, Mn, Ni	Al, P, Cl, Mn, Cu
Density		
Bulk density, $\text{g/cm}^3$	0.33	0.93
Pressed density, $\text{g/cm}^3$	1.37	2.35
Sulphate (soluble), % wt.	16.94	4.04
Nitrates (soluble), % wt.	<0.01	Not detectable
Chlorides (soluble), % wt.	0.18	0.01
pH	2.7	3.75
Acidity, mg as $\text{CaCO}_3/\text{g}$ of ash	38.3	3.6

Table 3.6. The physiochemical properties of carbonaceous particles (Cheng, 1983).

Coal-derived particles are denser than oil derived particles, and can contain higher concentrations of iron than oil particles, with an average of 73,000  $\mu\text{g/g}$  (Cheng, 1983). Iron and titanium trace elements in coal-derived particulates act as catalysts when they leach from particles, resulting in an increase in the oxidation rate of  $\text{SO}_2$  to  $\text{H}_2\text{SO}_4$  in surface moisture layers on stonework. Madnawat *et al* (1993) have found that leached trace elements (especially Fe, Cu and Mn) from the fly-ash interior are the main cause of catalytic oxidation, rather from those found on the surface of the particles.

### 3.3.3.3. Vehicle Derived Particulates.

Road transport, especially diesel engine vehicles, are thought to be the major source of  $\text{PM}_{10}$  (particulate matter with an aerodynamic diameter of less than 10  $\mu\text{m}$ ) in urban areas (QUARG, 1996). Diesel derived particulates are composed mainly of a high temperature origin carbon nucleus, coated with condensed organic and inorganic compounds, such as hydrocarbons and sulphate (QUARG, 1993b; QUARG, 1996). The composition of typical diesel particulates is shown in Figure 3.10.

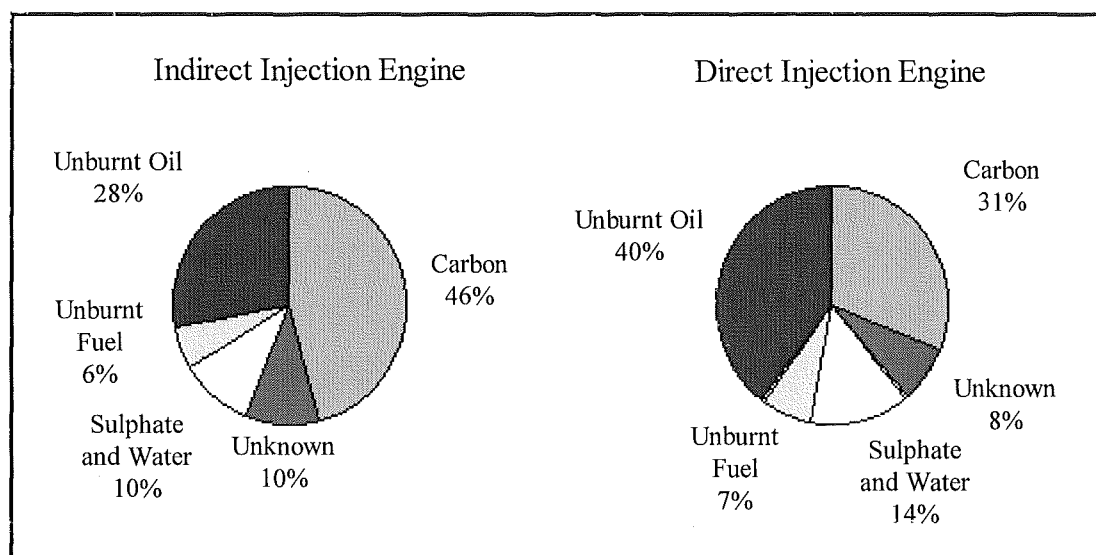


Figure 3.10. Diesel derived particulate composition (QUARG, 1993b)

Diesel vehicle engines emit particulate matter at a much greater rate than petrol engines, with estimates of emission factors around 4-7 g/litre of fuel for light duty diesel vehicles, 7-14 g/litre for heavy duty diesel vehicles and 0.65 g/litre for petrol vehicles (QUARG, 1993b). These Figures are supported by estimates (in ktonnes) of the exhaust emissions of PM<sub>10</sub> from road traffic. The 1995 Figures show that the contribution from all diesel vehicles (around 46.3 thousand tonnes) is approximately 4.3 times the size of the contributions from petrol engined vehicles (10.9 thousand tonnes) (QUARG, 1996).

#### 3.3.4. Black/Brown Crusts and Iron-Rich Patinas

As carbonaceous particles and Ca<sup>++</sup> ions are deposited on building surfaces, including granite, sulphation and gypsum growth can occur (Smith and Magee, 1990). Gypsum crystal growth is often initiated by deposited carbonaceous particles, which can act as nucleation centres (Del Monte *et al*, 1984).

Expanding gypsum crystals incorporate anthropogenic particulates and other wind-blown, deposited fines in their mineral structure. This will eventually lead to the relatively rapid formation of black or brown crusts in areas protected from rain washing. Limestone tablets exposed only to dry deposition in Milan, showed a luminous reflectance decrease of >30% over 18 months (Realini *et al*, 1995).

The presence of black crusts on the surface of building stones can affect the rock in a variety of ways, some of which are shown below in Figure 3.11. Although there are alterations to the thermal and hygrometric properties of the substrate stone, the presence of black crusts can also result in the physical fragmentation and incorporation of rock minerals within the crusts (Sequeira Braga *et al*, 1993; Schiavon *et al*, 1995). The fracturing of the surface minerals is thought to be due to crystallisation pressures generated by gypsum coming out of solution.

The presence of carbonaceous crusts on building stone surfaces can also alter the stones future physical weathering performance. Smith and Magee (1990) found a granite church in Rio De Janeiro that had large amounts of carbonaceous particles deposited below a projecting ledge, washed there by rain action. Where there had been an overlying carbonaceous crust the granite was stained brown, and was much more susceptible to decay by blistering and contour scaling. Nord *et al* (1994)

suggested that the presence of gypsum/deposited hydrocarbon crusts on the surface of building stones can act as a hydrophobic cover, preventing the free egress of moisture from the interior. This can lead to exfoliation of the stone surface.

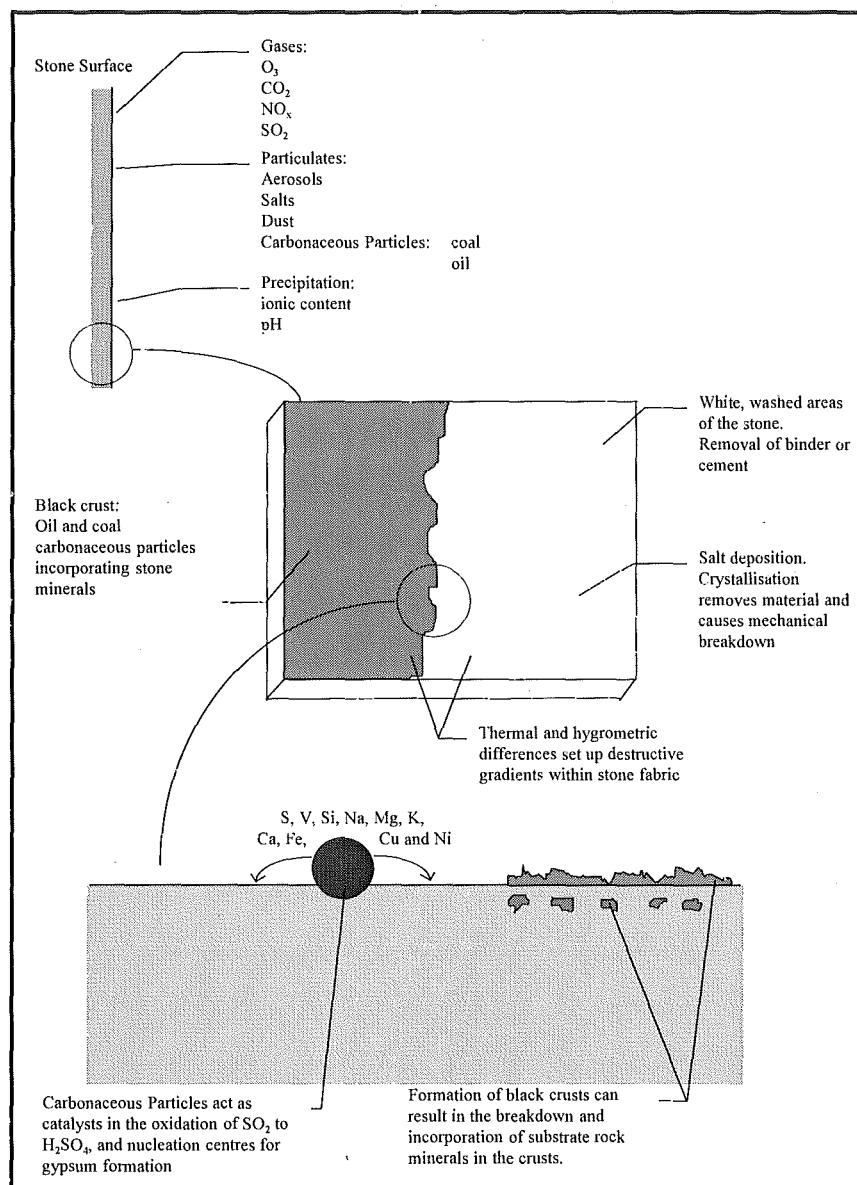


Figure 3.11. Some of the effects of carbonaceous particle deposition on a stone surface.

Black crusts can also result in rock deterioration through chemical processes. Schiavon *et al* (1995) found pseudomorphic replacement of primary silicate minerals in granite (mainly alkali and plagioclase feldspars, although there was also replacement of

some quartz grains) with gypsum. This was recorded in both Dublin and Edinburgh, along with further evidence of dissolution and fracturing on the surface of the quartz grains, suggesting that it is a common component of granite black crust formation. This is supported by Fe and oxide enrichment of black crusts forming on limestones due to dissolution of the underlying stone substrate (Hoke, 1978; Sabbioni and Zappia, 1992).

The presence of black crusts on stone surfaces suggests carbonaceous particle deposition. These particles have important implications for the chemical reactions that occur in the near surface water layer of the stone. As well as the formation of damaging gypsum crusts, carbonaceous particles can also increase the rate of  $\text{SO}_2$  oxidation.  $\text{H}_2\text{SO}_4$  formation was found to occur in water drops when fly-ash containing C, Fe and V was present (Cheng, 1983).

Iron-rich patinas have also been recorded on granites in urban environments. Composed of mineral fragments from the substrate rock, anthropogenic particles and soil dust embedded in an iron-rich matrix (Schiavon *et al*, 1995), the patinas are similar to black crusts without the gypsum binder. It is suggested that iron-rich patinas form where there is a combination of particulate deposition, biological activity and low levels of atmospheric  $\text{SO}_2$ .

In addition to iron-rich patinas, Fobe *et al*, (1993) found gypsum crusts developing on natural sandstone outcrops. Although there was no obvious source for the  $\text{Ca}^{++}$ , they suggest that the presence of moss aids in the concentration and precipitation of  $\text{Ca}^{++}$  and  $\text{SO}_4^-$  ions.

### 3.4. DEPOSITED IONS

Ions are transported to building surfaces through dry deposition or in solution, and can be derived from several sources, including carbonaceous particles, mortars, dust and exhaust particulates. Another contributory source for ion-rich solutions are limestone or sandstone rocks used in the same wall as poor ion-donators, i.e. granite.

The principle agent for study in this area, in relation to granite deterioration, are calcium ions. Although calcium ions are rare or even absent from granites, which often have  $\text{Ca}^{++}$  concentrations at less than 1% by weight (the calcium is found in plagioclase feldspars and apatite minerals), granites are still found in urban areas

with gypsum crusts (Smith and Magee, 1990; Sequeira Braga *et al*, 1993). The growth of gypsum crusts on calcium-free substrates was confirmed by Smith *et al* (1994), when they analysed the composition of crusts on Belfast sandstone, and by Schiavon *et al*, (1995) who found gypsum crusts and iron rich patinas on granite building stones in Dublin and Aberdeen.

Smith and Magee (1990) attempted to identify the sources of the  $\text{Ca}^{++}$  ions within granite, but could not find evidence that they were being leached from the feldspars, and suggested that the ions had arrived from a number of external sources. These included ions in solution from limestone mortar between the granite blocks, and in wind blown particulates from fly ash. Fobe *et al*, (1993) ascribed the source of  $\text{Ca}^{++}$  found in gypsum crusts on ferruginous sandstone buildings in Belgium to lime mortars used in the building fabric.

The distribution of mobile-ions or ion containing particulates around or on a building, monument or stone is determined by numerous interactions, such as rainfall parameters (intensity, duration, drop size), stone parameters (capillary size, surface roughness, porosity) and micro-climatic factors (relative humidity, air flow, wind speed and wind direction). Most importantly, Nord *et al* (1994) found a positive correlation between levels of air pollution and observed deposits (including soot, metals, salts, calcite, gypsum, fly-ash and quartz) on building stone.

In a study of several stone types exposed to the atmosphere in Germany, Steiger *et al* (1993) concluded that in polluted atmospheres gypsum formation can occur and proceed on silicate stones in the absence of a recognised  $\text{Ca}^{++}$  source (such as mortar). Indeed, gypsum crusts have been observed forming on bronzes of monuments, both in Vienna (Weber, 1985), and Sweden (Nord *et al*, 1994). These are attributed to depositing minerals from the atmosphere.

Steiger *et al* (1993) also found that in a Ca-poor sandstone, gypsum was the dominant constituent of the soluble minerals within the surface layers of the stone, leading to detachment of sand grains from rock binding agents. Decay rates for granite have also been found to increase when exposed to  $\text{Ca}^{++}$  rich run off, such as solutions derived from mortar and calcareous stones (Haneef *et al*, 1989).

Cooper *et al* (1989) have suggested a hypothesis for the higher rates of granite deterioration when calcium ions are present. They noticed increased decay of

granite facing in areas adjacent to mortared joints, areas washed by water deflected from limestone sills and overhangs, and areas located under decorative limestone surrounds. Areas of the facade where runoff water had not come into contact with limestone were in good condition, with minimal decay.

They suggest that limestone is reduced to calcium and sulphate ions under acid rain attack. The ions are transported to other sites, where crystallisation and hydration occur, disrupting the cracks and surface pores of the rocks involved. With granite this can occur wherever sources of calcium and sulphate ions are in proximity to the rock. Sulphate is normally deposited from the atmosphere, and calcium can be derived from the calcium-rich mortars that are currently used. The mechanism is shown in Figure 3.12.

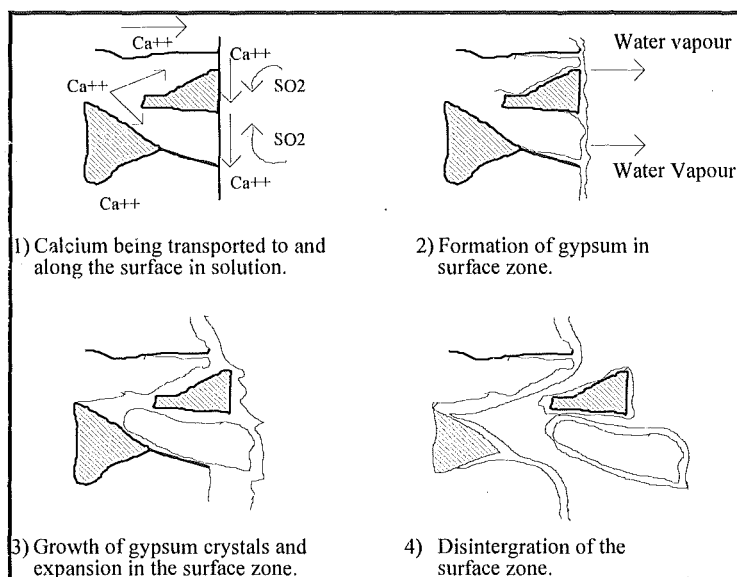


Figure 3.12. The possible actions of calcium and sulphates on granite (Cooper *et al*, 1989).

Haneef *et al* (1989) also tested the decay of granite in the presence of ions liberated by acidic solutions from limestones. They placed a variety of stone types, including granite, limestone, sandstone and marble, into a weathering chamber. The stones were either placed separately into the chamber, or in coupled pairs, i.e.: limestone resting on granite.



By analysing both the run-off solutions and the rocks, Haneef *et al* found that calcium and magnesium were released from carbonate bearing rocks, which resulted in weight changes in the coupled stones. The top stone of the pair lost weight as a result of acid dissolution, while the lower stone gained weight as a result of deposition of the dissolved products from the top stone. This was true for granite, which also showed severe degradation in the immediate area around the coupled carbonate stones, especially Portland limestone and Mansfield sandstone. The decay of the granite near the upper coupled stone is due to the presence of a 'meniscus' of solution in the coupling region, and this concentrates and contains the solution during the drying periods.

Haneef *et al* (1989) explained the recession of the granite surface, which was at a rate of approximately  $2 \times 10^{-2} \text{ mm yr}^{-1}$ , through the recrystallisation of dissolved salts from the acid rain and the coupled stone at and in the near surface pores and voids, such as grain boundary cracks, trans-granular microfractures and along cleavage lines (Warke and Smith, 1994).

The crystallisation of the salts  $\text{CaSO}_4 \cdot 2\text{H}_2\text{O}$  and  $\text{MgSO}_4 \cdot 7\text{H}_2\text{O}$ , results in a volumetric increase, which produces pressure within voids and microfractures, and can result in the extension and widening of the microfracture network (Rainey and Whalley, 1994). Ultimately this will cause the disaggregation of the surface, with the accompanying material loss.

### 3.5. DEPOSITION MECHANISMS

Deposition is the transfer of chemical species from the atmosphere to the surface of any given material, and the processes involved can be divided up in to two main classes: Wet deposition, which includes washout and rainout processes, and dry deposition, which involves all processes that lead to the deposition of airborne substances on a surface that do not involve precipitation (Lipfert, 1989). Total deposition is the sum of both wet and dry deposition processes.

Deposition around a building, or even within the same wall, is not uniform. Dolske (1995) reports of  $\text{SO}_2$  deposition to the south side of a building being  $\sim 60\%$  greater than to the north side of the same building

### 3.5.1. Dry Deposition

Dry depositional processes are of great importance in European weathering and decay, as it is the action of gas and particulate deposition that supplies the majority of aggressive chemicals in the surface moisture layer (Camuffo, 1993; Cooper, 1993; Dolske, 1995). Although Camuffo (1986) has suggested that dry deposition in urban environments accounts for over 90% of total pollutant deposition on a surface area, the relative importance of both wet and dry depositional processes is determined by the rainfall volume of an area (Conlan and Longhurst, 1993).

The rate of dry deposition (dry flux) onto a surface is controlled by a number of factors, including pollutant concentration, the transport and deposition velocities of the pollutant (a function of particle diameter) and the capture efficiency of the surface (which can be affected by surface roughness, the presence of moisture on the surface and surface water layer pH) (Judeikis and Stewart, 1976; Camuffo, 1993; Camuffo, 1995). Weber (1985) notes that the rates of aerosol deposition to a vertical surface increases with time, as surface roughness increases as a result of weathering.

The deposition rate is also affected by the amount of near-surface mixing, with dry deposition of  $\text{SO}_2$  and  $\text{NH}_3$  to wet surface layers maximised by co-deposition of pollutants (Erisman and Wyers, 1993). As surface deposition of a specific pollutant species occurs, the concentration of that pollutant in the air next to the material is lowered, limiting deposition of the pollutant. Therefore the rate of diffusion and gaseous mixing also determines the deposition rate (Judeikis and Stewart, 1976; Lipfert, 1989).

### 3.5.2. Wet Deposition

In addition to dry deposition mechanisms, there are other deposition processes that result in the incorporation of pollutants in precipitation and their removal from the atmospheric environment. As water droplets fall through the atmosphere, their ionic content changes as a result of gaseous diffusion, and the removal of aerosol particles. Wet deposition scavenging (washout and rainout) efficiency is described by the scavenging ratio  $W$  (Harrison, 1992).

$$W = \frac{\text{Concentration in rainwater (mg kg}^{-1}\text{)}}{\text{Concentration in Air (mg kg}^{-1}\text{)}} \quad (3.1)$$

Table 3.7 shows some scavenging ratios for selected ions. A large value implies a higher absorption rate, through increased precipitation scavenging.  $\text{Ca}^{++}$  has the highest rate of all the ionic species, and uptake is over 2.2 times greater than its nearest neighbour (Zn).

Species	W
$\text{Cl}^-$	600
$\text{SO}_4$	700
Na	560
K	620
Mg	850
Ca	1,890
Cd	390
Pb	320
Zn	870

Table 3.7. Table showing typical scavenging ratios (Harrison, 1992).

The size of individual raindrops can also influence the rate of pollution transfer to a given surface. Work by Bächmann *et al* (1992) shows that the smaller the radius of a individual rain drop, the higher the ionic and metal (Bächmann *et al*, 1995) concentration of the drop. It is thought this occurs as smaller particle condensation nuclei have a larger surface area/volume ratio (QUARG, 1993a). This is illustrated by Figure 3.13, where the lines represent different sampling periods at the same site.

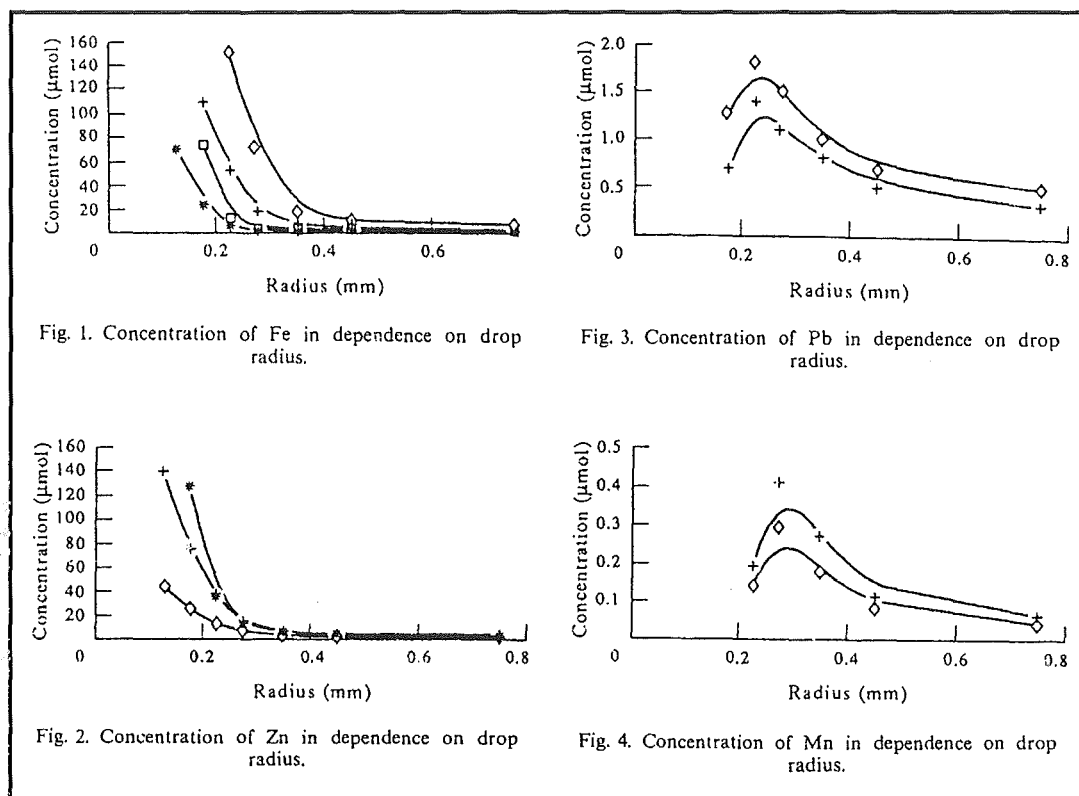


Figure 3.13. Characteristic ion concentrations as a function of drop radius (Bächmann *et al*, 1995).

Bächmann *et al* (1993) show that although concentration of any given species is strongly dependant on drop radius, this is also a function of rain event time - concentration increases inversely with drop radius at the beginning of the precipitation event, until a concentration maximum is reached. The length of the precipitation event also strongly influences ionic concentrations. Measurements taken in Manchester show ion concentrations in precipitation are inversely correlated to precipitation amount (Conlan and Longhurst, 1993).

### 3.6. ACID RAIN

Acidic precipitation, often called 'acid rain', occurs when pollutants go into solution in the atmosphere, and are deposited onto the surface of materials, sometimes over a thousand kilometres from the source. This differs from 'acid deposition', which tends to be more localised around a pollution source, and includes

the dry deposition of gaseous and particulate pollutants (Brimblecombe, 1986). The incorporation of pollutants into rain water can occur through two processes.

- 1) Rain-out, where the formation of raindrops around a dust or ice nucleus results in the adsorption of pollutants from the atmosphere.
- 2) Wash-out, where falling raindrops remove pollutants from the atmosphere by scavenging mechanisms.

The presence of pollutants in solution results in the lowering of the pH from a UK norm of  $\sim 5.6 - 6.4$ . Although there are regional variations in rain water pH, which can reach as low as 5 without the presence of anthropogenically-derived pollutants, rain with a pH of less than 5.6 is classed as acid rain, and can reach as low as pH 3.

Fogs and mists are also affected by the incorporation of pollutants, and they usually have a lower pH. This is associated with the increased ionic content of the water drop, a result of lower droplet deposition velocities and an increased residence time in the atmosphere (Bächmann *et al.*, 1992).

The two main causative components of acid rain are  $\text{H}_2\text{SO}_4$  and  $\text{HNO}_3$ , and although traditionally viewed as a minor component of acidification,  $\text{HNO}_3$  is increasing its contribution to pH decreases in the US (Galloway and Likens, 1981).

## CHAPTER 4. Sample Exposure Studies

### 4.1. SAMPLE EXPOSURE INTRODUCTION

Three sites of varying pollutant levels were used in the exposure programme: London (St. Paul's cathedral), Birmingham (Five-ways House) and Dartmoor (Yarner Wood) (see sections 4.4 for details). Each site contained stone samples divided into two groups; microcatchment units (M.C.U.s) and carousel tablets.

Four micro-catchment units were placed at each site, one acting as a blank, and three with differing surface finishes, so a estimation of the role of pollution and surface roughness on weathering rates could be made. Variations in surface roughness were used to determine the relative influence of surface roughness of granitic deterioration. The surface finish influences the deposition capture efficiency of the slabs and the duration of surface wetness - two factors that affect the amount and rate of weathering. The main method of weathering assessment was through the analysis of run-off water gathered from sites on a weekly basis, coupled with destructive analysis of the stones at the end of the exposure period. Higher pollutant concentrations are expected to elevate the weathering response of the granite, with London and Birmingham chosen as polluted urban sites, and Dartmoor as the 'clean' rural site.

The programme for the second group of samples was to measure weight changes associated with granites exposed to dry and net atmospheric deposition processes. Three granite types were divided up into small tablets and placed on carousels, with half the tablets protected from rainfall and surface flow. This allowed the accumulation and subsequent weighing of soluble reaction components (e.g. nitrate). The other half of the sample group was exposed to all atmospheric deposition processes, and will reflect changes engendered by the accumulation and removal of reaction products from the stone.

### 4.2. SAMPLE SELECTION

Granite samples with a varying physical and chemical properties were selected for use in the exposure programme. Three granite types were used in the

exposure programme, shown in Table 4.1, with the granitic characteristics and modal percentages listed below in Table 4.2.

Granite Type	Location	Calcium content (as % CaO)	Use in exposure Programme
Coarse biotite granite, Type B <sup>1</sup>	Merrivale Quarry, Dartmoor.	0.43	Carousel tablets
Fine biotite granite, Type C	Bolventor, Bodmin Moor.	0.67	Carousel tablets
Granodiorite	Mountsorrel Quarry, Leicester.	1.1	Micro-catchment unit slabs, Carousel tablets

Table 4.1. Type, location and use of granites in exposure programme.

Source	Granite Type	Modal Composition
Merrivale	Coarsely megacrystic tourmaline muscovite biotite granite	K - feldspar (mainly microperthite) 34%, quartz 33%, partly sericitized plagioclase 20%, biotite 6%, muscovite 3%, interstitial tourmaline 3%, opaque ore $\leq 1\%$
Bolventor	Medium to finely crystalline tourmaline biotite muscovite granite	K - feldspar (some microperthite) 34%, quartz 32%, partly sericitized plagioclase 20%, biotite 5%, muscovite 5%, interstitial tourmaline 3%, opaque ore and zircon $\leq 1\%$
Mountsorrel	Fine to medium crystalline granodiorite with thin quartz and feldspathic veins and rare brown xenoliths upto ~3cm diameter	highly sericitized plagioclase 30%, strained quartz 30%, perthitic orthoclase 22%, amphibole (cf. Hornblende) - altered to chlorite and opaque ores 12%, opaque ores 6%

Table 4.2. Granite type and approximate modal composition.

Carousel tablets were constructed from one of the three granite types tested, with four tablets from each rock type per carousel. Micro-catchment unit slabs were constructed from Mountsorrel granodiorite. This is because the granodiorite has a higher proportion of calcium containing plagioclase feldspars than alkali granites, and may have the potential to produce a larger decay response than granites with lower calcium quantities. Calcium has the highest degree of elemental mobility of ions in granite (Haneef *et al*, 1993).

<sup>1</sup> Granite Types B and C are described in chapter 2, section 2.3.4.

$\text{Ca}^{++}$  is also one of the most damaging ions in rock decay processes, leading to gypsum formation through the sulphation of calcium. This can result in the disruption of the rock surface, and affects hygrometric and thermal gradients within the rock, further promoting decay.

#### **4.2.1. Carousel Tablets**

Six carousels were used for the exposure programme, two at each site: London, Birmingham and Dartmoor. One of the carousels was located on the top of an exposure table, and was placed to measure either net or total deposition (the sum of wet and dry deposition processes), while the other was protected from precipitation, and designed to measure dry deposition. The second, protected carousel, still got wet during the exposure period, due to fogs and rain splashing, but was protected from surface flow removing soluble components from the rock.

Each carousel held twelve tablets, four from each rock type; Mountsorrel granodiorite, coarse biotite granite and fine biotite granite. These granite types were chosen to evaluate the influence rock composition has on weight changes as a result of exposure.

#### **4.2.2. Micro-catchment Units**

A total of four micro-catchment units (M.C.U.s) were deployed at each site, one acting as a control and three active sample collectors. The control unit had a sheet of ground glass in place of the samples (Sweevers, Peeters and Van Grieken, 1995). This was designed to simulate the surface roughness of the stones, without adding extra ions to the run-off, providing a measure of the particulate deposition and incident rainfall received by the slabs. Although weathering of the glass control might occur during the exposure period, contributing ions to the run-off, modern glass is durable (Butlin, 1991) and will only leach sodium, lead and potassium - components not measured during the project. Glass is also more suitable as a control than either perspex or copper (Halsey *et al*, 1995)

The other three M.C.U.s contained granodiorite slabs, with surface finishes of varying degrees of roughness. This will allow an evaluation of the relative importance of surface roughness on the contribution from the stone to the run-off



composition. The choice of surface finish on the slabs was designed to simulate a continuum of surface roughness that might be encountered on a typical building, ranging from the smooth polished finish, through the standard stone cut surface to the roughest flame textured finish. Varying stone roughness alters the rates of particle capture efficiency, duration of surface wetness and the rate of alteration product retention. It is during the time of wetness that aggressive chemical reactions can occur, degrading mineral constituents of the stone.

### 4.3. SAMPLE PREPARATION

#### 4.3.1. Carousel Tablets

The three stone types were cut to the required tablet dimensions ( $0.05 \times 0.05 \times 0.01\text{m}$ ,  $\pm 2\text{mm}$ ) using a Motacutter Mark II rock cutter with a diamond-tipped cutting blade. The carousel tablets were then measured for dimensional conformity before they had a small threaded stainless steel fixture attached, shown below in Figure 4.1.

Initially holes were to be drilled through the tablets, to allow them to be bolted to the carousels, but the thinness of the tablets and the strength of the granite resulted in the tablets breaking apart under the required drill pressure. To avoid this problem stainless steel fixtures, were obtained from the BigHead Fastener Company, and attached to one side of the tablets with high strength epoxy adhesive.

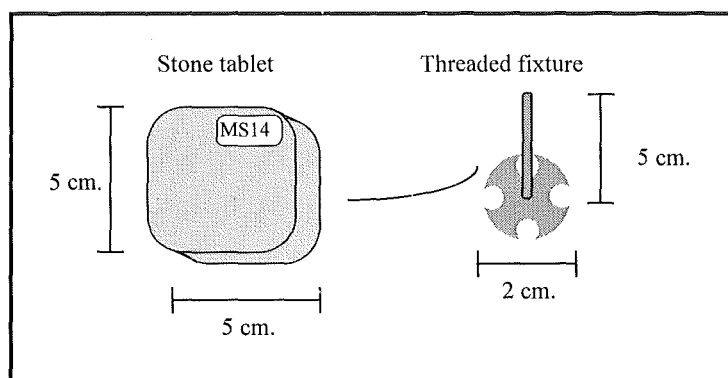


Figure 4.1. The carousel tablets and steel fixtures.

Once cut, the samples were labelled with individual identification numbers on the upper right corner of the tablet back (the side with the steel attachment) using an indelible marker. The samples were then washed in running water to remove coarse stone fragments and dust picked up during the cutting process, before being dried in an oven at 60 °C. Once dry the tablets were washed a second time in running double distilled, deionized water (DDDW) (following Jaynes and Cook, 1987).

The tablets then oven dried at 60°C for 90 hours before being placed in a desiccator to cool prior to weighing. The stones identification number and weight were recorded at the weighing, which was to four decimal places, before the samples were placed in individual sealed plastic bags to protect them from contaminants during transport to the site. Washed latex gloves were worn during the sample washing to minimise the transfer of ions and contaminants to the surface of the tablets.

#### **4.3.2. Micro-catchment Units**

The micro-catchment unit slabs were made from granodiorite (see Table 3.9) and were cut to the required dimensions ( 0.3 x 0.3 x 0.03m,  $\pm 4$ mm). Once cut, the slabs were given an identification code on the underside of the stone. After the slabs had been marked they were washed in running water and oven dried, before being washed a second time in running DDDW. The slabs were then placed in an oven at 60 °C for 90 hours.

The drying temperature of 60 °C was selected to avoid the burning or 'over-cooking' of the glue that was used in some of the Mountsorrel micro-catchment slabs. The glue was necessary to hold the fractured Mountsorrel granodiorite together. The drying procedure of 60 °C for 90 hours was adhered to for all other weighing of the stones over the exposure period.

After the drying period the slabs were weighed to two decimal places before being placed in sealed plastic bags. Washed latex gloves were worn while the samples were handled during and after the stone washes to minimise the transfer of ions and contaminants to the stone surface.

#### 4.4. SAMPLE SITES

Three locations around England were chosen as sample sites; London (St. Paul's Cathedral), Dartmoor (Yarner Wood) and Birmingham (Five-Ways House). The sites were chosen to represent urban and rural pollution regimes, with the air pollution levels for the three sites during the exposure period shown below in Table 4.3. Once at the sites, the exposure frames were orientated due south, to ensure that the granite slabs had as uniform a sunlight and heating regime as possible. Given the limited exposure period, thermal weathering of the slabs would not significantly influence alter rock properties.

Site	SO <sub>2</sub> (ppb)	NO <sub>x</sub> (ppb)
London	9.52	80.5495
Birmingham	7.81	49.512
Dartmoor	1.96	8.8-12.7*

Table 4.3. Mean air pollution levels during the exposure period. \* Background NO<sub>2</sub>, 1994 Newton Abbot NO<sub>x</sub> diffusion tube survey, AEA technology.

##### 4.4.1. London, St. Paul's Cathedral

The London site was located on the south side of St. Paul's cathedral roof, near the base of the central dome, as can be seen in Figures 4.2 and 4.3 below. The height of the sample site is equivalent to around six floors above road level.

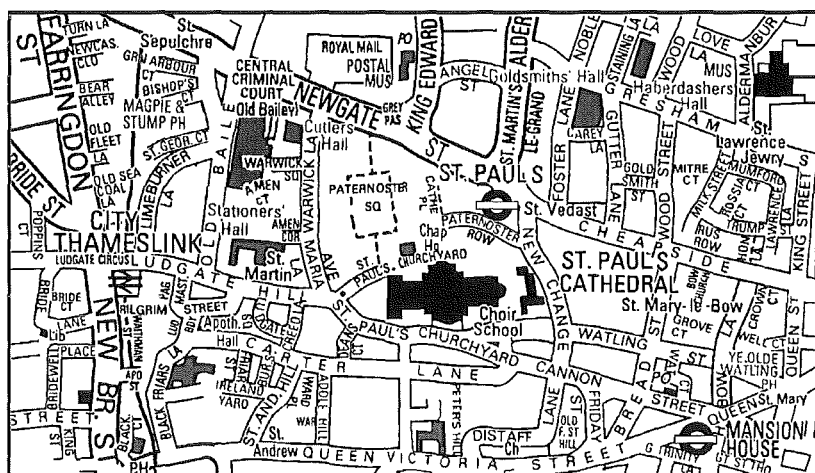


Figure 4.2. Street plan of London, showing St. Paul's Cathedral.

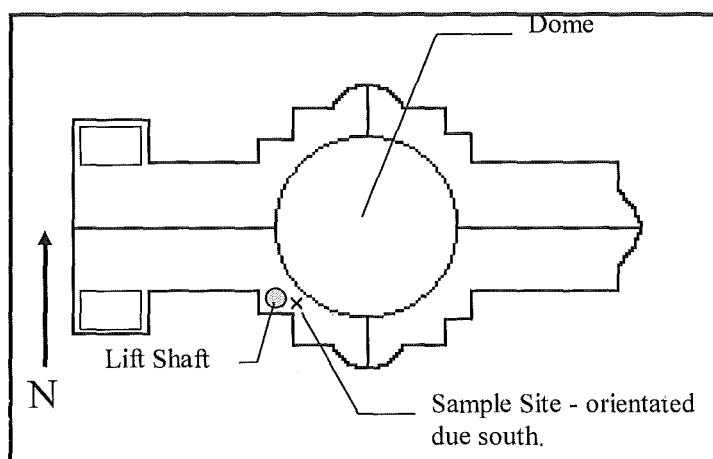


Figure 4.3. The location of exposure racks on the roof of St. Paul's.

#### 4.4.2. Birmingham, Five-Ways House

The Birmingham site was located on the roof of a six story local government building in central Birmingham. The building is next to a three lane road, and near to a major roundabout in the Birmingham ring road system. The frames are located on the roof of Five-Ways House, a Benefit Agency/Social Security office, shown below in Figure 3.4.

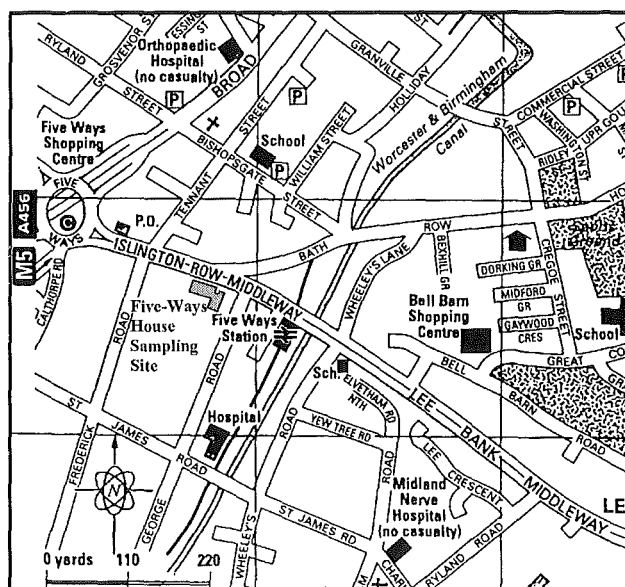


Figure 4.4. The location of exposure racks on the roof of Five-Ways House, Birmingham.

#### 4.4.3. Dartmoor, Yarner Wood

The site was located on a South West Water Authority covered reservoir near Yarner Wood at Trendlebere Down, Dartmoor, 119m above sea level. Grid reference: 783793 on Ordnance Survey map 191, shown below in Figure 4.5.

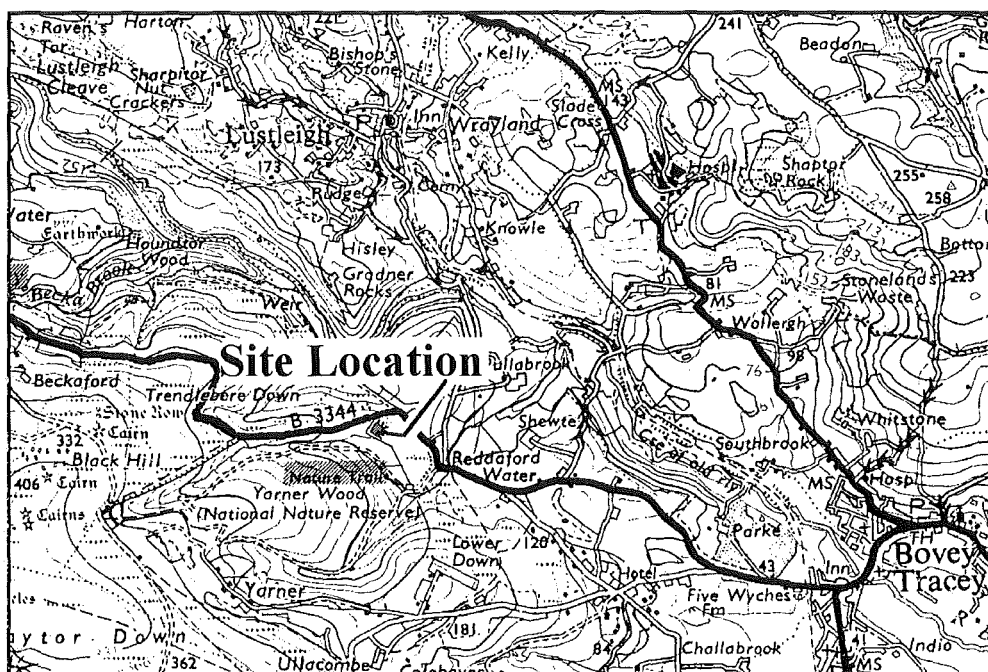


Figure 4.5. Diagram showing the location of the Dartmoor exposure site.

Average  $\text{NO}_2$  concentration at the Yarner Wood site, for the period June, 1987 - May 1990 was 5.8 ppb, with a minimum concentration of 2.0 and a maximum concentration of 26.0 ppb (Atkins and Lee, 1995). Atkins and Lee (1995) also report a winter/summer  $\text{NO}_2$  ratio of 1.38 for the Yarner Wood site. Although it is not known why there is a marked variation between summer and winter concentrations, Atkins and Lee feel that the higher winter concentrations are due to reduced photochemical activity and poorer dispersive conditions.

#### 4.5. SAMPLE EXPOSURE

All of the samples used in these experiments were exposed for a minimum period of ninety weeks, with various sampling strategies applied to the two principle

components of the exposure programme. The run-off was collected every week, while the carousel tablets and M.C.U slabs were collected and weighed at 45 and 90/91 weeks into the exposure period.

#### 4.5.1. Exposure Carousels

The exposure carousels, shown in Figure 4.6 and Plate 4.1, are freely rotating hubs with twelve arms radiating out from the centre of the hub. At the end of each arm is a stone exposure tablet, with the dimensions  $0.05 \times 0.05 \times 0.01\text{m}$  ( $\pm 2\text{mm}$ ). The carousels are standard exposure equipment, used originally by Jaynes and Cooke (1987) and then by the Building Research Establishment (B.R.E.), who loaned the carousels used in the experiment. The use of carousels prevents the sample tablets from resting in standing water, and reduces uneven weathering of the tablets by allowing the exposure of all sides to rainfall.

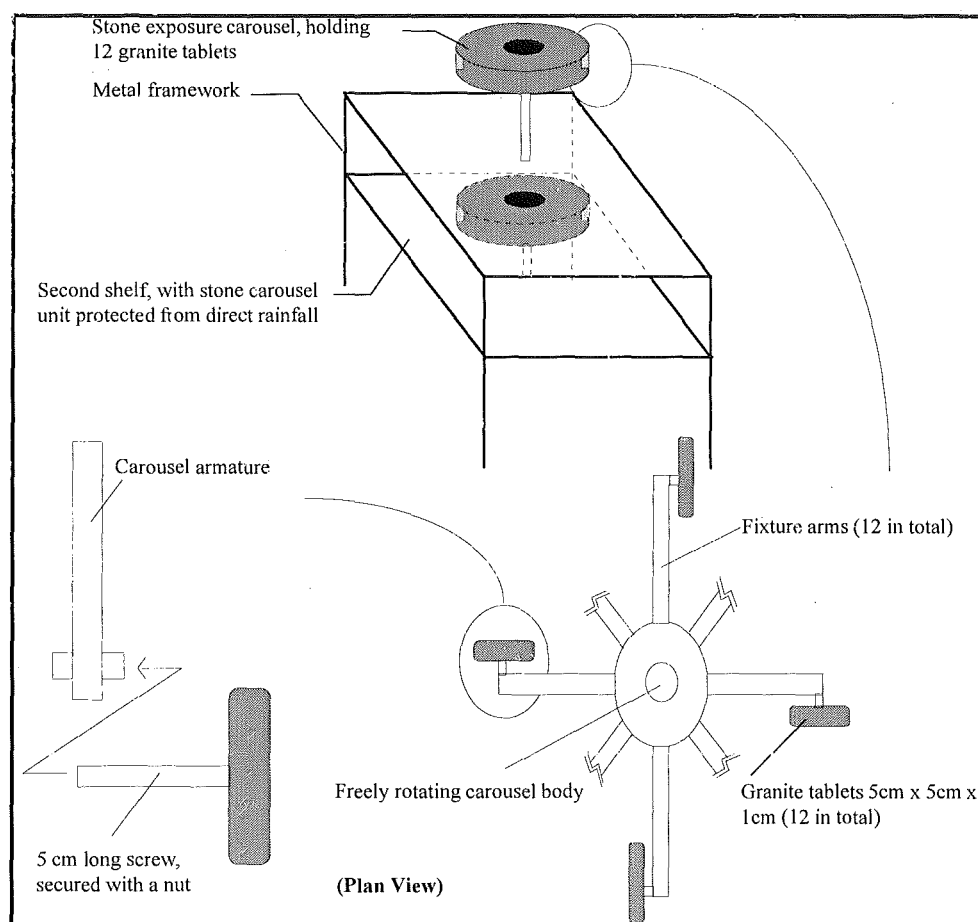


Figure 4.6. Diagram showing exposure carousel details.

#### 4.5.2. Micro-catchment Units

The micro-catchment slabs are 0.3 x 0.3 x 0.03m, and are located within perspex rainwater collectors inclined at 30° from the horizontal, designed after Reddy (1988), and shown below in Figure 4.7 and Plate 4.1.

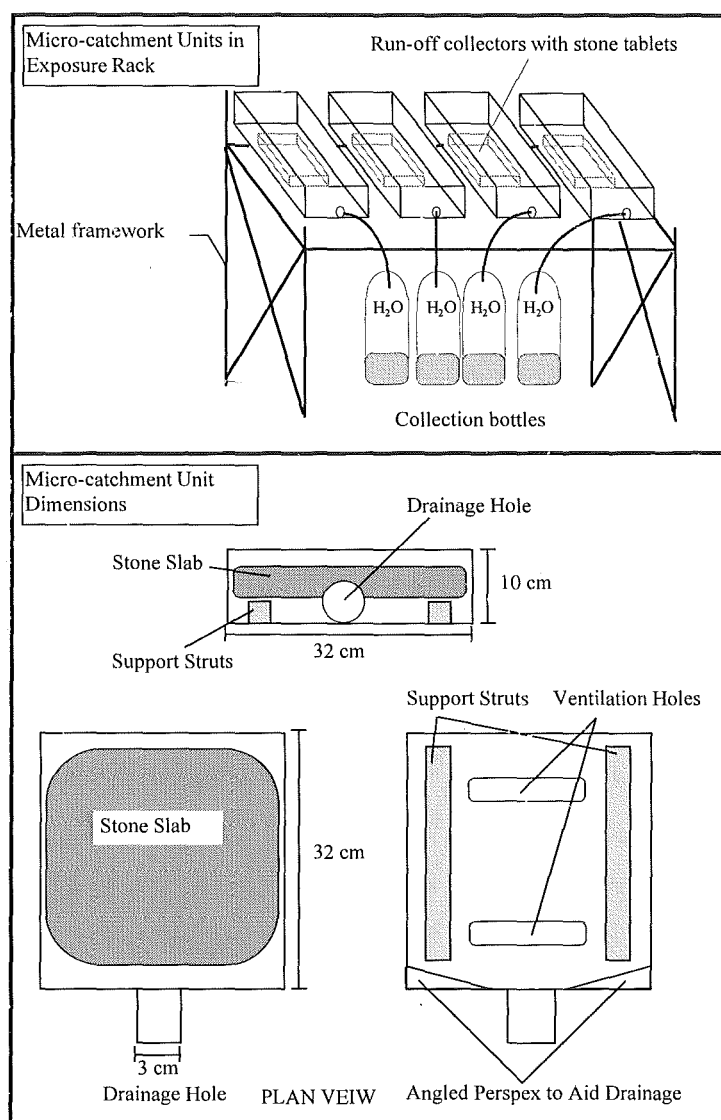


Figure 4.7. Micro-catchment unit and exposure rack dimensions.

The micro-catchment units are connected to 2.5 litre bottles with 1.5 m lengths of reinforced garden hose (plasticised PVC), with a plug of glass fibre in the

M.C.U. end of the hose. The glass fibre filter is designed to prevent the ingress of biological material, such as leaves, twigs and insects into the sample storage bottle.

The hoses were acid washed with 10% nitric acid for 24 hours to remove metal ions from the plastic, before being washed in DDDW and placed in sealed plastic bags until deployment on site. This was to protect them from contamination by mobile metal ions.

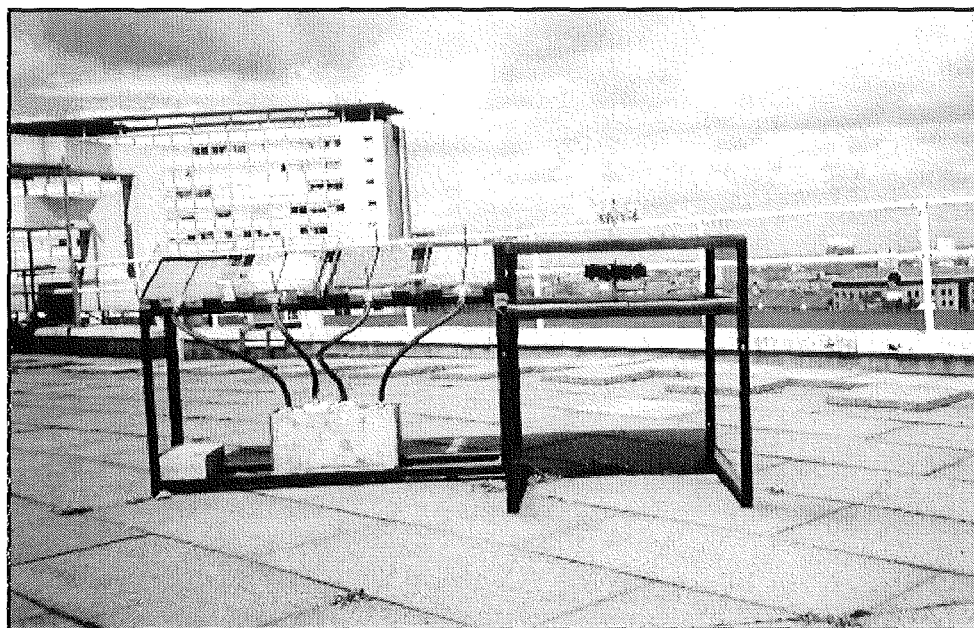


Plate 4.1. Microcatchment and carousel exposure rig, Birmingham.

The collection bottles were located under the stone samples on the rig, as seen in Figure 4.6. They were stored in drained wooden boxes that were designed to secure the bottles during the sampling period, and reduce the amount of sunlight falling on the samples. Sunlight falling on the samples during the collection period and subsequent storage can seriously influence the compositional stability of the sample, with concentrations of phosphates and ammonium decreasing as a result of prolonged exposure to light (Ridder *et al*, 1985).

The blank or control micro-catchment unit contained a ground glass sheet (30 x 30 x 0.4 cm) that had been sand-blasted to simulate the rough surface of the sample stones. The control sample was measured for incident rain characteristics (pH, volume, specific conductance, and the concentrations of sulphate, chloride, nitrate,



phosphate and a variety of metals). These values were then compared with the run-off generated by the sample M.C.U.s.

#### **4.6. SAMPLE ANALYSIS**

The analysis of the samples was split into two sections, based on the type of exposure the stones underwent. The carousel tablets were weighed during the exposure period, while the M.C.U slabs were also weighed and then destructively analysed at the end of the exposure period. The run-off generated during the exposure period by the M.C.U.s was analysed each week, and the data related to that of normal incident precipitation received by the blank. XRD analysis of the M.C.U slabs at the end of the exposure period was not conducted due to lack of time, a product of difficulties and delays encountered during the setting up of the exposure programme.

##### **4.6.1. Exposure Carousels**

###### **4.6.1.1. Weight loss and Gain**

The carousel tablets were dried and weighed before exposure, with additional weighing at the mid- and end-points of the exposure period. The process of drying the stone (a single drying period of 60 °C for 90 hours) was chosen to minimise the amount of re-weighing and handling of the stone, which Jaynes and Cook (1987) found affected the stone without significantly increasing the accuracy. The weight changes for the exposure period were calculated as percentage change from initial dry weight<sup>2</sup>.

##### **4.6.2. Micro-Catchment Units**

###### **4.6.2.1. Weight loss and Gain**

The M.C.U. slabs were dried and weighed before exposure began, with additional weighing occurring at 1 year and the end of the exposure period, to assess

---

<sup>2</sup> See section 5.4 for details.

the percentage weight change the slabs had undergone during the exposure period. The data was calculated as percentage change from initial dry weight<sup>3</sup>.

#### 4.6.2.2. Collection of Run-Off Water

The run-off generated from the M.C.U.s was collected in four 2.5 litre wide-mouthed FLPE bottles (Nalgene order code 2124-0005). The fluorinated high-density polyethylene bottles, with fluorinated polypropylene screw lids, were chosen to reduce the contamination of the sample by ions such as iron, manganese, zinc, cadmium and lead from the storage vessel. To further reduce the contaminative effects of storage in plastic bottles, the bottles have a protective fluorinated coating on the inside of the bottle, designed to reduce plastic phelate and ion contamination during sample storage.

The sample bottles were changed on a weekly basis, with the bottles sent back to Middlesex University for analysis. The week long collection period for each bottle was chosen to ensure that most of the sites would collect some run-off, while minimising the amount of biological growth that would occur in the bottles. Biological growth in the samples would have altered the composition of the run-off, and would have required the addition of a preservative such as formaldehyde. This would have resulted in the samples needing further treatment to remove the additional chemicals before they could be analysed by the ion chromatograph.

Oxidation of nitrite and sulphite after sample collection can result in increased nitrate and sulphate concentrations, providing potentially incorrect data for analysis. The weekly collection period will also help to reduce the amount of oxidation.

Once the sample had been received at Middlesex its volume was first measured, followed by pH and specific conductance measurements. The sample was then filtered and stored in the dark at 4°C. This was to minimise the degradation of the sample during storage; although nitrate and sulphate can undergo concentration decreases as a result of storage before analysis, the magnitude of the changes over a four week period is not more than 5-10%, which Ridder, Buishand, Rejnder, Hart

---

<sup>3</sup> See section 5.5.1. for results

and Slannia (1985) suggests has no practical relevance. The collection bottles were rinsed three times with DDDW after use, and were then sent out to the site again.

Anions in the run-off water (sulphates, phosphates, nitrates and chlorides) were detected and measured using a Dionex 2000i ion chromatograph, with a polystyrene packed column and running Dionex AI-450 chromatographic integration software.

Cation and metal analysis of the run-off was done using a Perkin Elmer Plasma 40 Emission Spectrometer (I.C.P), running Plasma 400 Inductively Coupled Plasma Emission Spectrometer software. The I.C.P. was used to detect and measure Al, Ca, Mg and Fe concentrations.

#### 4.6.2.3. Surface Roughness Analysis

The surface roughness of a stone is important in determining the rate of decay. As mineral weathering progresses, the stone surface roughness increases as a result of varying mineral dissolution rates. The increase in surface roughness will have two main effects:

- 1) It increases the particulate and gas capture efficiency of the stone, resulting in a higher rate of pollutant transfer to the stone surface.
- 2) It increases the stones surface area to volume ratio, resulting in a relative increase in pollution damage to the stone, which will expand as the surface area increases.

To determine the nature and rate of surface change, an average surface roughness of the three stone finishes was determined by measuring the finishes of the sample control stones using a CyberOptics laser profilometer. Measurement of the same transect before and after exposure was not a practical option as there are many procedural difficulties with the accurate positioning of the stone for a second measurement traverse at the end of the exposure period. As a result it was decided to generate average roughness values for the finishes, based on the control samples, which were then compared with the exposed sample data.

Differences in roughness values between the control and exposed samples allowed an estimation on the rate of surface roughness change over time. The measures of increasing surface roughness were then compared to data generated from

the run-off water to assess if the roughness increase was linked to an enlargement of the component concentration in the run-off, the result of an augmentation in the capture efficiency of the stone.

#### 4.6.2.4. End Analysis

Destructive analysis of the M.C.U slabs was undertaken at the end of the exposure period. Cross-sectional analysis of the composition of the stone was carried out by sectioning the slabs and using the scanning electron microscope with an EDX attachment to determine the elemental composition of the samples.

The surface roughness of the samples at the end of the exposure period was also measured, and compared to surface roughness measurements generated from the control samples at the start of the exposure period.

### 4.7. ANALYTICAL METHODS

Two instrumental methods were used to analyse the run-off water collected by the micro-catchment units, ion chromatography and inductively coupled plasma atomic emission spectrography.

#### 4.7.1. Ion Chromatography

Analysis of the run-off water for anions was carried out using a Dionex 2000i high performance ion chromatograph, or H.P.I.C., with Dionex AI - 400 integration software. Ionic detection was by conductivity.

The column used was an H.P.I.C. - AS4A anion exchange separator column, packed with a pellicular resin with positively charged fixed ionic sites. The column properties are shown below, in Table 4.4.

Anion Exchange Beads	
Cross Link Percentage	3%
Substrate Size	15 $\mu$
Efficiency	10,000
Operating pressure (PSI)	700 - 900
Dimension (mm)	4 x 250

Table 4.4. Properties of the ionic exchange column.

Ion chromatography involves the separation of sample components between two phases as a sample passes through a column, which is a function of the equilibrium distribution. The efficiency distribution determines whether the components favour the mobile phase, allowing the components to rapidly migrate down the column, or the stationary phase, which produces a slower migration rate as the components are more attracted to the column packing.

When the sample has passed through the column, the concentration of the component bands is measured by a conductivity detector. The concentration is determined by differences in conductivity between the background reading of the eluent and regenerant, and that of the sample.

The sample is injected into the system using a syringe with a 0.2  $\mu\text{m}$  syringe tip sample filter to remove any particulates and organics from the sample. DDDW was used for all standards, eluants, regenerants and reagents.

Calibration of the I.C. was undertaken using the external standard method, with the standards prepared at the start of each days analysis. Peak area, rather than peak height was used for measuring the detector response as it is less affected by minor changes in temperature, flow rate or analyte retention time.

#### 4.7.1.1. Determination of Anions

Analysis for:  $\text{Cl}^-$ ,  $\text{NO}_3^-$ ,  $\text{PO}_4^{3-}$ ,  $\text{SO}_4^{2-}$ .

Method: Anions are separated with an H.P.I.C. - AS4A column with a carbonate/bicarbonate buffer eluent, shown in Table 4.5. Detection is by conductivity with chemical eluent suppression.

Sample Loop Volume	50 $\mu\text{l}$
Guard Column	H.P.I.C. - AG4A
Separator Column	H.P.I.C. - AS4A
Eluent	2.00 mM $\text{Na}_2\text{CO}_3$
	1.90 mN $\text{NaHCO}_3$
Eluent Flow Rate	2.0 ml/min
Regenerant	0.025 N $\text{H}_2\text{SO}_4$
Regenerant Flow Rate	3 ml/min
Expected Background Conductivity: 15 - 20 $\mu\text{S}$ .	

Table 4.5. Ion chromatograph operating conditions

#### 4.7.2. Inductively coupled plasma - Atomic Emission Spectrophotometry

A Perkin-Elmer Plasma 40, running ICP 400 software, was used to determine and analyse the composition and quantity of metal species found in the run-off. This is achieved by exciting the ionic species of interest in an argon plasma, so that the atoms give off characteristic ultraviolet and violet radiation patterns as they change energy excitation states. These emissions pass through a monochromator to a detector, where the analytical data is recorded and used to indicate the elemental species present in the sample.

##### 4.7.2.1. Determination of Cations

Analysis for:  $\text{Al}^{3+}$ ,  $\text{Ca}^{2+}$ ,  $\text{Mg}^{2+}$  and  $\text{Fe}^{2+}$ .

A 1 ppm stock solution containing the required metals was used to calibrate the I.C.P. at the start of the analysis period. The standard was analysed, and the values obtained are plotted against values generated from a blank sample of DDDW with 1% nitric acid to create a calibration curve.

The samples were diluted 10 times before they were analysed on the I.C.P. To ensure that sample metal concentrations fell within the measurement range of the I.C.P., which lies between 1 - 400 ppm, 1 ml of sample was placed in a volumetric flask, and 9 ml of DDDW with 1% nitric acid was added. The solution was then immediately aspirated and measured by the I.C.P. The nitric acid was added to the samples to stabilise the solubility of metals prior to analysis, and was not designed to increase metal load through the dissolution of urban dusts and particulate matter.

#### 4.7.3. Surface Roughness Measurements

To quantify the influence of surface roughness on run-off, measurements were taken from the London site slabs and the sample control slabs. The measurements were taken by a laser profilometer (a Cyberoptics microscan 3D instrument), which expresses the roughness as a value,  $R_a$  which was used to assess roughness.  $R_a$  is defined as the arithmetic mean of the departures of the roughness profile from the arithmetic mean. Another quoted value is  $R_{\text{max}}$ , which is the

maximum deviation from the arithmetic mean (Massey, 1996), and provides a measure of the amount deviation of the surface.

To estimate the transect roughness, a laser is reflected off the sample surface, and the time of return is recorded. This is repeated at regular steps along the length of the transect, and it allows the instrument to construct a mathematical image of the transect. This is then interpreted by the software to obtain  $R_a$  and  $R_{max}$  values. The degree of light scatter is considered to be uniform across silicate minerals by the Building Research Establishment for the purposes of roughness evaluation.

A number of transects were measured from each stone, each at a different scale. This sampling strategy was taken to evaluate two levels of roughness at the stone surface, which will be referred to as 1<sup>st</sup> order and 2<sup>nd</sup> order roughness. The 1<sup>st</sup> order roughness readings were designed to measure larger scale surface undulations, shown in Figure 4.8, and readings were taken every 0.25mm over a 25mm traverse. The 2<sup>nd</sup> order roughness measurements were taken to assess the inter-grain roughness of the surface, with readings taken every 0.025mm over a 2.5mm traverse.

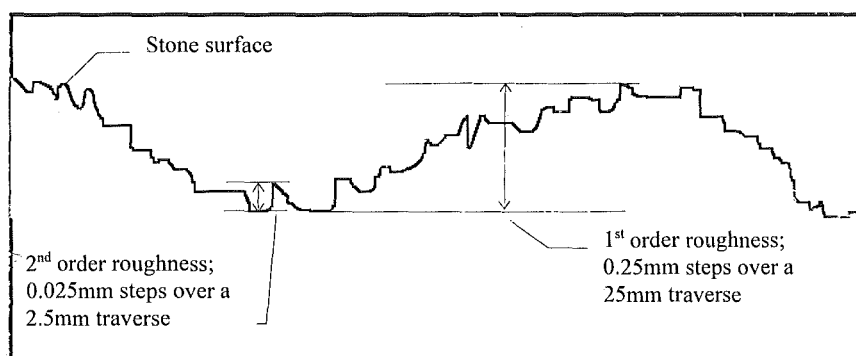


Figure 4.8. 1<sup>st</sup> and 2<sup>nd</sup> order roughness measurements.

A final traverse was taken from each slab, with 500 readings taken at 0.025mm intervals over a 12.5mm traverse, to generate a typical profile for the finish. The software used in the evaluation of the roughness profiles calculates the angle of any non-horizontal profile, and performs a least squares analysis to remove the slope before it calculates the roughness parameters.

#### 4.7.4. S.E.M. and E.D.X Analysis

The final analysis carried out on the stones was evaluation by Scanning Electron Microscope (SEM) and Energy Dispersive X-ray spectrometer (EDX). The EDX unit was used on the control and exposed slabs to determine if elemental leaching had occurred, and for the comparison of deposition rates of soluble minerals such as  $\text{Ca}^{++}$ , through the analysis of the elemental composition of selected areas within the slabs. The SEM was used for visual determination of decay features, such as dissolution pits or micro-fracture networks.

The samples used in the SEM were first sectioned, to provide a slab transect, and cut down to size for the vacuum chamber. The transects were then sputter coated with gold to provide a conductive surface and reduce back-scatter, and placed in the SEM for analysis.

A number of analyses were carried out using the EDX attachment, which allowed the determination of element type, in addition to distribution and concentration within the sample. The EDX unit analyses X-rays produced by an intense beam of electrons from the SEM, which bombards atoms within the sample. Each element produces X-rays with a characteristic and well-defined set of energies. As these hit the detector (which can detect all elements with an atomic number greater than 5), the X-rays are converted to electrical pulses (which are proportional in voltage to the original X-ray energy) which are fed to a multi-channel analyser (MCA) (each channel corresponds to a voltage level). The results are then continuously shown on a monitor, where they are displayed in the form of a spectrum, so the sample's elemental composition can be determined. This is shown overleaf in Figure 4.9.



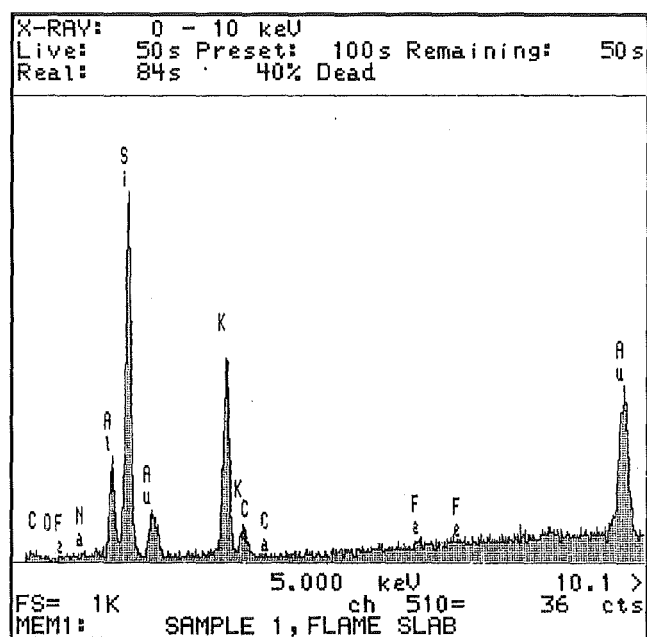


Figure 4.9. EDX elemental analysis of an orthoclase feldspar coated with gold.

## CHAPTER 5. Sample Exposure Results

### 5.1 INTRODUCTION

Over a period of about two years (91 weeks sampling from August 1994 to April 1996), a number of run-off samples were collected from three sites around England; 68 samples from each of the London micro-catchment units (allowing for non-precipitation weeks), 63 for the Birmingham M.C.U.s, and 58 for the Dartmoor M.C.U.s. By the end of the exposure trial, a total of 756 samples had been analysed.

Ambient pollution concentrations were calculated for the urban sites using data from the Enhanced Urban Air Quality Network. The daily averages for  $\text{NO}_x$  and  $\text{SO}_2$  were collected and presented as weekly averages, except for Dartmoor, where only  $\text{SO}_2$  values were collected. The figures for the analyses carried out on the exposure programme results are reported in the footnotes. Where average site means and the standard error range is reported, the values are drawn from the raw values for the entire site.

### 5.2. RUN-OFF ANALYSIS

During the course of the exposure program a number of different components were analysed. In order to characterise the data sets in the initial phase of data analysis, they were plotted using a frequency distribution graph. Distributions were then compared to the theoretical construct 'normal distribution'. This is a roughly bell-shaped symmetrical distribution with most items, or data points, falling near the mean, and the bell tapers off at the very high and very low scores. The normal distribution represents the likelihood that the items within a normally distributed population will depart from the mean by any amount.

The data collected during the course of the exposure program does not follow this idealised distribution, and is not symmetrically arrayed around the mean. When the distribution has a greater number of observations on the right side of the mean, it is 'positively skewed'. In the measured data sets, there was a greater number of observations at the high scores, which leads to the formation of a 'tail', shown below in Figure 5.1. The distributions in Figure 5.1 is representative of all the data sets, and reveals a moderate degree of asymmetry around the mean, or skewness.

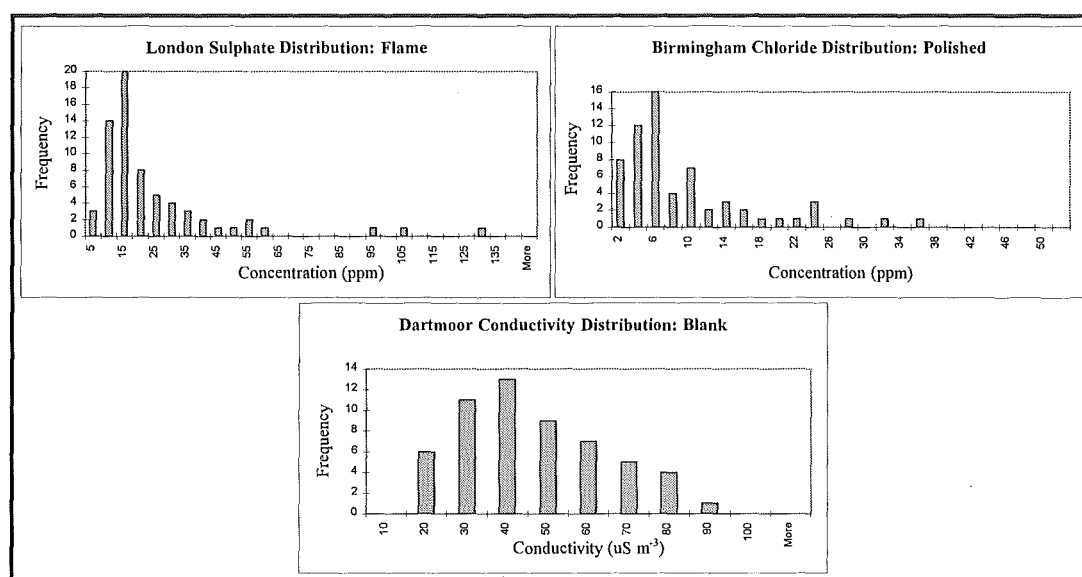


Figure 5.1. Frequency distributions for  $\text{SO}_4^{2-}$ ,  $\text{Cl}^-$  and conductivity measurements at different sites and finishes.

It is important to assess the distribution of the data sets so that it is possible to determine the most appropriate analyses. The exposure programme was designed to use analysis of variance (anova) primarily because it is crucial in understanding the decay rate as a consequence of the interaction of different factors, i.e. site and finish type. This means it is inappropriate to use non-parametric statistics. Another factor behind the choice of anova was that analysis of granite microcatchment unit run-off using multivariate principle component analysis (PCA) by Sweevers, Peeters and Van Grieken (1995) failed to produce any significant explanation of variance in their data sets. In their own words 'there was no point in carrying out PCA.'

There are three main assumptions that must be satisfied before it is appropriate to apply an analysis of variance; the data must be either interval or ratio measurements, there must be homogeneity of variance and most relevant to the discussion here, the data set must be normally distributed. In the event that the data set is not normally distributed, there are alternative approaches. Distribution free methods (non-parametric statistical techniques) is one alternative, but this option is inappropriate since it does not allow crucial experimental comparisons, and will result in the loss of information.

Another alternative is the transformation of the data set, through the application of a suitable mathematical function, to increase its conformity to the idealised normal distribution. As a result of the moderate positive skew observed in the exposure programme data sets, the most likely transformation would be a log normal transformation. This transformation is useful when the data is markedly positively skewed, because it will compress the right side of the distribution more than the left. Therefore, taking logs will reduce the standard deviation of the sample with large numbers more than it will reduce the standard deviation of the sample with small numbers. This alternative is also inappropriate.

The exposure programme examines the response of granite slabs over a short exposure period. As a consequence of this, and the fact that the rock composition will initially be the same across all finish types and all sites, the variations between data sets were not expected to be large. It is also predicted that the differences in the data sets between the finish types will be represented in the higher values. Log normal transformation will compress these scores, drawing them closer into the mean, and could well obscure the subtle variations engendered by finish type. Log normal transformation will therefore reduce the sensitivity of effects. As Everitt (1996) reports, it is almost always preferable to present results in the original scale of measurement.

One of the critical questions about the application of particular statistical analyses, such as anova, is how much a moderate deviation from the underlying assumptions of normal distribution will effect the reliability of the conclusions. Glass, Peckham and Sanders (1972) examined populations with the same mean, but with different distributions and different variances. After their assessment of the actual and theoretical sampling distributions of  $F$ , they concluded that the sampling distribution of  $F$  is amazingly robust, and that it is insensitive to even flagrant violations of the underlying assumptions. This is especially true for the assumption of normal distribution when compared data sets have similar distribution shapes (i.e. all positively skewed) (Howell, 1992). Keppel (1982) refers to an study by Norton (1952) who drew samples from normal, moderate and marked distributions, amongst others. He found that homogeneous distributions had a close match of empirical and theoretical percentages. The match of populations of markedly different form

showed discrepancies in the order of 1-2 percentage point over-estimation at the 1% significance level. It is safe to conclude that violations of normal distribution assumption do not significantly effect the reliability of the anova conclusions, except if violations are particularly severe.

Given that the exposure programme data sets only display a moderate deviation from the normal distribution, and that compared data sets are all positively skewed, there is no obvious reason to consider transforming the data. In addition, the experimental situation expects effects to occur in the higher values, and transforming the data sets would reduce the effects of these values, generating distributions that, while strictly normal, are essentially the same. It is for these reasons that the collected data sets were not transformed.

### 5.2.1. Run-Off Characteristics

#### 5.2.1.1 Volume

The role of site is one of the primary factors in determining run-off characteristics and composition. This was displayed immediately by run-off volume, which showed significant differences in the mean volumes from the three sites (shown below in Table 5.1, with the analysis significance reported in the footnotes), when analysed by anova<sup>1</sup>. Although there were significant effects when analysed as a group, individual comparisons of the sites showed that while there were significant differences between the London and Dartmoor sites<sup>2</sup>, there were no differences between the two urban sites<sup>3</sup>.

When the sites were analysed individually to assess the role of surface roughness on water retention by the stones, only London showed a significant difference between the blank and the three finish types when examined as a group<sup>4</sup>.

---

<sup>1</sup> An anova is an analysis of variance to test the hypothesis that means from two or more samples are equal (drawn from populations with the same mean).  $F(1, 254) = 16.1, P < 0.01$

<sup>2</sup> T-test;  $T(459) = 6.9, P < 0.01$

<sup>3</sup> London against Birmingham;  $T(498) < 1$

<sup>4</sup> London inter-finish;  $F(2, 178) = 3.13, P < 0.05$

	London			Birmingham			Dartmoor		
	Mean	Std. Error: lower limit	Std. Error: upper limit	Mean	Std. Error: lower limit	Std. Error: upper limit	Mean	Std. Error: lower limit	Std. Error: upper limit
Blank	1069.7	977.24	1162.1	1003.3	917.59	1089.1	1526.3	1432.8	1619.7
Polished	1038.9	944.85	1133	1088.9	1002.1	1175.6	1509.6	1412.3	1606.8
Cut	1084	990.66	1177.4	1091.7	1001.7	1181.7	1511	1413.4	1608.6
Flame	1044.7	950.91	1138.5	1082.3	993.02	1171.7	1526.4	1430.3	1622.6
<b>Average</b>	<b>1059.4</b>	<b>1013</b>	<b>1105.9</b>	<b>1066.4</b>	<b>1022.6</b>	<b>1110.1</b>	<b>1518.3</b>	<b>1470.6</b>	<b>1566.1</b>

Table 5.1. Run-off volume means (in ml) and standard error<sup>5</sup>, by finish and site.

This significance was not replicated at the other sites<sup>6</sup>, despite the low Birmingham blank volume, nor when post-hoc T-tests examined the interactions between the individual finishes at each site<sup>7</sup>. This suggests that although surface finish has some influence on the run-off volume from a given surface area, other site factors such as precipitation direction and micro-turbulence effects dominate.

### 5.2.1.2 pH

pH measurements were taken from the collected run-off samples to assess the effect of site and surface roughness on the acidity of surface solutions, and cross-site comparisons showed a significant difference between the sites when analysed as a group<sup>8</sup>.

When compared individually by site, there were significant differences between the two urban sites<sup>9</sup>, although not between Birmingham and Dartmoor<sup>10</sup>. There was, however, a strong effect between the polluted, urban London site, and the rural, 'clean' Dartmoor site<sup>11</sup>, with Dartmoor significantly lower than London, shown below in Table 5.2.

Although the distribution of the pH means was not as expected, with the 'clean' site showing the lowest mean, this might be explained by the presence of limestone at the London site. Leysen *et al* (1989) analysed aerosols around a sandy

<sup>5</sup> Standard error confidence limits reported at 95% confidence

<sup>6</sup> i.e. Birmingham inter-finish;  $F(2, 176) < 1$

<sup>7</sup> London flame against blank;  $T(126) < 1$ , Dartmoor polished against flame;  $T(110) < 1$

<sup>8</sup>  $F(1, 262) = 24.7$ ,  $P < 0.01$

<sup>9</sup>  $T(370) = 15.6$ ,  $P < 0.01$

<sup>10</sup>  $T(432) < 1$

<sup>11</sup>  $T(73) = 7.7$ ,  $P < 0.01$

limestone cathedral in Belgium, and found Ca-containing particles represented 37-56% of the total number of collected particles per m<sup>3</sup> at 33 m. They attributed the Ca<sup>++</sup> enrichment and high pH of the deposition particle's bulk chemical composition in comparison to standard results from the Netherlands and the Belgium rain network to particles that are generated by the erosion of the limestone building.

	London			Birmingham			Dartmoor		
	Mean	Std. Error: lower limit	Std. Error: upper limit	Mean	Std. Error: lower limit	Std. Error: upper limit	Mean	Std. Error: lower limit	Std. Error: upper limit
Blank	6.66	6.63	6.69	6.23	6.17	6.29	6.14	6.06	6.21
Polished	6.67	6.64	6.69	6.23	6.18	6.28	6.31	6.26	6.36
Cut	6.68	6.65	6.70	6.39	6.35	6.42	6.30	6.25	6.35
Flame	6.70	6.68	6.73	6.18	6.14	6.23	6.21	6.16	6.26
<b>Average</b>	<b>6.68</b>	<b>6.66</b>	<b>6.69</b>	<b>6.26</b>	<b>6.23</b>	<b>6.28</b>	<b>6.24</b>	<b>6.21</b>	<b>6.27</b>

Table 5.2. Mean finish and site pH and standard error.

St. Paul's, which was constructed from Portland limestone, may also be surrounded by a Ca-containing 'ionic cloud', which could be responsible for the buffering seen in the London site run-off. Roekens, Komy, Leysen, Veny and Van Grieken (1988) found that wet only (mean pH = 5.8) and total (mean pH = 6.7) deposition at St. Rombouts, a limestone cathedral in Belgium, was elevated in comparison to both the natural pH of rainwater (pH = 5.6) and a reference site some 6Km from the cathedral (mean pH = 4.9). The total deposition mean pH of 6.7 for the Belgium cathedral is very similar to the London run-off mean pH collected at St. Paul's cathedral (mean pH = 6.68). Roekens *et al* (1988) concluded the alkaline pH of deposition samples from the Belgium cathedral is due to neutralisation of rainwater by the washout of CaCO<sub>3</sub>, caused by urban dust or from erosion of the building (Delgado and Gil Saraiva, 1985), and with the similarities in total deposition mean pH between the two cathedrals, it is likely that a similar process is operating at the London site.

The Birmingham mean was lower than the London value, and this could be explained by the almost total absence of limestone around the MCU site, although it is not absent. The Dartmoor site had the lowest mean of all the sites, and this could

be explained by the surrounding acid geology of the south-west, which would not buffer rainfall pH levels, and the lack of urban dust, which has a high  $\text{Ca}^{++}$  concentration.

When the sites were examined individually for the effects of the different finishes, none of the sites showed any significant differences between finishes<sup>12</sup>. The lack of significance was repeated when analysed as a group (the blank and the finishes from all sites compared against each other).

This was also true for individual inter-finish comparisons for all finishes at London. Only Dartmoor and Birmingham showed any effect between individual finishes. At Dartmoor the polished and cut finishes were significantly higher than the blank<sup>13</sup>, while at Birmingham, the cut finish was significantly higher than the blank<sup>14</sup>. The lack of significant differences between the populations from London might be due to the masking effects of the theorised  $\text{Ca}^{++}$  clouds around the limestone cathedral, and inputs from  $\text{Ca}^{++}$ -rich urban dust which will reduce the level of response from individual finishes. Conlan and Longhurst (1993) report that the acidity of precipitation in greater Manchester area was a function of the spatial variability of calcium compounds and their buffering activity, which could explain the similar response from each finish type at the urban sites.

Birmingham and Dartmoor differed from this, in that the blank was significantly lower than the Birmingham cut finish, and Dartmoor polished and cut finishes. At Dartmoor, however, the flame finish was not significantly different from the blank. This could be explained by a slight buffering action from the stone itself, which was not available in the blank run-off, and was masked by an increase in acidic deposition to the rougher flame dressed finish surface.

### 5.2.1.3 Conductivity

Conductivity measurements were taken from all samples, and were used to provide an indication of the degree of overall ionic concentration within the run-off.

Inter-site comparison of the means, shown below in Table 5.3, revealed that there were significant differences between the sites when analysed as a group

<sup>12</sup> i.e. Birmingham;  $F(2,176) = 1.16$ ,  $P > 0.1$

<sup>13</sup> blank against cut;  $T(97) = -1.78$ ,  $P < 0.05$

<sup>14</sup> cut against blank;  $T(97) = 2.4$   $P = 0.01$



(examining all the sites together)<sup>15</sup>. Post-hoc comparisons also revealed significant differences between the means of the individual sites<sup>16</sup>. This indicates that the degree of pollutant concentration (as measured by conductivity) at each site was significantly different from the others, with London (urban site) as the most polluted site, and Dartmoor (rural site) as the cleanest (see Table 3.10 for average site pollution levels). The very high levels of variation in the data, however, reduced the reliability of the statistical inferences made from these values.

	London			Birmingham			Dartmoor		
	Mean	Std. Error: lower limit	Std. Error: upper limit	Mean	Std. Error: lower limit	Std. Error: upper limit	Mean	Std. Error: lower limit	Std. Error: upper limit
Blank	115.15	99.64	130.66	83.12	72.53	93.71	41.90	39.36	44.44
Polished	121.26	107.35	135.17	90.82	75.82	105.83	48.22	44.12	52.33
Cut	124.08	109.00	139.16	102.67	83.96	121.38	47.99	42.39	53.58
Flame	143.89	126.18	161.60	92.19	79.95	104.42	43.94	39.97	47.92
<b>Average</b>	<b>126.12</b>	<b>118.32</b>	<b>133.91</b>	<b>92.11</b>	<b>84.95</b>	<b>99.28</b>	<b>45.50</b>	<b>43.42</b>	<b>47.59</b>

Table 5.3. Mean conductivity measurements (in  $\mu\text{S m}^{-3}$ ), by finish and site.

When the role of finish type on conductivity was examined, as a group at each site, only the means calculated for London just reached significance between the finishes and the blank<sup>17</sup>. This result shows that the levels of conductivity from the stone run-off samples were higher than can explained solely by atmospheric deposition (the blank).

The other two sites did not show significant effects, either as a group, or through individual post-hoc T-test analyses between finish types<sup>18</sup>. Despite the significant group difference at London, there were no significant interactions between individual finishes<sup>19</sup>. This suggests finish type had a minimal role in influencing run-off concentrations. While the levels of component concentration might be higher for stone run-off in polluted atmospheres over atmospheric

<sup>15</sup> anova;  $F(1, 90) = 12.7$ ,  $P < 0.01$

<sup>16</sup> London against Birmingham;  $T(122) = 1.71$ ,  $P < 0.05$ , Birmingham against Dartmoor;  $T(69) = 3.27$ ,  $P < 0.01$

<sup>17</sup>  $F(2, 178) = 2.76$ ,  $P = 0.07$

<sup>18</sup> e.g. Birmingham, cut against blank;  $T(92) < 1$ , Dartmoor, polished against blank;  $T(92) = -1.31$ ,  $P = 0.1$

<sup>19</sup> flame against blank;  $T(124) = -1.22$ ,  $P = 0.1$

deposition alone, it is building placement within a given area that determines run-off concentrations.

### 5.2.2. Anions

Measurements of the anion components of the micro-catchment units run-off did not include  $\text{NH}_4^+$ . This was due to the weekly collection strategy, and the lack of temperature control at both the site and during transit to the laboratory. This would result in highly skewed ammonium values, and therefore it was decided to exclude any  $\text{NH}_4^+$  measurements from the study.

As a result of the lack of ammonium, however, it was not possible to ion balance the run-off measurements, which would provide a measure of the quality of obtained data set. Also, the measurement of  $\text{NH}_4^+$  would also allow an estimation of the sources of the pollution found in the run-off water.

Finally, if  $\text{NH}_4^+$  had been measured, analysis of the particulate sulphate-to-ammonium ratio would also provide information about scavenging efficiency and the dominant scavenging mechanism (Hidy and Countess, 1984). Concentration results are reported in parts per million (ppm (milligrams per litre)), to allow the comparison of the relative impact of both site and finish type.

Site	Chloride	Nitrate	Phosphate	Sulphate	SUM
London	11.5	11.38	2.95	21.63	<b>47.46</b>
Birmingham	9.08	6.62	1.88	15.45	<b>33.03</b>
Dartmoor	5.96	3.81	1.72	3.83	<b>15.32</b>

Table 5.4. Average site anion concentration (in ppm), across blank and finishes.

As can be seen in Table 5.4, the average anion concentration across the sites was highest for all species at the London site, situated at St. Paul's cathedral, while the rural Dartmoor site displayed the lowest concentrations. This pattern followed the pollution concentrations at the three sites.

#### 5.2.2.1. Chloride

When examined as a group, there were significant differences between

chloride concentrations (Table 5.5) at the three sites when analysed by anova<sup>20</sup>. This was confirmed by post-hoc T-tests, which showed each site was significantly different from the others<sup>21</sup>.

	London			Birmingham			Dartmoor		
	Mean	Std. Error: lower limit	Std. Error: upper limit	Mean	Std. Error: lower limit	Std. Error: upper limit	Mean	Std. Error: lower limit	Std. Error: upper limit
Blank	10.95	9.57	12.32	9.55	8.45	10.65	6.04	5.33	6.76
Polished	11.52	10.13	12.91	8.33	7.36	9.31	5.98	5.35	6.61
Cut	11.17	9.75	12.59	9.14	7.97	10.32	6.18	5.52	6.84
Flame	12.17	10.65	13.68	9.27	8.20	10.34	5.64	5.03	6.25
<b>Average</b>	<b>11.45</b>	<b>10.74</b>	<b>12.16</b>	<b>9.08</b>	<b>8.54</b>	<b>9.61</b>	<b>5.96</b>	<b>5.63</b>	<b>6.28</b>

Table 5.5. Chloride means (ppm) and standard error, by finish and site.

To determine the contribution ambient air quality played in  $\text{Cl}^-$  run-off concentrations at London, a correlation analysis was carried out on the chloride,  $\text{SO}_2$  and  $\text{NO}_x$  concentrations, shown below in Figure 5.2. Although a correlation does not imply a causal relationship between the examined pollutants, it does indicate the degree of co-occurrence of the values. It is on this basis that inferences were made. Although  $\text{NO}_x$  and  $\text{SO}_2$  were moderately correlated with each other ( $r = 0.62^{22}$ ) at the London site, the correlation with chloride concentrations was much lower ( $\text{SO}_2 = 0.29$ ,  $\text{NO}_x = 0.31$ ), and there was a seasonal distribution to  $\text{Cl}^-$  concentrations.

It seems likely, given the low levels of gaseous pollutant correlation, that the majority of  $\text{Cl}^-$  inputs were due to road de-icing salts, marine aerosols and mobile ionic sources such as carbonaceous particles. Road de-icing salts and marine aerosols are thought to be particularly important, as correlation analyses revealed a high degree of relationship between chloride and Ca ( $r = 0.74$ ) and Mg ions ( $r = 0.78$ ) (see appendix Table A.1).

Although the Birmingham chloride distribution appears similar to  $\text{SO}_2$  concentrations, shown below in Figure 5.3, correlation analyses showed that while

<sup>20</sup>  $F(1, 271) = 30.7$ ,  $P < 0.01$

<sup>21</sup> London against Birmingham;  $T(492) = 2.7$ ,  $P < 0.01$ , Birmingham against Dartmoor;  $T(405) = 6$ ,  $P < 0.01$

<sup>22</sup> All correlations are performed at the 95% confidence limit

SO<sub>2</sub> and NO<sub>x</sub> were highly correlated ( $r=0.78$ ), their relationship with chloride concentrations was much lower (correlation; SO<sub>2</sub> = 0.38, NO<sub>x</sub> = 0.36).

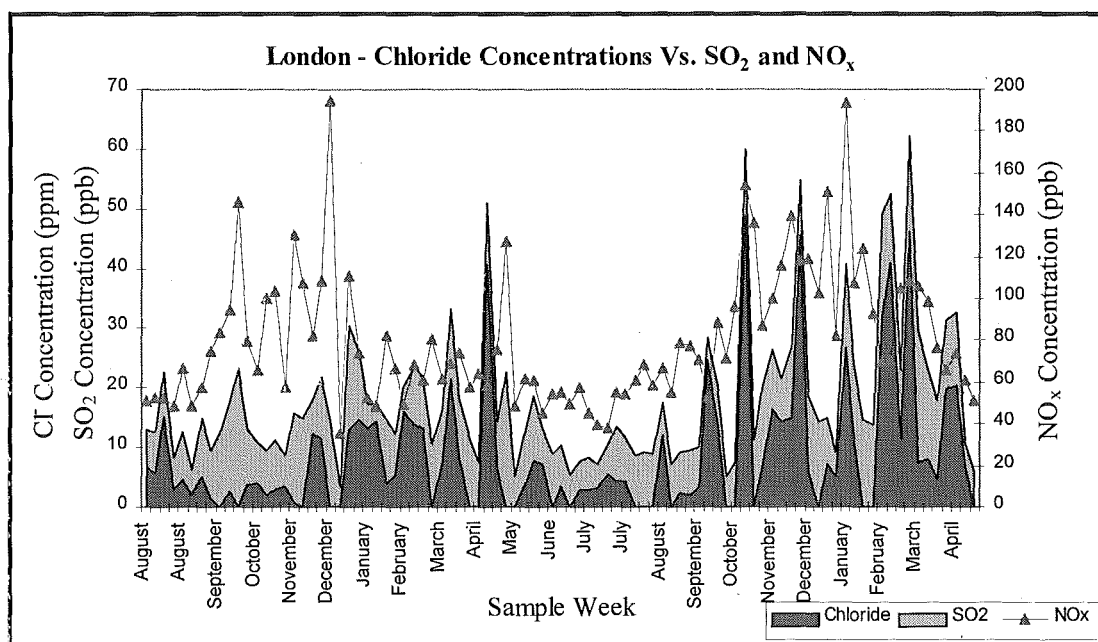


Figure 5.2. Weekly chloride, SO<sub>2</sub> and NO<sub>x</sub> distribution for London<sup>23</sup>.

This pattern was similar to that found at the London site (St. Paul's Cathedral), and with a similar seasonal distribution, although the degree of correlation between SO<sub>2</sub>, NO<sub>x</sub> concentrations and Cl<sup>-</sup> concentration in the run-off at Birmingham were marginally higher. This could possibly be explained by increased HCl deposition from coal pollution, produced by regional power stations (such as the Drax power station), which would increase the gaseous contribution to the chloride concentrations.

This route of chloride deposition was supported by correlation analyses, (see appendix Table A.2) which showed a reduced relationship between chloride and Ca<sup>++</sup> ( $r = 0.67$ ) and Mg<sup>++</sup> ( $r = 0.64$ ) ions, implying that salt deposition was not as important in determining Cl<sup>-</sup> run-off concentrations as it was at the London site. This conforms with an expected marine salt aerosol reduction as a result of Birmingham's inland position, although inputs from road de-icing salts were still important.

<sup>23</sup> Some months are mentioned twice comparison graphs. This is because five, rather than four, samples were taken during those months. Only one sample, however, was taken per week

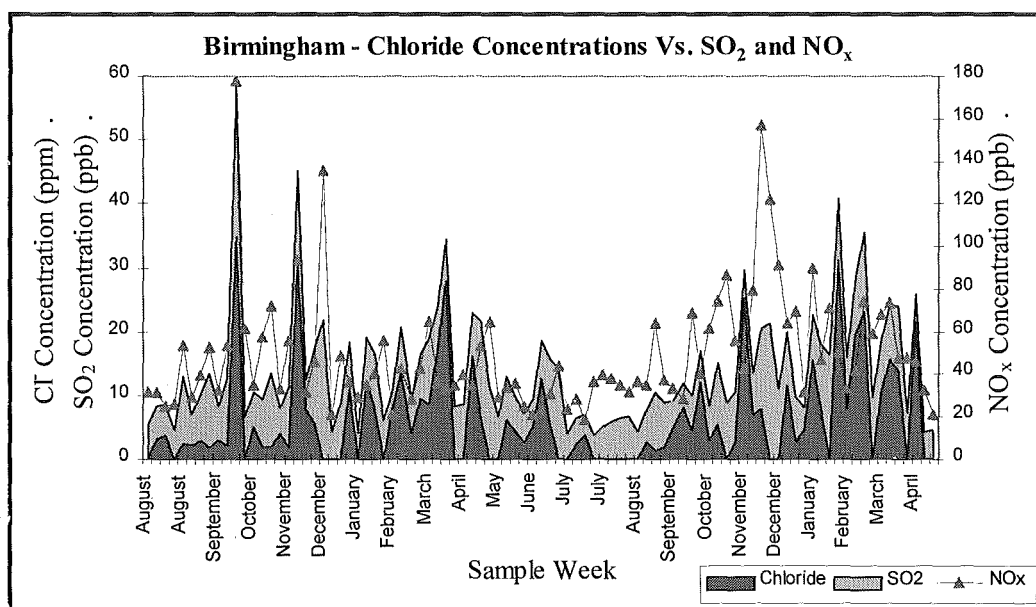


Figure 5.3. Weekly chloride, SO<sub>2</sub> and NO<sub>x</sub> distribution for Birmingham.

There was a strong seasonal distribution to the Dartmoor chloride values in Figure 5.4, one that was not reflected in the SO<sub>2</sub> levels measured at the site. As the weather became colder between October and March chloride values rise. They displayed approximately  $\frac{1}{4}$  their winter value during the summer months, which suggests there is a background run-off level of around 2-4 ppm at the Dartmoor site. Given the proximity to the ocean, the background Cl<sup>-</sup> concentrations may be produced by depositing marine aerosols.

During the colder months, the Cl<sup>-</sup> concentration rose. This could be due to increases from de-icing salts used during the winter period, but more likely from increased inputs from marine aerosols as a result of high winds and high seas. The correlation analysis, however, showed no clear relationship between chloride and any of the other measured pollutants (see appendix Table A.3), including SO<sub>2</sub> ( $r = -0.14$ ).

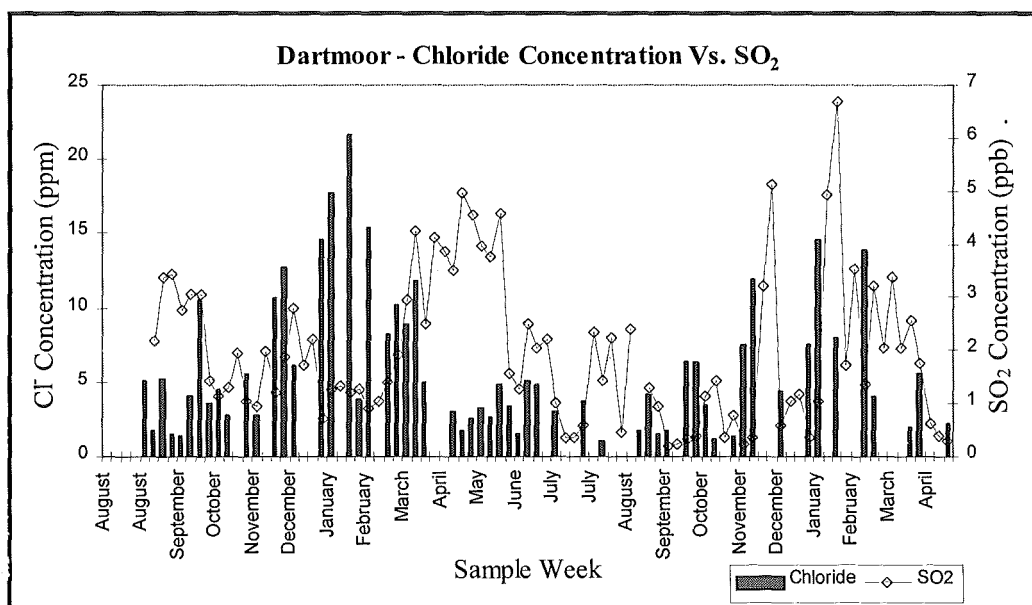


Figure 5.4. Weekly chloride and SO<sub>2</sub> distribution for Dartmoor.

When the role of finish type on chloride run-off concentrations across all three sites was examined, it was found to have a minimal effect. None of the sites showed any significant differences between the finishes and the blank when examined as a group<sup>24</sup>. Investigation of the relationship between individual finishes at each site by post-hoc T-test analyses also failed to show any significant differences<sup>25</sup>.

The lack of effect shown by the different finishes across all the sites, regardless of ambient pollution concentration, suggests that increasing roughness did not significantly increase the rate of Cl<sup>-</sup> deposition to the stone surface. However, this conclusion is only valid for the range of surface roughness represented by the exposed finish types ( $R_a = 0.016 - 0.134$ <sup>26</sup>). Given the significant differences between the values of the three site populations, and the lack of differentiation in the values from the different finish types, it would seem that the dominant factor in the determination of run-off concentrations was, as would be expected, the site, with London receiving major inputs from marine aerosols and road de-icing salts,

<sup>24</sup> i.e. St Paul's;  $F(2, 178) = 1.44$ ,  $P > 0.1$

<sup>25</sup> London, blank against flame;  $T(67) < 1$ , and Dartmoor, blank against cut;  $T(57) = 1.22$ ,  $P > 0.1$

<sup>26</sup> See section 4.7.3

Birmingham, road de-icing salts, as well as HCl deposition from coal burning, and Dartmoor from marine salts.

#### 5.2.2.2. Nitrate

Although  $\text{NH}_3$  was not measured nitrate stability was not an issue, with concentration degradation over a four week period at less than 5-10% (Ridder *et al*, 1985). An anova analysis of nitrate values across the three sites, with mean values shown in Table 5.6, showed a significant difference between the concentrations<sup>27</sup>. Post-hoc T-tests confirmed this, with significant differences found between all sites when analysed individually<sup>28</sup>.

	London			Birmingham			Dartmoor		
	Mean	Std. Error: lower limit	Std. Error: upper limit	Mean	Std. Error: lower limit	Std. Error: upper limit	Mean	Std. Error: lower limit	Std. Error: upper limit
Blank	10.82	9.27	12.37	7.38	6.30	8.46	3.97	3.37	4.56
Polished	11.36	9.95	12.78	5.97	5.05	6.89	3.78	3.29	4.26
Cut	11.41	9.93	12.89	6.81	5.73	7.90	3.54	3.06	4.03
Flame	11.21	9.78	12.64	6.41	5.48	7.34	3.85	3.30	4.40
<b>Average</b>	<b>11.20</b>	<b>10.47</b>	<b>11.93</b>	<b>6.64</b>	<b>6.14</b>	<b>7.14</b>	<b>3.79</b>	<b>3.52</b>	<b>4.05</b>

Table 5.6. Nitrate means (ppm) and standard error, by finish and site.

To determine the effect of air pollution levels on nitrate concentrations within the London run-off, correlation analyses were carried out (see appendix Table A.1). These showed no valid relationship between  $\text{SO}_2$ ,  $\text{NO}_x$  and nitrate concentration ( $\text{SO}_2 = 0.01$ , and  $\text{NO}_x = -0.13$ ). These values were much lower than the relationship between the gaseous pollutants and  $\text{Cl}^-$ . This suggests that a proportion of the deposited nitrate aerosols, formed by the reaction of  $\text{NO}_x$  with  $\text{HN}_3$  or Na, was non-atmospheric in origin and could be derived from other building run-off. This was supported by correlation values, which failed to show a high degree of correlation between nitrate and any other pollutant component except sulphate ( $r = 0.74$ ).

<sup>27</sup>  $F(1, 270) = 31.9$ ,  $P < 0.01$

<sup>28</sup> London against Birmingham;  $T(469) = 5.1$ ,  $P < 0.01$ , Birmingham against Dartmoor;  $T(375) = 5$ ,  $P < 0.01$

There was also a seasonal component to the London nitrate concentrations, shown below in Figure 5.5, however, with higher concentrations recorded during the summer months, and lower values reported during spring (January - March). It is possible that this was due to increased production of  $\text{NO}_2$  and photochemical smogs.

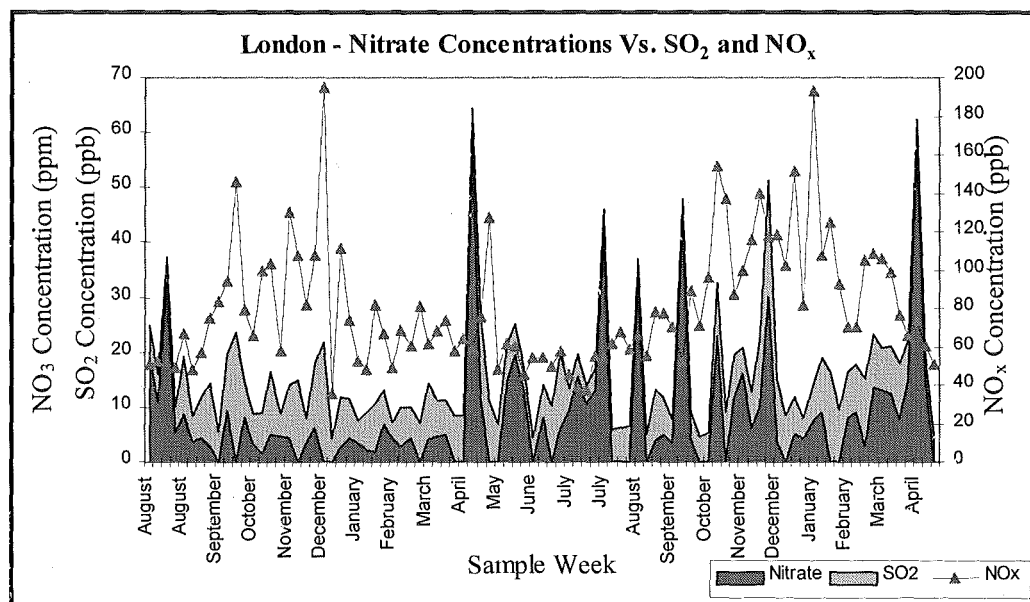


Figure 5.5. Weekly nitrate,  $\text{SO}_2$  and  $\text{NO}_x$  distribution for London.

The relationship between ambient air quality and run-off nitrate concentrations at the Birmingham site was determined by correlation analysis. This showed that the degree of relatedness between nitrate values and  $\text{SO}_2$  and  $\text{NO}_x$ , shown below in Figure 5.6, ( $\text{SO}_2 = 0.44$ ,  $\text{NO}_x = 0.5$ ) was once again higher at Birmingham than at London.

The higher degree of correlation (shown in appendix Table A.2) might be partially explained by a reduction in the number of atmospheric pollutants at the Birmingham site. A reduction in the degree of seasonality in the run-off concentrations could also increase the degree of relationship between the pollutants and the run-off concentration. More importantly, however, the correlation analysis showed that nitrate was the most strongly correlated with  $\text{Ca}^{++}$  ( $r = 0.86$ ) and  $\text{Mg}^{++}$  ( $r = 0.82$ ). This suggests that the majority of nitrate was deposited by salt aerosols.



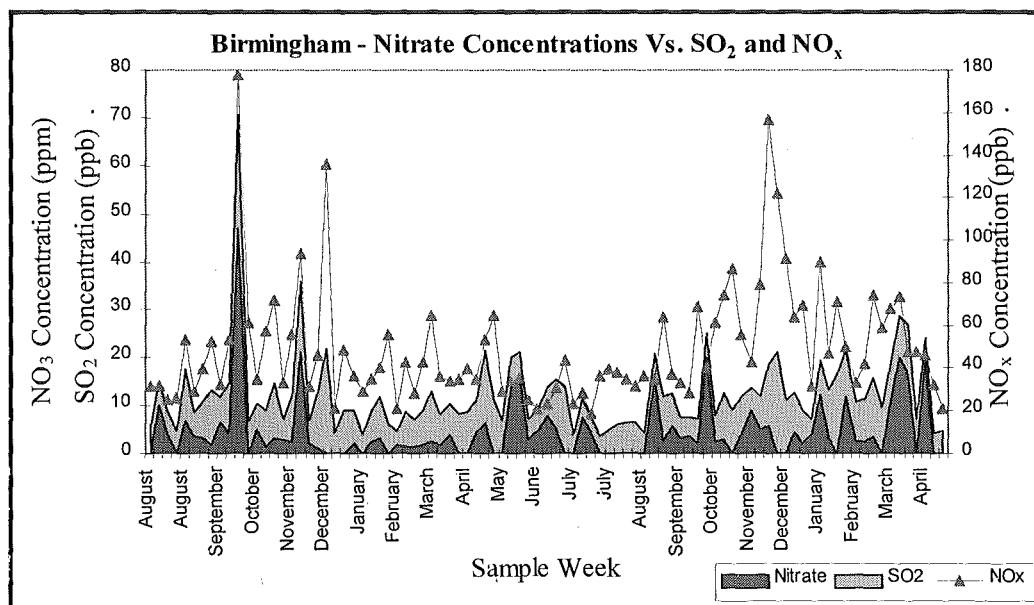


Figure 5.6. Weekly nitrate, SO<sub>2</sub> and NO<sub>x</sub> distribution for Birmingham.

The Dartmoor nitrate concentrations, shown below in Figure 5.7, were significantly lower than both of the urban sites, which is to be expected given the reduction in the number of NO<sub>x</sub> sources in the Dartmoor national park. It does, however, follow the seasonal distribution of London, rather than Birmingham, with a low correlation with SO<sub>2</sub> ( $r = 0.17$ ), and summer concentrations approximately 3 - 4 times as large as winter.

This might be explained by an increase in the number of tourists and visitors to the park, the majority of whom will drive. When examined by correlation analysis, shown in appendix Table A.3, the only significant relationship was between nitrate and sulphate levels ( $r = 0.85$ ). The high level of relationship between the two pollutants might be the result of co-deposition and adsorption by precipitation.

When the role of finish type was examined across all the sites, both London and Dartmoor showed no significant differences between the blank and finish sample populations when examined as a group. The lack of any main effect between the finishes at each site was further examined by post-hoc T-test comparisons between the individual finishes. These also failed to show any significant differences<sup>29</sup>. The Birmingham site almost reached significance between the stone finishes and the

<sup>29</sup> London, blank against cut;  $T(134) < 1$ , and Dartmoor, blank against cut;  $T(108) < 1$

blank when analysed as a group by anova<sup>30</sup>. The lack of significance was replicated by the analysis of individual finishes against each other by T-tests<sup>31</sup>.

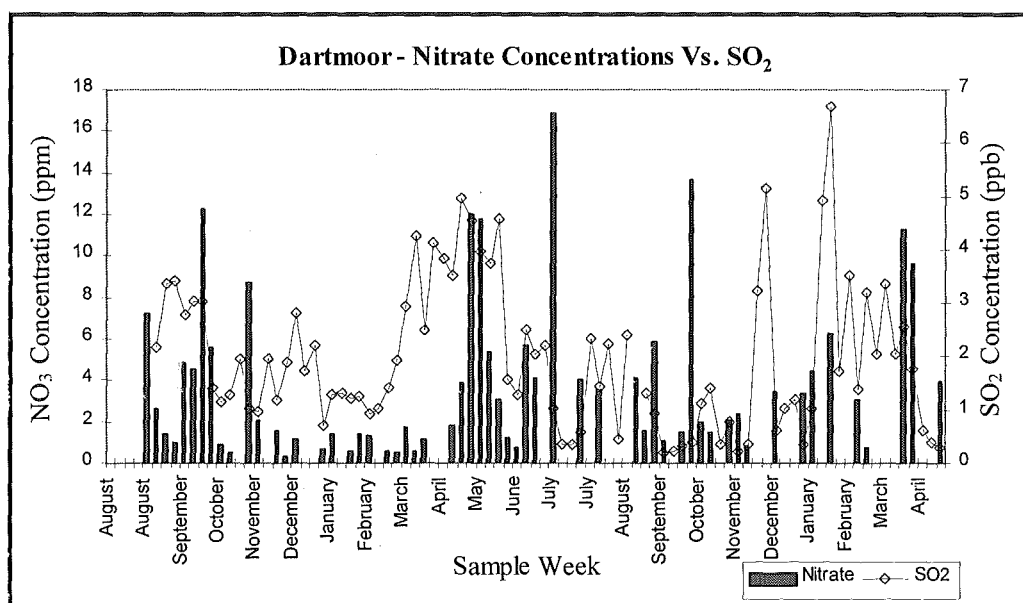


Figure 5.7. Weekly nitrate and SO<sub>2</sub> distribution for Dartmoor.

As with chloride concentrations in the run-off, nitrate values do not seem to have been influenced by changes in roughness between the finishes. Also, the lack of any significant difference between the blanks and the stone micro-catchment units at each site, suggests that once again, it was the site that is the determining factor for run-off concentration, not roughness.

#### 5.2.2.3. Phosphate

Although phosphate was one of the measured anion components in the M.C.U. run-off, it displayed a low degree of incidence within the sample period, and low averages (see Table 5.7 below) across the sites. As a result it will be primarily discussed as a cross-site component.

<sup>30</sup>  $F(2, 176) = 2.68, P = 0.07$

<sup>31</sup> blank against cut;  $T(122) < 1$ , blank against polished;  $T(121) < 1$

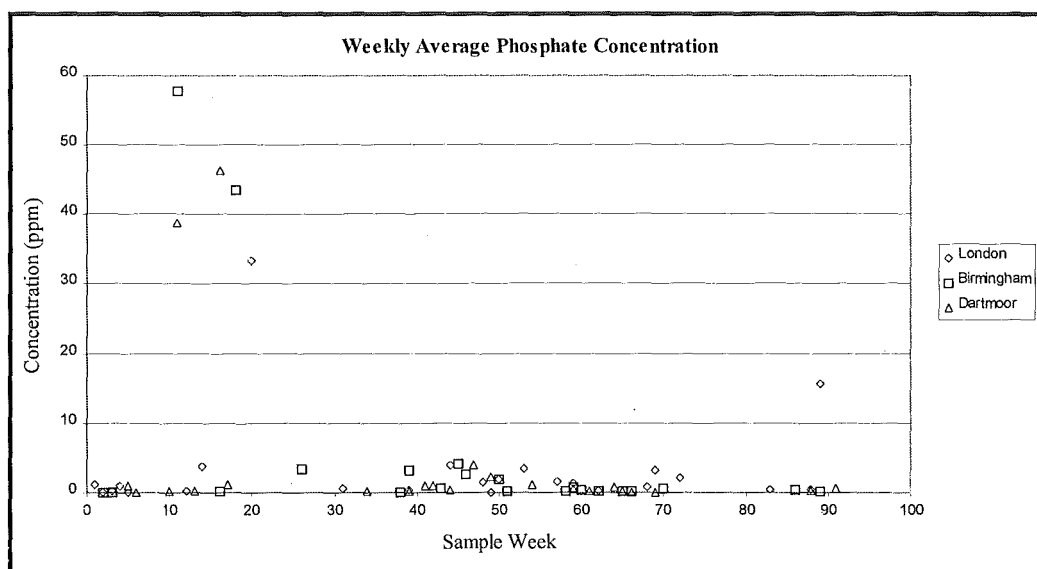


Figure 5.8. Weekly average phosphate concentrations.

Phosphate concentrations, shown above in Figure 5.8, were first analysed across all the sites, using average weekly values. anova analysis, however, showed no significant differences between the sites<sup>32</sup>. The lack of significance was confirmed by post-hoc T-tests, which showed no effects between the sites when examined individually<sup>33</sup>. The lack of significance between the sites is primarily explained by the low  $\text{PO}_4^{3-}$  means, and by the large number of times the phosphate was not detected in the run-off samples.

	London			Birmingham			Dartmoor		
	Mean	Std. Error: lower limit	Std. Error: upper limit	Mean	Std. Error: lower limit	Std. Error: upper limit	Mean	Std. Error: lower limit	Std. Error: upper limit
Blank	2.37	0.81	3.92	1.86	0.83	2.90	1.33	0.53	2.14
Polished	3.03	1.01	5.05	2.56	0.96	4.16	2.04	0.71	3.37
Cut	2.32	0.98	3.67	1.83	0.61	3.05	2.24	0.82	3.67
Flame	4.12	1.44	6.81	1.29	0.49	2.08	1.36	0.19	2.53
<b>Average</b>	<b>2.96</b>	<b>1.98</b>	<b>3.93</b>	<b>1.89</b>	<b>1.29</b>	<b>2.48</b>	<b>1.74</b>	<b>1.14</b>	<b>2.34</b>

Table 5.7. Phosphate means (ppm) and standard error, by finish and site.

<sup>32</sup>  $F(1, 271) < 1$

<sup>33</sup> London against Dartmoor;  $T(271) = 1.1$ ;  $P > 0.1$

When phosphate values were examined by group analysis across all sites, the phosphate distribution between the blank and the three finishes failed to show any significant interactions at any of the sites<sup>34</sup>. The lack of any effect between the finishes by group was supported by post-hoc T-tests between individual finishes at each site<sup>35</sup>. Given the low occurrence in the run-off samples, the lack of significance between any of the finishes at the three sites, and the low degree of correlation (shown in appendix tables A.1 and A.3) with any other major component, it may be that the majority of the phosphate was of biological origin, i.e. bird droppings.

The exception to this was the Birmingham site (Table A.2), where phosphate showed a high degree of correlation with four other species (correlation;  $\text{SO}_4 = 0.94$ ,  $\text{Al}^{3+} = 0.9$ ,  $\text{Ca}^{++} = 0.9$  and  $\text{Mg}^{++} = 0.9$ ). Why these elements showed a strong relationship with phosphate is not obvious at this point.

Unlike the other measured anions in the exposure programme, phosphate showed no significant changes in concentration between either the sites or the finishes. This, coupled with the infrequent detection of the component within run-off samples, could be explained if the source was biological in origin.

#### 5.2.2.4. Sulphate

Analysis of weekly average sulphate concentrations, in Table 5.8, showed a significant difference between the three sites, when examined as a group<sup>36</sup>. Further investigation of the interactions of individual sites by post-hoc T-tests also showed significant differences between all the sites<sup>37</sup>.

A correlation analysis was carried out on the sulphate concentration of the London run-off, and the ambient concentrations of  $\text{SO}_2$  and  $\text{NO}_x$  (shown below in Figure 5.9) to determine the relationship between pollutant concentration and gaseous deposition and sulphate concentration in the run-off. It was found that although  $\text{SO}_2$  was low ( $r = 0.26$ ), the role of  $\text{NO}_x$  was (as expected) much lower ( $r = 0.05$ ).

<sup>34</sup> e.g. . London site,  $F(2, 176) = 1.52$ ,  $P > 0.1$ , and Dartmoor,  $F(2, 180) < 1$

<sup>35</sup> Birmingham, blank against polished;  $T(108) < 1$ , and Dartmoor, blank against cut;  $T(87) < 1$

<sup>36</sup>  $F(1, 90) = 15.2$ ,  $P < 0.01$

<sup>37</sup> London against Birmingham;  $T(270) = 2.7$ ,  $P < 0.01$ , and Birmingham against Dartmoor;  $T(256) = 7.2$ ,  $P < 0.01$

	London			Birmingham			Dartmoor		
	Mean	Std. Error: lower limit	Std. Error: upper limit	Mean	Std. Error: lower limit	Std. Error: upper limit	Mean	Std. Error: lower limit	Std. Error: upper limit
Blank	19.02	16.29	21.75	12.64	10.69	14.60	3.43	3.16	3.71
Polished	20.92	18.52	23.32	13.47	11.03	15.91	3.90	3.57	4.23
Cut	22.27	19.43	25.11	18.40	14.14	22.65	4.18	3.64	4.72
Flame	22.12	19.38	24.86	17.46	13.69	21.23	3.78	3.46	4.10
<b>Average</b>	<b>21.08</b>	<b>19.74</b>	<b>22.42</b>	<b>15.47</b>	<b>13.86</b>	<b>17.08</b>	<b>3.82</b>	<b>3.63</b>	<b>4.01</b>

Table 5.8. Sulphate means (ppm) and standard error, by finish and site.

The analysis also showed that sulphate levels were most strongly related to calcium ( $r = 0.93$ ) and magnesium ( $r = 0.71$ ) levels. This could be due to gypsum and magnesium sulphate (epsomite, hexahydrate or thenardite) deposition on the surface of the granite slabs from external sources, such as carbonaceous particles, urban dust and  $\text{CaCO}_3/\text{CaSO}_4$  from St Paul's itself. Roekens *et al* (1988) and Leysen *et al* (1989) have recorded higher pH and  $\text{Ca}^{++}$  concentrations in wet and total-deposition samples taken from around a limestone cathedral in Belgium than results from rain collection networks in Belgium and the Netherlands.

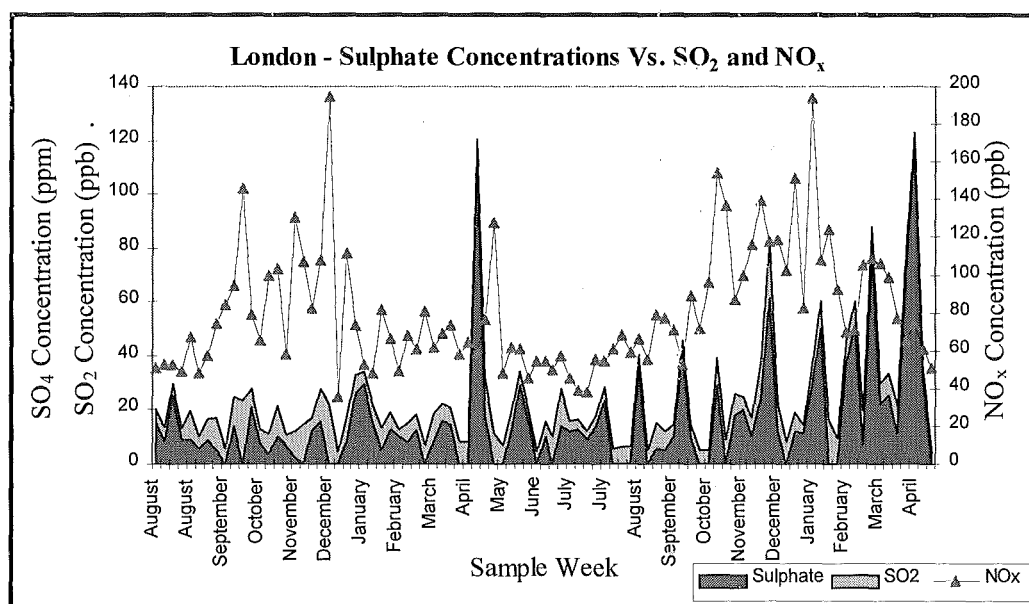


Figure 5.9. Weekly sulphate,  $\text{SO}_2$  and  $\text{NO}_x$  distribution for London.

Analysis of the ambient air quality and sulphate levels in the Birmingham run-off, shown in Figure 5.10, showed a moderate level of relationship, with  $\text{SO}_2$  ( $r = 0.56$ ) and  $\text{NO}_x$  ( $r = 0.53$ ) concentrations both co-occurring with sulphate levels. Sulphate was, however, most related to phosphate ( $r = 0.94$ ), aluminium ( $r = 0.86$ ), calcium ( $r = 0.94$ ) and magnesium ( $r = 0.85$ ) levels. The latter three are strongly suggestive of  $\text{CaSO}_4$ ,  $\text{MgSO}_4$  and  $\text{AlSO}_4$  formation and deposition.

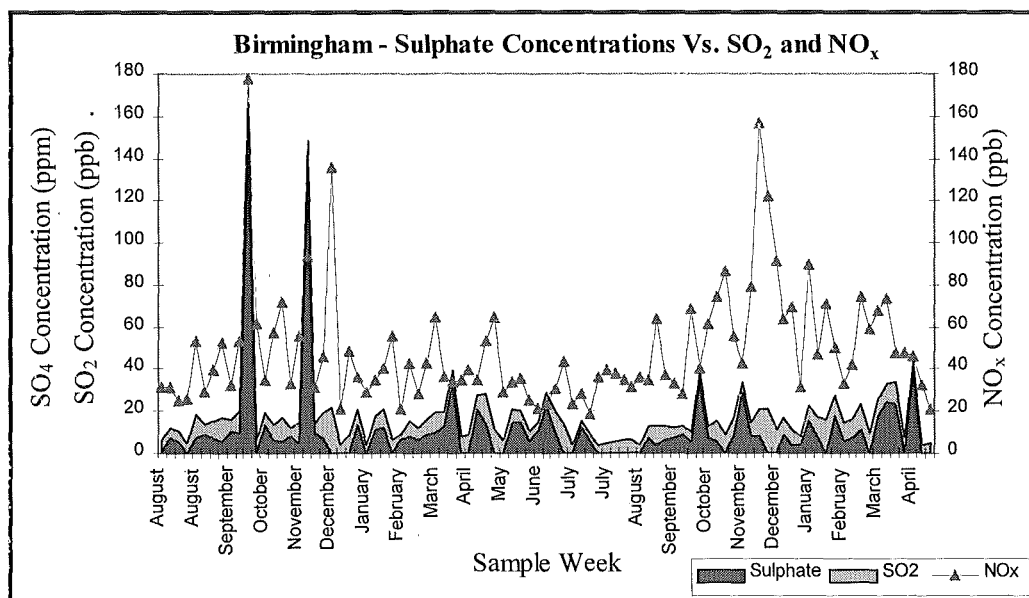


Figure 5.10. Weekly sulphate,  $\text{SO}_2$  and  $\text{NO}_x$  distribution for Birmingham.

The correlation between sulphate values and the major pollutant species at Dartmoor showed a similar distribution to the other two sites, with the most highly correlated ions being  $\text{Ca}^{++}$  ( $r = 0.73$ ) and  $\text{Mg}^{++}$  ( $r = 0.7$ ) (see appendix Table A.3).  $\text{SO}_2$  showed no correlation with sulphate values in the run-off ( $r = 0.19$ ). Although the Dartmoor site was a rural site, surrounded by acid, igneous rocks and removed from large urban centres, the correlation values suggest that there was still a major sulphate contribution from gypsum and one of the magnesium sulphate species (i.e. epsomite,  $\text{MgSO}_4 \cdot 7\text{H}_2\text{O}$ , hexahydrate,  $\text{MgSO}_4 \cdot 6\text{H}_2\text{O}$  or thenardite,  $\text{MgSO}_4$ ).

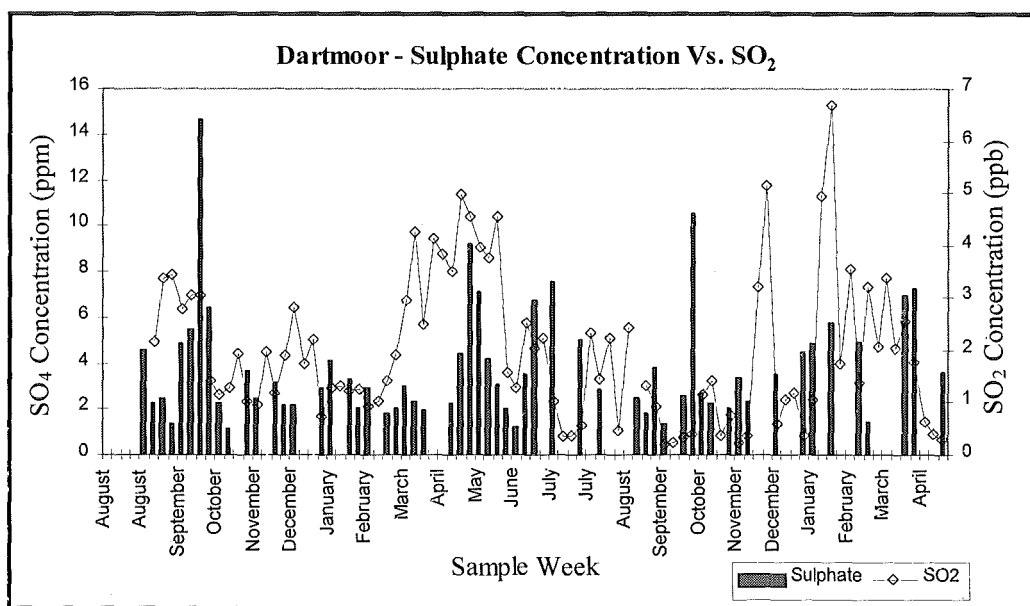


Figure 5.11. Weekly sulphate and SO<sub>2</sub> distribution for Dartmoor.

To examine the impact of surface finish on run-off concentrations, further analyses were carried out, across the blank and finish types, at each site. Although London and Dartmoor showed no significant differences in the sulphate concentrations, when examined by group, Birmingham revealed a main effect<sup>38</sup> between the finishes and the blank. Post-hoc T-test examinations of the individual finishes at each site failed, however, to show any other significant interactions<sup>39</sup>.

Sulphate followed the pattern of all the measured anions, except phosphate. Although there were significant differences between the population values for each site, with the most polluted site (London) having the highest mean concentrations, the finish seemed to have little effect on sulphate concentration. Although sulphate values from the Birmingham stones were higher than the blank, this was not repeated at the other sites, and there were no significant inter-finish variations.

### 5.2.3. Metals

Four major metals were measured in the run-off from the three sites; Al<sup>3+</sup>, Ca<sup>++</sup>, Mg<sup>++</sup> and Fe<sup>++</sup>. While Mg<sup>++</sup> is mainly derived from sea salt and terrestrial dust, Al<sup>3+</sup>, Ca<sup>++</sup> and Fe<sup>++</sup> are usually associated with anthropogenic processes such as

<sup>38</sup>  $F(2, 176) = 3.1, P = 0.05$

<sup>39</sup> e.g. London, blank against flame;  $T(133) < 1$ , and Dartmoor, blank against cut;  $T(83) = -1.23, P < 0.1$

industry and power generation, and generally occur in the fine fraction of airborne particles (QUARG, 1996). Although there are differences in the compositional variation between the coarse and fine particle fractions, metal ions are approximately 5% of the total composition of typical urban particles (QUARG, 1993a).

Measurement of metal concentrations in the run-off samples was by Inductively Coupled Plasma Spectrometer (ICP), as described in section 4.7.2, and was designed to provide a relative indication of the rates of leaching of the minerals within the granite slabs. Aluminium and calcium are found within feldspars, while iron and magnesium are found within biotite minerals, both of which are susceptible to weathering processes and secondary alteration.

### 5.2.3.1. Aluminium.

Initial analysis of the weekly average aluminium concentrations for the three sites showed a significant level of difference between the means<sup>40</sup>, shown in Table 5.9. This was confirmed by post-hoc T-test analyses of individual sites, which revealed that Birmingham values were significantly higher than either London or Dartmoor<sup>41</sup>, and that Dartmoor was lower than London<sup>42</sup>.

	London			Birmingham			Dartmoor		
	Mean	Std. Error: lower limit	Std. Error: upper limit	Mean	Std. Error: lower limit	Std. Error: upper limit	Mean	Std. Error: lower limit	Std. Error: upper limit
Blank	98.44	86.14	110.73	149.26	120.96	177.56	71.38	61.70	81.07
Polished	88.51	78.69	98.33	145.93	116.66	175.20	82.31	71.13	93.48
Cut	89.20	76.52	101.89	134.30	104.31	164.30	75.66	67.73	83.58
Flame	87.76	76.85	98.66	122.76	98.76	146.76	80.28	69.55	91.02
<b>Average</b>	<b>91.14</b>	<b>85.41</b>	<b>96.87</b>	<b>138.04</b>	<b>124.18</b>	<b>151.89</b>	<b>77.42</b>	<b>72.46</b>	<b>82.37</b>

Table 5.9. Al<sup>3+</sup> runoff means (ppm) and standard error, by finish and site.

The role of ambient air quality in terms of the contribution to aluminium concentrations, shown below in Figure 5.12 in the London run-off was assessed by a correlation analysis, shown in appendix Table A.1. This showed that although the

<sup>40</sup>  $F(1,188) = 22.9, P < 0.01$

<sup>41</sup>  $T(237) = -3.1, P < 0.01$

<sup>42</sup>  $T(83) = 1.8, P < 0.05$



gaseous pollutants  $\text{SO}_2$  and  $\text{NO}_x$  were moderately correlated at the London site ( $r=0.62$ ), their co-occurrence with  $\text{Al}^{3+}$  concentrations was limited ( $\text{SO}_2 = 0.14$ , and  $\text{NO}_x = 0.15$ ). This indicates that  $\text{Al}^{3+}$  concentrations do not rise in line with increases in  $\text{SO}_2$  or  $\text{NO}_x$  or any other measured component. Coupled with the apparent seasonal distribution, it is suggested that concentrations within run-off were generated by internal dissolution, or by aluminium leached from deposited particulates generated by point sources such as coal-fired power stations and industrial plants.

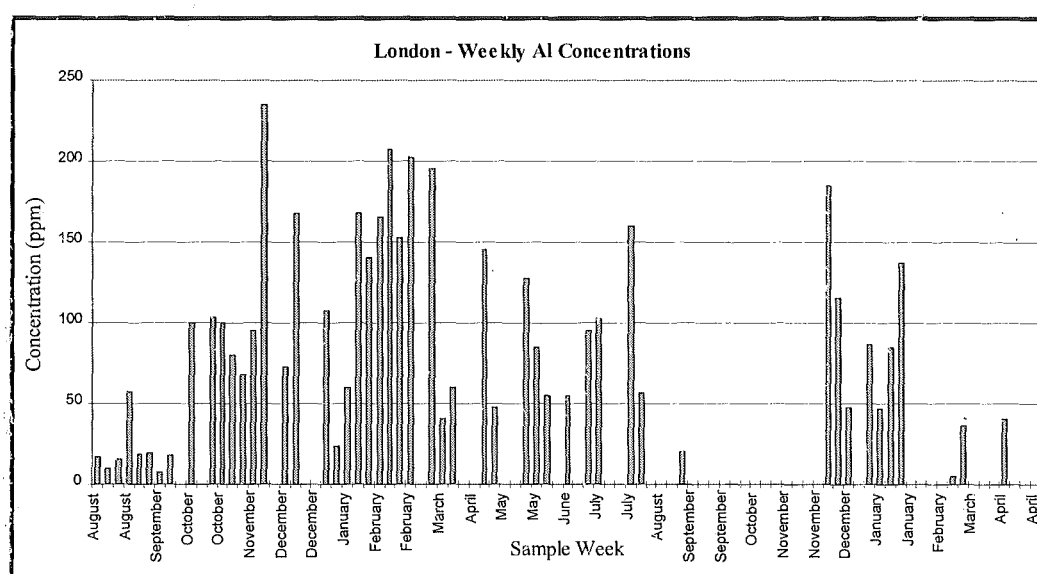
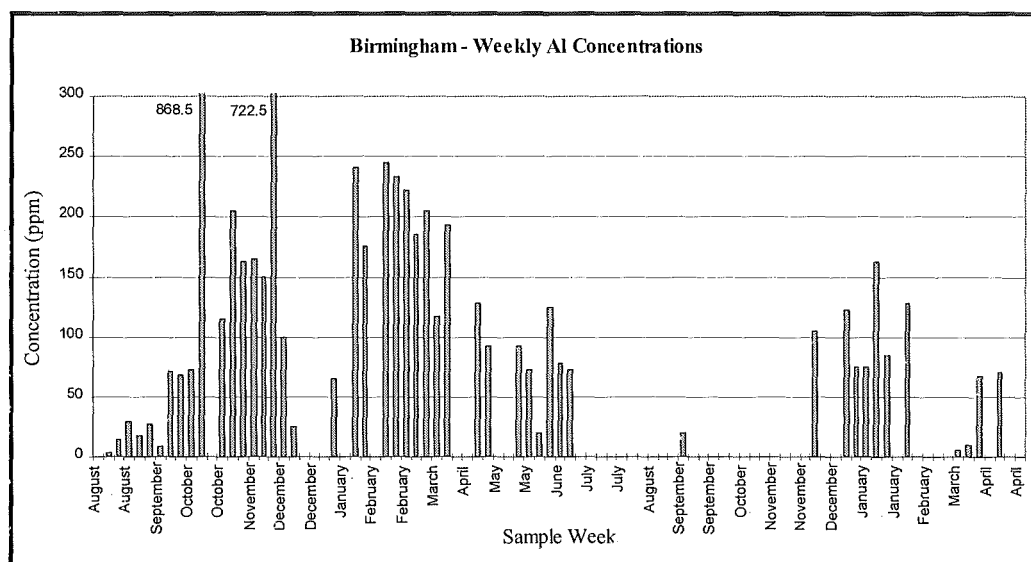


Figure 5.12. London runoff; average weekly aluminium distribution.

A correlation between the gaseous pollutant concentrations at Birmingham and Al concentrations in the run-off water (shown below in Figure 5.13) showed a far higher degree of correlation than that found at the London site, with  $\text{SO}_2$  and  $\text{NO}_x$  highly correlated with each other ( $r = 0.78$ ), and moderately correlated with  $\text{Al}^{3+}$  concentrations ( $\text{SO}_2 = 0.58$ , and  $\text{NO}_x = 0.57$ ). The similarity in their correlation with  $\text{Al}^{3+}$ , however, is explained by their own relatedness, rather than a true independent relationship.

The correlation also showed that  $\text{Al}^{3+}$  was actually most related to  $\text{Ca}^{++}$  ( $r = 0.79$ ) and  $\text{Mg}^{++}$  ( $r = 0.95$ ) - which may indicate that they were deposited from the same source, i.e. carbonaceous particles from power plants, which are rich sources of

metal ions and other pollutants. This theory was supported by the seasonal distribution of  $\text{Al}^{3+}$  concentrations, which increased in winter as power plant output increases and dropped during the warmer, summer months when power output decreases.



significance in the group analysis was repeated with individual finish comparisons by T-test<sup>44</sup>.

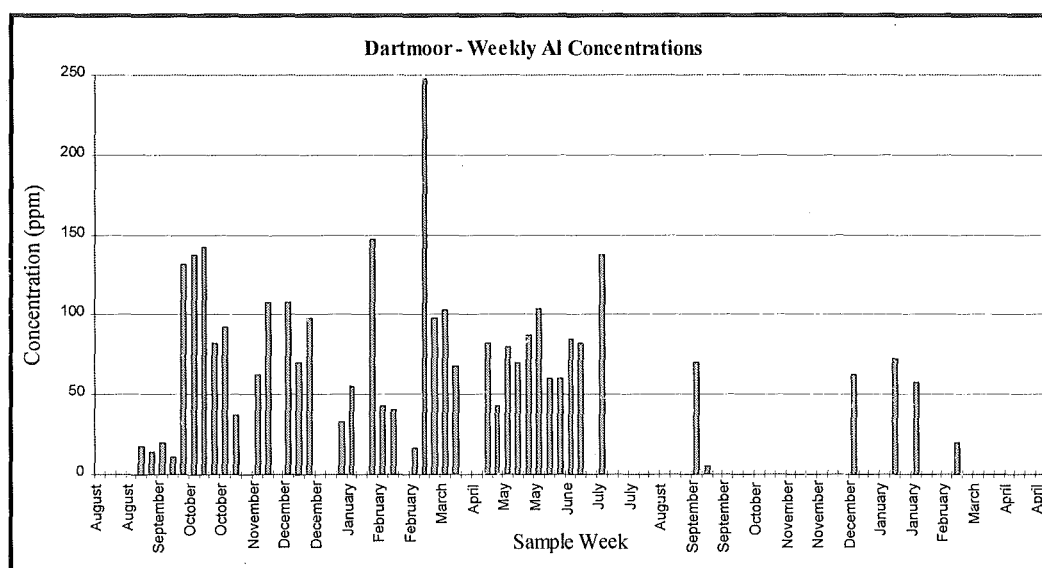


Figure 5.14. Dartmoor runoff; average weekly aluminium distribution.

Dartmoor was the cleanest of the three sites, and unlike the urban sites had mean stone finish values that were higher than the blank mean. There were no significant differences between the finishes and the blank when analysed as a group. There were also no differences found between individual finishes.

With a similar distribution to the anion analyses,  $\text{Al}^{3+}$  showed a significant difference between all three sites. It differed from the anion concentration pattern, however, in that Birmingham, the urban site with lower gaseous pollution levels, displayed the highest concentrations of  $\text{Al}^{3+}$  in the run-off, and it was significantly higher than either the London or Dartmoor sites. This would suggest that the Birmingham site location was, on average, positioned closer to one or more point sources than either of the other sites, which would produce an increase in concentration levels as Al-rich particulates deposited on sample stone surfaces.

The importance of deposition in  $\text{Al}^{3+}$  run-off concentrations is demonstrated by the individual blank and finish means. At the more polluted sites (Birmingham and London), blank mean values were higher than those from the stones. It was only

<sup>44</sup> e.g. blank against flame;  $T(90) > 1$

the least polluted Dartmoor site that had stone finish values higher than those generated by the blank. This, coupled with the lack of significant differences between the finishes, suggests that the role of surface roughness was minimal in affecting  $\text{Al}^{3+}$  concentrations.

### 5.2.3.2. Calcium.

Investigations of the role of site in calcium concentrations, shown below in Table 5.10, reveal there are significant differences between the sites when examined overall<sup>45</sup>. This was supported by post-hoc tests, which showed significant differences between London and Birmingham<sup>46</sup>, and Birmingham and Dartmoor<sup>47</sup>.

All of the sites followed the expected distribution, with the London site, St. Paul's (located on the roof of a Portland limestone building), having twice the  $\text{Ca}^{++}$  concentration of the Birmingham site, and six times that of the Dartmoor site.

	London			Birmingham			Dartmoor		
	Mean	Std. Error: lower limit	Std. Error: upper limit	Mean	Std. Error: lower limit	Std. Error: upper limit	Mean	Std. Error: lower limit	Std. Error: upper limit
Blank	10114.8	8830.8	11398.8	4043.2	3463.8	4622.6	1203.1	1050.3	1355.8
Polished	10461.6	9372.8	11550.3	4316.4	3573.8	5058.9	2005.8	1826.1	2185.5
Cut	10632.6	9462.6	11802.6	5126.0	4423.4	5828.5	1638.9	1508.1	1769.7
Flame	11578.3	10392.1	12764.5	4869.2	4142.7	5595.7	1297.9	1145.2	1450.7
<b>Average</b>	<b>10698.2</b>	<b>10107.9</b>	<b>11288.4</b>	<b>4583.3</b>	<b>4239.2</b>	<b>4927.5</b>	<b>1535.5</b>	<b>1455.5</b>	<b>1615.5</b>

Table 5.10.  $\text{Ca}^{++}$  runoff means (ppm) and standard error, by finish and site.

Correlation analysis of calcium concentrations in the London run-off, shown in Figure 5.15, in comparison to  $\text{SO}_2$  and  $\text{NO}_x$  showed a low degree of relatedness ( $\text{SO}_2 = 0.29$ ,  $\text{NO}_x = 0.16$ ). This result indicates that the concentrations of these gaseous pollutants had no more effect on  $\text{Ca}^{++}$  concentrations than that ascribed by chance. Calcium had a much higher degree of relationship with other measured components, however, with strong correlation values occurring with  $\text{Mg}^{++}$  ( $r = 0.84$ ), sulphate ( $r = 0.93$ ) and chloride ( $r = 0.74$ ) levels.

<sup>45</sup>  $F(1, 271) = 76.9$ ,  $P < 0.01$

<sup>46</sup>  $T(429) = 8.9$ ,  $P < 0.01$

<sup>47</sup>  $T(226) = 8.6$ ,  $P < 0.01$

This suggests that the majority of  $\text{Ca}^{++}$  was deposited as calcium sulphate ( $\text{CaSO}_4$ ), and the high level of relationship with Mg indicates that they are of atmospheric origin, such as urban dust (QUARG, 1996). Aerosols derived from the dissolution of limestone of St. Paul's cathedral will also contribute the  $\text{Ca}^{++}$  measured in the London run-off.

Although there was no obvious seasonality to the  $\text{Ca}^{++}$  distribution, the mean of the run-off concentration increased over the length of the exposure period. While this was undoubtedly modified by several exceptionally high values towards the end of the sampling period, the increasing mean could have been due to the dissolution of  $\text{Ca}^{++}$  contained within the M.C.U.s granodiorite plagioclase feldspars, or to increased inputs from the limestone fabric of the cathedral.

However, as the increasing mean was not repeated at the other two sites, which displayed a decrease in mean run-off  $\text{Ca}^{++}$  concentrations over the length of the exposure period, it is suggested that it was inputs from the body of St. Paul's Cathedral that resulted in the increased  $\text{Ca}^{++}$  concentrations.

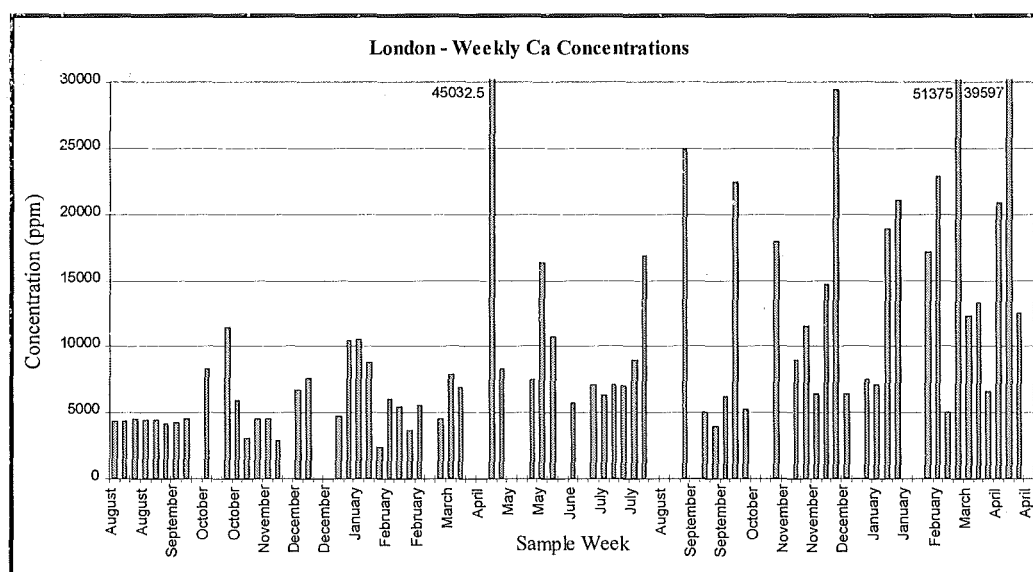


Figure 5.15. Weekly calcium runoff distribution, London.

To assess the impact of ambient pollution levels on  $\text{Ca}^{++}$  concentrations (shown in Figure 5.16) at the Birmingham site, a correlation analysis was carried out between the measured components. As found in the aluminium analysis, the

Birmingham correlation figures ( $\text{SO}_2 = 0.54$ , and  $\text{NO}_x = 0.54$ ) were over twice as large as those for London. This would suggest that there were less pollutant species at the Birmingham site, producing higher levels of correlation. Other analyses provide support for this claim, showing that  $\text{Ca}^{++}$  was highly correlated with  $\text{Mg}^{++}$  ( $r = 0.95$ ),  $\text{Al}^{3+}$  ( $r = 0.79$ ), sulphate ( $r = 0.94$ ) and nitrate ( $r = 0.86$ ).

The high levels of correlation between the  $\text{Ca}^{++}$  and  $\text{Mg}^{++}$ ,  $\text{Ca}^{++}$  and  $\text{SO}_4^{2-}$  and  $\text{Mg}^{++}$  and  $\text{SO}_4^{2-}$  point to an atmospheric input from particulates such as urban dust, rather than to material lost by the stone (Sweevers et al, 1995). Urban dust contains high levels of  $\text{Ca}^{++}$  and  $\text{Mg}^{++}$  (mean  $\text{Ca}^{++}$  concentration of dust sample from Lancaster:  $0.400 \mu\text{m}/\text{m}^3$ ,  $\text{Mg}^{++}$ :  $0.146 \mu\text{m}/\text{m}^3$  (QUARG, 1996)), and could explain the elevated  $\text{Ca}^{++}$  concentrations found in the run-off water in comparison to Dartmoor, and the high level of correlation with  $\text{Mg}^{++}$ .

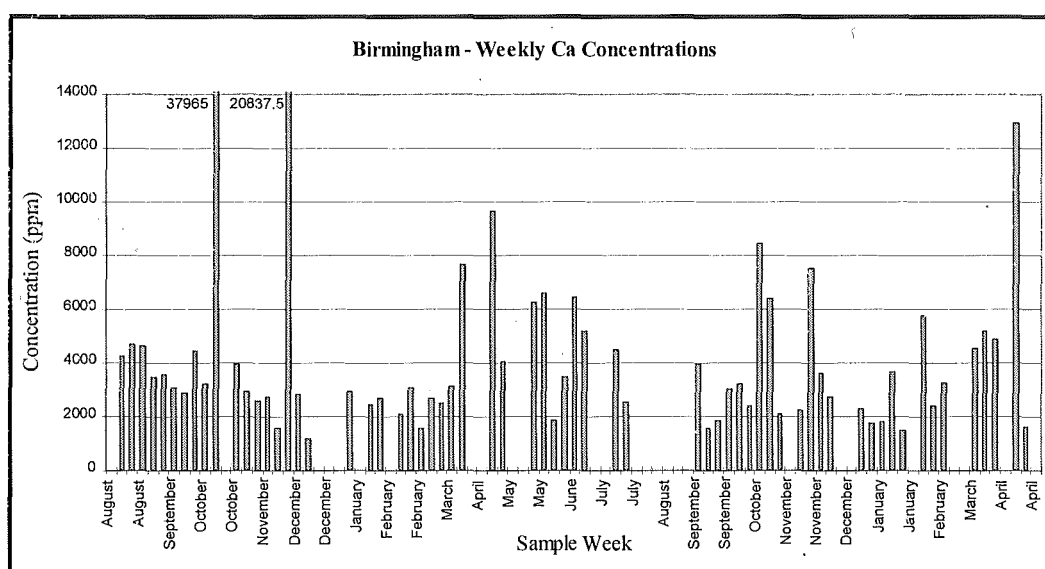


Figure 5.16. Weekly calcium runoff distribution, Birmingham.

With a correlation pattern more similar to London than Birmingham, the Dartmoor Ca concentrations (see Figure 5.17) were closely associated with only  $\text{Mg}^{++}$  ( $r = 0.83$ ) and sulphate ( $r = 0.73$ ) levels. The high level of relationship between the  $\text{Ca}^{++}$  and  $\text{Mg}^{++}$  again indicates that these ions could be derived from the same source, and may be transported to the exposure site in carbonaceous particles from power stations. There were no seasonal variations in the concentration, however, to

aid in source assignment. There was no relationship with  $\text{SO}_2$  concentrations at the site ( $r = 0.08$ ), which is probably due to low background levels of gaseous pollutants.

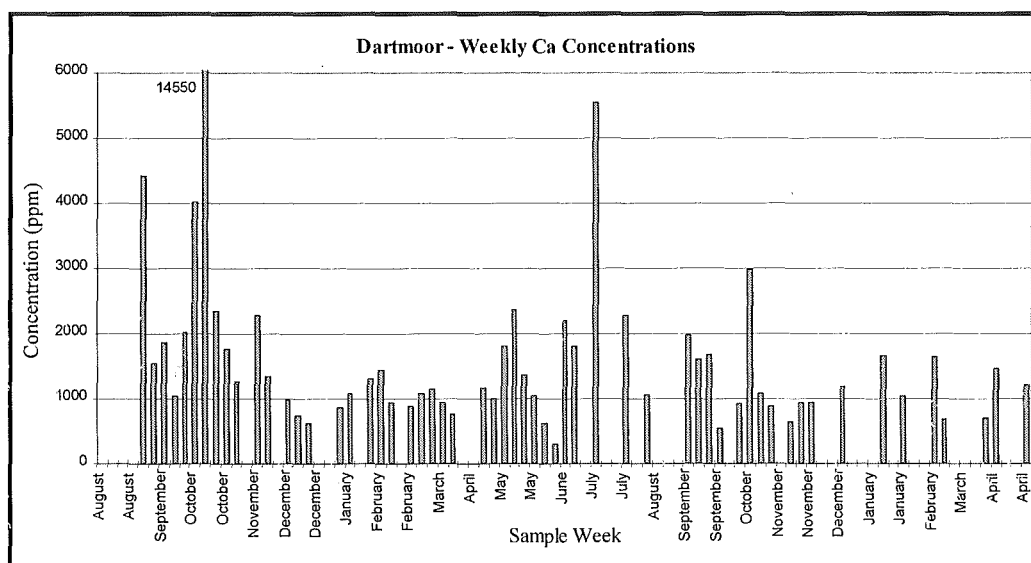


Figure 5.17. Weekly calcium runoff distribution, Dartmoor.

To determine the influence of finish on the run-off concentrations (whose average values were higher than those of the blank), an analysis of the London site, collapsed by finish, was conducted. The anova<sup>48</sup> only just failed to reach significance, and this was probably due to the high levels of variability in the data sets, shown in Table 5.10. Post-hoc T-test analyses between the individual finishes also failed to show any significant differences<sup>49</sup>.

The Birmingham site showed no significant differences between the sample populations from the four micro-catchment units, when examined as a group. The lack of significance was repeated by T-test analyses between individual stone finishes at the Birmingham site. The Dartmoor site, however, showed a main effect between the finishes and the blank<sup>50</sup>.

Post-hoc T-tests were used to examine the interactions between the individual finishes in greater detail. These revealed no significant interactions between the

<sup>48</sup>  $F(2, 178) = 2.83, P = 0.06$

<sup>49</sup> e.g. flame against blank;  $T(133) < 1$

<sup>50</sup>  $F(2, 158) = 4.8, P < 0.01$

finishes, except between the polished and cut against the blank<sup>51</sup>. The increased  $\text{Ca}^{++}$  concentrations of the polished and cut run-off could be the result of increased deposition rates to the stone surfaces, although this is not replicated with other components or at other sites, nor does it explain the low performance of the flame-dressed finish, which was the roughest of the exposed slabs.

Unlike  $\text{Al}^{3+}$ , there were clear differences between all three sites. The London site, located at St. Paul's, showed the highest levels of concentration, with a value 2.3 times the size of the Birmingham value, and 6 times that of the Dartmoor concentrations. The most probable explanation for this is the proximity of a large  $\text{Ca}^{++}$  source near the MCU slabs - the body of the Cathedral itself. The elevated  $\text{Ca}^{++}$  levels of the urban sites over the rural site could also be explained by greater concentration and deposition rates in urban areas.  $\text{Ca}^{++}$  is the main component of urban dust, and is derived from construction and extraction activities, transportation and fuel combustion (Conlan and Longhurst, 1993).

At individual sites, only Dartmoor showed any significant differences between the blank and finish, when examined as a group. This was replicated with individual T-test analyses, which only revealed significant differences between the cut/polished finishes and the blank/flame finishes at the Dartmoor site. The lack of difference between the means of the finishes at the other sites could be explained by a masking effect of the urban dust and possible  $\text{Ca}^{++}$ -rich aerosols around limestone buildings (Leysen *et al*, 1989)

#### 5.2.3.3. Magnesium.

Analysis of weekly average magnesium concentrations for each site, with the finish and site means shown below in Table 5.11, revealed significant differences between the sample populations<sup>52</sup>. This was replicated by post-hoc T-tests, which showed significant differences between the Birmingham and Dartmoor populations when analysed individually<sup>53</sup>, and between London and Birmingham<sup>54</sup>. This

---

<sup>51</sup>  $T(62) = -1.66, P = 0.05$

<sup>52</sup>  $F(1,271) = 27.6, P < 0.01$

<sup>53</sup>  $T(412) = 4.3, P < 0.01$

<sup>54</sup>  $T(500) = 3.6, P < 0.01$



suggests that the urban background level was significantly higher than rural concentrations.

	London			Birmingham			Dartmoor		
	Mean	Std. Error: lower limit	Std. Error: upper limit	Mean	Std. Error: lower limit	Std. Error: upper limit	Mean	Std. Error: lower limit	Std. Error: upper limit
Blank	809.0	690.6	927.4	518.2	456.8	579.6	365.3	329.9	400.7
Polished	1248.3	1091.4	1405.3	803.4	700.8	905.9	667.12	601.6	732.6
Cut	1247.2	1108.3	1386.0	1011.1	877.4	1144.8	577.53	509.4	645.7
Flame	1304.6	1147.3	1461.9	941.5	806.2	1076.8	454.9	416.9	493.0
<b>Average</b>	<b>1151.2</b>	<b>1078.7</b>	<b>1223.7</b>	<b>816.6</b>	<b>759.8</b>	<b>873.3</b>	<b>517.7</b>	<b>489.8</b>	<b>545.6</b>

Table 5.11.  $Mg^{++}$  runoff means (ppm) and standard error, by finish and site.

Magnesium concentrations in the London run-off, shown in Figure 5.18, were first correlated with ambient air pollution levels, to assess the impact of  $SO_2$  and  $NO_x$  on stone decay. The low levels of correlation ( $SO_2 = 0.29$ , and  $NO_x = 0.22$ ) suggest that the majority of  $Mg^{++}$  was deposited from other sources. There was no clear evidence that the pH lowering effect of the two pollutants had a significant effect on the rate of metal leaching in the central London environment for igneous rocks. This was confirmed by the correlation, which showed that pH had non-significant levels of relationship with each component, across all sites. The highest correlation value was  $r = 0.61$  with Mg at London, which was suggestive of a relationship, but was not statistically reliable.

Magnesium was then correlated with other measured components of the study, and showed a high degree of relationship between  $Ca^{++}$  ( $r = 0.84$ ), and sulphate ( $r = 0.71$ ) and chloride ( $r = 0.78$ ) ions. Although  $Mg^{++}$  was undoubtedly deposited in a sulphated form, it was also possibly derived from sea salt aerosols (due to the high chloride correlation). The lack of a seasonal distribution removes the possibility of de-icing salts being an ion source and suggests that deposition as urban dust or aerosol was the primary route.

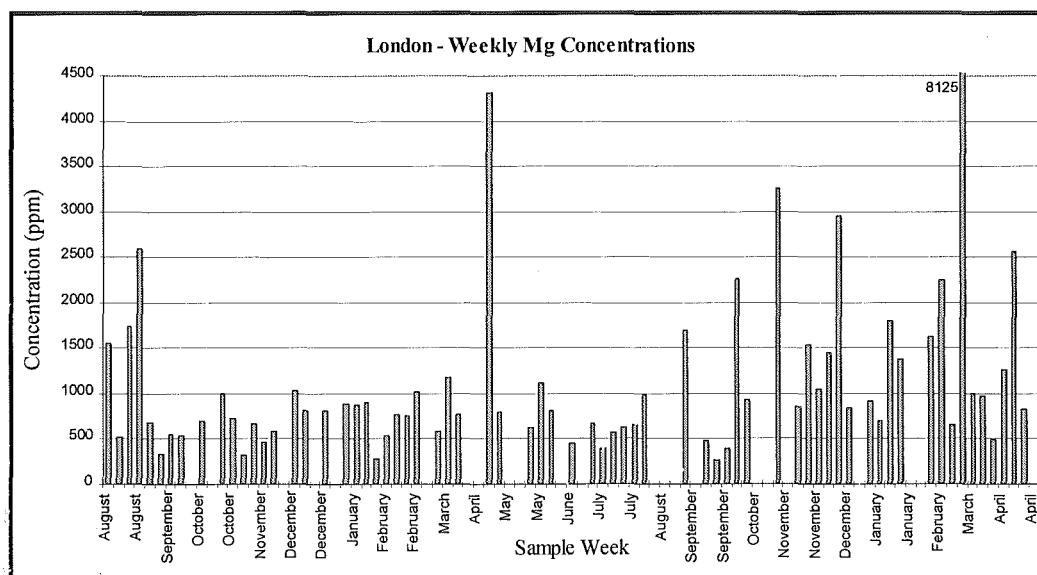


Figure 5.18. Weekly magnesium runoff distribution, London.

Birmingham, which has systematically shown higher levels of correlation between ambient pollution and metal species concentration in the run-off, continues this trend with magnesium. Weekly concentrations are shown in Figure 5.19. The higher levels of correlation ( $\text{SO}_2 = 0.61$  and  $\text{NO}_x = 0.6$ ) between increasing pollutant concentrations and increasing levels of magnesium in the run-off suggest that the effect of the pH reducing gases on metal release from the stones could be more important than at the London site. This conclusion was not, however, supported by the pH correlation values across the three sites (St Paul's, 0.61, Birmingham, -0.02, Dartmoor, 0.29).

There are high levels of correlation between nitrate ( $r = 0.82$ ), sulphate ( $r = 0.89$ ), aluminium ( $r = 0.82$ ) and calcium ( $r = 0.95$ ). This leads to the conclusion that the Mg in the run-off was derived from atmospheric deposition from a number of sources - such as industrial sources and urban dust, which is rich in magnesium, aluminium and calcium (QUARG, 1993; Nord et al, 1994). Due to its inland position, the contribution from sea salts was likely to be minimal.

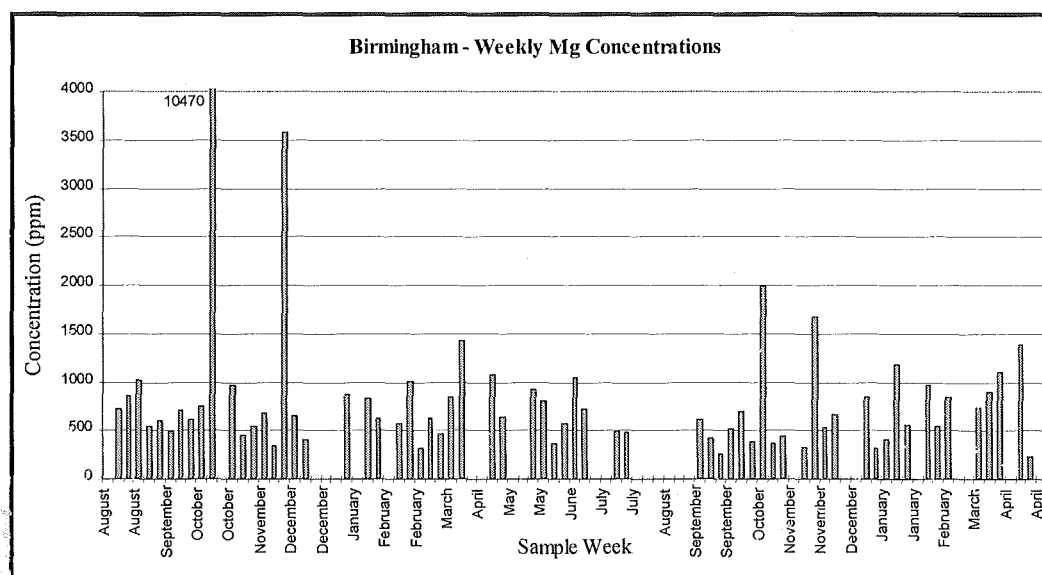


Figure 5.19. Weekly magnesium runoff distribution, Birmingham.

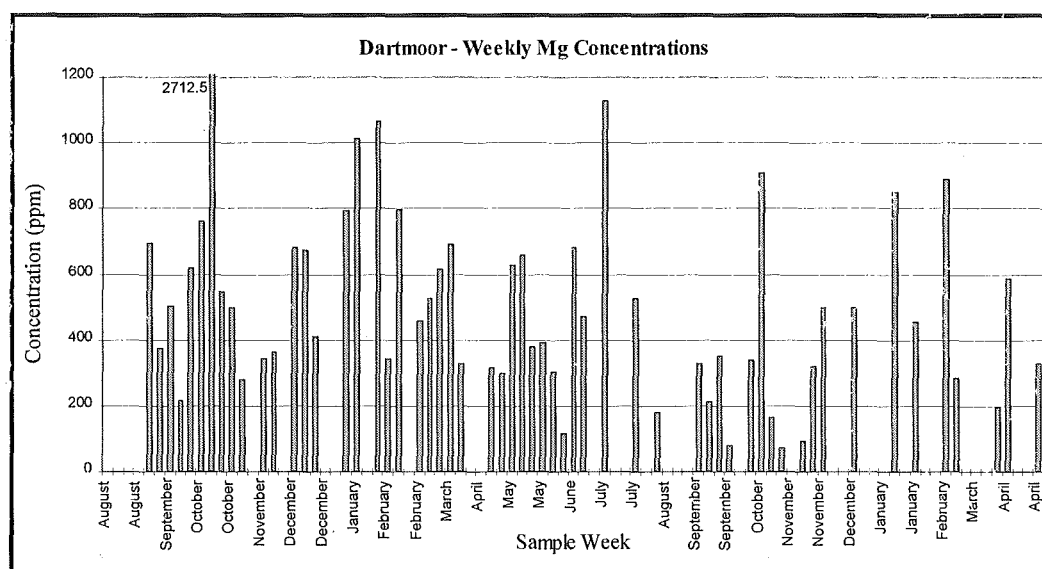


Figure 5.20. Weekly magnesium runoff distribution, Dartmoor.

Dartmoor concentrations, shown in Figure 5.20, were consistent with the other sites by being strongly correlated with  $\text{Ca}^{++}$  ( $r = 0.83$ ), and moderately related to sulphate concentrations ( $r = 0.7$ ). The high levels of correlation with both chemical species indicated they could be derived from the same source. This might be carbonaceous particles, which can act as sources of  $\text{Ca}^{++}$ ,  $\text{Mg}^{++}$  and S (Cheng, 1983; Sabbioni, 1995), allowing the formation of gypsum on deposition surfaces

(Del Monte *et al.*, 1984). There were no other significant relationships between  $Mg^{++}$  and any other pollutant or run-off component, shown in appendix Table A.3.

To determine the role of finish on magnesium concentrations in the run-off, a group anova (where the blank and three finish types are analysed together) was carried out on the St Paul's samples. This showed that, although all of the finish concentrations were a minimum of 400 ppm higher than the blank, there were no significant differences within the group<sup>55</sup>. This pattern was present in the Birmingham site. The Dartmoor site, however, showed significant differences between the M.C.U.s when examined as a group<sup>56</sup>.

To analyse the interaction of individual finishes at each site, post-hoc T-tests were carried out. These showed that while the stone finishes at the sites were significantly higher than the blank<sup>57</sup>, there was little inter-finish variation between the stones<sup>58</sup>. Dartmoor was the only site that showed a marginal significance between the stone slabs<sup>59</sup>.

With  $Mg^{++}$ , as with the majority of other measured run-off components, site was the determining factor in run-off concentration, with the two urban sites significantly higher than the rural site, and London significantly higher than Birmingham.

Analyses of individual finishes against the blank, across all sites, showed that the runoff from the stone slabs had significantly higher  $Mg^{++}$  concentrations than could be explained by atmospheric deposition alone. This, coupled with the lack of inter-finish significance suggests that although the granodiorite slabs contribute  $Mg^{++}$  to the run-off through the dissolution of minerals within the stone matrix, the influence of finish on  $Mg^{++}$  concentrations was marginal.

#### 5.2.3.4. Iron.

Analysis of the weekly average iron concentrations (which originate from a combination of petroleum fuelling, industry, traffic and dissolution of iron containing

<sup>55</sup>  $F(2, 178) = 1, P > 0.1$

<sup>56</sup>  $F(2, 180) = 6.4, P = < 0.01$

<sup>57</sup> e.g. St. Paul's, blank against cut;  $T(128) = -2.4, P = 0.01$ , and Birmingham, flame against blank;  $T(88) = -2.9, P = < 0.01$

<sup>58</sup> e.g. Birmingham, flame against cut  $T(89) < 1$

<sup>59</sup> flame against cut;  $T(69) = 1.48, P = 0.07$

minerals in the rock (Nord *et al*, 1994)) from the three sites, shown below in Table 5.12, showed no significant differences between the sample populations<sup>60</sup>. Post-hoc T-tests of the individual populations supported this, with no effect found between London and Dartmoor<sup>61</sup>, the two extreme sites in terms of Fe concentration.

	London			Birmingham			Dartmoor		
	Mean	Std. Error: lower limit	Std. Error: upper limit	Mean	Std. Error: lower limit	Std. Error: upper limit	Mean	Std. Error: lower limit	Std. Error: upper limit
Blank	60.00	49.22	70.78	74.39	57.57	91.22	61.39	47.05	75.74
Polished	56.71	46.58	66.84	55.64	44.12	67.16	53.23	45.30	61.15
Cut	87.38	61.10	113.65	85.62	62.43	108.82	79.70	50.64	108.76
Flame	126.56	91.74	161.38	57.94	48.67	67.21	75.88	52.57	99.18
<b>Average</b>	<b>82.49</b>	<b>70.95</b>	<b>94.04</b>	<b>68.82</b>	<b>60.59</b>	<b>77.05</b>	<b>67.71</b>	<b>57.50</b>	<b>77.92</b>

Table 5.12. Fe<sup>++</sup> runoff means (ppm) and standard error, by finish and site.

Iron concentrations in the London run-off, shown in Figure 5.21 were correlated with ambient pollution levels to help estimate the role of pollutant concentration on the rates of metal ion release. The low levels of correlation ( $\text{SO}_2 = 0.26$ , and  $\text{NO}_x = 0.3$ ) imply it was the interaction of a variety of pollutants that were responsible for controlling the rates of ion release. There were, however, no significant relationships between Fe<sup>++</sup> and any other measured component.

Unlike other metal species correlation analyses, the levels of Fe<sup>++</sup> in Birmingham run-off, shown in Figure 5.22, were only slightly correlated with the concentrations of  $\text{SO}_2$  and  $\text{NO}_x$  ( $\text{SO}_2 = 0.32$ , and  $\text{NO}_x = 0.31$ ). The low levels of correlation also apply for other measured components, which showed no values above  $r = 0.58$  ( $\text{Al}^{3+}$ ). Low measurement rates of iron in the run-off, which was intermittent and at low concentrations, may explain this result.

<sup>60</sup>  $F(1, 186) < 1$

<sup>61</sup>  $T(164) < 1$

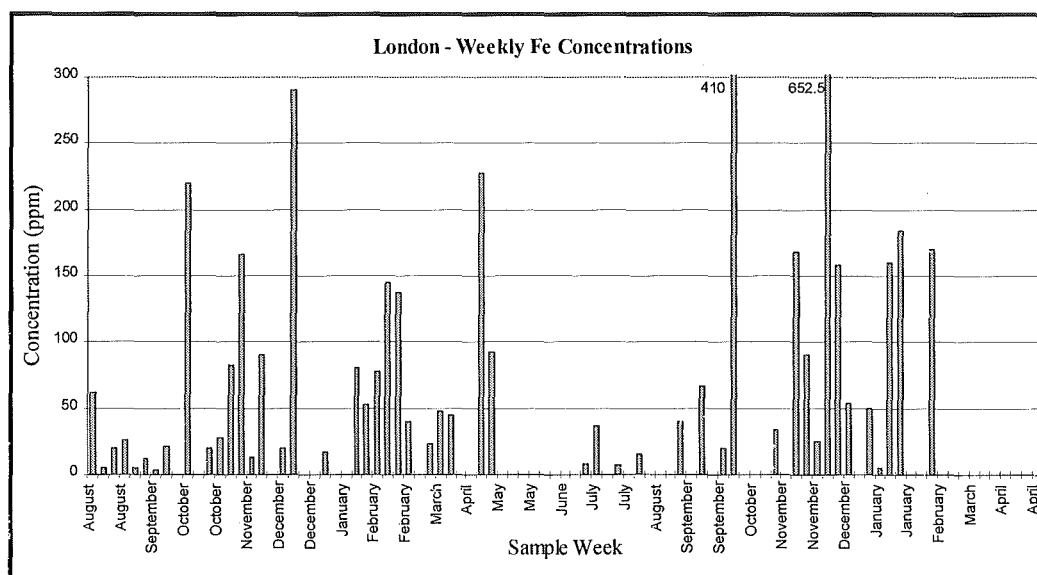


Figure 5.21. Weekly iron runoff distribution, London.

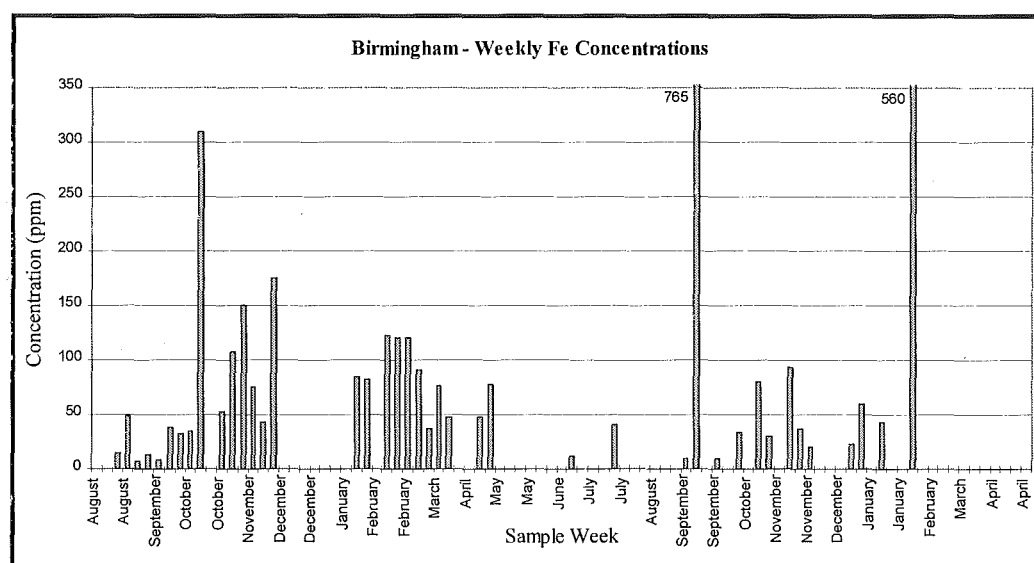


Figure 5.22. Weekly iron runoff distribution, Birmingham.

Dartmoor concentrations, shown in Figure 5.23, follow a similar pattern to London and Birmingham, and also showed no significant degree of relatedness with any of the measured components. Once again  $\text{Al}^{3+}$  showed the highest effect ( $r = 0.36$ ), although this was not significant.

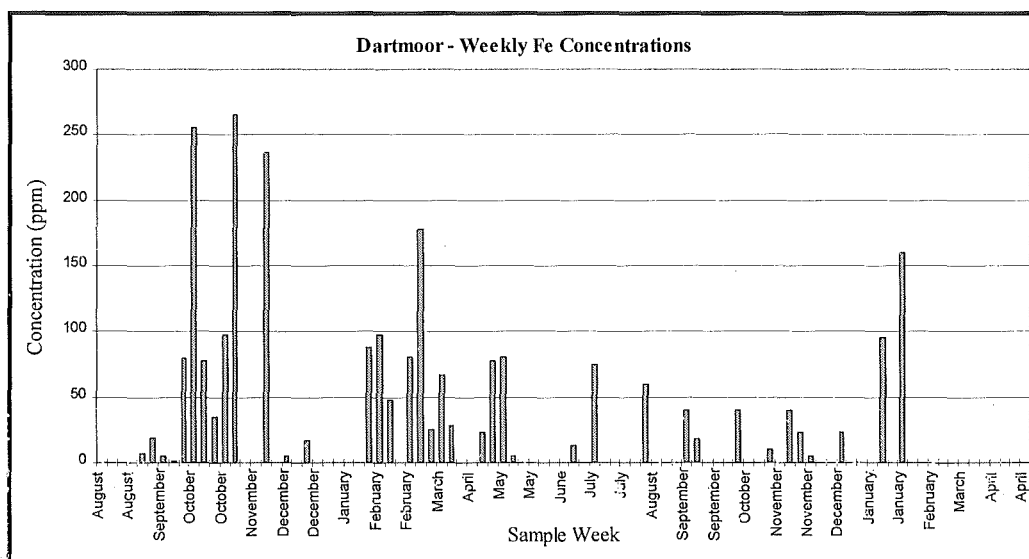


Figure 5.23. Weekly iron runoff distribution, Dartmoor.

The roughness of the stone surface used in the micro-catchment units can influence the deposition rate of particulates and other pollutants, and to examine the role they played in component concentrations, group anova's were carried out on the four M.C.U.s at each site. London, however, like Birmingham and Dartmoor, showed no significance between the M.C.U.s<sup>62</sup>.

To further examine the role of finish, individual finishes were compared by post-hoc T-test analyses - while London showed an effect between the stone finishes<sup>63</sup> (although not between the finishes and the blank), this was not replicated at any of the other sites<sup>64</sup>.

$\text{Fe}^{++}$  differs from other metals and anions measured in the exposure programme, in that there was no variation between the urban and rural sites. The lack of significant differences was replicated by group finish analyses, and individual inter-finish comparisons. The only site that displayed any variation was London, which had a significant difference between the polished (56.7 ppm) and flame-dressed (126.6 ppm) finishes. This may be the result of low levels of occurrence in the run-off, and the extremely high levels of variability in the sample populations.

<sup>62</sup> London  $F(2, 160) = 1.88, P > 0.1$

<sup>63</sup> e.g. polished against flame  $T(47) = -1.93, P = < 0.05$

<sup>64</sup> Birmingham, cut against flame  $T(47) = -1.1, P < 0.1$ , and Dartmoor, blank against flame;  $T(52) < 1$

These factors would reduce the possibility of detection of any significant interaction between population groups.

Although they were not significantly different from other MCU values, the mean blank values for the urban sites were either the largest or second largest values, which was indicative of high levels of atmospheric deposition. There was no indication why the smoothest finish (polished), which would be expected to have a faster rate of run-off generation than the roughest finish (flame-dressed), had consistently lower concentrations than all the other finishes.

#### 5.2.4. Site Effects on Run-off Characteristics.

Site was the strongest characteristic in the determination of component concentration. Of the eleven measured parameters (run-off volume, pH, conductivity,  $\text{Cl}^-$ ,  $\text{NO}_3^-$ ,  $\text{PO}_4^{3-}$ ,  $\text{SO}_4^{2-}$ ,  $\text{Fe}^{++}$ ,  $\text{Al}^{3+}$ ,  $\text{Mg}^{++}$ , and  $\text{Ca}^{++}$ ), only two ( $\text{PO}_4^{3-}$  and  $\text{Fe}^{++}$ ) showed no significant differences between the sites. Both of these parameters, however, differed from the rest of the studied characteristics in their low levels of incidence and concentration, and the high levels of sample variation. This reduces the statistical reliability of any tests carried out on them.

The rest of the parameters showed differences between the sites, with all but run-off volume and pH showing significant differences between each of the sites. London, the most polluted site, consistently showed the highest concentrations, except for  $\text{Al}^{3+}$ , which was significantly higher at Birmingham than at London and Dartmoor.

Run-off volume and pH also differed from the normal distribution, with volume significantly higher at the rural site than at either of the urban sites, which showed no significant differences between them. pH also differed from the other components, in that the highest pH values were recorded from the London site run-off, while Birmingham and Dartmoor were significantly lower (there was no significant difference between those two sites). The variation in pH could possibly be explained by buffering  $\text{Ca}^{++}$  clouds that are hypothesised to surround calcium carbonate buildings. Conlan and Longhurst (1993) reported that spatial variability of hydrogen ion concentrations was a function of buffering by calcium compounds in Manchester, and as a result of precipitation amount. Despite minor concentration



distribution variations, such as  $\text{Al}^{3+}$ , the higher values from the polluted London site suggests, as would be expected, that it was the pollution regime and ambient air quality at a site that determined the levels of pollutants in run-off water from buildings. This is confirmed by the significant correlations between  $\text{Ca}^{++}$  and  $\text{SO}_4^{2-}$ ,  $\text{Mg}^{++}$  and  $\text{SO}_4^{2-}$  and  $\text{Ca}^{++}$  and  $\text{Mg}^{++}$  which point towards atmospheric input, rather to material lost by the stone through weathering processes (Sweevers *et al*, 1995).

#### 5.2.5. Roughness Effects on Run-off Characteristics.

Surface roughness was examined during the exposure programme to attempt to evaluate the relative impact that changes in the stone surface had on dissolution rates for minerals within the stone matrix. The programme found two main types of distribution for roughness effects, when individual finishes were examined by site. The majority of measured components fell into the first type, where there were differences between the finishes when the whole site was examined, by group. There were, however, no differences between individual population values, either between the blank and the stone slabs, or between the different finish types. This implies that individual slab variation between the blank and the stone, and between the finishes, was not sufficient to produce measurable difference in the dissolution and weathering rates of minerals within the granite slabs.

The second type of distribution was where stone finishes differed significantly from the blank, indicating that the stone slabs significantly altered the run-off composition from that derived solely by atmospheric deposition processes. Only pH,  $\text{Ca}^{++}$  and  $\text{Mg}^{++}$  showed any variation between blank and stone slabs, and then only Dartmoor showed significant inter-finish variations. This indicates that over the period of exposure, mineral dissolution from the stone was minimal, with only  $\text{Ca}^{++}$  and  $\text{Mg}^{++}$  showing a higher concentration than that explained by atmospheric deposition. Roughness variation also had little influence on deposition or dissolution rates, with only Dartmoor showing any inter-finish effects between  $\text{Mg}^{++}$ .

This suggests that it was only when there were low background pollutant levels, that differences in the deposition surface were revealed. Even Dartmoor, the cleanest of the three sites, only approached inter-finish significance (between the cut

and flame finish ( $\text{Mg}^{++}$ ) once, when there were significant differences between the finishes and the blank. The higher ambient pollutant levels, and increased pollutant interaction that occurs in urban areas, masks the weak effects of the stone and finish types, resulting in similar run-off concentrations, regardless of the surface roughness of the exposed slabs.

The lack of detectable differences between the concentrations of the finish run-off at each site is consistent with the resistant nature of the stone, and the slower rate at which weathering effects granite. The paucity of significant results replicates another granite micro-catchment unit study conducted by Sweevers *et al* (1995) under ambient atmospheric conditions at sites in Holland and Belgium. After over 2 years of exposure and analysis, they concluded that the weathering of fresh Leinster granite was negligible.

### 5.3. CAROUSEL TABLET ANALYSIS

The carousel tablets, described in section 3.8.1 and 3.9.1, were collected after 45 and 91 weeks exposure at the three sites around England; London, Birmingham and Dartmoor. To determine the modifying effects of total and dry deposition, the tablets were divided into two groups; the upper suite, which was completely exposed to the atmosphere, and the lower suite, which was protected from direct rainfall.

The most significant variations in tablet weight change were shown across the upper and lower suite, at each site. Therefore the different suites will be examined first, followed by analysis of the individual stone types.

The Dartmoor carousel tablets were only weighed at the initial and end point of the exposure study, due to restrictions in site access. The Dartmoor analyses will therefore focus on differences between these two weighing points. The urban site analyses will examine all three weighing points.

	1/2 Way		End Weight	
	upper	lower	upper	lower
<b>London</b>	100.083	100.172	99.966	99.991
<b>Birmingham</b>	100.021	100.039	99.959	99.978
<b>Dartmoor</b>	--	--	100.826	100.028

Table 5.13. Mean percentage change from initial carousel tablet weight.

When the values, expressed as percentage change from initial dry weight (shown in Table 5.13), were analysed, significant differences were found between the upper and lower suites end weights at Dartmoor and Birmingham, which also displayed differences at the half-way measurements<sup>65</sup>. This pattern was not replicated at the London site, for either the half-way or end weights<sup>66</sup>. As a result of their general cross-site differences, however, the two suites will be examined separately.

### 5.3.1. Upper Suite Weight Changes

The carousel tablets were weighed twice during their exposure period, the half-way point (around 45 weeks into the exposure period) and at the end (around week 91). The values, expressed as the percentage change from initial dry weight, can be seen in Figure 5.24. Although weighing error was not determined, care was made in selecting the initial set of balance scales, which was then used in every subsequent weighing period. In addition, although the tablets were weighed in g to four decimal places, the results were only reported to three, absorbing some of any potential error.

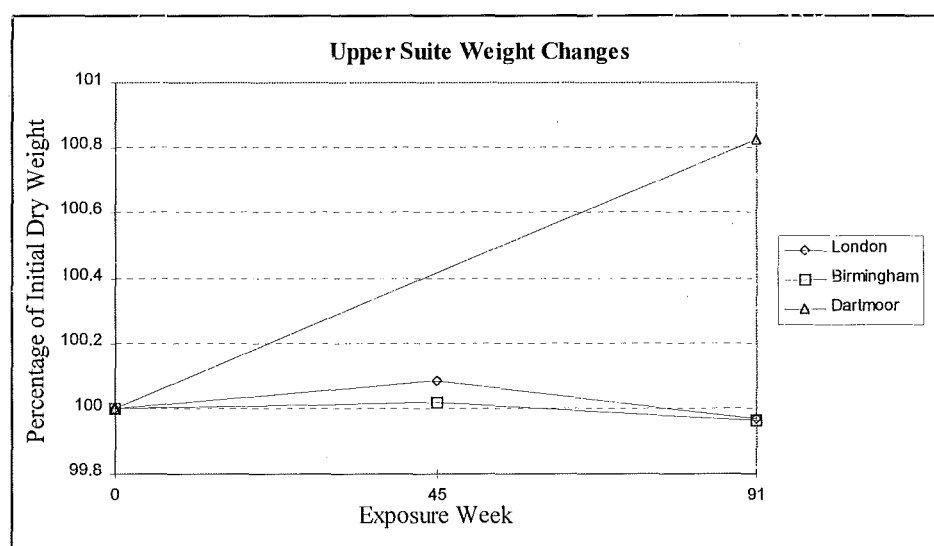


Figure 5.24. Mean carousel tablet weight changes; upper suite.

<sup>65</sup> Birmingham, ½ -way;  $T(20) = -3.6$ ,  $P < 0.01$  and Dartmoor, end weight;  $T(22) = -19.8$ ,  $P < 0.01$

<sup>66</sup> e.g. ½-way;  $T(22) = -1.4$ ,  $P < 0.1$

The upper suite stones at each site were then analysed, across all stone types, to identify significant differences between the initial, mid-way and end point weights.. The analyses showed that there were significant differences between the weights at all three sites<sup>67</sup>.

When these relationships were examined more closely by post-hoc T-tests, each upper suite interaction was significant; i.e. between the end and mid-point values at London<sup>68</sup>. Although there was no mid-point weight for the Dartmoor, site, shown below in Table 5.14 and Figure 5.25, there were significant differences between the initial and end point values<sup>69</sup>.

When the upper suite carousel tablet weight changes were examined by stone type (modal analysis of the stone types is shown in Table 3.9), only Birmingham displayed any significant differences between the stone types at the half-way or mid-point stage<sup>70</sup>, where there were main effects observed between all three stone types<sup>71</sup>.

Site	Stone Type	Weighing Point (weeks)		
		0	45	91
London	Mountsorrel	100	100.065	99.989
	Bolventor	100	100.138	99.933
	Merrivale	100	100.046	99.976
Birmingham	Mountsorrel	100	100.02	99.946
	Bolventor	100	100.035	99.963
	Merrivale	100	100.008	99.968
Dartmoor	Mountsorrel	100	--	100.755
	Bolventor	100	--	100.859
	Merrivale	100	--	100.865

Table 5.14. Upper suite percentage change from initial dry weight.

<sup>67</sup> e.g. London;  $F(1,11) = 8.5$ ,  $P = 0.01$ , and Birmingham;  $F(1,11) = 38.4$ ,  $P < 0.01$

<sup>68</sup>  $T(22) = 3.1$ ,  $P < 0.01$

<sup>69</sup>  $T(22) = -42$ ,  $P < 0.01$

<sup>70</sup> group anova;  $F(2,9) = 93.6$ ,  $P < 0.01$

<sup>71</sup> Mountsorrel against Merrivale;  $T(4) = 6$ ,  $P < 0.01$

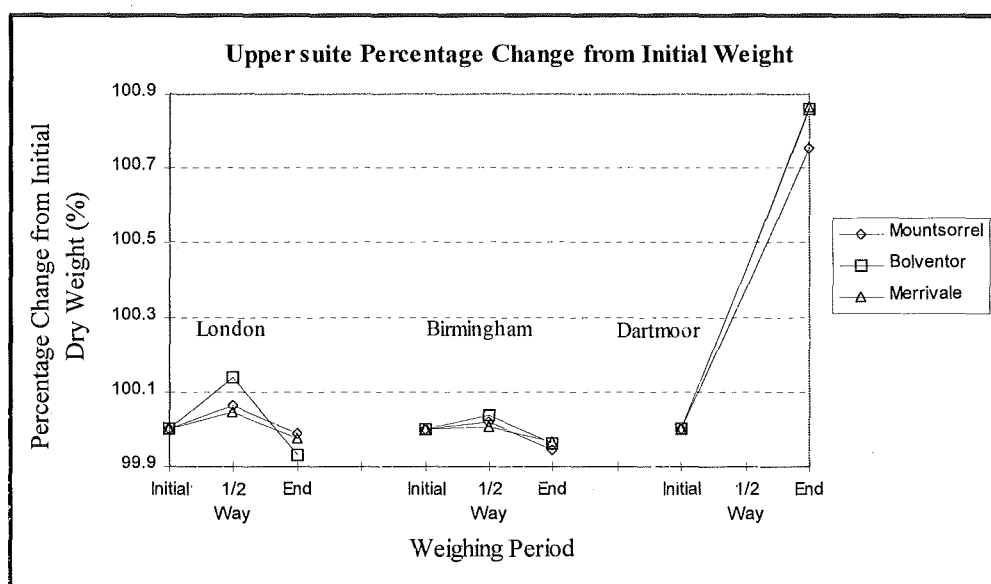


Figure 5.25. Upper suite weight changes from initial condition.

The analyses were also carried out on the upper suite end stage values at each site. Although there were significant differences between the stones when examined as a group at London and Dartmoor<sup>72</sup>, there were no main effects between the Birmingham stone types.

Examination of the interaction between the individual stone types at the three sites showed that while there were significant differences between the Bolventor and Mountsorrel stones, comparisons between Bolventor and Merrivale failed to reach significance. Furthermore, while there were significant weight change differences between the Mountsorrel and Bolventor stone types at the half-way and end-point weighing, this was not consistently in one direction. Consequently it is difficult to assign reasons for this variability. However, differences in the  $\text{Ca}^{++}$  content of the three stone types (shown in Table 3.5), suggest that it was not a function of  $\text{Ca}^{++}$ -induced gypsum formation.

The weight gain and loss shown by the upper suite carousel tablets, shown in Figure 5.25, is likely to be a combination of particulate deposition onto the tablets surfaces, and increased reaction rates affecting friable particles produced by the cutting process that formed the tablets. Due to an increased surface area to volume

<sup>72</sup> London anova;  $F(2,11) = 7.1$ ,  $P = 0.01$ ; Dartmoor anova;  $F(2, 11) = 6.8$ ,  $P < 0.02$

ratio, it is likely that the particles will undergo rapid change, increasing in size and weight, before falling off or being removed by atmospheric processes such as wind and rain. From the lack of results from analyses conducted at the end of the exposure period on the exposed microcatchment units, it is unlikely that any significant chemical change occurred to the carousel granite's constituent minerals, which might have partly accounted from weight loss.

### 5.3.2. Lower Suite Weight Changes

To examine the role of exposure on the lower suite tablet weight change values, shown in Figure 5.26, the three sites were analysed across all stone types. These showed that while there were significant differences between the mid-point and end point weight values at London and Birmingham, there were none at the Dartmoor site<sup>73</sup>.

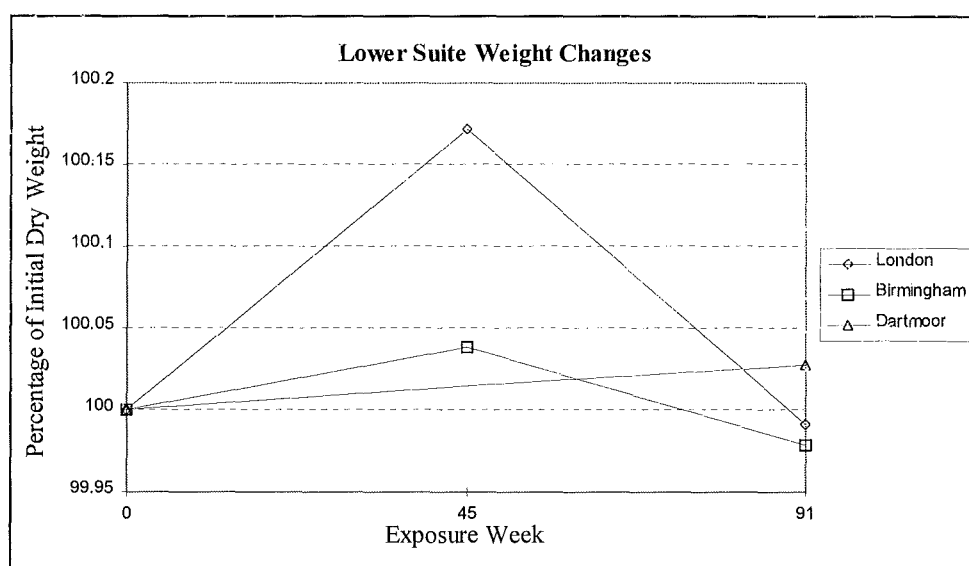


Figure 5.26. Mean carousel tablet weight changes; lower suite.

Post-hoc T-tests of the London and Birmingham weight change values showed that while there were significant differences between the end weight and the initial and mid-point values at Birmingham<sup>74</sup>, there was only an effect between the

<sup>73</sup> e.g. London;  $F(1,11) = 3.1$ ,  $P < 0.01$ , and Dartmoor,  $T(22) < 1$

<sup>74</sup> e.g. initial against end weight;  $T(22) = 10$ ,  $P < 0.01$

end and mid-point values at the London site<sup>75</sup>. The lower suite values, by stone type and site, are shown in Table 5.15 and Figure 5.27.

Site	Stone Type	Weighing Point (weeks)		
		0	45	91
London	Mountsorrel	100	100.17	100.025
	Bolventor	100	100.273	99.962
	Merrivale	100	100.071	99.988
Birmingham	Mountsorrel	100	100.037	99.97
	Bolventor	100	100.053	99.985
	Merrivale	100	100.026	99.98
Dartmoor	Mountsorrel	100	--	100.049
	Bolventor	100	--	100.027
	Merrivale	100	--	100.007

Table 5.15. Lower suite percentage change from initial dry weight.

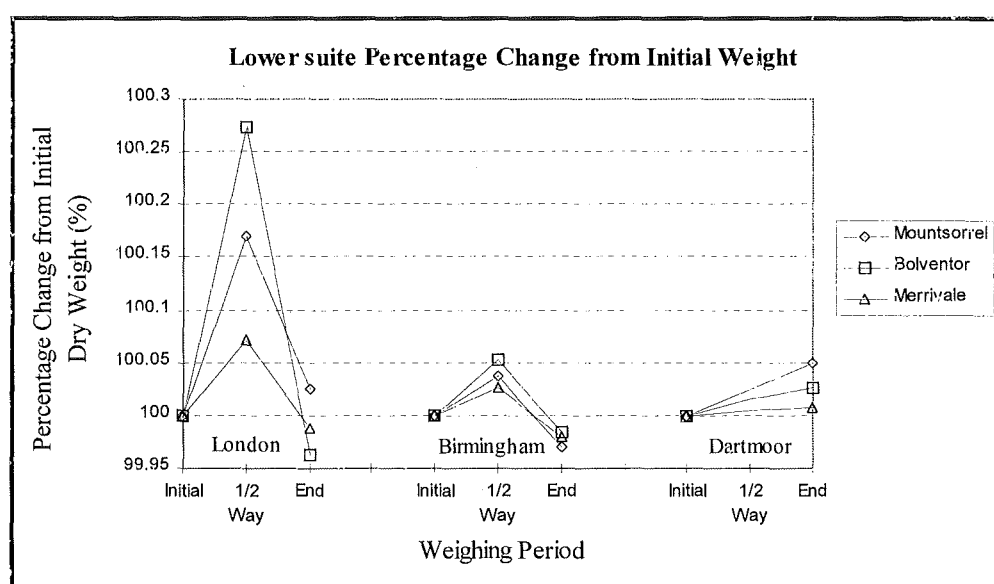


Figure 5.27. Lower suite weight changes from initial condition.

As can be seen in Figure 5.27, the greatest variability in weight change at the urban site occurred at the half-way measurement period, before the weight changes become more uniform. The rapid weight increase during the first 45 weeks of

<sup>75</sup> e.g. initial against end weight;  $T(22) < 1$

exposure, which leads to the greater degree of weight variation, could be explained by the reaction of friable particles (with a high surface area/volume ratio) to atmospheric processes such as oxidation. This would result in a weight increase before their removal, as the stone adjusts to its environment. The similarity between the start and end points for the urban sites could indicate that the stone tablets have reached equilibrium at the end of the exposure programme, and that an extended period of exposure would be needed for characteristic weight changes to reveal themselves.

To determine if stone type (Merrivale, Mountsorrel and Bolventor  $\text{Ca}^{++}$  concentrations are shown in Table 3.8) had an effect on weight change values, group analyses of the mid-point and end values were carried out. The half-way values showed that while significant differences exist between the Birmingham lower suite tablets<sup>76</sup>, there were no main differences between the London stone types<sup>77</sup>. Post-hoc T-test analyses between individual stone types showed that while the Birmingham site showed a main effect between all three stone types<sup>78</sup>, the London site only showed a significant difference between Bolventor and the other two stone types<sup>79</sup>.

Analysis of the end weight differences on the lower suite tablets revealed that the impact of stone type was much less after 91 weeks of exposure than it was during the first 45 weeks. Although there were significant differences between stone types at Birmingham when analysed by group<sup>80</sup>, neither London or Dartmoor followed this distribution<sup>81</sup>. Examinations of the role of individual stone types by post-hoc T-tests showed that once again Birmingham was the only site to display any differences<sup>82</sup>, with an effect between Mountsorrel and the other two stone types<sup>83</sup>.

### 5.3.3. Site and Suite Variations

There was a clear trend across the urban sites for weight increases in both the upper and lower suite tablets by the mid-stage of the exposure period. Although the

---

<sup>76</sup>  $F(2, 11) = 60.8, P < 0.01$

<sup>77</sup>  $F(2, 11) = 1.4, P > 0.1$

<sup>78</sup> e.g. Merrivale against Bolventor;  $T(6) = 13, P < 0.01$

<sup>79</sup> e.g. Bolventor against Merrivale;  $T(6) = 2.1, P < 0.05$

<sup>80</sup>  $F(2, 11) = 10.1, P < 0.01$

<sup>81</sup> e.g. Dartmoor,  $F(2, 11) < 1$

<sup>82</sup> e.g. London, Mountsorrel against Bolventor;  $T(3) = 1.2, P > 0.1$

<sup>83</sup> Mountsorrel against Merrivale;  $T(3) = -2.5, P < 0.05$



two suites followed the same weight gain and loss pattern as each other, shown in Figure 5.28, the lower suite stones underwent a greater degree of weight gain. This was as expected, with the build-up of soluble salts such as gypsum and nitrates on the protected stones, and its removal from the unprotected upper suite stones. The weight increases by the upper suite stones were explained by the surface deposition of insoluble dust and particles, which would have affected the weight of both suites.

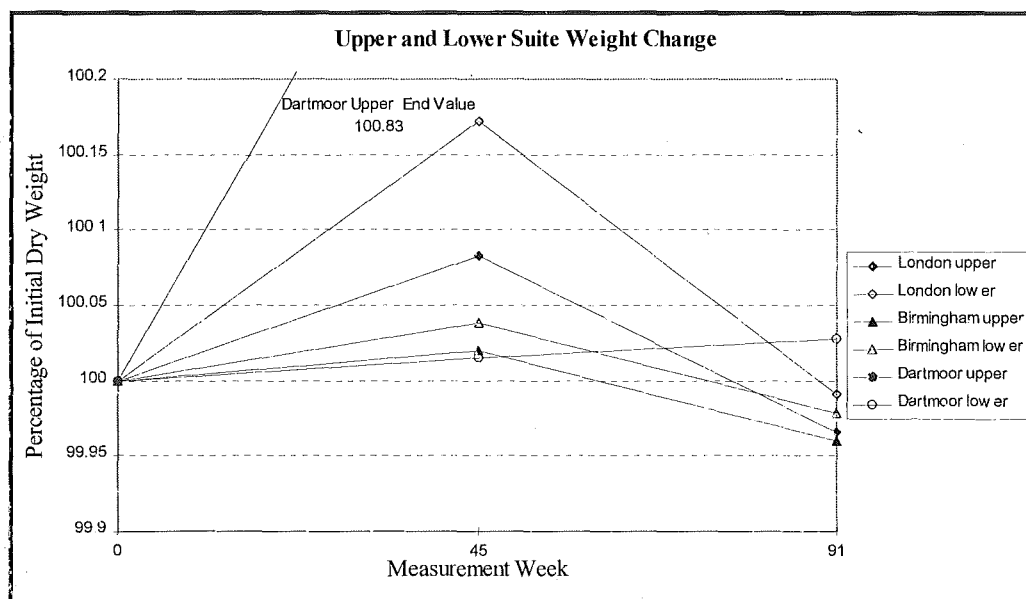


Figure 5.28. Upper and lower suite weight change.

The greatest degree of carousel weight variability, for both the upper and lower suites, was shown during the mid-point weighing. It is suggested that this is the result of the reaction of loosely attached, friable particles generated by the cutting procedure. These react with atmospheric process and undergo a weight increase before detachment. This is part of the equilibrium process as fresh granite adjusts to the changes in ambient conditions. By the end of the exposure period, urban site carousel tablet weights are much more uniform, and it could be that the two years of exposure was required for the tablets to reach equilibrium. The rural Dartmoor stones still show a high degree of variability at the end stage, and this could be due to slower rate of reaction as a result of the lower levels of atmospheric pollution recorded at the site.

When inter-site differences were analysed by group, there were no significant differences between the tablets of the upper suite across all sites, at both the mid-point and end weighing<sup>84</sup>. Although an individual analysis of the mid-point values for the London and Birmingham site tablets approached significance<sup>85</sup>, only London and Dartmoor at the end of the exposure period actually reached significance<sup>86</sup>.

Suite Type	Mid-point		End Stage	
	Upper	Lower	Upper	Lower
<b>London</b>	100.026	100.119	99.966	99.991
<b>Birmingham</b>	100.01	100.03	99.96	99.978
<b>Dartmoor</b>	--	--	100.826	100.028

Table 5.16. Site and suite variation in weight changes.

When the lower suite tablet values, shown in Table 5.16, were analysed as a group, there were significant differences between the sites at the mid-point or half-way weighing<sup>87</sup>. These were not, however, replicated at the end point weighing, where there was no significant differences between the sites<sup>88</sup>. Individual analyses of the end point site values show no significant differences between the sites, although Dartmoor and Birmingham comparisons approached significance<sup>89</sup>.

The lack of significant results from the carousel tablet exposure programme is indicative of the resilience of granite, and of the length of time it takes for the fresh granite to adjust to changes in the ambient environmental conditions (Sweevers *et al*, 1995). Although one possible method for increasing the speed of adjustment would be to expose thinner tablets, producing a large surface area/volume ratio. This is undesirable, for while the tablets are small enough to handle and rotate, they are large enough for a meaningful weathering response to be measured, should it occur. This, coupled with the practical considerations of producing the tablets from hard and resistant granite stones, renders thinner carousel tablets undesirable.

<sup>84</sup> end weighing,  $F(1, 11) = 2.4$ ,  $P > 0.1$

<sup>85</sup>  $T(20) = 1.6$ ,  $P = 0.07$

<sup>86</sup>  $T(22) = -39.7$ ,  $P < 0.01$

<sup>87</sup>  $T(22) = 2.6$ ,  $P < 0.01$

<sup>88</sup>  $F(1, 11) = 2$ ,  $P > 0.1$

<sup>89</sup>  $T(22) = -1.4$ ,  $P = 0.09$

#### 5.3.4. Stone Type Variations

At the midpoint weighing stage, the lower suite Bolventor stones, like the upper suite tablets, had higher in weight change values than the other stone types. At the end-point, however, the effect on the Bolventor stone type was no longer consistent for the upper stones, with Merrivale and Mountsorrel stones undergoing greater degrees of weight change over the last 45 weeks of exposure.

The pattern of rapid weight change during the first 45 weeks of exposure, followed by a slower weight change as Bolventor was caught by the other two stone types at the end point was similar in both stone suites. It is suggested that the initial weight changes are explained by attached mineral particles (not removed by the pre-exposure washing), formed by the tablet cutting procedure. These would have an increased surface area in relation to the rest of the stones, and therefore will react quickly to atmospheric processes. Alternatively the increase in tablet weights could be explained by the build-up of insoluble particulates such as dust and carbonaceous particles on the stone surfaces.

The later stage weight changes are explained by the removal of soluble reaction products from the upper stone surfaces, and the loss of friable stone particles from the cutting process as binding minerals were removed. The general lack of any main effect between the stone types at the end point indicates the stones have reached equilibrium with the atmosphere, and therefore a longer period of exposure would be necessary for systematic results between the different stone types to become obvious. The effect of the higher calcium content of the Mountsorrel stone in comparison to the other two stones types has been effectively non-existent, and it is suggested that this may be a long-term method of stone decay.

It should also be remembered that although there are significant differences between the initial and end weights for the different stone types at the two suites, the over-all weight changes for the tablets were very small (fractions of a percent). It could be argued that although these changes are significantly different from the other weight measurements in statistical terms, the variations could be explained by instrument error during the weighing process, and might not be the result of exposure changes on the stone.

#### 5.4. MICRO-CATCHMENT STONES ANALYSIS

There were four micro-catchment units per site, three with finished stone slabs which were evaluated at the end of the exposure period for material change within the stones, and one with a ground glass sheet to act as a blank.

##### 5.4.1. Weight Changes

The M.C.U slabs were weighed at two points during the exposure period, half-way through (45 weeks into exposure), and at the end of the exposure period (91 weeks). Weight changes were recorded after the slabs were oven-dried for 60°C for 90 hours (see section 4.3.2). The weight changes, expressed as percentage change from the initial dry weight, are shown in Table 5.17, and in Figure 5.29.

Site	Finish	Measurement Week		
		0	45	91
London	Polished	100	99.995	99.833
	Cut	100	100.002	99.826
	Flame	100	99.971	99.802
<b>Average</b>		<b>100</b>	<b>99.989</b>	<b>99.82</b>
Birmingham	Polished	100	99.987	99.847
	Cut	100	99.939	99.830
	Flame	100	99.951	99.884
<b>Average</b>		<b>100</b>	<b>99.959</b>	<b>99.854</b>
Dartmoor	Polished	100	99.883	99.826
	Cut	100	99.870	99.957
	Flame	100	100.023	99.812
<b>Average</b>		<b>100</b>	<b>99.925</b>	<b>99.865</b>

Table 5.17. Percentage change from initial dry weight, by finish and site.

As can be seen in Figure 5.29, the two urban sites (London and Birmingham) displayed the same weight change pattern, with a slow period of weight loss during the first 45 weeks, followed by an increased rate of weight change. At London, the slabs showed weight change values at the end-point commensurate with increasing finish roughness. This pattern was not repeated at Birmingham, where the roughest

finish (the flame-dressed stone) had the least amount of weight change, while the median roughness slab (the cut finish) had the greatest degree of change.

Dartmoor, however, showed a more random distribution. Although the cut and polished slabs mimicked each other during the first period of exposure with a high degree of weight loss, they diverged during the second phase, with the cut slab gaining weight, while the polished slab continued to lose weight. Despite gaining weight during the first exposure phase, the flame finish then rapidly decreased in weight to finish as the most altered of the Dartmoor slabs.

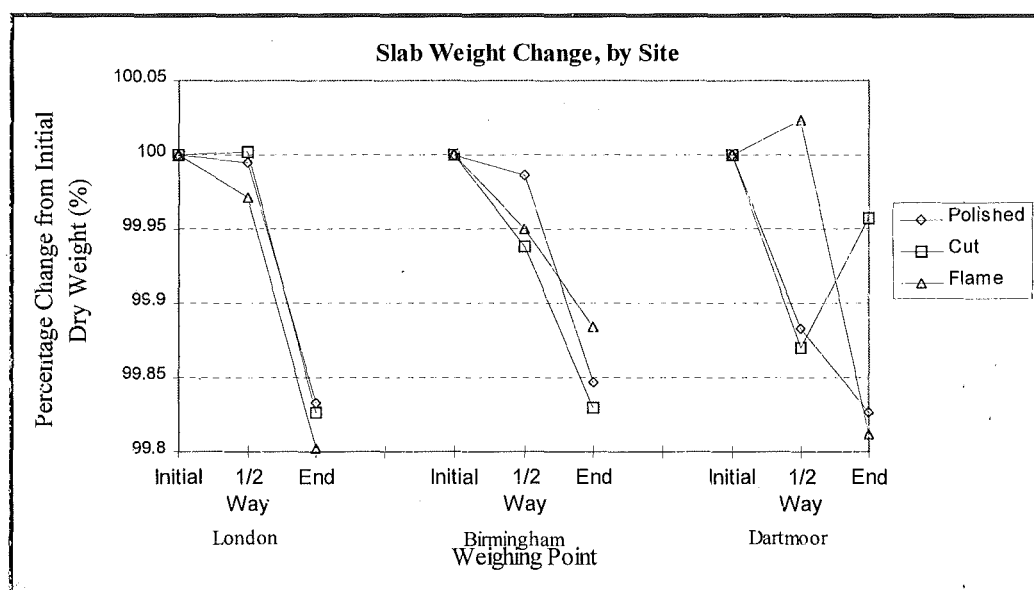


Figure 5.29. Changes from initial slab weight between exposure sites.

To determine the importance of site on weight change, a group analysis of the two weighing periods was carried out, collapsed by site. This showed no significant differences between the sites at either the half-way<sup>90</sup> or end point<sup>91</sup> weighing period. Post-hoc T-test analyses confirmed this by failing to show any main effects between individual sites when compared against each other at the two weighing periods<sup>92</sup>. As a result of the lack of site effect, the M.C.U slabs were then examined by finish, to

<sup>90</sup>  $F(2, 8) = 1.14, P > 0.1$

<sup>91</sup>  $F(2, 8) < 1$

<sup>92</sup> London against Dartmoor,  $T(2) = 1.1, P > 0.1$

ascertain if the surface roughness of the stone can effect the rate and amount of material loss.

The finish analyses followed the site effect analyses, in that they failed to show any significant differences between the finishes, either by group analysis<sup>93</sup>, or by individual T-tests<sup>94</sup>. This suggests that the micro-catchment unit slabs reached equilibrium with their environment during the length of the two year exposure period. A longer period of exposure would be required for the small differences engendered by the finish to become significant in affecting the weight of the slabs.

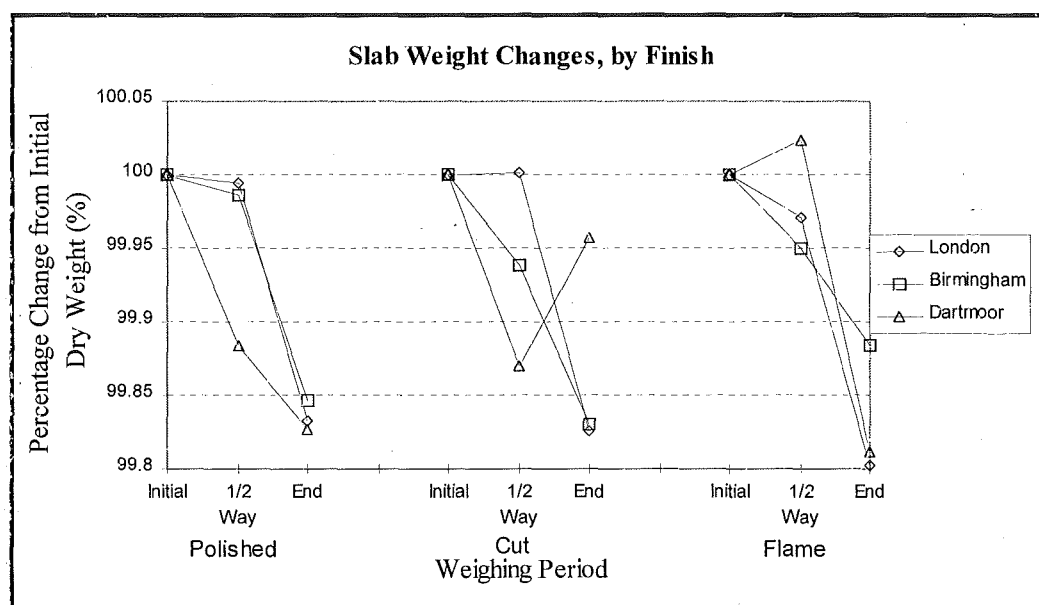


Figure 5.30. M.C.U slab weight changes, by finish.

Although there were no significant differences found between the sample populations from the different finishes, the distribution of the slab weight changes, shown in Figure 5.30, can still be informative. In contrast to the predicted distribution, it was the Dartmoor finishes that displayed end weights lower than, or similar to, the urban sites for two of the finishes. The behaviour of the Dartmoor cut slab was due to material problems with the slab during the exposure period. Slab failure necessitated re-gluing of the broken stone, and although the percentage

<sup>93</sup>  $F(2, 6) < 1$

<sup>94</sup> e.g. end analysis, cut/flame;  $T(2) < 1$

change for the end weight was linked to the new value of the slab, there were still inconsistent weight changes.

If the role of finish is examined graphically in Figure 5.30, it can be seen that the polished finish slabs produce the most similar weight loss patterns, across the sites. This could be explained by the limited surface relief (as measured by a laser profileometer, see section 4.7.3) of the polished slabs, which had the least profile deviation of the finishes. This will promote a degree of homogeneity in the weathering response by the stone at the three sites.

The Dartmoor site polished slab weight distribution differs from the urban site, with a rapid weight loss, followed by a more gradual weight decrease. Although different from the urban polished slabs, the rate of Dartmoor polished weight loss is similar to that experienced by the Dartmoor cut finish. This could be due to a characteristic of the site that promotes a high initial weathering rate, such as a high intensity, high frequency driving rain, which will remove any friable particles generated by the cutting process.

The amount of weight change displayed by the cut slabs at the two urban sites was similar to that of the polished slabs, and it is suggested that weight changes experienced by the polished and cut stones were the result of the M.C.U slabs reaching equilibrium with the atmosphere. Two of the three flame-dressed slabs displayed a greater degree of weight loss than the other, smoother finishes. Although there were no statistically significant differences between the finishes at this stage of the exposure programme, it is suggested that a longer period of exposure would see the development of distinct differences between the finishes as surface relief altered the degree of deposition and run-off concentration.

#### **5.4.2. Finish Roughness Variation**

A detailed examination was conducted on the slabs from one of the sites. The London site was chosen for roughness analyses as it had the highest levels of run-off concentrations across all sites, shown below in Table 5.18.

Measurements of the three finish types were conducted on the control slabs to determine the initial average finish prior to exposure, and on the exposed slabs to determine the effect of weathering on surface roughness.

Component	London	Birmingham	Dartmoor
Cl <sup>-</sup>	11.5	9.1	6
NO <sub>3</sub> <sup>-</sup>	11.2	6.6	3.8
PO <sub>4</sub> <sup>3-</sup>	3	1.9	1.7
SO <sub>4</sub> <sup>2-</sup>	21.6	15.5	3.8
Al <sup>3+</sup>	91.1	138	77.4
Ca <sup>++</sup>	10698.2	4583.3	1535.5
Mg <sup>++</sup>	1151.2	816.7	517.7
Fe <sup>++</sup>	82.5	68.8	67.7

Table 5.18. Mean run-off concentrations (ppm), by site.

The roughness readings from all slabs were taken on two scales; 1<sup>st</sup> and 2<sup>nd</sup> order roughness<sup>95</sup>. 1<sup>st</sup> order measurements detailed the general surface roughness, while 2<sup>nd</sup> order readings investigated inter-grain roughness. The values from the control and sample slabs are shown below in Table 5.19, where  $R_a$  is the arithmetic mean of the departures of the roughness profile from the arithmetic mean, RMS is the root mean square calculation of all profile values of the roughness profiles, and  $R_{max}$  is the maximum deviation from the arithmetic mean.

		1 <sup>st</sup> Order Roughness			2 <sup>nd</sup> Order Roughness		
		Polished	Cut	Flame	Polished	Cut	Flame
Control Slabs	$R_a$	0.016	0.026	0.134	0.012	0.014	0.032
	RMS	0.026	0.032	0.164	0.018	0.018	0.044
	$R_{max}$	0.134	0.166	0.696	0.098	0.09	0.218
Exposure Slabs	$R_a$	0.026	0.02	0.129	0.022	0.016	0.036
	RMS	0.034	0.028	0.159	0.028	0.024	0.044
	$R_{max}$	0.19	0.15	0.703	0.14	0.102	0.194

Table 5.19. Roughness measurements (in mm) from control and sample slabs

When roughness values from the protected control slabs and the exposed sample slabs were compared, shown in Figure 5.31, there was a consistent increase in the roughness values for the exposed slabs in the 2<sup>nd</sup> order. This trend was not

<sup>95</sup> See section 4.7.3 for details.



repeated, however, in the 1<sup>st</sup> order, where only the exposed polished slabs showed an increase over the control values.

These differences were further examined through T-tests, which showed that the only statistically significant differences, in both the 1<sup>st</sup> and 2<sup>nd</sup> order measurements, were those between the polished slabs<sup>96</sup>.

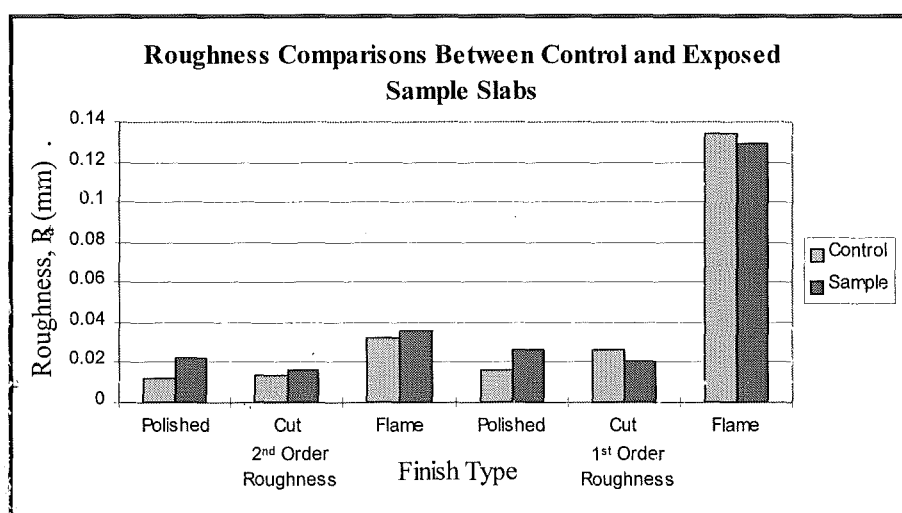


Figure 5.31. Control and sample slab roughness comparisons.

The overall lack of significance between the control and exposed slabs was not unexpected. Only the polished slabs, with the most homogeneous surface relief, showed significant differences between the weathered and unweathered finishes. As weathering occurred, there was an increase in the 1<sup>st</sup> order roughness of the polished slabs, through the removal of friable material and mineral dissolution. The same mechanisms will result in an initial decrease in the relief of the more variable surface finishes, such as the flame-dressed finish, shown in Figure 5.31. This is likely to be due to increased erosion of the peaks of the finish, which have a higher surface area/volume ratio than other areas of the stone surface. If the exposure programme was extended, an increase in the flame-dressed and cut finish 1<sup>st</sup> order roughness values would be expected.

There was a finish-wide increase in the 2<sup>nd</sup> order (inter-grain) roughness

<sup>96</sup> Polished finish, sample/control slabs; 2<sup>nd</sup> order;  $T(4) = -2.24$ ,  $P < 0.05$ , 1<sup>st</sup> order  $T(4) = -3.2$ ,  $P < 0.05$ . Cut finish sample/control slabs; 2<sup>nd</sup> order  $T(4) < 1$

values in Figure 5.31, although only the polished slabs showed any significant increase. It may be that the 2<sup>nd</sup> order increase was due to the dissolution of soluble binding minerals, or more importantly, the initiation and expansion of micro-crack networks. This would increase the roughness of the MCU finishes, without generating detectable quantities of alteration minerals.

Below in figures 5.32 -5.34, are roughness transects taken from the three exposed finish types at the London site. Measurements were taken in 0.025mm steps along a 12.5mm traverse (500 readings).

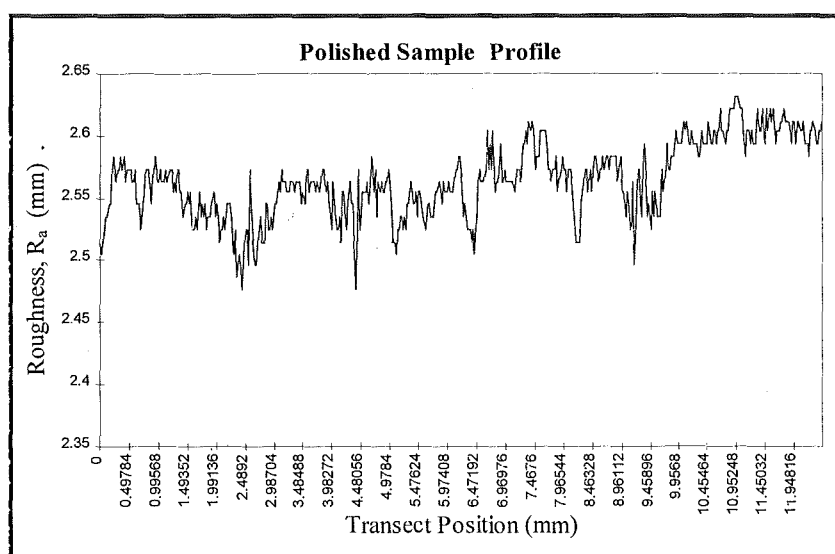


Figure 5.32. Polished exposure slab transect.

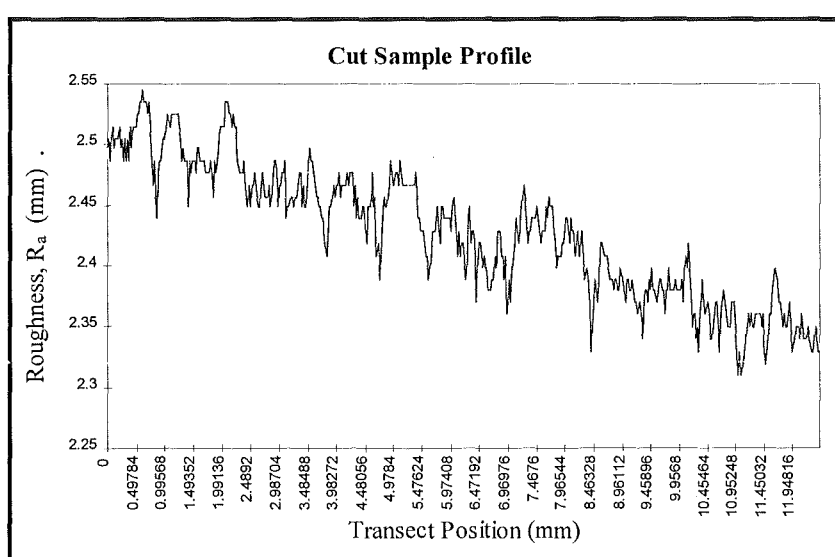


Figure 5.33. Cut exposure slab transect.

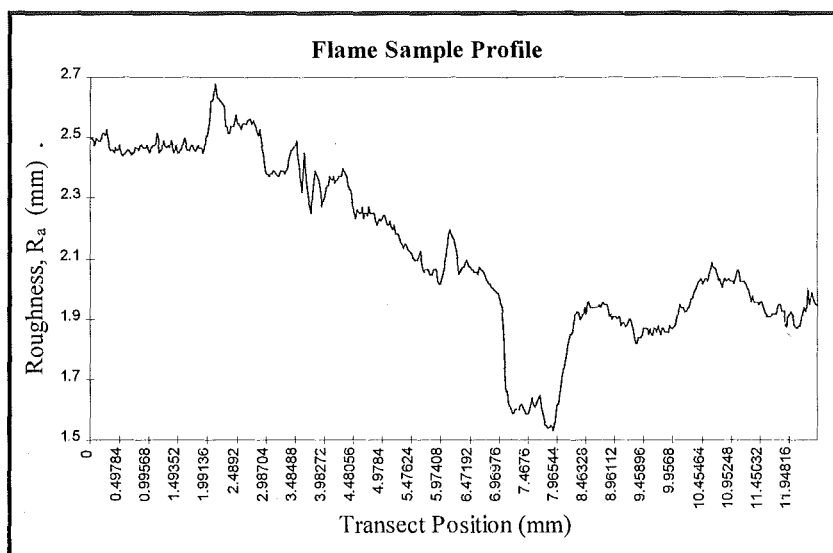


Figure 5.34. Flame exposure slab transect.

#### 5.4.3. SEM/EDX Analysis

The SEM and EDX analyses were carried out on the control and exposure slabs from the London site. These slabs were chosen as they were sited in the most polluted atmosphere of the study and had the highest run-off concentrations, shown in Table 5.18. They would, therefore, be expected to have undergone the greatest degree of change of all the sites.

After sectioning, a number of samples were visually examined under the SEM, although no deterioration features were found on the samples. Numerous elemental analyses between the control and exposed slabs were also carried out, although they also revealed no apparent differences between the results from the two groups.

The lack of stone alteration was further confirmed by incremental depth analyses of selected minerals within the exposure slabs. Several minerals were examined in each of the studied microcatchment unit slabs, and instead of showing a decrease in concentration for elements such as potassium and aluminium as they are replaced by hydrogen ions, there was no significant variation in composition with increasing depth, even though the minerals chosen abutted the surface of the selected transects. This is shown in Figure 5.35, which shows a orthoclase mineral within the London flame-dressed exposure slab. Figure 5.36 shows the elemental spot analyses

carried out on the same mineral at increasing depths. As can be seen, the spectra are extremely similar, regardless of increasing depth.

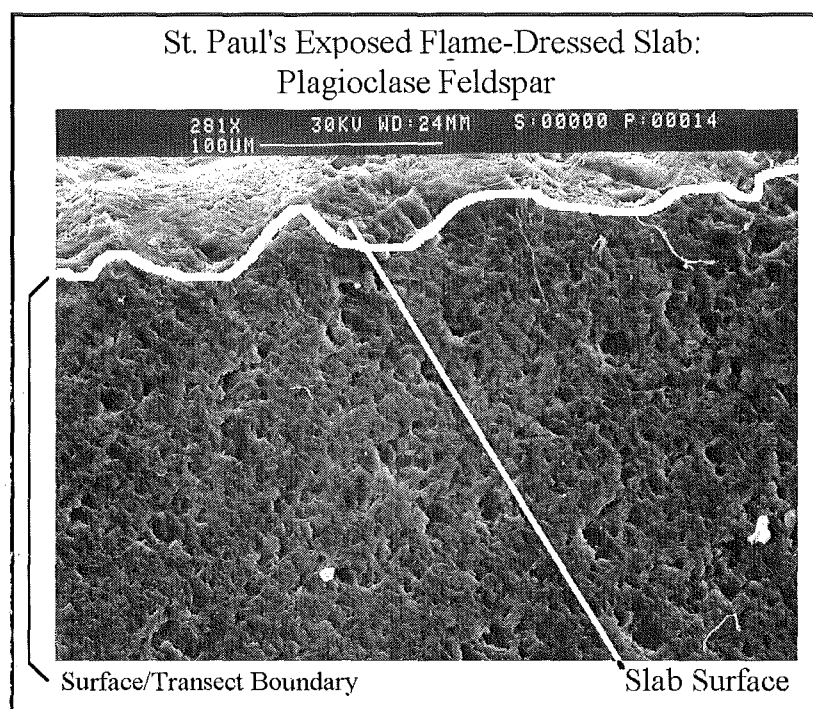


Figure 5.35. Detail of the London flame-dressed transect, showing a orthoclase mineral.

The lack of difference in the depth analysis, coupled with no significant variations in the elemental analysis of other minerals, where elements such as iron and calcium were examined, suggests that the length of exposure was insufficient to generate significant deterioration features. A longer period of exposure could allow the formation of extensive micro-fracture networks, alteration minerals and other weathering features such as dissolution pits.

It is only when the different finishes and sites have sufficient deterioration features, that SEM/EDX comparisons will become worthwhile. At this stage of exposure, there were not enough modifications to the original chemical or physical composition of the slabs for differentiation to occur.

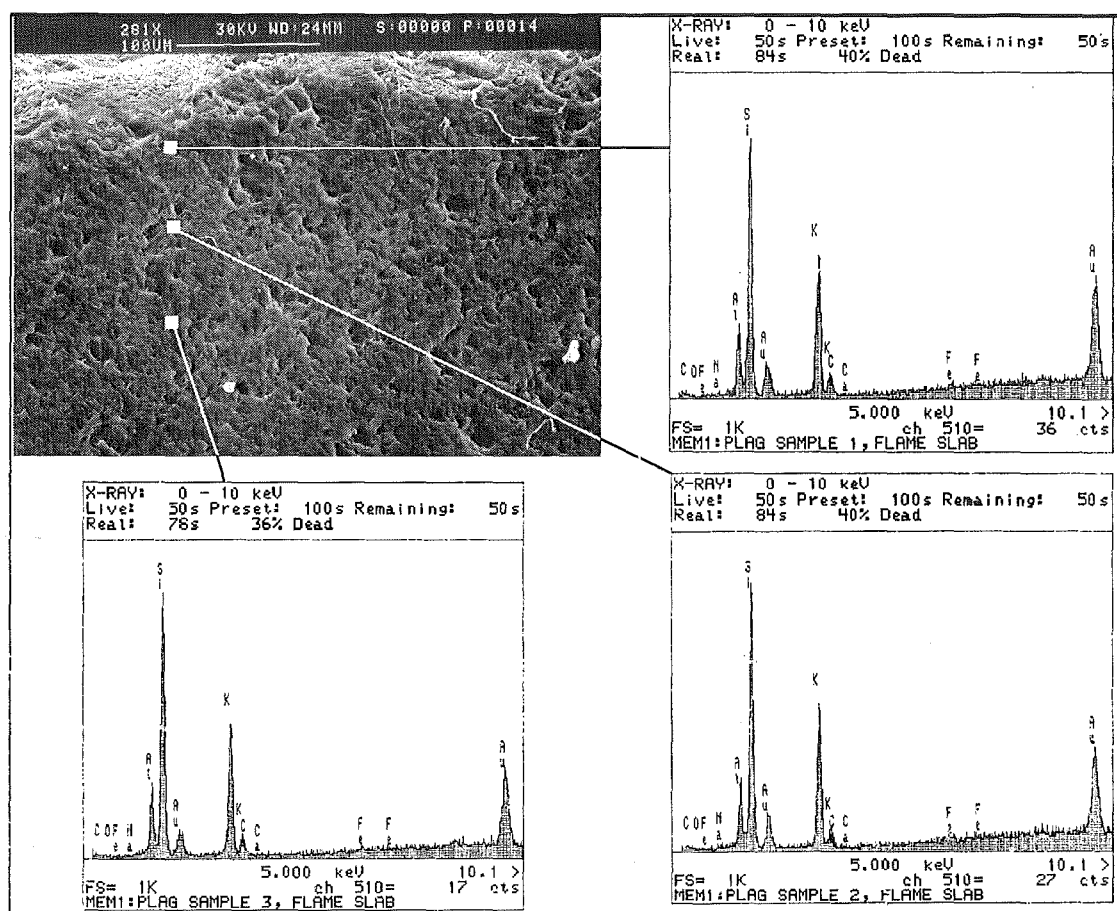


Figure 5.36. Incremental depth composition spectra, orthoclase mineral.

## 5.5. CONCLUSIONS

There were two main sections to the exposure programme; analysis of the run-off characteristics, and analysis of the physical changes the micro-catchment unit slabs and carousel tablets underwent.

The main parameter in controlling run-off composition and concentration was, as would be expected, site. This had a much stronger effect on parameter characteristics than whether the MCU contained glass or granodiorite, or what finish the stone slabs had. To illustrate this, only two of the eleven measured parameters showed no significant differences between the sites, while the other nine all showed significant differences between the rural and urban sites, even if it was not possible to detect differences between the urban sites.

The role of deposition surface and finish type was much more difficult to quantify. Only three of the eleven characteristics showed a significant difference

between the population of the blank and the stone slab populations, indicating that although the stone surface might be an important factor in deposition velocity over the course of a buildings lifetime, it had little impact over the 91 weeks of the study.

The role of finish was the most marginal of the independent factors, with only Dartmoor, the cleanest of the three sites, showing a difference between the finish concentrations. This may be due to: 1) Ambient pollutant concentrations of the urban sites masking the very subtle variations in concentration engendered by the finish variations. 2) Insufficient differences in slab roughness, although commercial stone finishes were used to reflect current practices.

The second section of the exposure programme was the analysis of the physical characteristics of the exposed stone. There were two groups of stone used at each of the three sites. The first were the carousel tablets, which consisted of three stone types; Mountsorrel granodiorite, Merrivale granite and Bolventor granite.

The carousel tablets were weighed three times during the course of the exposure period (except Dartmoor, which was only weighed twice). When the weights for the different stone types were compared, it was found that there were significant weight loss variations between Bolventor and the other stone types at Birmingham and London at the half way point. Differences in weight between the stones types were only detected at Birmingham, however, at the end of the end of the exposure period, when the granodiorite was significantly lighter than the other two stone types.

This suggests that there was a period of rapid adjustment to the environment from the stone tablets as they moved towards equilibrium. This adjustment period occurred over the length of the exposure period, and resulted in a similar level of weight loss across the tablets. Once adjustment has occurred, it is likely that a period of more gradual weight changes would occur as differences between the stone types started to emerge

Comparisons between the upper (total deposition) and lower (dry deposition) suites showed that while all of the tablets (both upper and lower) gained weight during the first 45 weeks of exposure, the protected lower suite tablets gained weight more rapidly. The weight gains were most likely explained by a combination of

insoluble particulate deposition and the build-up of soluble salts i.e. nitrates. The weight gains appeared to be partially influenced by site.

Comparison of the upper and lower suites at different sites showed little variation between the upper suite stones, except between London and Dartmoor at the end point weighing. In comparison, the lower suite urban half-way weights were significantly different from each other, but by the end of the exposure period, these differences had gone, and only Birmingham and Dartmoor approached significance.

At the end of the exposure period, the carousel tablets at the urban sites had lost weight (with the rate of lower suite weight loss lower than for the exposed tablets), and weighed, on average 99.99% (lower) and 99.96% (upper) of their original weights. The rural tablets were only weighed at the beginning and end of the exposure programme, and showed a weight gain by the end of the period. This could be explained by the rural stones following the same pattern as the urban stones, but as a result of the lower ambient pollution levels, over a longer period of time.

The weight gain and loss of the granite samples of the exposure programme differed from the response of limestone tablets prepared by Janyes and Cooke (1987), and exposed in south-east England, where both sheltered and exposed samples lost weight, with tablet weight loss significantly higher in central London than in the surrounding country. The difference in response between the granite and limestone tablets can be ascribed to the mineral composition of the two stone types. The calcium carbonate of the limestone tablets reacted quickly with  $\text{SO}_2$  concentrations to produce soluble gypsum which was leached away, while the more resistant granite gained weight through atmospheric deposition processes before the removal of friable stone fragments produced by the cutting of the tablets. A more lengthy period of exposure could well produce systematic differences between the stone types, as the tablets adjust to ambient condition before producing gradual effects.

Analysis of the micro-catchment unit slabs again revealed the limitations of the length of exposure. Although site had been determined to be the most important aspect in determining run-off concentrations, and affecting carousel tablet weights, it had no significant effect on the weight of the MCU slabs at either weighing period. Inter-finish comparisons also failed to show any significance between the slabs, regardless of site.

The lack of variation between the initial and end condition of the MCU slabs was confirmed by SEM and EDX analysis of the London and control slabs, and implies that the length of exposure was not sufficient for changes to become detectable. This holds true for the roughness measurements, in which only the polished slabs showed any significant roughening over the exposure period, at both the 1<sup>st</sup> and 2<sup>nd</sup> order scales. This increase in roughness is only detectable due to the relative uniformity of the unexposed polished surfaces, and would not be evident on rougher stones.

The lack of response from the granite microcatchment units, which have been used successfully for other stone types such as marble (Reddy, Sherwood & Doe, 1986; Sweevers and Van Grieken, 1992; Torfs and Van Grieken, 1996), sandstone (Halsey *et al*, 1995; O'Brien *et al*, 1995) and limestone (Cooper, 1986; Reddy, 1988), illustrates the resistant nature of granite. Although the exposure program was constructed to determine the relative influence of surface roughness on the weathering rate and response of granite building stone, the lack of significant results from variations in the run-off concentrations only showed the importance of site in determining run-off characteristics.

Variations in the surface finish had no significant impact on either the run-off concentrations or the physical condition of the stone slabs used in the experiment. The lack of significant results from the granite exposure programme is in accordance with a study of Leinster granite microcatchment units in Holland and Belgium, where Sweevers *et al* (1995) reported that 2-3 years ambient atmospheric exposure had a negligible effect on the granite samples.



## CHAPTER 6. *In Situ* Building Deterioration Assessment Study: SDI Scheme

### 6.1. INTRODUCTION

Building stone undergoes weathering when exposed to the atmosphere. Rain, pollution, thermal variation and the constituents of air (CO<sub>2</sub>, O<sub>2</sub> etc.) all promote decay. As detailed in Chapter 2, deterioration occurs through a variety of mechanisms as the rock material adjusts to changes in its environment. The weathering can take many forms, and will not always be visible to the casual observer.

One of the problems with the assessment of cultural heritage decay is determining not only how far the building stone has altered from its 'original' condition, but also at what rate it weathered. This can have important implications for both the physical and aesthetic condition of a building. 'Original' in this case is the state that the stone was in when the building was first completed.

The amount of deterioration a building has undergone is an important, but a difficult, parameter to measure. If it is known that areas of any given building are at risk, a preventative and protective strategy can be implemented to conserve the building. With modern remedial techniques, it is possible to reduce the effects of atmospheric exposure on building surfaces, but the application of such silicone water-repellents is expensive and can promote the rate of decay by inhibiting the free egress of moisture within the rock.

There have been many methods developed for the assessment and characterisation of building decay features and rates, ranging from a visual study of the building and its decay features (Smith, Whalley and Magee, 1992; Quinlan, O'Daly and Lewis, 1994; Halsey, Dews, Mitchell and Harris, 1996; Robinson and Williams, 1996) to photogrammetric assessments (Cooper, 1993; Emerick, 1995; Sequeira Braga, 1996), both of which have problems with the subjective interpretation of decay features and the qualitative assessment of the effected areas. Geochemical (Fort González, Bustillo Revuelta, Mingarro Martín, & López De Azcona, 1993; Vargas, Maqueda, Franquelo, García-Talegón and Pérez Rodríguez, 1996) and petrographic analysis of the building stone (Sequeira Braga, Simões Alves

and Begonha, 1993; García-Talegón, Molina and Vicente, 1996) have also been carried out on historic monuments and buildings, although there are several problems associated with these forms of building decay analysis, primarily the need for material samples for destructive testing from the examined buildings, and the removal of the samples for lab-based analysis procedures such as XRD.

Recently, as a result of rapid increases in instrumental and computational power, i.e. computer-aided tomography (Montoto, Valdeón, and Esbert, 1996; Valdeón Montoto and Esbert, 1996), X-ray fluorescent spectrometer (Stillman, 1996) and laser-scan roughness plotting, it has become possible for the non-destructive measurement of a variety of internal and external building stone parameters in great detail to classify the degree of weathering. Common elements of these analytical methods are, however, the high levels of expertise needed both by the operator and data analyst, and the high cost of purchasing and running the instruments. Another problem that often affects the application of these techniques is the inability to conduct the exploration *in situ*, at the building site - a major hurdle in their application.

In contrast, the proposed SDI (Stone Deterioration Index) assessment scheme differs from the previous methods of building decay evaluation, in that it is composed of a number of quantifiable, cheap, quick and easy to perform measurements. These measurements are carried out *in situ* on individual building stones, and are repeated a number of times to provide a reliable average for the rock.

The results from the parameter or index tests are referenced against a rating index, where the variables are assigned a number of rating points, depending on the rock response. The rating of each building stone, in both internal and external walls, can be used to provide: 1) a measure of change from the assumed initial condition (the interior blocks); 2) information on the rate of stone weathering and how it is affected by pollution concentration; 3) the formation of deterioration maps, detailing areas of higher than average weathering. This will allow the pin-point targeting and application of remedial strategies to protect the rock, and the prediction of future decay patterns.

The concept of using a number of parameters to derive a single rating figure is not new, and has been used in many engineering geology schemes i.e.  $Q$  (Rock

Mass Quality). Formulated by Barton *et al* in 1974,  $Q$  was designed to measure and classify tunnel stability. Based on six parameters, including the RQD (Rock Quality Designation) index, water inflow rate, joint density and degree of alteration,  $Q$  could be used to estimate rock mass quality from heavy squeezing-ground to sound unjointed rock.

## 6.2. ROCK CLASSIFICATION SCHEMES IN ENGINEERING GEOLOGY

Rock rating and index schemes are used extensively in engineering geology where they provide a description of the engineering characteristics for zones of rock of similar quality (Anon., 1995). This permits an engineer to quickly and reliably assess a site's suitability for construction purposes. The utilisation of the numerous grading and ratings schemes allows a relative evaluation of the strength or quality of a rock, on both large (mass) or small (material) scales. This is achieved by either a visual assessment of the rock (Price, 1993), the measurement of selected physical characteristics of the material (index testing), or a combination of both modes (Selby, 1982).

Rating and classification systems have traditionally been applied on one of two scales, with parameter boundaries and index performance differing in the separate systems. Rock material schemes attempt to evaluate and grade small scale rocks that are either free, or virtually free, of major discontinuities, and can be regarded as uniform for engineering purposes (Martin and Hencher, 1986). Rock mass schemes are applicable to either larger faces or areas of rock, where more variation in zones of rock quality will occur, and rocks need to be zoned in terms of engineering performance.

The SDI study is carried out on the material scale, with measurements taken from each stone within a particular building wall. This is for two reasons: 1) each building stone is a discrete rock entity, free from any major discontinuities and of a similar quality; 2) neighbouring blocks would not have been contiguous to each other in the quarry. A judgement on the mass rating of a wall can be made by averaging the values obtained for the individual blocks.

By using a material scale assessment scheme that can be applied to larger rock faces, the SDI scheme avoids some of the problems that have affected other engineering classifications, i.e. confusing terminology, no clear definition of material

grades, and unjustified boundaries for mass weathering zones (Hencher and Martin, 1986).

The first engineering classification of rock mass was purely descriptive, and was formulated by Terzaghi (1946) for use with tunnelling excavations. In 1964 Deere introduced a rough quantitative assessment of rock quality with the Rock Quality Designation (RQD). This has been followed by numerous other schemes (Bieniawski, 1974; Barton *et al*, 1974; Bieniawski, 1976; Irfan and Dearman, 1978a; Lee and de Freitas, 1989), all of which attempted to evaluate rock quality through the measurement of selected physical parameters (i.e. strength, fracture density, slakeability etc.).

Bieniawski (1989) listed the important uses of engineering rock classifications as; 1) Identification and quantitative measurement of selected physical parameters from identified rock units. 2) Separation of a rock mass into units of varying quality, with the conditions of each unit applied in a consistent and unified way from site to site, and from worker to worker. 3) Provision of distribution maps and data about the condition of the rocks at a site prior to design and building.

### 6.2.1. Engineering Rock Mass Rating Schemes

There are numerous rating schemes in operation, each with differing levels of differentiation between physical defects and weathering phenomena. The two most commonly used rock mass classification systems are Rock Mass Rating (RMR) (Bieniawski, 1974; Bieniawski, 1976), and Rock Mass Quality (*Q*) (Barton *et al*, 1974).

Bieniawski's 1974 Rock Mass Rating Geomechanics Classification (RMR) was initially formulated to predict the performance of rock masses in tunnelling, but has also been used in rock quality assessment for dam foundations, mining applications and slopes (Bieniawski, 1976). Incorporating RQD, groundwater condition, material strength, and information about joint spacing, condition and orientation, the RMR scheme rated each parameter to derive an overall figure for rock quality between <20 to 100, with very good rock rated as 81-100 RMR. This allowed the prediction of unsupported stand-up time for various rock masses, with obvious implications and applications for engineering geology.

Barton *et al* (1974) also evaluated the condition of a rock mass by rating six rock parameters (RQD, number of joint sets, joint roughness, joint alteration, amount of joint water reduction and the amount of stress reduction) to provide a figure between 0.001 and 1000. Using this figure, engineers could then estimate the amount of support any given tunnel in that rock mass would require.

Recently, Price (1993) suggested one way of accurately evaluating the suitability of a rock mass for geo-engineering purposes was to construct a rating system where a number of rock parameters are rated and applied to a table of values. This system gave rock masses a rating from -20 (geotechnical soil with relict discontinuities) to 140 (effectively unweathered), and is applicable to all rock types.

The rock under investigation is graded according to a predetermined set of scales, which assign numerical values to the amount of rock decayed (i.e.  $\pm 1/4$ ,  $\pm 3/4$ ,  $\pm \text{All}$ ), and the level of decay. The weathering intensity is also quantified by measuring parameters such as joint staining, joint waviness and bedding plane infilling, resulting in a total rating for rock quality. The total rock rating is then entered in to a weathering classification table, shown in Table 6.1.

Class	Rating	Descriptive Term	Igneous Rocks
<b>A</b>	140	Effectively unweathered	Engineering problems related to material properties, discontinuity properties etc. No influence of weathering
<b>B</b>	100	Significantly weathered	Reduction in joint strength gives problems in slope stability, tunnelling.
<b>C</b>	50	Severely weathered	Major slope stability problems by release of corestones, irregular bearing capacity particularly for small dimension foundations. Corestone/soil strength contrast difficult for tunnelling.
<b>D1</b>	0 - 20	Geotechnical soil - without relict discontinuities	Weathered material geotechnically a soil so all engineering works designed on soil parameters.
<b>D2</b>	-20	Geotechnical soil - with relict discontinuities	Weathered material geotechnically a soil so all engineering works designed on soil parameters, but with added handicap of potential sliding planes of relict discontinuities.

Table 6.1. The Price classification, based on rock parameters (Price, 1993).

There are problems with the utilisation of rating schemes and the imposition of weathering classes, such the categorisation of ambiguous rock in the field, the initial weighting of the rating mechanism and the combination method of parameter ratings to

provide an end figure. These problems are outweighed, however, by the ease and speed of use of the visual schemes, allowing the rapid characterisation of a site, prior to more in depth investigations.

### 6.2.2. Weathering Grade Classifications

The first attempt at a progressive weathering grade classification was that of Moye (1955) for the Snowy Mountains granite of Australia. Moye first introduced the much used terms Fresh, Slightly Weathered, Moderately Weathered, Highly Weathered and Completely Weathered. The grades were distinguished by simple hand tests on borehole cores, although not specifically for engineering purposes. Table 6.2 shows the current weathering classifications suggested by the Geological Society Engineering Group Working Party.

1: Classification for Uniform Materials			2: Classification Incorporating Material and Mass		
Grade	Classifier	Typical Characteristics	Class	Classifier	Typical Characteristics
I	Fresh	• Unchanged from original state	A	Unweathered	Original strength, colour, fracture spacing
II	Slightly Weathered	• Slight discolouration, slight weakening	B	Partially Weathered	Slightly reduced strength, slightly closer fracture spacing, weathering penetrating in from fractures, brown oxidation
III	Moderately Weathered	• Considerably weakened, penetrative discolouration • Large pieces cannot be broken by hand	C	Distinctly Weathered	Further weakened, much closer fracture spacing, grey reduction
IV	Highly Weathered	• Large pieces can be broken by hand • Does not readily disaggregate (slake) when dry sample immersed in water	D	Destructured	Greatly weakened, mottled, ordered lithorelicts in matrix becoming weakened and disordered, bedding disturbed
V	Completely Weathered	• Considerably weakened • Slakes • Original texture apparent	E	Residual or Reworked	Matrix with occasional altered random or 'apparent' lithorelicts, bedding destroyed. Classed as reworked when foreign inclusions are present as result of transportation
VI	Residual Soil	• Soil derived by in situ weathering but retaining none of original texture if fabric			
3: Classification for Heterogeneous Masses					
Zone	Proportion of Material Grades		Typical Characteristics		
1	100% G I - III (not necessarily fresh rock)		Behaves as rock; apply rock mechanics principles to mass assessment and design		
2	>90% G I - III <10% G IV - VI		Weak materials along discontinuities. Shear strength, stiffness and permeability affected		
3	50 to 90% G I - III 10 to 50% G IV - VI		Rock framework still locked and controls strength and stiffness; matrix controls permeability		
4	30 to 50% G I - III 10 to 50% G IV - VI		Rock framework contributes to strength; matrix or weathering products control stiffness and permeability		
5	<30% G I - III >70% G IV - VI		Weak grades will control behaviour. Corestones may be significant for investigation and construction		
6	100% G IV - VI (not necessarily all residual soil)		May behave as soil although relict fabric may still be significant		

Table 6.2. Rock weathering classifications for rock mass and material rating currently recommended for engineering purposes (Anon., 1995).

### 6.2.3. Rock Index Classifications for Engineering

Investigation of a rock mass, for both classification and rating schemes, can also be achieved through index testing, petrological analysis and laboratory testing (Broch and Franklin, 1972; Anon, 1977; Irfan and Dearman, 1978a; Dearman, 1978; Zhao *et al*, 1994; Anon 1995). These tests and procedures, some of which can be applied *in situ*, are designed to be easy to apply to the rock, reproducible and quickly completed.

The Rock Quality Designation (RQD) scheme is a simple index used widely in the evaluation of rock core quality, and therefore the engineering performance of a rock mass. Devised by Deere in 1964 for borehole cores but now extended for use at *in situ* rock exposures, the RQD is the sum of intact core lengths  $\geq 100\text{mm}$  as a percentage of the total length drilled (equation 6.1).

$$\text{RQD} = \frac{\sum c \geq 100\text{mm}}{\sum C} \times 100\% \quad (6.1)$$

where **C** is the total core length drilled, and **c  $\geq 100\text{mm}$**  is the number of core sections that are over 100mm in length. When the RQD value is calculated, it is referenced against Table 6.3, shown below, to provide a rock quality grade.

RQD Value	Rock Quality
<25%	Very poor
25 - 50%	Poor
50 - 75%	Fair
75 - 90%	Good
90 - 100%	Very good

Table 6.3. The RQD rock quality evaluation table (Deere, 1964).

Broch and Franklin (1972) also used classes for their simple point-load strength index test to classify rock strength on the material scale, which allowed quick, *in situ* testing (in comparison to the previous uniaxial (unconfined) compression test which required machined specimens and a laboratory environment). They produced a scale of

seven classes (six subdivisions), which could classify material between a residual soil and fresh rock.

Another way of quantifying the state of material weathering, as opposed to rock mass rating schemes, is by petrographic study, particularly for igneous rocks such as granite. The mineralogy of granite alters as it weathers, and it is possible to classify the degree of weathering granite samples have undergone by analysis of the rock under thin-section. Lumb (1962) created a weathering index,  $X_d$ , from observations of weathered Hong Kong granites. In fresh rock,  $X_d=0$ , while in completely weathered granite  $X_d=1$ .  $X_d$  is a weight ratio of quartz to feldspars, shown below

$$X_d = (N_q - N_{qo}) / (1 - N_{qo}) \quad (6.2)$$

where  $N_q$  is the weight ratio of quartz and feldspar in the soil sample, and  $N_{qo}$  is the weight ratio of quartz and feldspar in the original rock.

Weathering Class	Grade	Rock mass/material description	Strength	RQD (%)	$I_p$ values
Fresh	I	No visible signs of material weathering. Near boundary with grade II some slight discolouration on major defects	Very high	Very high 90-100	>12
Slightly weathered	II	Discolouration indicates weathering of rock material and defect surface. Discolouration ranges from defect surface only to completely stained.	Very high to 50-60% of fresh rock strength	75-90	12-6
Moderately weathered	III	Less than 50% of material decomposed and disintegrated to intact soil. Rock core discoloured and weakened.	30% of fresh rock strength	40-75	4-6
Highly weathered	IV	More than 50% of material decomposed and disintegrated to intact soil. Rock core discoloured and weakened.	15% of fresh rock strength	10-40	2-4
Completely weathered	V	Intact friable soil which may be weakly cohesive. Soil has fabric of parent rock.	Extremely low	0-10	2
Residual soil	VI	Friable soil with original rock fabric completely destroyed.	Extremely low	0	--

Table 6.4. Rock weathering classes and granite indices test values (modified from Irfan and Dearman, 1978a).  $I_p$  = Micropetrographic index (after Irfan and Dearman, 1978b).



Another material weathering index classification, the micropetrographic index, has been created by Irfan and Dearman (1978b) who also classified rock material weathering by analysis of the petrography of the sample. Macroscopic analysis included an assessment of the amounts of discolouration, decomposition and disintegration, while the microscopic analysis involved determining the mineral composition, degree of alteration and microfracture density. This is then converted to the micropetrographical index,  $I_p$ , using the following equation, with rock quality grades shown in Table 6.4.

$$I_p = \frac{\% \text{ sound or primary minerals}}{\% \text{ unsound constituents}} \quad (6.3)$$

### 6.3. STONE DETERIORATION INDEX

The stone deterioration index (SDI) is designed to assess the weathering levels of historic granitic buildings. This is achieved by the index measurement of a number of building stones in each wall of the examined building. By plotting and analysing the distribution of individual building stone values, it is possible to not only achieve a rating average for the whole wall, but also a distribution pattern for stone decay. Repeated use of the SDI scheme on the same building over time will allow the long-term monitoring of weathering rates, as building stone can show marked deterioration over engineering time, i.e. tens of years (Fookes *et al*, 1988).

The existing engineering classifications are useful for rating macro-scale site areas and rock masses, but are less applicable and informative for the oligo- and micro-scale weathering found on buildings. To counter this, the SDI scheme will allow the non-destructive and *in situ* quantification of parameters on the micro-scale for building stones within existing buildings, rather than for engineering construction site assessment. In addition, it will also be quick and simple to apply; Cragg and Ingman (1995), practising engineering geologists state that present classifications in engineering geology are difficult to apply. They suggest that a simple quantifiable and detailed scheme is needed to reduce the amount of misinterpretation and misapplication of current schemes, especially at material scales.

By concentrating on stones as individuals (equivalent to rock material rating), rather than the wall as a whole (rock mass rating), it is possible to account for a wide range of decay vectors that affect the stone.

Mortar, especially  $\text{Ca}^{++}$ -rich mortar can have a significant role in the rate of granitic stone deterioration. Cooper *et al* (1993) found that limestone mortars acted as salt reservoirs, promoting granular decay. The presence of the mortars also increased the time of wetness, especially when old mortar was exposed.

These findings were supported by further work on mortars by O'Brien *et al* (1993). They also found that repointing mortars, a harder mortar used as a seal between building stones to limit the ingress of water from the atmosphere, has several important interactions with the surrounding stones. Crucial areas are the hardness of the mortar, permeability and salt content.

If the pointing mortar is too strong for the surrounding building stones, then surface failure of both sound and weakened rock can occur if there is the slightest movement of the building (Duffy and Perry, 1994). The hardness of the mortar can also prevent the movement of moisture through the mortar, forcing it to through the stone, increasing decay (Emerick, 1995).

Dissolution of  $\text{Ca}^{++}$  in lime-rich mortars can also contribute to granite decay and mineral alteration, as mobile ions are liberated from the mortars and precipitate either on or in the surrounding granite (depending on the development of micro-fracture networks with the stones). These are cracks that can form inter-, intra-, and trans-granular microfracture networks throughout the stone body (Delgado Rodrigues, 1996), and can be the result of volume expansion or scaling (Smith *et al*, 1993).

The presence of microfractures can increase the secondary porosity of the stone, allowing the ingress of  $\text{Ca}^{++}$  and salts from the mortars, which can then accumulate at preferred depths with the stones and cause scaling and plaque formation. With time the microfracture network can propagate and widen, allowing a greater degree of decay (Rainey and Whalley, 1994). This activity is promoted by an increased time of wetness, which in turn is due to increased roughness of the inter-block mortars and the presence of poor sealing between the blocks and the mortar (O'Brien *et al*, 1993; Cooper *et al*, 1993).

Another important factor to consider is the historical legacy of the building, which could have been repointed some 10-15 times during the course of its life, each time with a mortar of differing composition. By analysing the actual building stones themselves, this will allow the integration of mortar-induced decay with deterioration produced by more general atmospheric processes.

It is obvious that the role of mortars in granite building stone decay is complex, with many different processes acting on the granite and promoting decay. Although the SDI scheme does not specifically account for the role of mortars in the decay of building stone, the end results of the decay processes can be measured. It is felt that this is a more versatile and robust system of decay assessment that will account for the different types of mortar used in a historic building.

### **6.3.1. Building Decay Parameters and Class Boundaries**

There are three fundamental criteria for measurements in the SDI scheme:

- 1) Simple - so all workers can achieve the same results.
- 2) Effective - the selected tests must measure discrete parameters that are relevant to rock properties.
- 3) Non-destructive - the tests are carried out *in situ* on building walls and changes to the wall as a result of measurement is not allowed on the grounds of aesthetic and material conservation.

A variety of physical index tests have been used in the past for the assessment and classification of rock material and mass weathering.

As shown in Table 6.5, there are a number of tests that can be used to physically characterise building stone. However, several of the tests can not be carried out without either destruction of the sample, or removal of samples for laboratory testing. These conditions clearly exclude lab-based physical tests, such as the consistency index, point load index or the quick adsorption index.

Other possible tests, such as the micro-resistivity testing and sonic velocity, do not address a clear component of stone deterioration, where there is difficulty in accurately assigning variability to specific aspects of stone decay (Lumb, 1985). The components of stone deterioration are shown below in Figure 6.1.

A high number of the physical tests cited in Table 6.5 are used to assess rock material strength. Although this is an important component of rock weathering evaluation, even the same rock type with the same weathering grade can produce strength values with a high level of variability (Lee and de Freitas, 1989). Therefore it is important to have strength as only *one* of the parameters used to evaluate the deterioration level of building stone.

Physical Test	Parameter Measured	Reference	Comments
Schmidt Hammer	Surface Strength	Irfan and Dearman, 1978; Lee and de Freitas, 1989; McCarroll, 1991; Hencher and Martin, 1982	Quick, easy and non-destructive
Point Load Index	Rock Strength	Fookes <i>et al</i> , 1971; Irfan & Dearman, 1978; Lumb, 1983	Not applicable to <i>in situ</i> testing
Quick Absorption Index	Permeability	Fookes <i>et al</i> , 1971; Irfan & Dearman, 1978; Dearman and Irfan, 1978	Not applicable to <i>in situ</i> testing
Hand Penetrometer	Soil Strength	Hencher and Martin, 1982	Not applicable to fresh, slightly and moderately weathered rock
Surface Roughness	Surface Variability	Grimm, 1983;	Quick, easy and non-destructive
Slake Durability Test	Slakability and strength	Irfan & Dearman, 1978; Lee and de Freitas, 1989	Destructive and requires material extraction
Consistency Index	Weathering Degree	Martin, 1988	Not applicable to <i>in situ</i> testing, and does not measure a single weathering parameter
Micro-resistivity/ Conductivity Testing	Moisture Content		Difficult to test, unreliable data, difficult in assigning variability to specific parameters
Seismic/Sonic Velocity	Porosity/ fissuring	Dearman and Irfan, 1978; Lumb, 1983; Martin, 1988	Not applicable to <i>in situ</i> testing and not an accurate measure of a single aspect of deterioration

Table 6.5. Physical tests used in rock quality assessment.

The choice of the assessment parameters for the SDI scheme is one that has to account for all of the deterioration that can be observed on building stone, as well as providing a balanced, and repeatable, estimation of the weathering level of the stone and its importance to conservators. As a result of the variability of measured parameters such as strength, a combination assessment of stone weathering was felt to be the most reliable method of decay evaluation.

This was for two main reasons: A) A combination SDI rating drawn from the mean of a number of readings per stone could absorb a greater degree of variation within individual measured parameters without dramatically affecting the end reading, which will result in a more accurate and stable end rating value. B) The combination approach to decay assessment was needed to fully account for all the products of decay that result from stone deterioration.

There are several aspects of building stone deterioration that would have to be covered by any assessment scheme, as shown in Figure 6.1. The first, and most important, is surface strength. This is affected by a variety of disintegration and decomposition process, such as the formation of alteration products within the stone and microfracturing, and it can be used to provide a measure of the material strength of the building stone - crucial for a load-bearing stone.

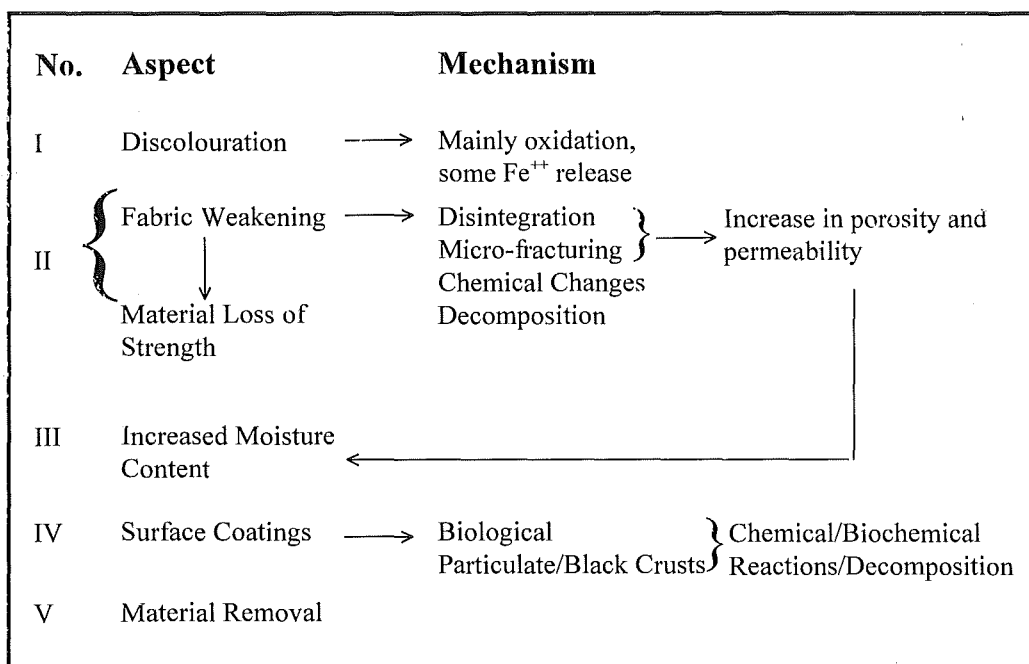


Figure 6.1. Aspects of stone deterioration.

There are a number of methods than can be used to assess material strength, but the majority of them are not only confined to lab-based assessment, but also involve the unacceptable destructive analysis of samples, as shown in Table 6.5. This leaves the Schmidt hammer, which has been found to be able to distinguish between the

weathering sub-grades of a coarse-grained granite (Irfan, 1996), as the most applicable method of strength assessment. Quick and easy to apply, the Schmidt hammer was designed for *in situ* testing of the surface hardness of concrete by impacting the sample surface with a weight at a known force. Measurement of the rebound distance can then be used to provide a measure of the surface unconfined compressive strength, allowing an insight into the amount of fabric weakening the building stone has experienced. Although a rapid, simple and non-destructive test of surface strength, the Schmidt hammer can be affected by the degree of sample surface roughness, and requires multiple readings to produce a reliable mean for individual building stones. It also provides no measure of the amount of material lost from the building stone over time, which is covered by the second SDI parameter.

The second most important measure of stone deterioration is surface roughness, which can provide a measure of surface variability and material loss, as well as an indication of the amount of disintegration the rock has undergone (surface strength and surface roughness have a strong negative relationship (McCarroll, 1991)). These factors all have important ramifications for the aesthetic and material conservation of the building stone. The surface roughness measurements in the SDI evaluation of building stone deterioration were acquired through the use of a contour comb, described in section 6.3.3, and is equivalent to coarse 1<sup>st</sup> order roughness.

Surface roughness, however, despite being correlated with surface strength, should not be used as the sole deterioration assessment parameter. Work by Grimm (1983) on the roughness profiles of granitic gravestones in Munich, showed that once a certain level of roughness was reached, any increase in roughness ceased, and parallel surface retreat occurred. This will not effect the SDI scheme as the roughness evaluation range can account for the cessation of roughness increase, but it is enough to prevent roughness being the sole assessment criteria.

Together, surface strength and surface roughness are the two most important parameters of stone decay evaluation, covering the loss of material strength through the formation of microfracture networks and alteration products, and material loss. They are also inversely related (albeit weakly) to each other in pilot studies on two Dartmoor churches (see section 6.3.1.1) (regression analysis; Sheepstor  $r = -0.52$ , Widecombe  $r = -0.45$ ,  $P > 0.01$ ). Consequently they are used to allocate the majority

of the rating points, with 75 of a maximum of 100 determined by strength and roughness, shown in Table 6.14., accounting for 75% of the potential rating value of any individual building stone. They do not, however, assess all of the possible deterioration factors that can affect building stone, and as a result two more parameters were considered necessary for inclusion in the SDI scheme.

The third parameter is a visual assessment of the amount of sample building stone discolouration, which will allow a degree of measurement for the amount of chemical weathering the stone has undergone. This not only has implications for stone performance, but it also provides a measure of aesthetic deterioration. Although surface strength will account for the majority of the decay instigated by chemical weathering processes in the near-surface area of the stone, a visual assessment of the amount of stone surface affected by discolouration will allow a refinement of the SDI scheme.

The final parameter to be included in the SDI scheme, shown below in Table 6.6, is a visual evaluation of the amount of black/brown crust or biological coverage on the surface of the sample stone. Although the other three parameters assess the overall products of the various weathering processes that can affect building stone, while an assessment of surface coatings (either black/brown crusts or biological coverage) measures a decay instigator, it is needed in the SDI scheme for two reasons. 1) The presence of crusts on the stone surfaces can result in deterioration and decay. This can range from the alteration of the physical structure of the stone in the near-surface environment (Schiavon *et al*, 1995), making it more susceptible to blistering and contour scaling (Smith and Magee, 1990) to the dissolution of the substrate stone itself (Ascaso *et al*, 1990; Prieto Lamas *et al*, 1995). 2) Crustal coverage is in itself a form of deterioration, albeit aesthetic, and as such needs to be rated.

The last two parameters, surface coatings and discolouration, are less important in determining the condition of building stone, although they are needed to provide a degree of refinement and discrimination for the values generated by surface strength and roughness. This is reflected by the lower weighting values for these parameters, which have a combined total of 25 points. Biological and crustal coverage is considered the more important of the two parameters, with a significant part of chemical weathering effects on stone already accounted for by surface strength and

roughness measurements. Therefore, surface coatings is allocated 15 points, while stone discolouration is allocated 10 SDI points.

By using these deterioration parameter tests, and combining their values, a rating scheme can be formulated to provide an assessment of the amount of weathering building stone has undergone. Measuring individual blocks, and combining them for an entire wall, it is possible to rate both the entire building and individual wall areas with varying aspects, in terms of the amount of general stone decay.

Parameter Test	Aspect No.	Deterioration Aspect
Discolouration Assessment	I	Surface Discolouration
Schmidt Hammer (relates to surface unconfined compressive strength)	II	Material Loss of Strength
Black Crust and Biological Coverage	IV	Surface Coatings
Surface Roughness	V	Material Loss

Table 6.6. Minimum tests required to account for all weathering aspects.

Although the measured deterioration parameters are expressed in different units, e.g. surface roughness in mm, surface strength in  $R_{\%}$  (percentage of rebound return), it is possible to combine these and other parameters to provide a single index figure using the SDI. This is similar to the method of obtaining the RMR (rock mass rating), a scheme extensively used by engineering geologists (Bieniawski, 1974; Bieniawski, 1976). The SDI value is achieved by rating the four decay parameters (surface strength, surface roughness, surface coatings/crusts and discolouration); assigning a number of points to their value, depending on their response to the condition of the subject stone. The measured values and their range is shown in Table 6.14. The SDI rating points are then summed, and the total value is a measure of rock quality.

The total rating value of the stones can highlight areas of dramatic change if an entire wall is measured, or if the studies are carried out over a number of years, allowing the relative weathering rates of the subject building to be monitored. Knowledge of the weathering profile of culturally significant buildings can allow either the selective application of remedial techniques in order to protect or repair areas that



are weathering rapidly, or the implementation of a more detailed, and expensive, examination of the stone condition.

Resistivity was considered as one of the evaluation parameters, but there were several areas of concern about the resistivity values obtained in the pilot study of two churches, discussed in section 6.3.1.1. The study was conducted to allow testing of the measurement equipment, and the collection of raw data to allow the formulation of the rating ranges for each of the assessed decay parameters. The results from the preliminary micro-resistivity survey showed there was an unacceptably wide range of resistivity values obtained within blocks, and from block to block. Also, there was no clear association of high resistivity values with sound rock, or low values with friable, weathered rock. The values also included an unrealistic value distribution between the interior and exterior walls, and a high number of anomalous readings from all churches.

Finally, resistivity values, unlike other assessed parameters, were not discrete measures of rock quality; they reflected water content, water quality and the amount of secondary clay minerals within the rock matrix. It was decided, therefore, that resistivity values would not be included in the index formulation. Increased porosity, permeability and moisture content, which might be assessed by resistivity, are all functions of fabric break-up and would be reflected in loss of rock strength and the Schmidt Hammer results.

#### **6.3.1.1. Pilot Study**

A pilot study was undertaken in November 1995 on two churches on Dartmoor to allow the formulation of the SDI rating tables. The churches were Widecombe-in-the-Moor, with a tower built in the early 16<sup>th</sup> century (the construction date was considered to be 1500 for the study), and Sheepstor, which was rebuilt between 1500 -1520. Sheepstor is considered to have a construction date of 1510 for the study.

Both of the churches measured in the pilot study, and the quarry at Burrator reservoir, were constructed from Dartmoor granite Type B<sup>1</sup> (classified as a coarse-

---

<sup>1</sup> See Table 2.3, and section 2.3.4.1 in chapter 2 for details.

grained megacrystic biotite granite by Floyd *et al*, 1993). This is a coarse-grained porphyritic biotite granite with feldspar megacrysts of 2 - 5 cm length.

Two pieces of equipment were used in the building assessment;

- Profile gauge, with height and levelling guides to ensure reproducible results, shown in Figure 6.5.
- Schmidt Hammer (Type N, power:  $2.227 \text{ Nm}^{-1}$ ).

The studied buildings were first characterised in terms of orientation, number of courses (horizontal rows of building stones) and number of building blocks per course. A plan of the building, showing orientation, measurement areas and the layout of the courses was also constructed. This was marked with any anomalous regions that might affect the measurements (e.g.: areas with later alteration, cleaning or repair of the surface), as determined by visual assessment. Measurements were then taken from the stones, using only building blocks with vertical faces, to allow the formulation of the range and class boundaries for each of the rated values.

#### **6.3.21. Surface Strength (Schmidt Hammer Rebound Test)**

The Schmidt Hammer was originally designed for *in situ* testing of concrete structures by civil engineers, which it does through recording the distance of rebound from the subject surface of a spring-loaded mass for a given force. It is simple to use, with readings taken perpendicular to the sample surface, and is now used by a wide range of geologists and geomorphologists for rapid field measurement of rock surface hardness.

Rock strength is reduced by weathering processes, and particularly by the development of soft secondary minerals, microcracks and an increased water absorption capacity (Fookes *et al*, 1988). This reduction in strength has been used by Hencher and Martin (1982), who correlated 'N'-type Schmidt Hammer values with the unconfined compressive strength and shear strength of rock samples.

McCarroll (1991) supports this by showing that there is a clear negative relationship between the degree of rock surface weathering and Schmidt Hammer rebound values ( $R_{\%}$ ). His measurements were taken from a small area of recently uncovered, uniform gabbroic rock, and the N-type Schmidt Hammer values have a

negative correlation with both surface roughness ( $r^2 = 0.89$ ) and degree of weathering ( $r^2 = 0.9$ ), shown in Figure 6.2.

There is a wide range of Schmidt Hammer values for *in situ* granite at outcrop, with fresh granite masses producing  $R_{\%}$  values of over 60, while moderately weathered granite gives values between 20-40  $R_{\%}$  (Zhao *et al*, 1994). Sjöberg (1994) measured culturally important granite exposures in south-west Sweden, and found an  $R_{\%}$  range of 0 - 62 when using the less powerful Type L Schmidt hammer (0.735 Nm, as opposed to 2.227 Nm for the common Type N). Typical Schmidt Hammer values are given for the different weathering grades in Table 6.7.

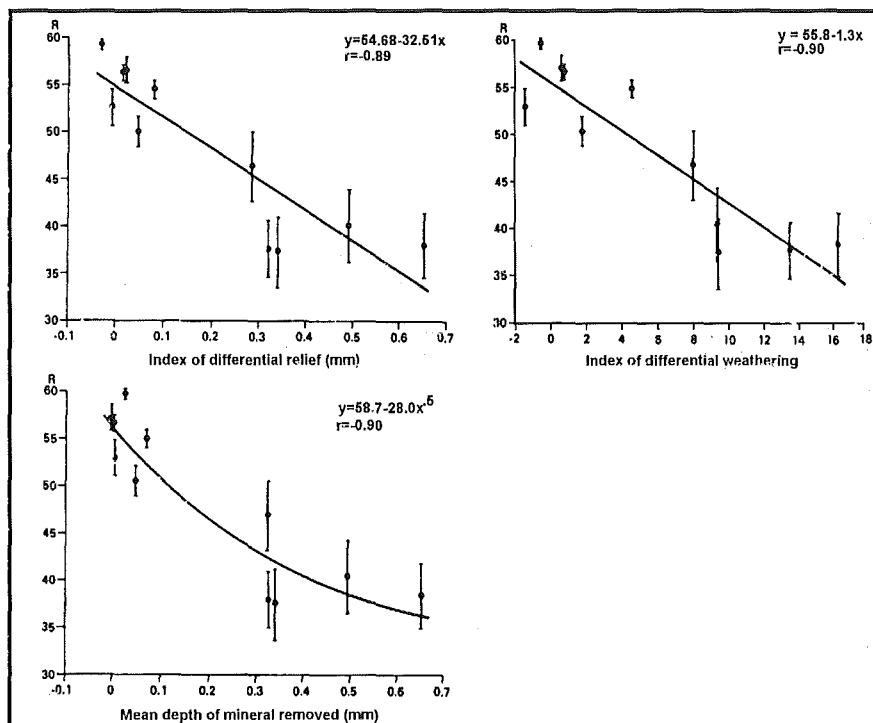


Figure 6.2. The relationship between Schmidt Hammer rebound values ( $R_{\%}$ ) ( $\pm 2$  standard error), and different measures of rock surface weathering (McCarroll, 1991).

Surface strength is the most important and robust measure of rock quality in the Stone Deterioration Index, and is weighted accordingly, with a maximum of 40 points. This is divided up equally throughout the range of possible values, as determined by the pilot study measurements. Schmidt Hammer values for a granite

mass, which are measured as percentage of rebound return ( $R_{\%}$ ), can vary between  $<20$  to  $>60$ , with a typical response from a slightly weathered granite as  $40 - 60 R_{\%}$ .

Readings taken from the Dartmoor churches and other buildings are considerably lower than those measured at *in situ* outcrops at a local quarry, where an average value of  $53.08R_{\%}$  was recorded for 'engineering' slightly weathered rock. The quarry used in the study was located by the side of the Burrator reservoir, and was rated as approximately grade II by Fookes, Dearman and Franklin (1971).

Rock Grade	Term	Granite Korea <sup>1</sup>	Granite Singapore <sup>2</sup>	Granite UK <sup>3</sup>	Granite Hong Kong <sup>4</sup>	Granite Hong Kong <sup>5</sup>	Granodiorite Hong Kong <sup>6</sup>
I	Fresh	59 - 62	60 - 67	$>58$	57 - 60	--	59 - 68
II	Slightly Weathered	51 - 56	40-60	53 - 58	$> 55$	$> 45$	45 - 68
III	Moderately Weathered	37 - 48	20-40	45 - 53	30 - 58	25 - 45	25 - 50
IV	Highly Weathered	12 - 21	$<20$	20 - 45	14 - 32	0 -25	15 - 30
V	Completely Weathered	--	--	$< 20$	0 - 18	--	0 - 18
VI	Residual Soil	--	--	--	--	--	--

Table 6.7. Weathering grades with N-Type Schmidt Hammer values. -- = no value or not reported. <sup>1</sup> = Values from Korean granite masses (Lee and de Freitas, 1989). <sup>2</sup> = Values from granite masses in Singapore (Zhao *et al*, 1994). <sup>3</sup> = Values from granites in the United Kingdom (Dearman and Irfan, 1978). <sup>4</sup> = Values from course-grained granites in Hong Kong (Irfan, 1994). <sup>5</sup> = Values from Hong Kong granites (Hencher and Martin, 1982). <sup>6</sup> = Granodiorite readings from Hong Kong (Irfan and Powell, 1985).

These values were significantly different<sup>2</sup> from the average values recorded at the two churches used in the pilot study, where Sheepstor church produced an average external strength value of  $27.03R_{\%}$  and Widecombe-in-the-moor church an average value of  $29.14R_{\%}$ . (See appendix, Table 8.4, 8.5 and 8.6).

The disparity between measurements from the Dartmoor churches, and the values cited for granite rock masses in Table 6.7, is due to the extraction (which

<sup>2</sup>  $T(5) = -11.56$ ,  $P < 0.01$

might include blasting), working and processing of the stone prior to building. These processes instigate and expand the microfracture network within the stone (Fookes *et al*, 1988; Smith *et al*, 1992; Smith *et al*, 1993), which will appreciably reduce the strength of the rock (Irfan, 1996). Winkler (1987) has recorded the development of spalling of parallel layers in urban granite building stones, which he attributes to a combination of salt action and the stresses induced by the finishing processes used to shape and polish the stones. This will lead to a high rate of building decay in the first 100 years of construction, with a possible decrease in the decay rate once spalling of the fractured surface layers has occurred.

Dibb *et al* (1983) mention limestone breakwater armourstone that weighed 20-25 tonnes at the quarry face, but only 12 tonnes at the coastal site. The halving of the weight was due to the transportation of the blocks to the site. Although this is not directly comparable to the situation faced by the granite blocks used in the Dartmoor churches, it provides an indication of the amount of stress transmitted to transported stones.

The data gathered from the surface strength tests were expressed as  $R_{\%}$ , or the percentage of rebound return. These values are related to the surface strength (MPa) of the rock. Engineers frequently convert the rebound percentage values to strength, but this is not required here.

Following the pilot study measurements of two churches on Dartmoor (Widcombe-in-the-Moor and Sheepstor), the highest class boundary was set at  $36R_{\%}$ . Consequently, any value  $\geq 36R_{\%}$  is allocated the highest number of points (40), and this allocation decreases with each decrease of  $5R_{\%}$ .  $R_{\%}$  values that fall below  $20R_{\%}$  are allocated 0 points. The distribution of rating points can be seen below in Table 6.8.

Class	Surface Strength ( $R_{\%}$ )	Rating
Effectively unweakened	$\geq 36$	40
Slightly weakened	31 - 35	30
Moderately weakened	26 - 30	20
Highly weakened	20 - 25	10
Extremely weakened	$< 20$	0

Table 6.8. Surface strength assessment chart.

Schmidt Hammer readings can vary markedly within the same weathered heterogeneous rock (Lee and de Freitas, 1989), such as granite, as the measured point moves from minerals such as quartz to weathered mica or feldspar. To counter this a *minimum* of four measurements were taken per block, evenly spread out over the surface of the block, and the readings were then averaged to produce a single value figure for the building stone or measurement site. Care was taken to ensure that none of the readings were made on any surface coating. Where surface coatings approached 100%, or there was an anomalous reading, extra measurements were made.

### **6.3.3. Surface Roughness**

Surface roughness can also provide information about the weathering levels of rock, as it gives an indication of material lost. It is highly correlated with surface strength, and can provide a measure of differential relief (McCarroll, 1991).

Grimm (1983) studied the roughness profiles of gravestones in the New Nordfriedhof area of Munich, by laser analysis of silicone peals taken from the gravestones. He found that the surface roughness of gravestones increased for a number of decades, dependant on the stone type. However, once a certain level of roughness was achieved, any further increase stopped, and the stone underwent general surface regression. Despite this, surface roughness is still an important indicator of material loss, stone quality, and the exposure level of the building block location. Analysis of the variation in roughness values can be used to identify areas that experience more localised erosion, such as regular surface flow or gutter overflow.

Surface roughness is considered the second most important parameter in the evaluation of the amount of building stone decay. To determine the roughness (depth of material removed), measurements were made using a fine-toothed contour gauge with a measuring front of 14.9cm and 0.83mm wide pins fitted with levelling guides, which was pressed against the subject stone to obtain a profile. The guides were used to position the gauge parallel to the stone surface, and to aid in the accurate

transferral of the profile to paper. There was no preferred orientation to the measurements, providing the readings are taken from an uncoated surface.

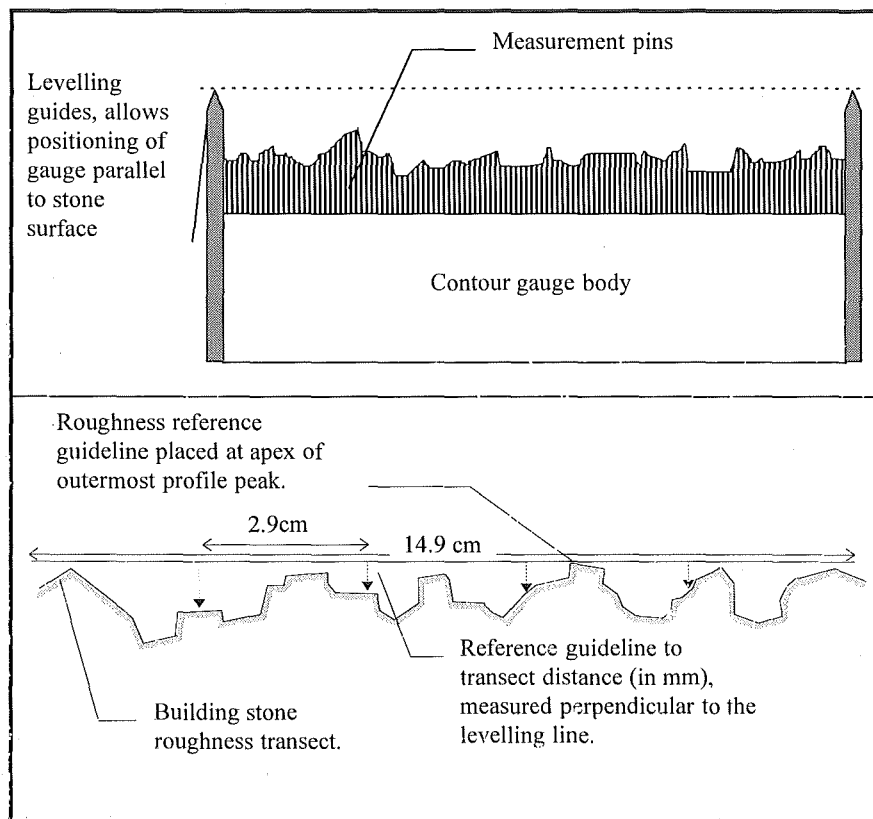


Figure 6.3. Surface variability measurement.

After the profile had been traced on to paper, a horizontal reference line was added to the outer-most point of the profile, as shown in Figure 6.3. Four regularly spaced measurements were then taken perpendicular to the reference line, one every 2.9cm along the profile to provide a systematic assessment of the surface variability, and the results recorded in mm. The average roughness for individual block is the mean of the four readings., were taken from the stone to provide an indication of surface variability and material loss through spalling and grain detachment. The roughness values for each stone are given a rating value using the rating chart, shown in Table 6.9.

Although one roughness transect per sample area was considered sufficient to characterise the stone for the SDI scheme, in areas of high surface variability the distance between the outer-most profile peak and the stone surface profile could be

reduced to 2 cm along the transect. An analysis of the effectiveness of increased reading from the roughness profile was undertaken on Sheepstor church, with six readings taken from the roughness profile as opposed to the standard four readings. T-test analysis showed no significant differences between either the profile means<sup>3</sup> or the raw values<sup>4</sup>, therefore it is as effective to use four measurements to characterise stone roughness as it is to use six, except in areas of high surface relief.

Initially, interpretation of the roughness profiles used a horizontal reference line positioned at the apex of the levelling guides, rather than at the apex of the outermost profile peak, with roughness expressed (in mm) as variation from the median line. This method, however, only provided information on surface variability, rather than the mean depth of material removed, and it was decided to change the evaluation method to the current practice. Correlation analysis between the raw roughness values from the two methods produced a value of 0.59 at the 95% confidence limit, while another analysis between the final SDI block totals for each church produced an average correlation value of 0.85 across all churches. This implies that both of the roughness evaluation methods are valid procedures for the assessment of the churches SDI value.

Class	Surface Roughness (mm)	Rating
Smooth	0 - 0.5	35
Slightly rough	0.6 - 1.0	30
Moderately rough	1.1 - 1.7	24
Rough	1.8 - 2.5	18
Very rough	2.6 - 3.5	9
Extremely rough	≥ 3.6	0

Table 6.9. Surface roughness assessment chart.

The range used in the SDI rating scheme, derived from the raw values obtained by the pilot study, rates the values from an average roughness of 0mm to >36mm, shown in Table 6.9.

<sup>3</sup>  $T(1, 284) < 1$

<sup>4</sup>  $T(1, 31) < 1$



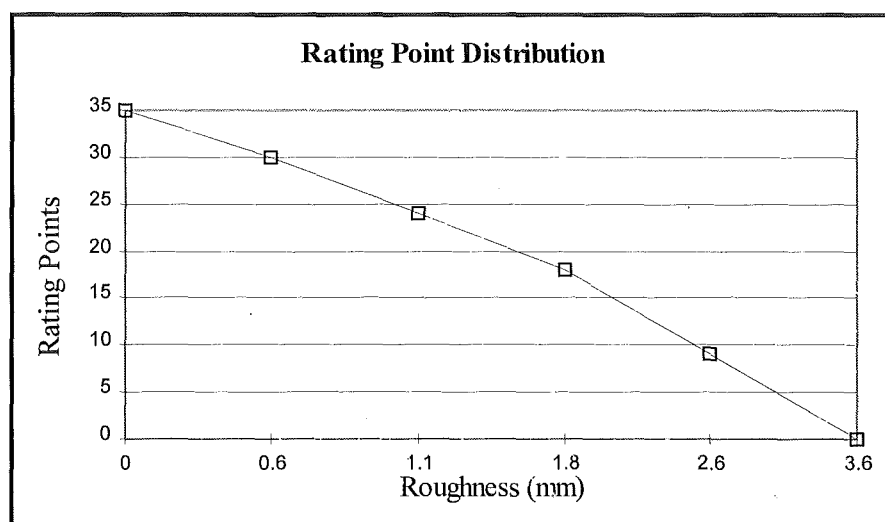


Figure 6.4. Surface roughness rating point distribution.

The distribution of rating points against surface roughness can be seen in Figure 6.4. The rating for this parameter is more discriminatory at the smoother end of the assessment scale, as this is thought to be the more critical zone of roughness increase. Initial increases in surface roughness will have a greater relative impact in terms of increased time of wetness, increased surface area, particle deposition etc., than an increase in surface variability at the rougher end of the scale. Therefore, the classes for the allocation of points increase in size as the roughness increases. To capture all possible surfaces, the end class includes all values over 3.6 mm. This addresses concerns about general surface recession once the rock has reached a certain level of roughness.

#### 6.3.4. Surface Coatings (Biological Cover and Black Crusts)

The formation of crustal deposits on the surface of a building stone can influence the near-surface regime of the stone (Bell *et al*, 1994), and strongly affect the aesthetic appeal of a building or monument. As result it should be included as a parameter in the SDI study. The impact of crustal coverage, however, is not uniform across all of the different aspects (North, South, West and Interior), as shown in Table 6.10.

Percentage Surface Coverage		
Aspect	Sheepstor	Widcombe
South	20.9	22.9
West	40.9	10.9
North	94.3	94.6
Interior	0	0

Table 6.10. Cross-church average coverage for different walls.

As a result, the contribution of the surface coating evaluation is less than surface strength and roughness in the overall weathering evaluation, but still contributes to 15% of the rating total. The surface coatings rating allows the presence of both biological growth and black crust formation to be accounted for, and permits a degree of discrimination in the overall SDI value. Although the presence of surface coatings on building stones will have an adverse effect on Schmidt Hammer readings, care is taken to locate areas of the rock that are free from coatings for testing.

Biological organisms, such as lichens, algae and endolithic and epilithic bacteria can all grow successfully on building stone surfaces, and their metabolic by-products can further promote weathering when deposited on stone surfaces (Ascaso *et al*, 1990; McGee, 1989). Although more frequent in rural, non-polluted areas, biological organisms can be found on almost all buildings of cultural significance (Camuffo *et al*, 1994; Pireto Lamas *et al*, 1995)

Black and brown crusts (Camuffo, 1995; Dolske, 1995; Schiavon *et al*, 1995) are also common on granite stone surfaces in urban environments, and can have an important influence on the near-surface regime and weathering rate of building stone. Incorporation of fly-ash and road-side dust from vehicles into black crusts is also detrimental to granite, and will promote decay (Smith *et al*, 1993).

The presence of both crusts and biological growth is evaluated by the SDI scheme, with the overall weathering grade for a particular building stone altered according to amount of block coverage (see Table 6.11). Only one grading parameter is used for both types of block coverage, although the final value can be suffixed with either 'B' or 'C' to indicate either *biological* coatings, or a pollution *crust*. Rural buildings tend to have higher biocolonisation rates and lower crustal

coverage, while urban buildings tend to have lower organism counts and a higher percentage of crustal coverage.

Class	Surface Cover (%)	Rating
Uncovered	0	15
Slightly covered	1 - 25%	12
Moderately covered	26 - 50%	10
Highly covered	51 - 75%	6
Very highly covered	76 - 90%	4
Completely covered	91 - 100	0

Table 6.11. Surface coating/crustal coverage assessment chart.

The impact of surface coatings (both biological growth and black and brown crustal coverage) is visually assessed by rating the degree of colonisation or coverage on the building stone in 25% increments until 90% coverage is reached. This is shown in Table 6.11. There is no distinction made between crustal coverage and biological growth. If there is a mixture, both of the coating types are assessed and the values added together to produce an overall rating for the stone.

The rating distribution for surface coatings in the SDI scheme is not regular. Zero coverage is awarded the most points, while anything upto 25% is rated as only slightly below this. This is because the organisms found at this level of coverage only sparsely colonise a stone surface, and their impact on a stone will be almost insignificant. The final group in the surface coating/crustal coverage covers a range of only 10%, with zero points award for the group. During the pilot studies on Dartmoor, it was found that a distinction should be made to separate very highly covered and completely covered stone. Stones in a northerly aspect frequently had sufficient coverage to clearly distinguish between the very highly and completely covered classes.

### 6.3.5. Surface Discolouration

Surface discolouration or mineral colour change, brought about by weathering, is the fourth variable to be assessed in the determination of the SDI value. The discolouration of mineral grains and the rock generally is one of the signs

of chemical weathering. Ions are liberated from the crystal lattice of primary minerals by acidic solutions (Smith *et al*, 1994). Biotite, tourmaline and other iron oxides are sources of  $\text{Fe}^{++}$  ions in granite, which then precipitate on the surface and in inter- and intra-granular cracks. This can eventually lead to the formation of a thin, iron-rich patina on the surface of the stone (Schiavon *et al*, 1995), as well as an expansion of the micro-fracture network.

As weathering solutions penetrate the rock, feldspars can undergo dissolution and sericitization, resulting in increasing cloudiness and staining (Irfan and Dearman, 1978b). The presence of weathering solutions and precipitating iron oxides can also lead to the formation of an extensive micro-crack network within the stone, further altering mineral appearance. Visual assessment of the amount of chemical change apparent on the surface of individual building stones provides an indication of the amount of chemical weathering the building stone has undergone (even though chemical weathering can continue after complete staining has occurred). This parameter measures chemical weathering that has occurred before quarrying and while part of the building fabric, and also the amount of aesthetic deterioration the building is experiencing.

Although the majority of weathering grade classification schemes take account of discolouration as one of the defining parameters for the boundary between fresh and slightly weathered rock (see Table 6.4), they make little distinction between the amount of surface discolouration. The SDI scheme addresses this by visually evaluating the percentage of block discolouration, and assigning a rating value to each class. Increasing discolouration results in decreasing rating points, as shown in Table 6.12. This allows any post-solidification alteration to be accounted for by the scheme, increasing the refinement of the block rating.

Class	Discolouration (%)	Rating
Fresh	0 - 10%	10
Slightly discoloured	11 - 30%	8
Moderately Discoloured	31 - 50%	6
Highly Discoloured	51 - 80%	4
Completely Discoloured	81 - 100%	0

Table 6.12. Discolouration assessment chart.

When a building stone has biological coverage of higher than 90% (complete coverage), the stone is assigned a discolouration rating of 2 (completely discoloured). This is to account for the chemical changes the stone surface undergoes under either black crusts or biological cover, which would be unseen by any observer.

Surface discolouration is a rapid measurement, using five classes of perceived percentage of surface discoloured, i.e. marked areas of chemical weathering and colour change, and this allows the amount of discolouration to act as a modifying mechanism to allow the rating scheme a greater degree of discrimination.

As measure of the accuracy of the SDI scheme in assessing rock deterioration from buildings of a variety of ages, a correlation analysis between the total SDI rating for individual blocks and their age. This was followed by individual parameter analysis, which compared the raw index test block value against building age. The results of the analyses are reported below in Table 6.13, which shows that the SDI values have the highest correlation values, and therefore the SDI scheme offers the most accurate description of stone deterioration levels.

Parameter	Correlation Value
Surface Strength	0.69
Surface Roughness	-0.49
Surface coatings	-0.30
Discolouration	-0.15
SDI Block Rating	0.74

Table 6.13. Correlation between SDI parameters and building age.

Parameters		Value Range					
Surface Strength	R <sub>%</sub>	≥36	31-35	26-30	20-25	<20	
	Class	Effectively unweakened	Slightly weakened	Moderately weakened	Highly weakened	Extremely weakened	
	Rating	40	30	20	10	0	
Surface Roughness	mm	0-0.5	0.6-1.0	1.1-1.7	1.8-2.5	2.6-3.5	≥3.6
	Class	Smooth	Slightly rough	Moderately rough	Rough	Very rough	Extremely rough
	Rating	35	30	24	18	9	0
Surface coatings	%	0	1-25	26-50	51-75	76-90	91-100
	Class	No crustal coverage	Slight coverage	Moderate coverage	Extensive coverage	High coverage	Complete coverage
	Rating	15	12	10	6	4	0
Discolouration	%	0-10	11-30	31-50	51-80	81-100	
	Class	Fresh	Slightly discoloured	Moderately discoloured	Highly discoloured	Completely discoloured	
	Rating	10	8	6	4	2	
If biological cover is over 90% no rating for discolouration will be made, and two (2) rating points should be assigned.							

Table 6.14. The SDI rating Table.

## CHAPTER 7. Results of the Dartmoor Churches Study

### 7.1. INTRODUCTION

Ten churches, built in the Dartmoor region between 1410 and 1870, were analysed by the Stone Deterioration Index rating scheme. Using the SDI to rate the buildings, and one monument, it is possible to determine not only the over-all exterior weathering level, but also if there is any modification in the performance of the stones due to aspect variation. As well as distinguishing between differing orientations (aspect), the SDI assessment will also consider variations in height above ground (course height).

The selection of churches with a wide age range permits the formation of a reliable base-line for the rate of granite weathering in a clean, rural site. This can be used in later studies as a reference mark when analysing granitic churches in urban environments. By referencing the SDI rating of urban churches against rural churches, it may be possible to determine if the presence of pollutants accelerates the rate of granite decay, and more importantly, the SDI scheme will be able to provide a quantifiable measure of the degree and rate of change in the SDI rating.

Although the SDI scheme does not arrive at an estimation of rock quality through the assessment of decay and deterioration features, it was noted that all of the churches, except Mary Tavy Vestry, showed extensive friability, the result of the micro-fracturing of quartz and feldspars and the sand-disaggregation of the surface zone. Areas of discolouration were also common, especially close to tourmaline and, to a limited extent, biotite. Plaque formation was not noted.

### 7.2 CHURCH DETERIORATION RATING

When the buildings used in the SDI survey were assessed, shown in Figure 7.1, the majority of the studies were carried out on the church towers. These were selected for three main reasons:

- 1) There has often been rebuilding or expansion of the churches throughout their history. In order to assure that the stones measured were contemporaneous with surrounding blocks, the towers were selected as they were usually completed within five years of the start of construction.

2) The naves of the churches used in the study that were built before 1550 all ran along the same west-east orientation. Using the towers, which are normally located at the west end of the building, allowed continuity between the aspects of the buildings.

3) The construction of the tower is usually more regular than that of the rest of the church, and allows the study to differentiate between the course number and block position with a greater degree of accuracy.

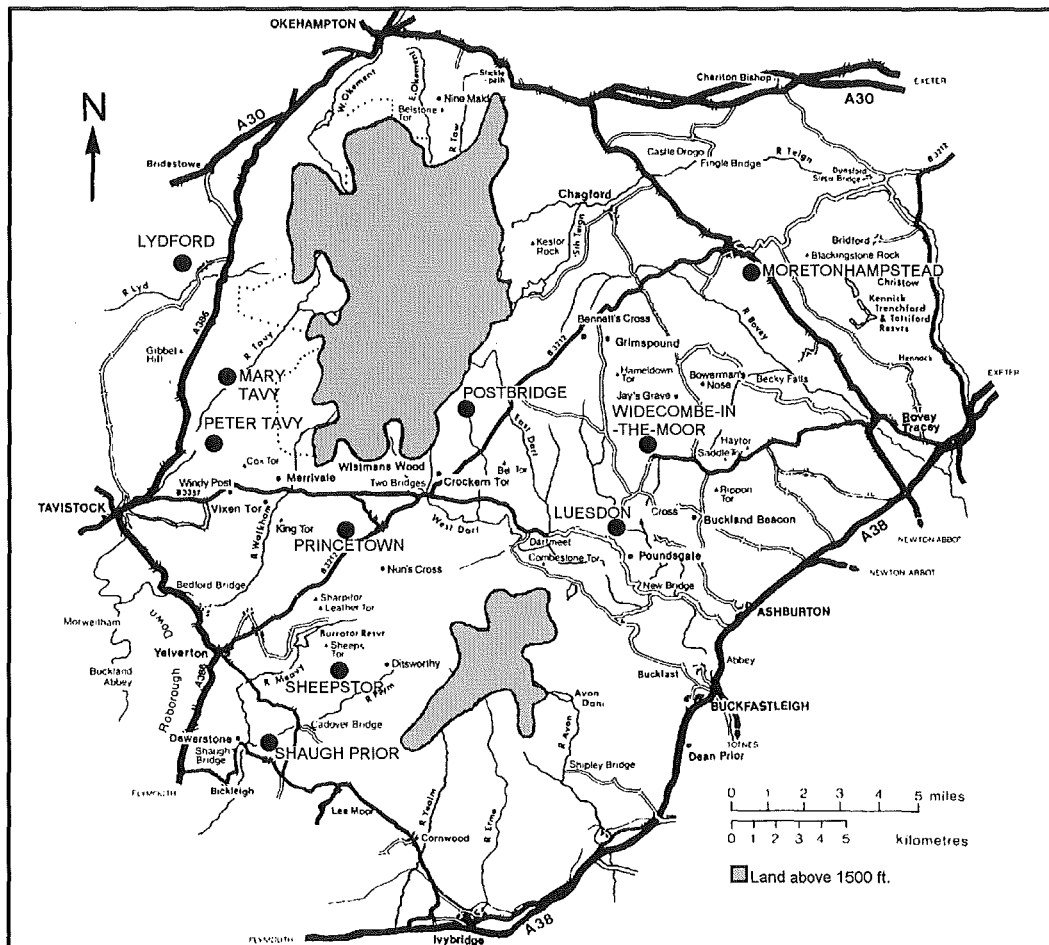


Figure 7.1. Church and monument locations around Dartmoor. Modified from Dartmoor National Park Authorities Map. ● = measured churches.

Furthermore, the churches selected for the SDI survey are mainly constructed of Cornubian Granite Type B (Floyd *et al*, 1993) - a coarse-grained megacrystic biotite tourmaline granite. This stone type was used for the SDI measurements, and other



granite types were removed from the study (see 7.2.4). Other individual site variations are recorded within the church descriptions.

Aspect values for the measured churches as reported as South-West-North, as this follows the pattern of tower orientation found at the churches, and best represents the changing conditions experienced by the building stones in the different walls, as shown below in figure 7.2.

Where the term 'course' is used, this refers to one layer of horizontal stones or ashlar within the building fabric, with an average thickness of ~30cm. 'Course' is used instead of height above ground to remove variations in the measuring heights caused by changes in the positioning of each course at between churches. The course number increases with height above ground, shown in Figure 7.2, with course 1 positioned at ground level, unless specified otherwise. Within each church is a summary of the course and overall aspect averages.

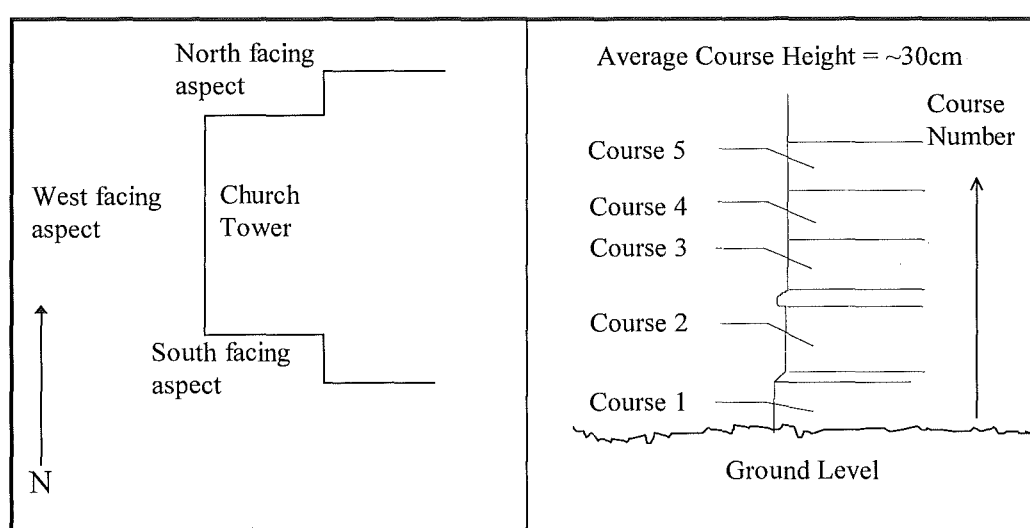


Figure 7.2. Generic tower and course position within churches.

### 7.2.1. Luesdon Cross

Luesdon church was built in 1863 to replace a chapel in a neighbouring village. Situated on the side of a valley with a WNW - ESE orientation, shown in Figure 7.3, there was a mixture of rock types in the fabric of the church. Examination of the exterior church walls failed to reveal any rock that appeared to have been quarried expressly for the church. The lack of provenance of the stones,

and the removal of the possibilities for cohort comparison excluded the church from the study.

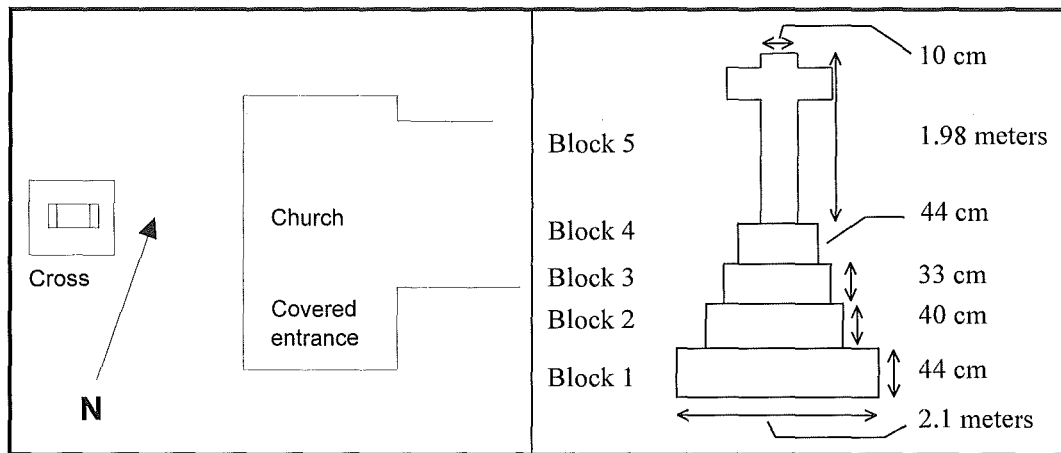


Figure 7.3. Orientation, position and dimensions of Luesdon cross.

The lack of suitable stone, coupled with a total absence of exposed stone in the all-plaster interior, meant that a large memorial cross, erected with the church in 1863, was used in the study. The cross, shown in Figure 7.3, Plate 7.1 and Figure 7.4, was constructed from granite Type B (Floyd *et al*, 1993).

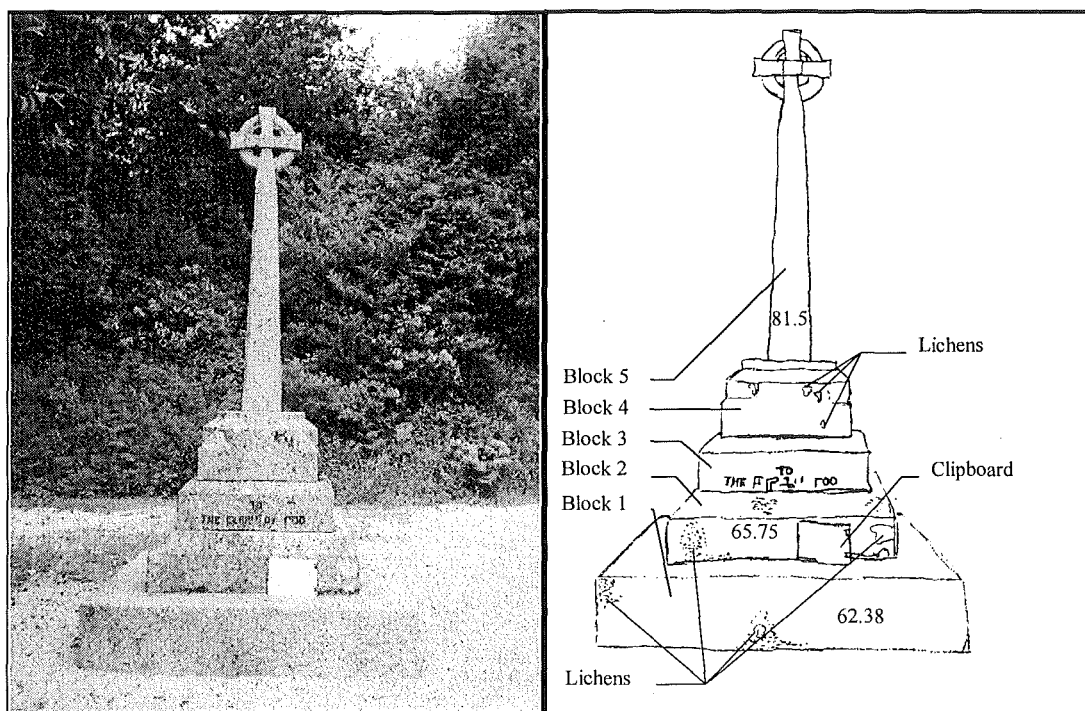


Plate 7.1. Luesdon Cross, south facing, and Figure 7.4. Sketch plan of Luesdon Cross.

Total Block Rating: Luesdon Cross			
Average Block Values	South	West	North
Block 1	62.38	64.88	62.29
Block 2	62.75	62.688	58.63
Block 5	81.5	66.25	67.88
<b>Average</b>	<b>65.69</b>	<b>64.38</b>	<b>62</b>

Table 7.1. Average block ratings, by aspect, for Luesdon cross.

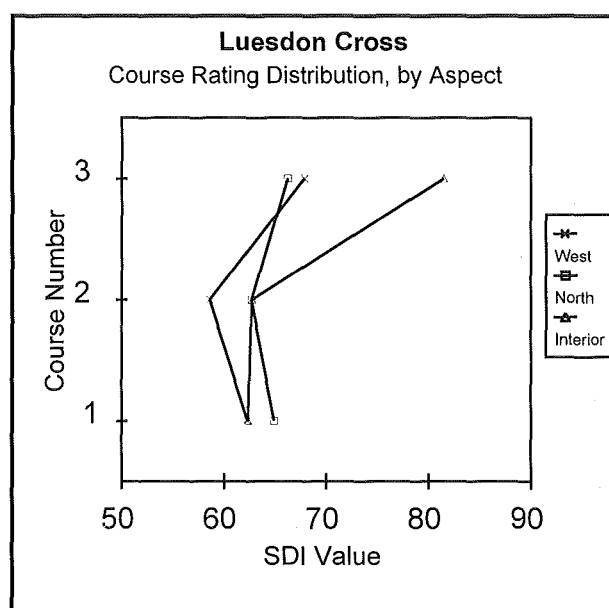


Figure 7.5. Luesdon cross course rating distribution

Analysis of the total block ratings, shown in Table 7.1 and Figure 7.5, by ANOVA showed that there were no significant differences between the different measured aspects of the Luesdon cross<sup>1</sup>. The lack of variation in readings taken from different aspects of the monument was not unexpected, given the small size of the memorial (total block values are shown in appendix Table A.7). This will tend to produce homogeneous results as there is less variation in the conditions affecting each part of the monument. It was also small enough for thermal and moisture gradients within the stone to affect the whole monument, equally effecting all orientations. With the homogeneity of the rock characteristics, the changes in the total rating values between the aspects is due to changes in the percentage biological

<sup>1</sup>ANOVA;  $F(1,11) = <1$

cover, with the north facing aspect showing a greater degree of biological colonisation than the west facing aspect, which is itself larger than the south-facing aspect.

This differs from the analysis of the data, by block (height above ground), which found a significant effect<sup>2</sup>. When further analysed by planned, post-hoc, two-tailed T-tests<sup>3</sup>, there was a marginal difference between block 1 and block 5, while significant differences were found between block 1 and 2 against block 5<sup>4</sup>. There were no significant differences between blocks 1 and 2<sup>5</sup>.

This suggests that while significant differences between the blocks exist, with course two presenting a lower SDI rating value than the other two courses, there was no uniform relationship between height above ground and rating values. Stone quality variations between the blocks is the most reasonable explanation for the performance of block 5. This block had the highest surface area to volume ratio of all the blocks, and would be considered the most vulnerable to weathering, yet has the highest values of the monument, indicating the least weathered rock.

The lack of any interior readings precluded any interior/exterior comparisons.

### 7.2.2. Lydford

Lydford church, shown in Figure 7.6, was built in 1450, and was orientated in an east-west direction in a flat and open churchyard. The church and tower was constructed from granite Type B (Floyd *et al*, 1993).

Part of the south facing wall of the tower had been recently cleaned (shown below in Plate 7.2 and Figure 7.7), and although any readings from the cleaned areas were marked, the cleaning seemed to have a negligible effect on the overall rating of the blocks (total SDI block values are shown in appendix A.8). It is suggested that

<sup>2</sup> ANOVA;  $F(1, 17) = 4.82$ ,  $P < 0.05$

<sup>3</sup> When multi-comparison post-hoc T-Tests were made, two tests were conducted. The first analysed interior/exterior differences by comparing the interior values, and the external wall with the highest mean value (i.e., the value closest to the interior). This ensured that if there was a significant difference between these two factors, the other walls, with lower means, would also be significant. This was repeated for the external wall comparisons, where the two external walls with the closest means were analysed. Again, a significant difference between these factors would mean a significant difference between the others. When the test was not significant, another T-Test comparison between the other two walls was conducted. This reduced the number of T-Tests that were required.

<sup>4</sup>  $T(20) = 1.8$ ,  $P < 0.05$

<sup>5</sup> Block 1 & 5;  $T(6) = -1.56$ ,  $P = 0.08$ , block 2 & 5;  $T(26) = < 1$

this is due to the very low percentage of surface coatings that south facing walls normally display. This is demonstrated by the mean crustal coverage SDI rating for the external aspects (with a maximum of 15 SDI points for a 0% coverage of the building stone): South, 12.3; West, 9.3; North 0.9. Cleaning, which involves the removal of these crusts, will therefore have less effect on the southern walls than it would on the north facing walls, where heavy biological coverage is more prevalent.

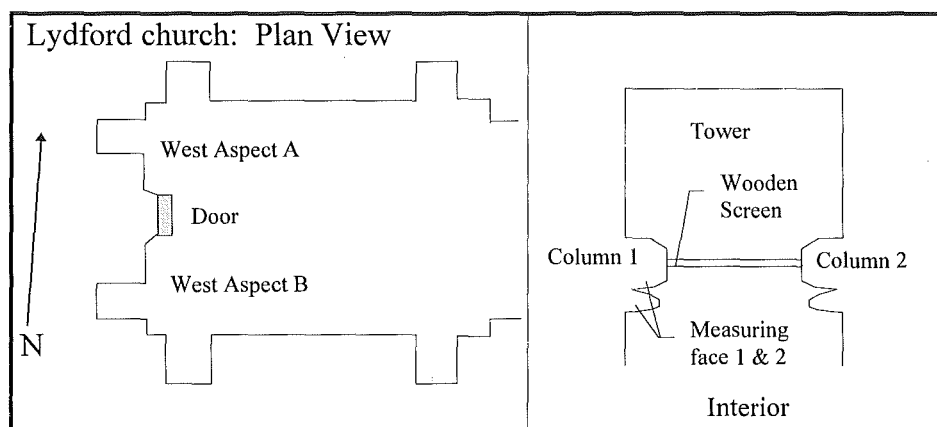


Figure 7.6. Plan view of Lydford church and interior.



Plate 7.2. Lydford church, south facing wall, showing cleaned area.

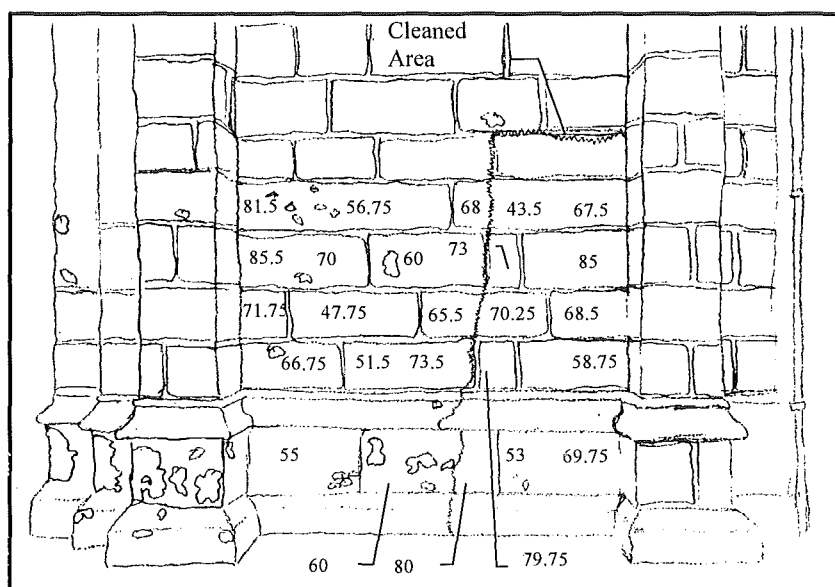


Figure 7.7. Sketch plan for Lydford church, south facing wall.

When the average total block rating values for Lydford church were analysed, there were significant differences shown between the wall aspects<sup>6</sup>, and post-hoc T-tests revealed significant differences in mean values between the interior and all exterior wall readings<sup>7</sup>, shown in Table 7.2. There were also significant differences between each of the external walls<sup>8</sup>.

Rating totals				
Average Course Values	South	West	North	Interior
Course 1	63.55	55.63	49	90.81
Course 2	66.05	55.5	41.75	92.69
Course 3	64.75	50.63	39.6	84.19
Course 4	74.7	54.63	42.75	83.13
Course 5	63.45	47.88		
<b>Average</b>	<b>66.5</b>	<b>52.85</b>	<b>43.28</b>	<b>87.7</b>

Table 7.2. Average course ratings, by aspect, for Lydford.

<sup>6</sup> ANOVA;  $F(2, 48) = 7.38$ ,  $P < 0.01$

<sup>7</sup>  $T(39) = -7.34$ ,  $P < 0.01$

<sup>8</sup>  $T(37) = 2.82$ ,  $P < 0.01$

As the church is on a level site, without earth banks or walls in the proximity, the majority of SDI rating variation can be explained by changes in the degree of exposure. Caneva *et al* (1992) related rates of building biodeterioration to the amount of incident rainfall buildings receive, which is determined by the aspect of individual walls. This was also a significant factor in determining biological growth on the Dartmoor churches and, coupled with changes in the degree of insolation, evaporation and thermal cycling, could result in changes in the SDI values for the individual walls.

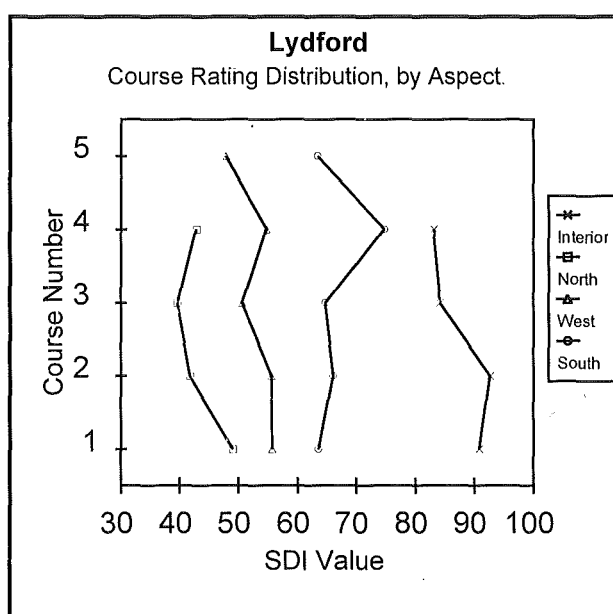


Figure 7.8. Lydford course rating distribution

There were also significant differences between the average external block values when analysed by course (height from the ground), shown in Table 7.2 and Figure 7.8. Although the ANOVA shows an over-all effect<sup>9</sup>, post-hoc T-test comparisons showed that there were no significant differences between the courses when they are compared individually<sup>10</sup>.

The failure to reach significance when courses were analysed individually is explained by the decreasing populations involved in the analysis. This excludes the

<sup>9</sup>  $F(3, 39) = 6.36, P < 0.01$

<sup>10</sup> course 3 & 4;  $T(25) = < 1$

possibility of successfully determining any trends within the data sets. Analysis of the internal course values also failed to show any significance between the courses with increasing height<sup>11</sup>.

### 7.2.3. Mary Tavy

Mary Tavy is situated on the northern side of the Tavy River valley. Built from granite Type B (Floyd *et al*, 1993), the church was orientated in a WSW-ENE direction, perpendicular to a slight slope. This means the eastern end of building was partially surrounded by an earth bank, while the western end was fully exposed to the atmosphere, shown in Plate 7.3 and Figure 7.10. The tower was on the western end of the building, while the vestry was located on the southern side of the church. This is shown in Figure 7.9.

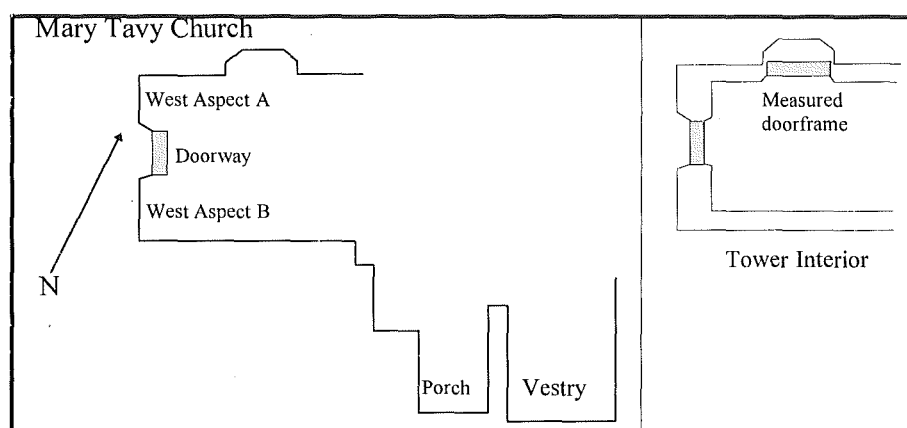


Figure 7.9. Site plan of Mary Tavy, the tower and vestry.

Built in 1440, the church was composed of granite Type B (Floyd *et al*, 1993). The total rating values, by block, for each aspect is shown in appendix A.9, while a summary of the total block ratings is shown in Table 7.3.

<sup>11</sup> ANOVA;  $F(2, 6) = 2.35$ ,  $P > 0.1$





Plate 7.3. Mary Tavy church, south facing wall

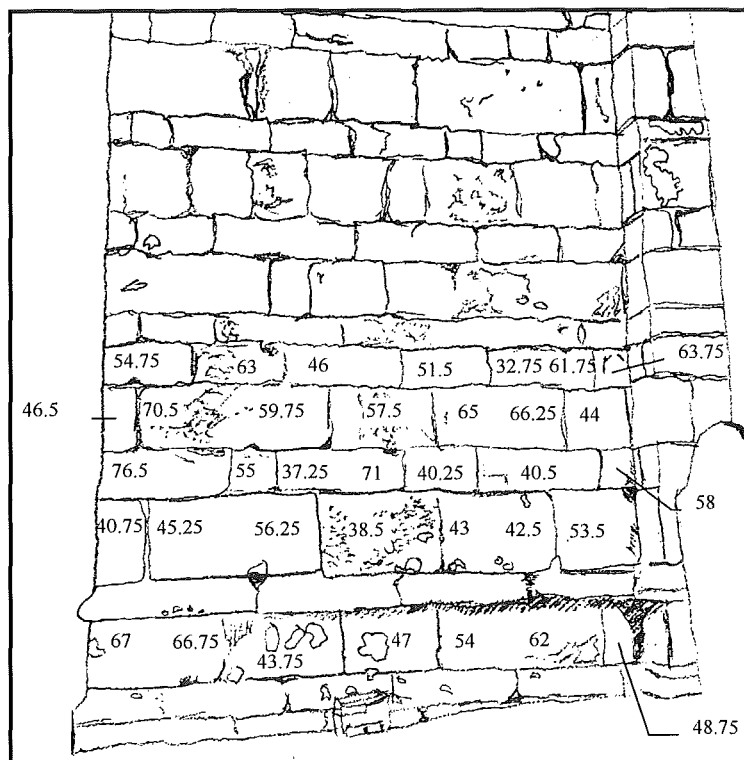


Figure 7.10. Sketch plan of Mary Tavy Church, south facing wall.



Plate 7.4. Mary Tavy Vestry, south facing wall

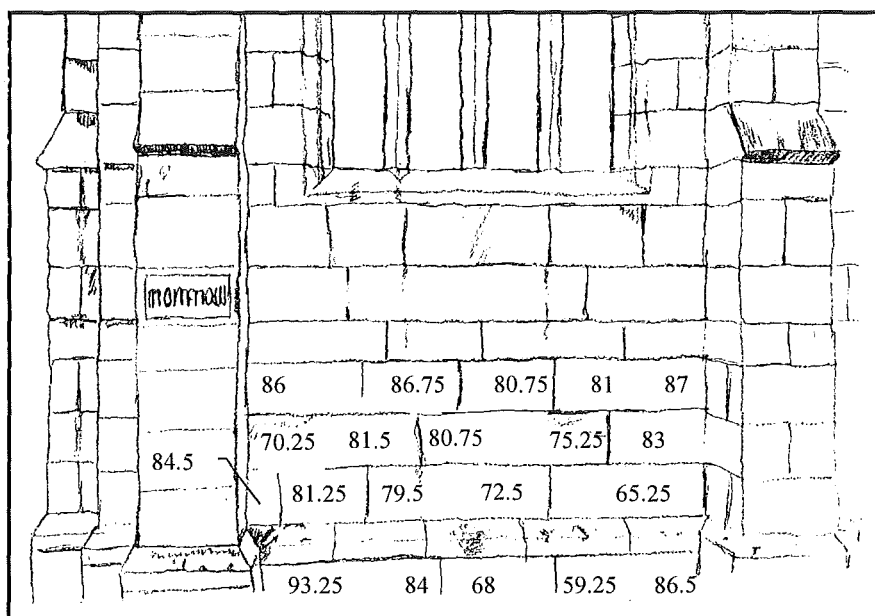


Figure 7.11. Sketch plan of Mary Tavy Vestry.

Later, in 1895, a vestry was attached to the south side of the church, which was slightly recessed into the slope. The vestry, built of Type B granite (shown in Plate 7.4 and Figure 7.11), was also measured and rated, and the values are shown

below in Table 7.4. A summary of the total SDI values for each block for Mary Tavy Vestry is in the appendix (Table A.10).

Total Block Rating: Mary Tavy Church				
Average Course Values	South	West	North	Interior
Course 1	55.61	55.17	44.75	81.69
Course 2	45.68	52.88	50.13	79.25
Course 3	54.07	39.13	53.63	
Course 4	58.5	59.38	66.5	
Course 5	53.36	40.46	59.19	
<b>Average</b>	<b>53.44</b>	<b>49.4</b>	<b>54.22</b>	<b>80.64</b>

Table 7.3. Summary of the average course ratings for Mary Tavy church.

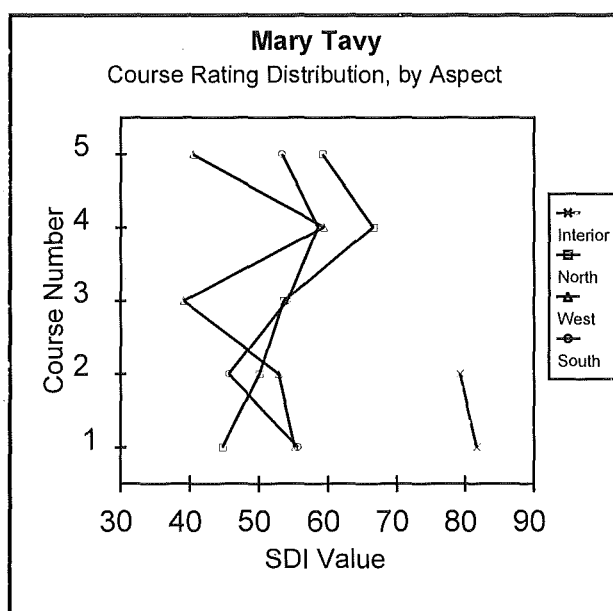


Figure 7.12. Mary Tavy course rating distribution.

Analysis of the average total block rating values, shown in Figure 7.12, for Mary Tavy church by ANOVA, showed that there were significant differences between values, by aspect<sup>12</sup>. Post-hoc T-tests confirmed this by showing significant differences between the interior values and all exterior walls<sup>13</sup>. There were, however,

<sup>12</sup> ANOVA;  $F(2, 68) = 10.17$ ,  $P < 0.01$

<sup>13</sup> North against interior  $T(12) = -6.05$ ,  $P < 0.01$

no significant differences found between the exterior walls<sup>14</sup>. Although it is difficult to ascribe reasons for the lack of variation between the external walls, the position of the church in a small river valley could result in the homogeneity of ambient conditions. This would produce similar weathering conditions for all walls, with only the slightly protected north wall displaying a higher (not statistically significant) mean value. The unusual aspect ranking (i.e. north > south > west) for this church could be another product of the homogeneous conditions, and was not found in other churches.

Analysis of the rating values by course (height above ground), showed that there were no significant differences between the values<sup>15</sup>. Post-hoc T-tests between individual courses revealed that course 4 (around 120cm above ground level) contained significantly higher rating values than every other external course<sup>16</sup>, except course 1<sup>17</sup> (measurements taken within 30cm of ground level), where the effect was marginal. No other significant interactions were found by course analysis. The lack of a clear trend between the courses would suggest that the differences are due to natural variations in stone quality, rather than a function of increasing exposure.

Block Rating Totals: Mary Tavy Vestry		
Average Course Values	Exterior	Interior
Course 1	78.2	96
Course 2	76.6	
Course 3	78.15	
Course 4	84.3	
<b>Average</b>	<b>79.31</b>	<b>96</b>

Table 7.4. The average course ratings for Mary Tavy Vestry.

Mary Tavy vestry, an addition to Mary Tavy church in 1895, was also rated for the SDI scheme. Analysis of the total rating values showed that there were significant differences between interior and exterior values<sup>18</sup>, with course means

<sup>14</sup> North against west facing wall values;  $T(45) = 1.14$ ,  $P > 0.1$

<sup>15</sup> ANOVA;  $F(3,48) = 1.13$ ,  $P > 0.1$

<sup>16</sup> Course 4 against course 5;  $T(26) = 2.43$ ,  $P = 0.01$

<sup>17</sup> Course 4 against course 1;  $T(24) = 1.62$ ,  $P = 0.06$

<sup>18</sup> Exterior against interior;  $T(21) = -7.06$ ,  $P < 0.01$

shown in Figure 7.13. Analysis of variation by course number, however, failed to show any significant differences between the building stones by group ANOVA<sup>19</sup>.

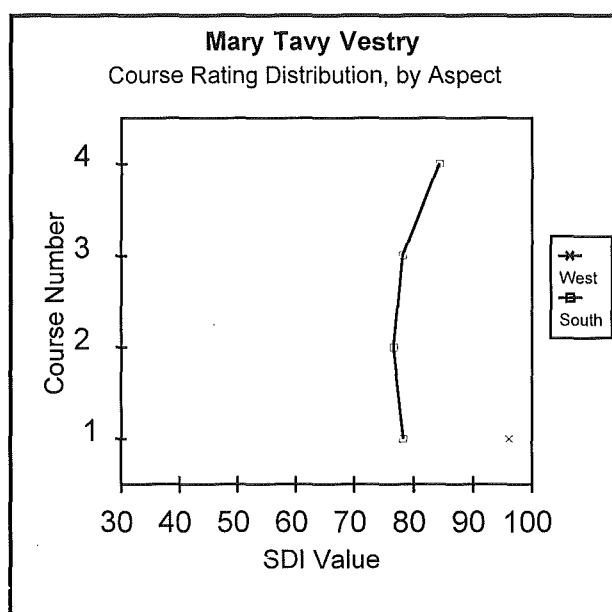


Figure 7.13. Mary Tavy Vestry course rating distribution.

When individual courses were compared by T-test analyses, there was only a significant difference between the means of courses 2 and 4<sup>20</sup>. The general lack of variation between courses could be explained by two factors; 1) External measurements for Mary Tavy Vestry were only taken from one south facing wall, due to physical limitations of the measuring site. The measurements were also reasonably close together, and only spanned a measurement front of about two meters. This, coupled with the fact that the vestry was partly surrounded by a wall of earth (the church was cut into a slight slope, with a small stone path between the church and the walled earth), would help promote homogeneity in the environment affecting the vestry stones. 2) The reduced time of stone exposure, in comparison to the other churches used in the study, could help suppress any variation in stone weathering.

<sup>19</sup> ANOVA;  $F(2,8) = 2.13$ ,  $P > 0.1$

<sup>20</sup> T-test;  $T(5) = -2.07$ ,  $P < 0.05$

#### 7.2.4. Moretonhampstead

Moretonhampstead church was built throughout the fourteenth and fifteenth centuries, with the tower constructed around 1418. Situated at the edge of Moretonhampstead town, the church had a basic east-west orientation, with the tower (shown below in Plate 7.5 and Figure 7.15) situated on the western end of the building. The site plan for the church, which was located on a flat and open site, is shown in Figure 7.14.

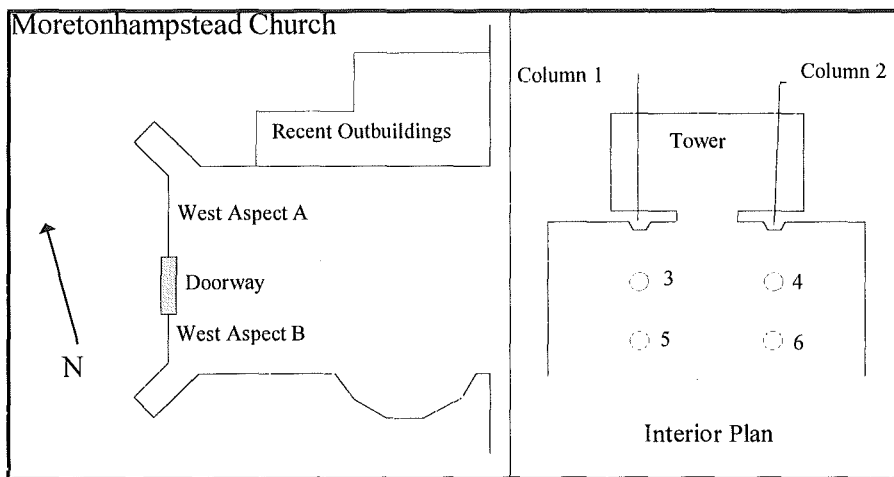


Figure 7.14. Site plan of Moretonhampstead church and interior.

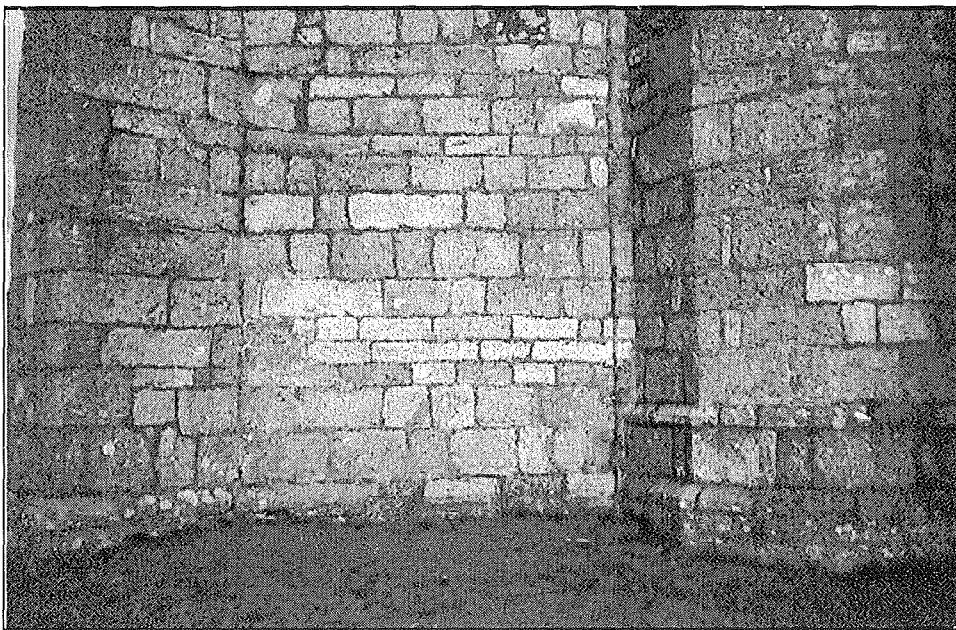


Plate 7.5. Moretonhampstead church, south facing wall.

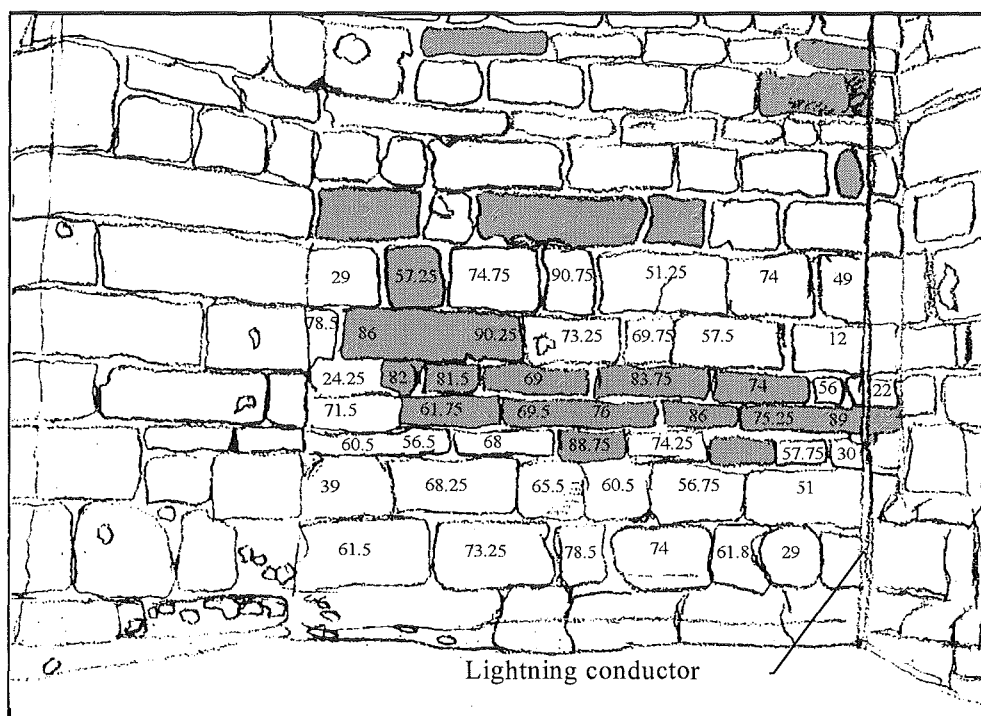


Figure 7.15. Sketch of Moretonhampstead Church, South wall. Shaded blocks are Type C granite. The first course above ground was excluded from the evaluation as it was not horizontal.

Unlike the other churches and monuments examined in the study, Moretonhampstead church contained two main stone types in its fabric. The first was the common Dartmoor porphyritic granite, Type B (Floyd *et al*, 1993), found exclusively in all of the other churches of the study. The second was a white fine-grained Cornubian Type C Granite (Floyd *et al*, 1993).

Although index tests were carried out on both types, the Type C was excluded from the final comparative study of all the churches, as this rock type only occurred at this one church. The surface strength results from these fine-grained Type C stones were, as would be expected, significantly higher than the porphyritic Type B granites<sup>21</sup>.

Subsequent analysis of the data distribution between the interior and exterior Type B granites, and the interior and exterior white, fine-grained Type C granites, showed that there were no significant differences in the strength ratio between the

<sup>21</sup> ANOVA;  $F(1, 128) = 62.6, P < 0.01$

two rock types. This is shown below in Table 7.5. This suggests that the SDI study can be used with different granitic types, provided that enough comparative readings are taken.

Ratio of external wall strength to internal values (% of internal values)		
	Type C Granite White, Fine-grained granite	Type B Granite Megacrystic Biotite granite
South	92.15	82.91
West	86.57	90.49
North	77.66	84.13
<b>Average</b>	<b>85.46</b>	<b>85.84</b>

Table 7.5. Internal/external surface strength ratios of Moretonhampstead Church.

The total SDI values for separated Type B and Type C blocks are shown in appendix A.11, while their total rating values are shown in Table 7.6, along with the total rating values for Type C granite blocks.

	Type B Block Rating Totals				Type C Block Rating Totals			
Average Course Values	South	West	North	Interior	South	West	North	Interior
Course 1	63.00	56.30	60.00	76.83		36.00		
Course 2	56.83	55.95	53.05	87.33		75.50		
Course 3	57.75	57.25	55.45	77.75	88.75	70.00		
Course 4	71.50	52.88	65.17	87.42	76.25	82.38	67.00	
Course 5	34.08	75.88	45.83		71.83	71.88	46.00	91.67
Course 6	58.20				88.13			91.92
Course 7	61.46				42.38			
<b>Average</b>	<b>57.55</b>	<b>58.21</b>	<b>55.98</b>	<b>82.33</b>	<b>72.84</b>	<b>72.38</b>	<b>54.40</b>	<b>91.79</b>

Table 7.6. Average course rating values for Moretonhampstead church.

Analysis of average Type B block rating values showed significant differences between the different wall aspects of the church<sup>22</sup>. This was supported by post-hoc T-tests which showed significant differences between the interior and exterior walls<sup>23</sup>, although there were no differences between the external walls.

<sup>22</sup> ANOVA;  $F(3, 96) = 8.97$ ,  $P < 0.01$

<sup>23</sup>  $T(25) = -5.85$ ,  $P < 0.01$



Despite the west facing wall having the highest mean of all exterior walls, it was not significantly different from either the north and south walls<sup>24</sup>.

There was no significant difference, however, between those two walls, which could be due to the difference in the measuring heights of the north and south walls. The north wall, shown below in Plate 7.6, had an outbuilding that covered the lower 7 courses, which results in measurements that start 2.1 metres above ground level.

Further analysis of the aspect data, with rating values collapsed by course, revealed significant differences between the rating values<sup>25</sup>. Post-hoc T-test analysis on the exterior course values showed that despite a strong effect when the courses were measured as a whole (across all walls), there were no statistically significant differences between any of the courses when they were compared individually with each other<sup>26</sup>.

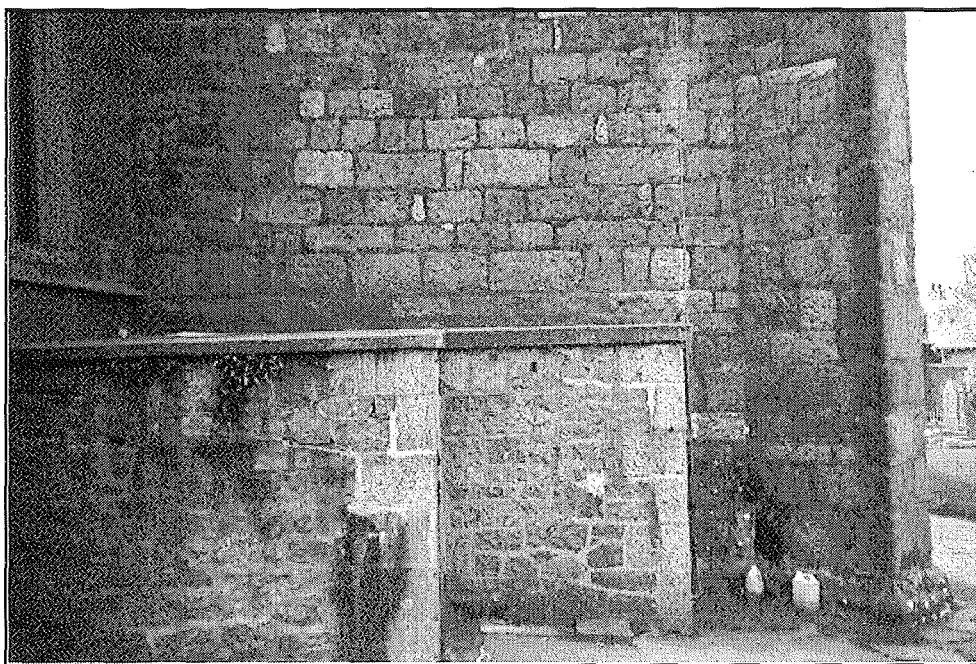


Plate 7.6. Moretonhampstead church, north facing wall.

<sup>24</sup> West against north exterior wall values;  $T(34) < 1$

<sup>25</sup> ANOVA;  $F(5, 85) = 27.92$ ,  $P < 0.01$

<sup>26</sup> Course 7 (around 2.1 metres) against course 4 (around 1.2 metres)  $T(6) = -1.45$ ,  $P = 0.1$

The lack of a clear trend by height for Moretonhampstead church was not unexpected, for two reasons: A) a reduction in the number of data points when the courses are analysed individually reduces the statistical reliability of the results, and decreases the chance of a significant outcome. B) to obtain readings for the north facing wall, it was necessary to climb an outbuilding constructed against the wall, shown above in Figure 7.14 and Plate 7.6. This means that course 1 for the north facing wall was located around 2.1 metres above ground level. Although this did not produce a significant difference between the south and north walls, it added variability to the data, reducing the probability of significance between the courses.

As can be seen in Figure 7.16, when course ratings were plotted by aspect, the distribution pattern for the north and south walls were very similar up to course 4, where they diverge from each other. One possible explanation for the almost parallel distribution is that the roof of the outbuilding had a similar effect as the ground in protecting the courses immediately above it.

Once the level of protection has been reduced by increasing course number, the effect of the higher northern course height was reflected in the effective course number 5 results (actual course number = 12 (equivalent to 360 cm above ground level)). The similar distribution and lack of significant differences between the north and south walls mean that north course values will be included in other analyses.

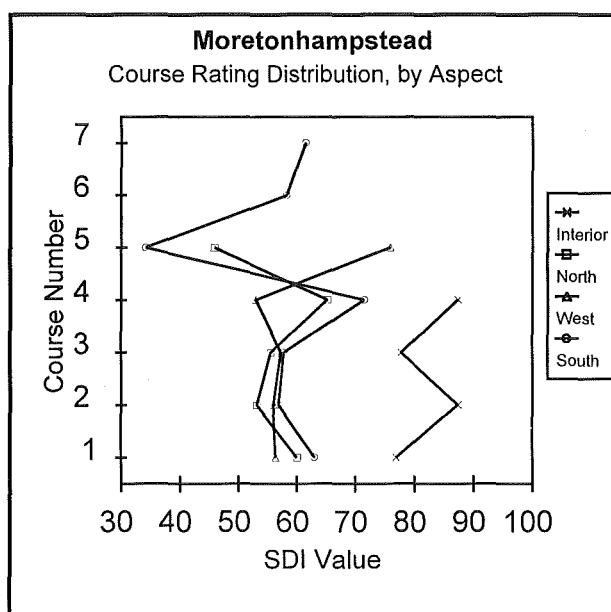


Figure 7.16. Moretonhampstead course rating distribution.

### 7.2.5. Peter Tavy

Located on the southern side of the Tavy valley, Peter Tavy church was built in the fourteenth and fifteenth centuries, with the tower constructed by 1520. The building, constructed of Type B granite (Floyd *et al*, 1993) was orientated in an east-west direction on a relatively flat site (see Plate 7.7 and Figure 7.18), with the tower at the western end of the building, shown in Figure 7.17.

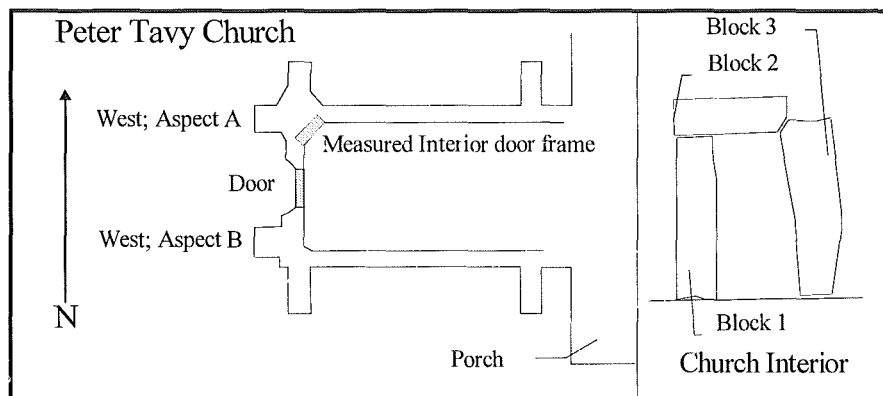


Figure 7.17. Site plan of Peter Tavy church and interior doorway.

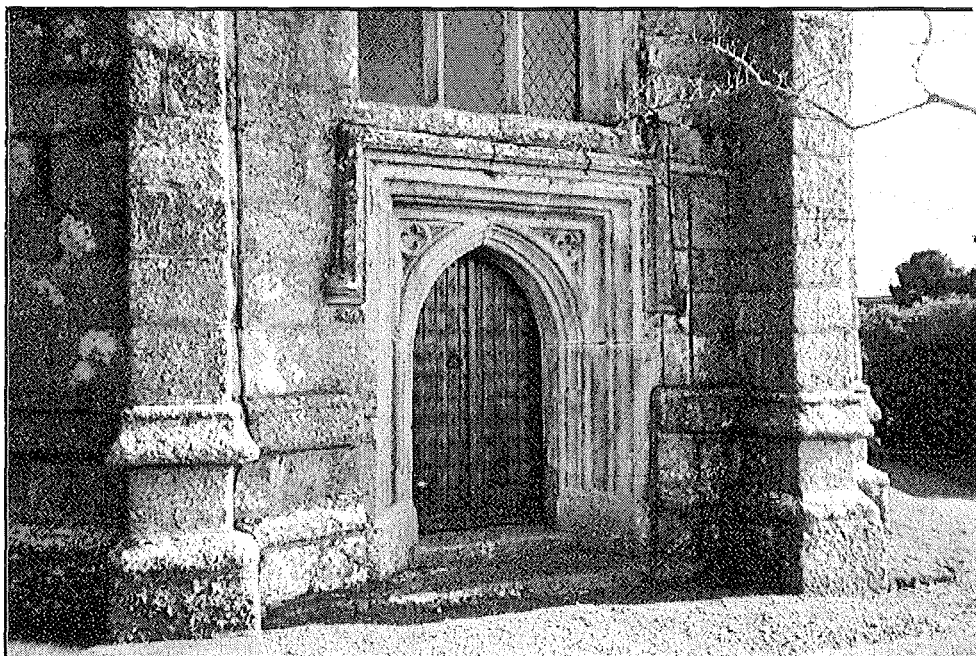


Plate 7.7. Peter Tavy church, west facing wall

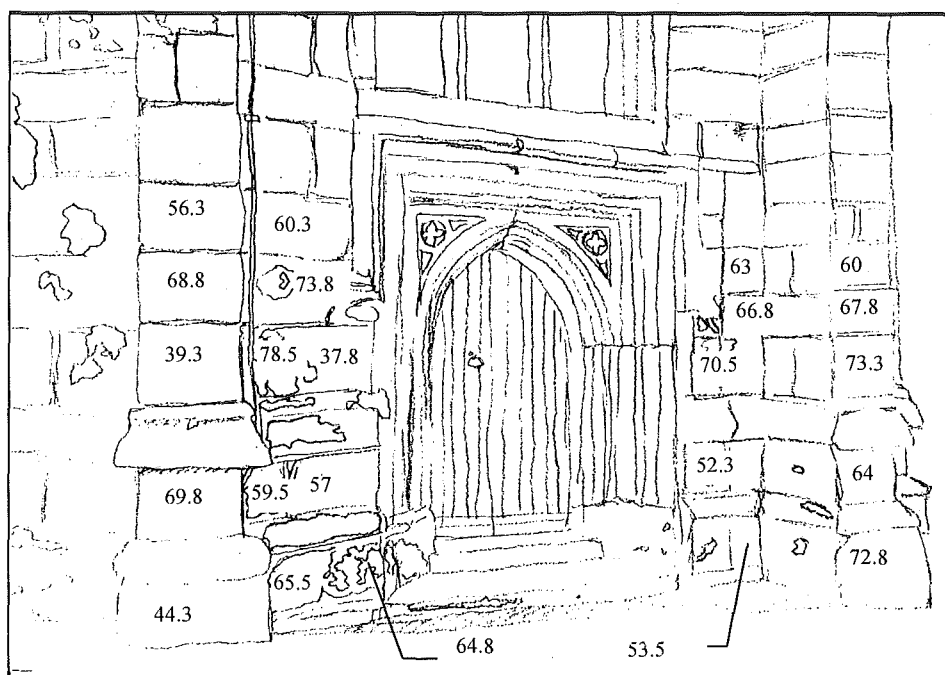


Figure 7.18. Sketch plan of Peter Tavy Church, West facing wall.

A summary of the total SDI rating for each block is shown in the appendix (Table A.12), with the total rating value for the building stones in Table 7.7.

Total Block Rating: Peter Tavy				
Average Course Values	South	West	North	Interior
Course 1	62.1	60.15	63.6	77.85
Course 2	66.9	60.51	72.25	73.2
Course 3	60.3	59.85	59.05	60.5
Course 4	64.5	69.25	55.9	
Course 5	70.05	59.875	52.1	
<b>Average</b>	<b>64.77</b>	<b>61.7</b>	<b>60.58</b>	<b>70.52</b>

Table 7.7. Average course rating for Peter Tavy church.

A group analysis of the total block rating values revealed significant differences between the different wall aspects<sup>27</sup>. This was confirmed by post-hoc T-tests, which showed significant differences between the interior and all of the exterior

<sup>27</sup> ANOVA;  $F(2, 48) = 5.02$ ,  $P = 0.01$

walls<sup>28</sup>. There were no significant interactions between the means of the exterior aspects<sup>29</sup>.

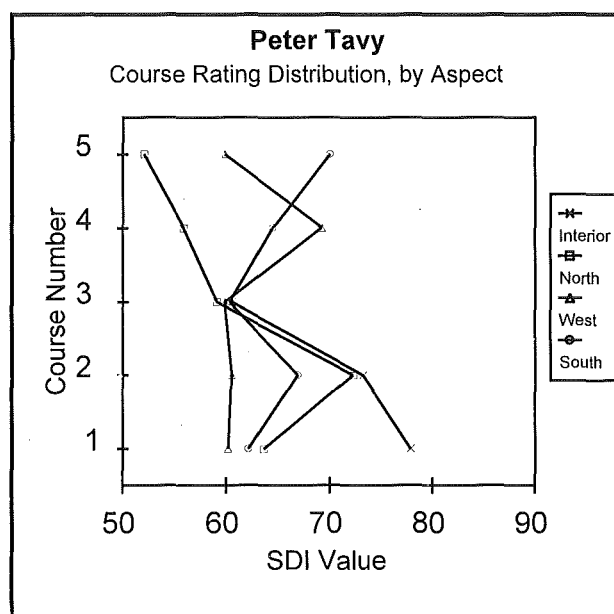


Figure 7.19. Peter Tavy course rating distribution.

When analysed by course the block rating totals, shown in Figure 7.19, showed no significant differences between the courses when examined by group<sup>30</sup>. Post-hoc T-test analyses between individual courses also revealed no main effects between the external wall courses, except between courses 2 (measurements taken within 60cm of ground level) and 3<sup>31</sup> (around 90cm above ground level), and courses 2 and 5<sup>32</sup>. This would indicate that there was no uniform weathering process that affected the external stones, and, given the low interior values, it is also possible that their SDI values were subject to greater modification by their initial weathering condition than other stones examined in the study.

Although the rating values for the church interior were significantly higher than the external values, they are low in comparison to other churches in the study. The low interior rating was perhaps due to the high degree of discolouration

<sup>28</sup> Interior values against south facing block values;  $T(24) = -1.98$ ,  $P < 0.05$

<sup>29</sup> South facing values against west facing stones;  $T(38) = 1.14$ ,  $P > 0.1$

<sup>30</sup> ANOVA;  $F(3, 48) = 1.5$ ,  $P > 0.1$

<sup>31</sup> course 2 and 3;  $T(22) = 1.81$ ,  $P < 0.05$

<sup>32</sup> course 2 and 5;  $T(24) = 1.83$ ,  $P < 0.05$

(chemical weathering) the interior stones of Peter Tavy displayed during sampling. The increased level of chemical weathering (in comparison to other study church interiors) could be the result of higher than average dampness in the church. Although efforts were made to locate a second sampling site for the interior values, to produce values in conjunction with those from the first site, the plastering of the church interior precluded this.

### 7.2.6. Postbridge

Postbridge church was built in 1868, in the small community of Postbridge. Located almost at the exact centre of Dartmoor, the church was situated beside the B3212, one of Dartmoor's largest roads. The eastern end of the church, constructed from granite Type B (Floyd *et al*, 1993), has been covered with shotcrete, although the other aspects are still uncovered. A site plan of the church is shown in Figure 7.20, and the north facing wall is shown in Plate 7.8 and Figure 7.21.

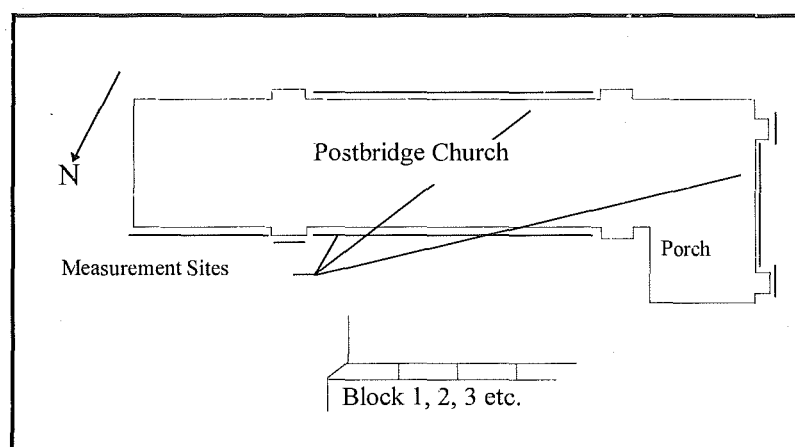


Figure 7.20. Site plan of Postbridge church.

Readings were taken along the length of the three remaining walls, with measurements taken from a layer of stone sills that ran around the building at 120 - 130cm high. The sills were selected because they were the same Type B granite that has been measured at other Dartmoor churches. A summary of the Postbridge block values is shown in Table 7.8, while the complete block totals are in appendix A.13.



Plate 7.8. Postbridge church, north facing wall.

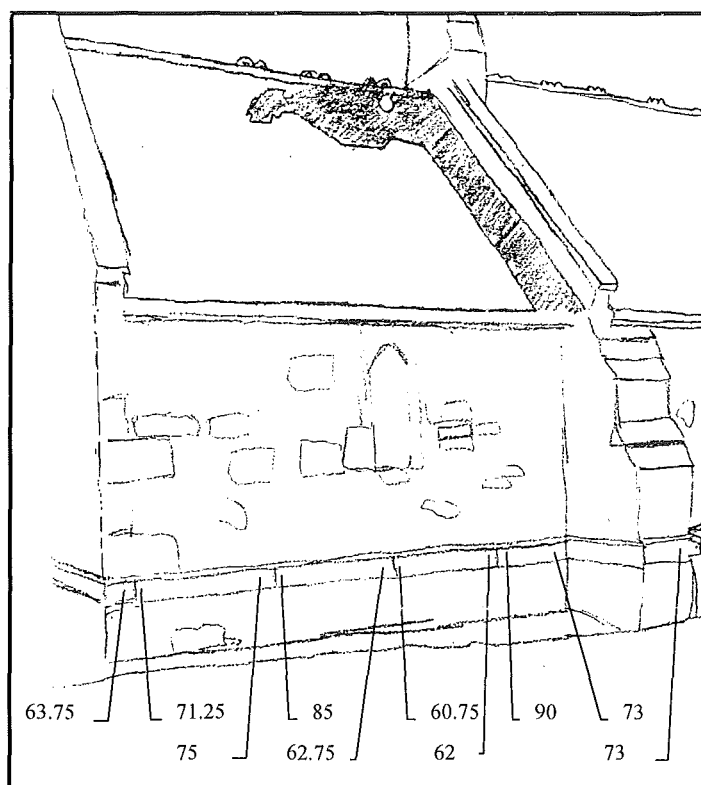


Figure 7.21. Sketch plan of Postbridge church, north facing wall.

Block Rating Totals: Postbridge								
South	West	North	Interior		South	West	North	Interior
63.75	75.25	48.5	95		73.5	75.75	46	92.5
71.25	59.75	50.25	95		70	59.75	45	96.25
75	68.25	35.5	89		39.5	75.5	47	96
85	61.75	44	79.75		63	55.25	69.25	80
62.75	63.75	33	88.25		58.5	50.75	59.5	90.75
60.75	67	55.25	96.25		80	66.75	70.5	
62	89.5	51.25	85		67.25	73	70.5	
90	66.25	43.5	96.75		80.25	54		
73	70	50	95		50.75	54.5		
73.25	70.5	42.75	87		64.5	61.5		
62.25	67.25	30.5	92.25					
Values continue from top of next column				<b>Average</b>	<b>67.92</b>	<b>66</b>	<b>49.57</b>	<b>90.92</b>

Table 7.8. Total block ratings for Postbridge church.

Analysis of the total rating values for Postbridge showed significant differences between the aspects<sup>33</sup>, and this was confirmed by post-hoc T-test analyses, which showed a significant difference between the interior and exterior walls<sup>34</sup>. Within the exterior walls, there were significant differences between the west and north walls against the lower rating values of the south wall<sup>35</sup>, but no significant difference between the west and north walls<sup>36</sup>.

Postbridge church displayed an external wall SDI distribution that was unlike the majority of other churches, in that the south wall was the lowest average value, while the north (which was usually the most weathered) has the highest external average. This might be due to two factors: A) Measurements from the church were only taken at one height, along almost the whole length of the wall. It is possible that this sampling strategy, which differs from the other evaluated churches, had some effect on the results. B) The church orientation and position is different from those of the other churches. Trees were found within close proximity of both the west and south faces, but not for the north face. It is possible that the presence of the trees,

<sup>33</sup> ANOVA;  $F(2, 40) = 8.18$ ,  $P < 0.01$

<sup>34</sup> interior against north facing block values;  $T(31) = -8.03$ ,  $P < 0.01$

<sup>35</sup> west against south facing block values;  $T(32) = 4.79$ ,  $P < 0.01$

<sup>36</sup>  $T(38) < 1$



which were closer to the south facing wall than the others, and the shade they cast, increased both the ambient moisture content (humidity) and the time of wetness. Both of these factors could increase the building's weathering rate in a localised area.

### 7.2.7. Princetown

Princetown church was built between 1810 -1814 (with a median date of 1812 used in the study to describe the average date of exposure) by French and American prisoners of war. The church was a rugged granite building, constructed of unfinished Type B granite (Floyd *et al*, 1993), and was set on level ground. The only stones that were measured for the study were large finished blocks used in buttresses at the eastern end of the building, as shown in Figure 7.22. This was because; a) there were many inappropriate rocks in the building fabric, including non-igneous rocks, b) a lack of an appropriate course structure, and c) no evidence that the bulk of the stones in the walls were ever worked to provide a flat surface. The east end of the building is also shown in Plate 7.9 and Figure 7.23.

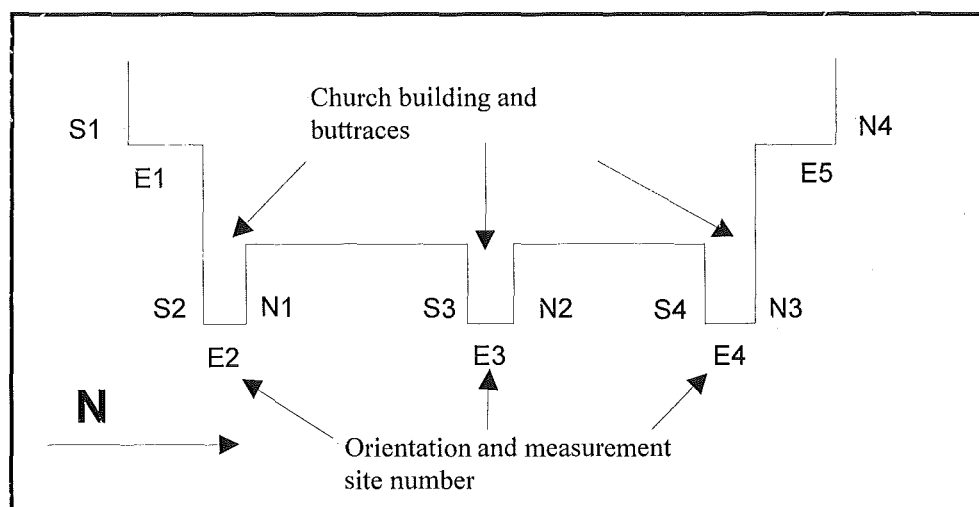


Figure 7.22. Site plan and measurement site distribution of Princetown church.

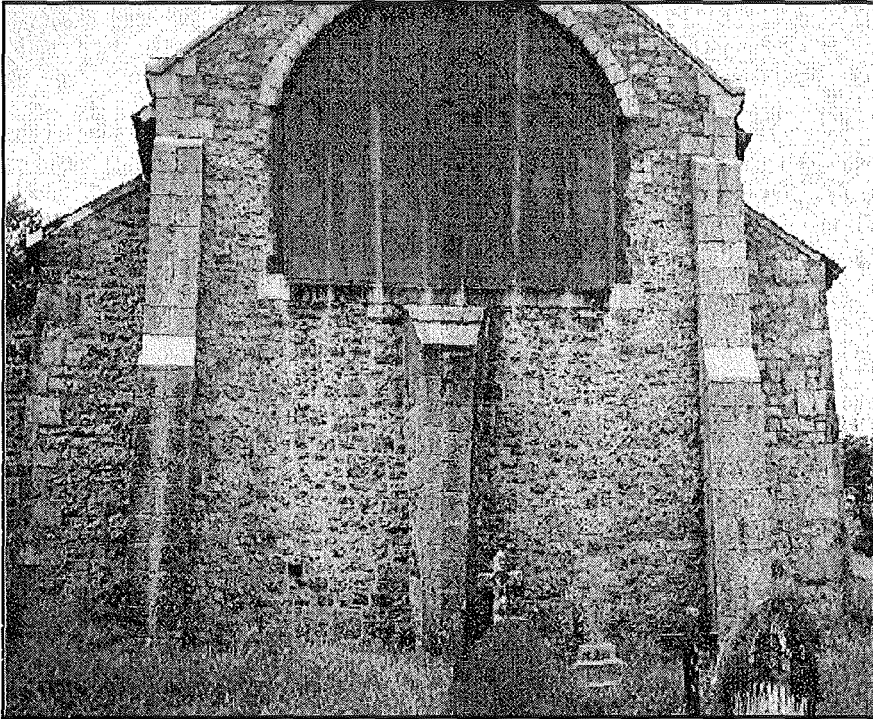


Plate 7.9. Princetown church, east end.

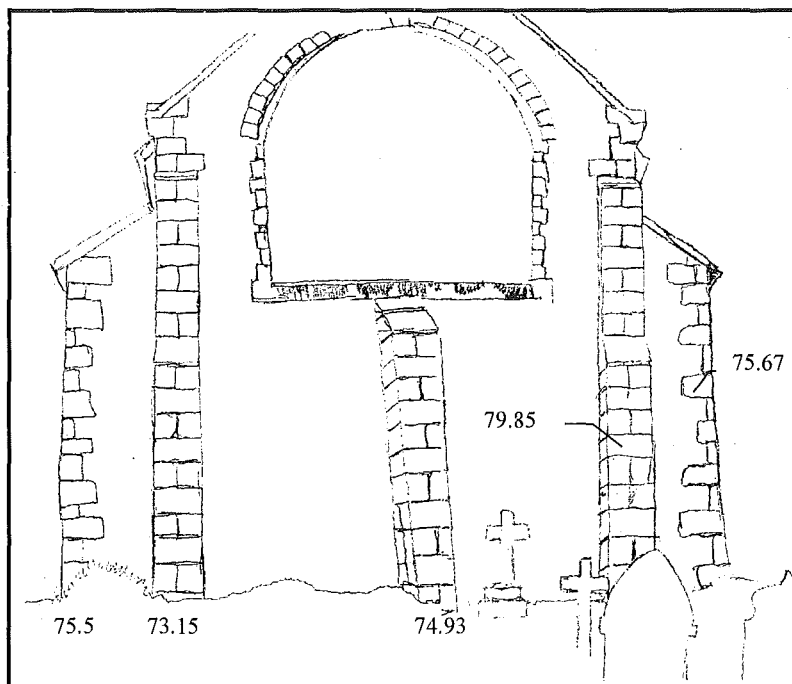


Figure 7.23. Sketch plan of Princetown Church, east end average values.

A summary of the block rating values for Princetown church is shown below in Table 7.9, while the total block rating for each stone is shown in appendix A.14.

Block Rating Totals: Princetown Church			
Average Course Values	South	East	North
Section 1	75.6	75.5	71.82
Section 2	72.82	73.15	79.97
Section 3	71.31	74.93	72.47
Section 4	79.75	79.85	68.4
Section 5		75.67	
<b>Average</b>	<b>74.57</b>	<b>75.85</b>	<b>73.37</b>

Table 7.9. Average block rating values for Princetown church.

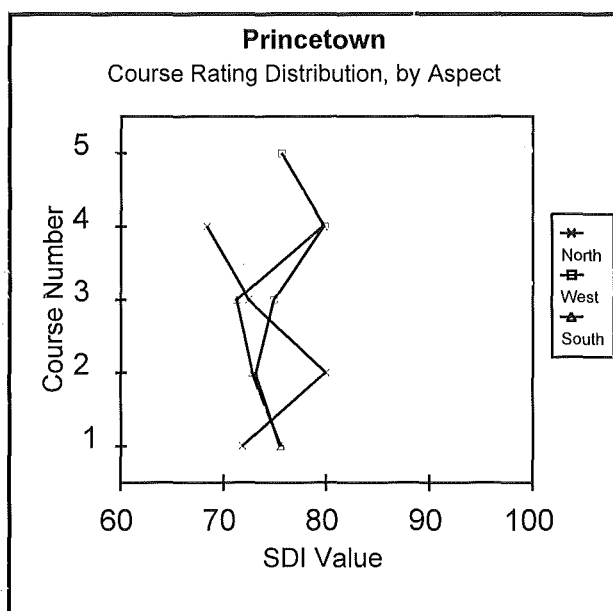


Figure 7.24. Princetown course rating distribution

Given the scattered distribution of the stones which could be rated, and the lack of interior readings (access was not possible during the sampling period), the analysis for this church was more limited.

Unexpectedly, given the close nature of the means from the three different aspects (see Table 7.9 and Figure 7.24), there was a significant difference between

the aspects when analysed together<sup>37</sup>. However, when the exterior aspects were compared individually against each other, there were no significant differences, i.e., between east and north facing walls<sup>38</sup>.

Despite the strong initial effect between the different aspects, the lack of effect between individual measurement areas could be explained by three factors: 1) The decrease in the data population for the individual aspects will decrease the power of the statistical analysis, reducing probability of significance. 2) The measurements were all taken within close proximity of each other, where the effects of the atmosphere and exposure would be almost identical on each face. 3) The measurements were taken from projecting buttresses, which would reduce the amount of inertia to change a large rock volume would impart, and this could also play a contributory role in the lack of differentiation between the rock aspects.

#### 7.2.8. Shaugh Prior

Shaugh Prior was built throughout the 15<sup>th</sup> century, with the tower constructed in 1430. The building was orientated in an east-west direction, with the tower on the western end of the building, shown in Figure 7.25. Details are shown in Plate 7.10 and Figure 7.26.

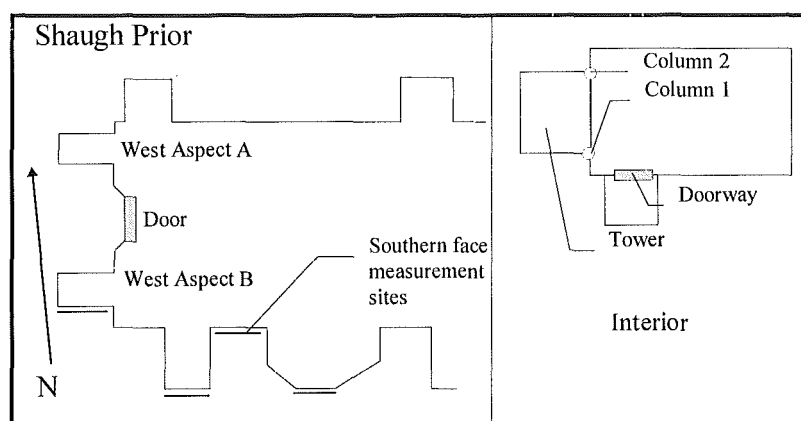


Figure 7.25. Site plan of Shaugh Prior and interior.

<sup>37</sup> ANOVA;  $F(1, 43) = 20.61$ ,  $P < 0.01$

<sup>38</sup>  $T(44) < 1$

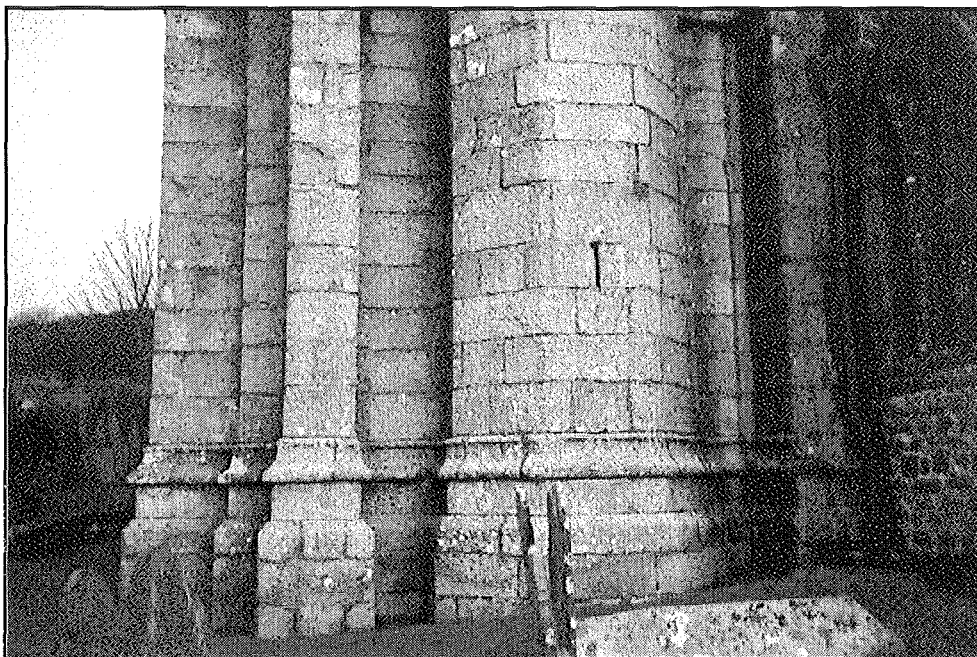


Plate 7.10. Shaugh Prior, south facing wall

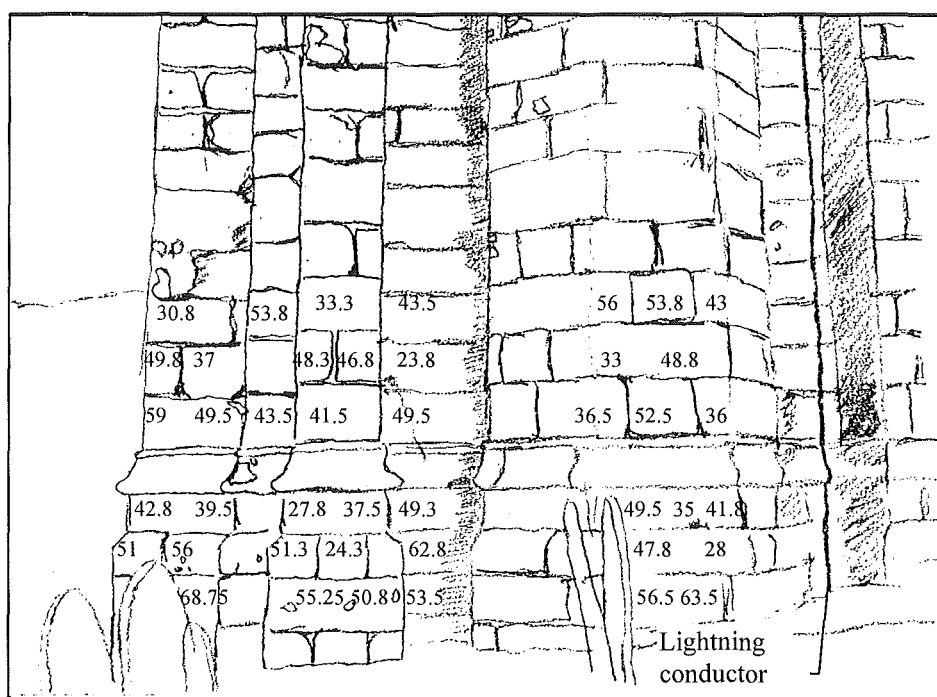


Figure 7.26. Sketch plan of Shaugh Prior, south facing wall.

Shaugh Prior was constructed from porphyritic granite, Type B (Floyd *et al*, 1993), and was located on a gently sloping church site that was raised above the

neighbouring road. A summary of the rating values is shown in Table 7.10, while the total rating values for the blocks are in appendix Table A.15.

Block Rating Totals: Shaugh Prior				
Average Course Values	South	West	North	Interior
Course 1	54.68	41.75	36.29	87.04
Course 2	45.31	37.03	38.8	85.75
Course 3	40.38	40.38	36.33	84.25
Course 4	46	44.06	32.21	
Course 5	41.04	50.5		
Course 6	44.86	50.97		
<b>Average</b>	<b>45.28</b>	<b>44.45</b>	<b>35.78</b>	<b>86.02</b>

Table 7.10. Average course rating values for Shaugh Prior.

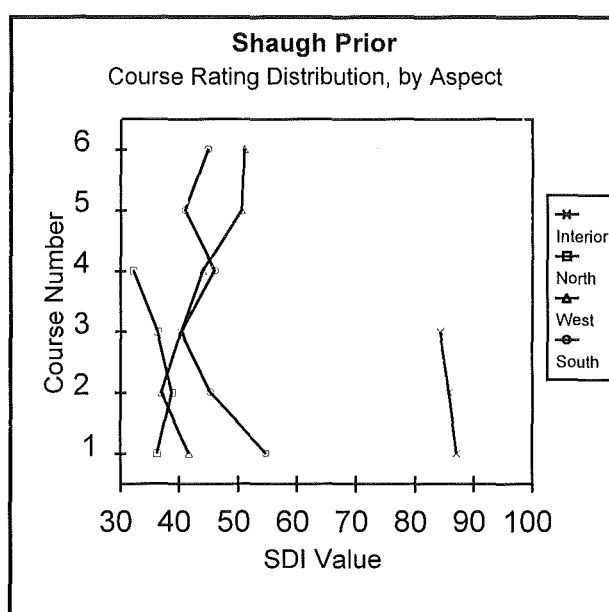


Figure 7.27. Shaugh Prior course rating distribution.

Group analysis of the total block rating values for Shaugh Prior revealed significant differences between the different wall aspects<sup>39</sup>. Further analysis by post-hoc T-tests also showed significant differences between the interior and exterior

<sup>39</sup> ANOVA;  $F(2, 88) = 11.5$ ,  $P < 0.01$

walls<sup>40</sup>, and between west and north exterior walls<sup>41</sup>. No significant differences were found between the south and west facing walls<sup>42</sup>.

Further analyses were carried out on the rating totals to determine if there was any effect by course (height off the ground), with course means shown in Figure 7.27. Although there was no overall effect when examined as a group<sup>43</sup>, some individual courses showed significant differences<sup>44</sup> between them and their neighbours. There was, however, no systematic pattern to the distribution.

The significant differences between the external walls was related to the degree of exposure the building undergoes. Located on the side of a valley, and elevated above most of the village around it, Shaugh Prior tower had three clear zones of exposure; the south which was open and unprotected by any vegetation. The west, which was partially protected by the tower structure from driving rain, etc., and the north which was the most protected by the presence of windbreak trees and walls some ten to fifteen meters away, and possibly by the rising land in front of it.

Although there are a number of factors that influence the deterioration rate of the tower fabric, it would seem likely that the determining factor was the drying rate of the three walls. The south facing wall was the most exposed to solar radiation, and this, coupled with wind that flows up the valley in front of the church, would result in the lowest time-of-wetness of all the walls. This is in comparison to the north facing walls, which are protected from both direct sun-light and the impact of the majority of wind. This will increase the time-of-wetness, and the amount of biological growth - producing the lowest external aspect rating for the building.

### 7.2.9. Sheepstor

Sheepstor church, constructed from granite Type B (Floyd *et al*, 1993), was substantially rebuilt in the early 16<sup>th</sup> century, with the tower constructed by 1510. The church building was orientated in an east-west direction, with the tower located on the western end of the building. The site was gently sloping (parallel to the church orientation), and was located some thirty meters away from a small stream.

<sup>40</sup> Interior against south facing block values;  $T(36) = 18.39$ ,  $P < 0.01$

<sup>41</sup>  $T(58) = 4.24$ ,  $P < 0.01$

<sup>42</sup> South against west facing block values;  $T(85) < 1$

<sup>43</sup> ANOVA;  $F(4, 84) = 2.17$ ,  $P = 0.08$

<sup>44</sup> i.e. course 3 and 1;  $T(21) = -1.77$ ,  $P < 0.05$ .

Below are two plans of the Sheepstor church. Figure 7.28 shows a plan view of the church tower, the areas of measurement, and the course structure. Figure 7.29 shows an overall plan of the whole church, and details of the internal measurement sites. Details of the west facing tower wall are given in Plate 7.11 and Figure 7.30.

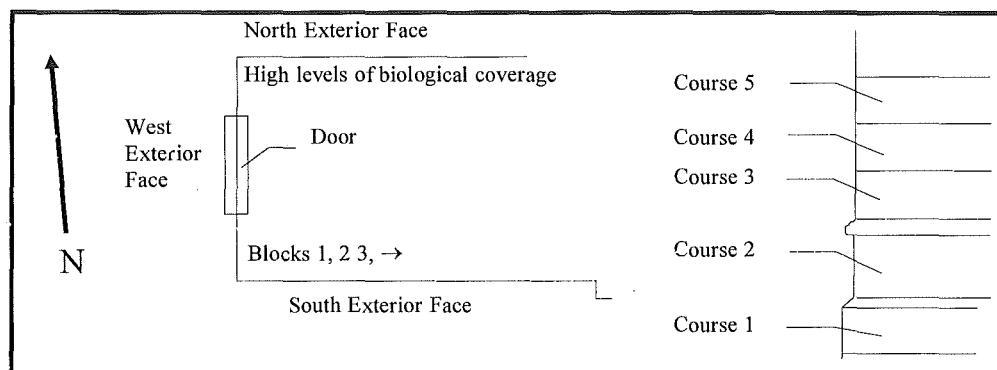


Figure 7.28. Site plan of Sheepstor church tower.

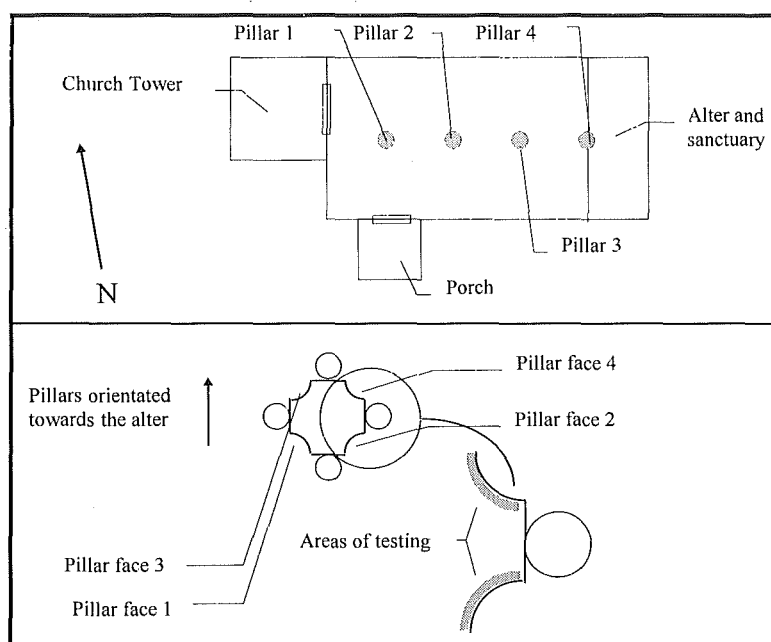


Figure 7.29. Site plan of Sheepstor church and interior details.



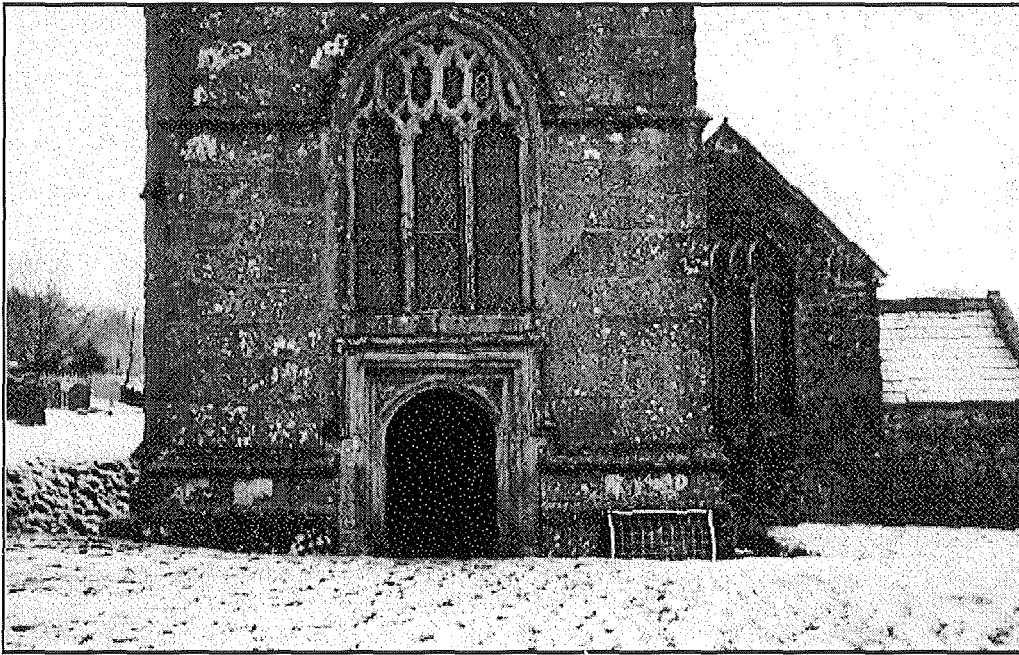


Plate 7.11. Sheepstor church, west facing wall.

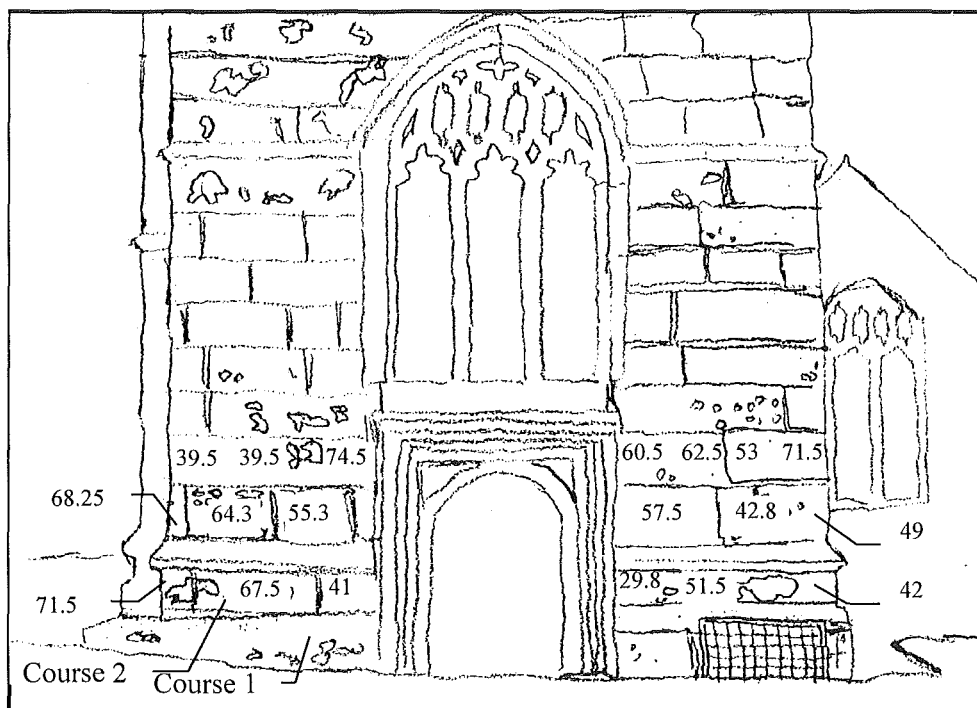


Figure 7.30. Sketch plan of Sheepstor Church, west facing wall.

There is a summary of the separate index test results for the blocks of Sheepstor church in Table 7.11, while appendix Table A.16 shows the total block rating values for the church.

Rating Totals: Sheepstor Church				
Average Course Values	South	West	North	Interior
Course 1	40.33	51.25	57.25	81.69
Course 2	50.29	46.71	35.00	94.00
Course 3	56.17	50.17	37.81	89.00
Course 4	57.29	51.88	40.44	
Course 5			20.94	
<b>Average</b>	<b>51.27</b>	<b>50.00</b>	<b>38.29</b>	<b>88.23</b>

Table 7.11. Average course ratings for Sheepstor church.

The total block rating values from Sheepstor church were analysed to find variation by wall. Although there was a marginal effect between the different aspects when studied overall, significance was not reached<sup>45</sup>. Further study by T-tests, however, found a significant difference between the interior and exterior walls<sup>46</sup>. There are also significant differences between most of the exterior walls; west against north<sup>47</sup> and south against north are both significant, but there was no statistical difference between west and south<sup>48</sup>.

This supports the relationship found between west and south facing walls at other churches in the study, where there has been a small, often marginal, difference between the two, while the north facing wall was usually significantly lower. This would indicate that increased moisture content, and biological growth were the main agents of granite deterioration in the Dartmoor region.

When analysed by course, with course means shown in Figure 7.31, the Sheepstor data showed significant differences between the external courses<sup>49</sup>. Further post-hoc T-test analyses showed that there were significant differences between course 5 (around 150cm above ground level) and course 2 (around 60cm

<sup>45</sup> ANOVA;  $F(2, 56) = 2.94$ ,  $P = 0.06$

<sup>46</sup> Interior against south facing block values;  $T(34) = 10.31$ ,  $P < 0.01$

<sup>47</sup> West against north facing block values;  $T(40) = 3.09$ ,  $P < 0.01$

<sup>48</sup> West against south;  $T(43) < 1$

<sup>49</sup> ANOVA;  $F(3, 48) = 51.85$ ,  $P < 0.01$

above ground level)<sup>50</sup>, although there were no other significant relationships found between the courses<sup>51</sup>. This difference, while significant, fails to reveal any trends with the individual church courses, the result of decreasing power of the statistical analyses used to examine the data (which, in turn, is due to decreasing data sets as courses are analysed separately). It is suggested that the differences between courses 2 and 5 was due to natural variation within the rock.

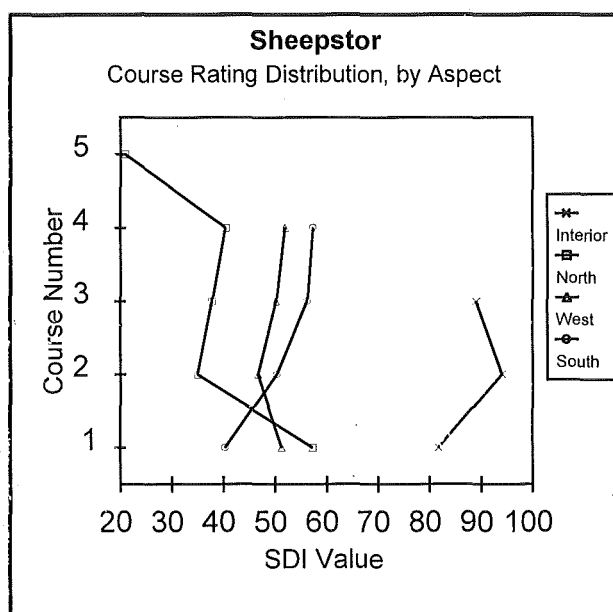


Figure 7.31. Sheepstor course rating distribution.

#### 7.2.10. Widecombe in the Moor

Widecombe-in-the-Moor had a church on the site of the present building in the late 14<sup>th</sup> century, although it was rebuilt and enlarged in the late 15<sup>th</sup> and early 16<sup>th</sup> centuries. Built from granite Type B (Floyd *et al*, 1993), and located in a slightly sloping and undulating churchyard on the crest of a hill, the construction date for the tower in the SDI study is taken as 1500. A site plan, showing both the west wall measurement site breakdown and the arrangement of the interior columns is shown in Figure 7.32, and details of the west facing wall is shown in Plate 7.12 and Figure 7.33. The individual block values are shown in appendix A.17.

<sup>50</sup> Course 5 against course 2;  $T(5) = 3.77$ ,  $P < 0.01$

<sup>51</sup> Course 2 against course 4;  $T(31) = -1.34$ ,  $P = 0.1$

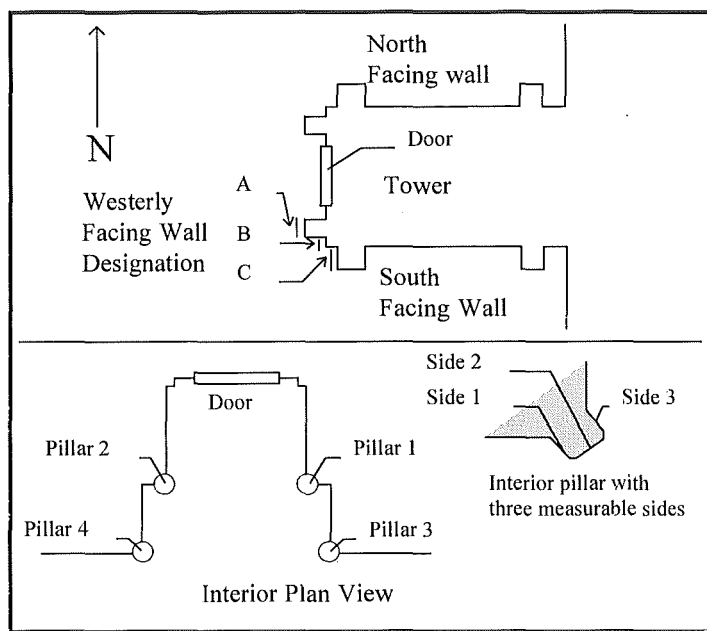


Figure 7.32. Plan view of Widecombe Church and interior.

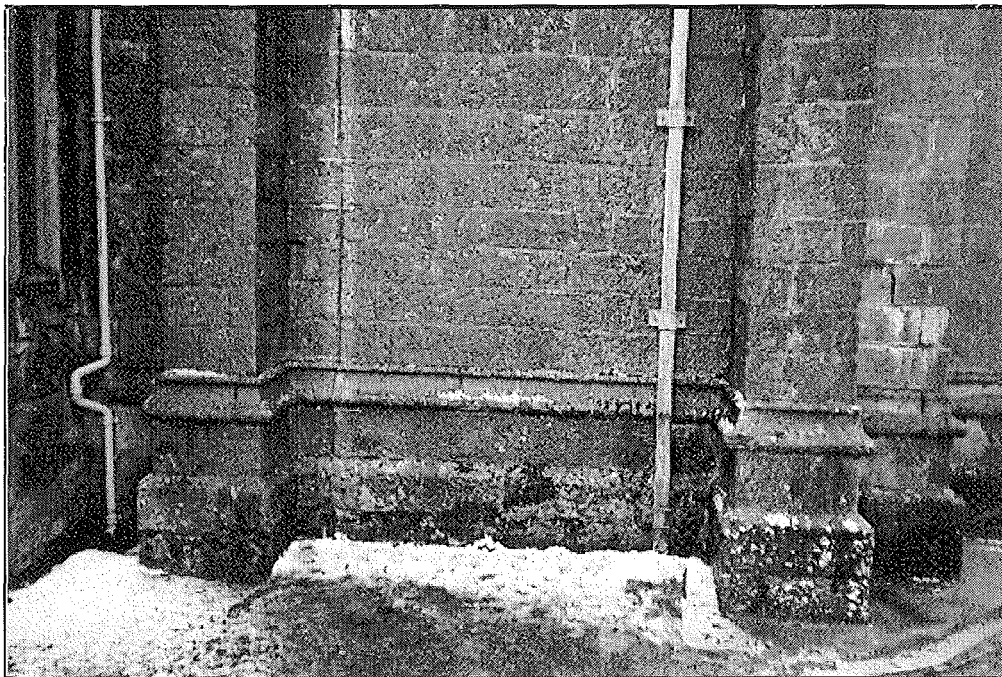


Plate 7.12. Widecombe-in-the-Moor church, north facing wall.

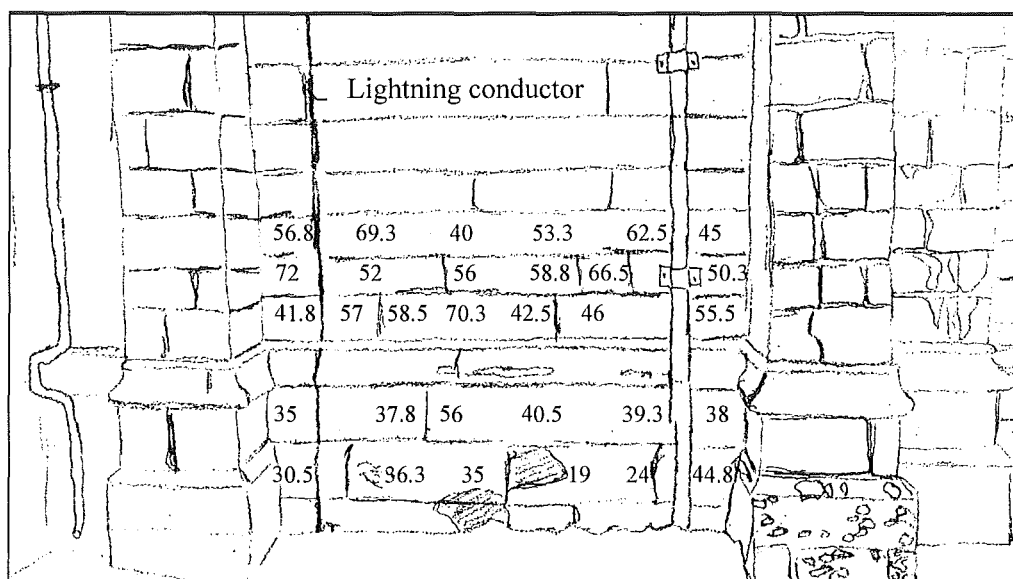


Figure 7.33. Sketch plan of Widecombe-in-the-Moor, north facing wall.

Analysis of the Widecombe-in-the-Moor block rating totals showed that there was a significant difference between the different wall aspects<sup>52</sup>. Post-hoc T-tests confirmed the differences between the interior and all exterior walls<sup>53</sup>, as well as between the some of the exterior walls<sup>54</sup>. Comparisons between north and west facing walls, however, were not significant<sup>55</sup>.

Rating Totals: Widecombe-in-the-moor church				
Average Course Values	South	West	North	Interior
Course 1	56	49.63	31.58	74.5
Course 2	67.4	54.96	41.08	90.25
Course 3	61.3	54.13	53.07	96.92
Course 4	58.3	47.54	59.25	
Course 5	59.2		54.46	
<b>Average</b>	<b>60.83</b>	<b>51.56</b>	<b>48.06</b>	<b>88.61</b>

Table 7.12. Average course ratings for Widecombe-in-the-moor church.

<sup>52</sup> ANOVA;  $F(2, 60) = 8.17$ ,  $P < 0.01$

<sup>53</sup> Interior values against south facing block values;  $T(10) = -6.16$ ,  $P < 0.01$

<sup>54</sup> i.e. south against west;  $T(45) = 2.88$ ,  $P < 0.01$

<sup>55</sup>  $T(52) = -1.05$ ,  $P > 0.1$

The significant differences between the south and the west and north aspects was expected, given the level of exposure at the site. Situated at the edge of a wide valley near one of the highest points on Dartmoor, the church was very exposed, and therefore slight changes in wall orientation can provide substantial changes to the micro-environment around a building wall. Once again, the north facing wall was the lowest rated wall of the church, which was not unexpected. During the numerous site visits to the church, water has frequently been seen running over the surface of the north facing wall stones, and there was a very high level of biological growth evident on the stones.

When the exterior walls were analysed by course (shown in Figure 7.34), it was found that overall there were significant differences between the courses when examined as a group<sup>56</sup>. Subsequently, however, post-hoc T-test analysis showed only one significant difference between the courses; course 1 (measurement taken within 30cm of ground level) was significantly lower than all other courses<sup>57</sup>. There were no other effects between the courses<sup>58</sup>.

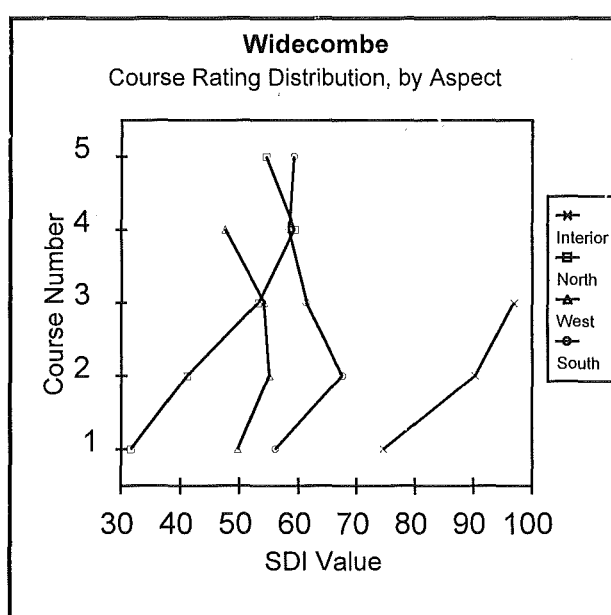


Figure 7.34. Widecombe Church course rating distribution.

<sup>56</sup> ANOVA;  $F(3, 51) = 5.2$ ,  $P < 0.01$

<sup>57</sup> course 1 against course 2;  $T(30) = 2.02$ ,  $P < 0.05$

<sup>58</sup> course 2 against course 5;  $T(26) < 1$

When the rating value distribution of the walls is viewed graphically in Figure 7.34, it can be seen that there are two types of distribution for the exterior walls. The south and west wall follow similar distribution patterns; the rock quality increases slightly as course number increases (up to around 120 cm from ground level), and then the SDI values start to decrease, most likely as a result of increasing exposure to wind and rain etc.

The north facing wall, which had much higher biocolonisation rates than the other two external walls, displays a different pattern, with SDI values increasing as course number increases. It is suggested that this is a function of a decreasing organism count, which in turn is the result of changes in the micro-climate surrounding the stone (decreasing moisture levels, increasing exposure etc.).

### 7.3. COURSE AND ASPECT RATING VARIATION

Stone deterioration does not affect a building or monument in a uniform fashion. Differences in height and aspect can have profound effects on the micro-environment of the stone (Emerick, 1995; Price, 1995), influencing the surface flow regime (Trudgill *et al*, 1990), the degree of thermal weathering, the rate of pollutant deposition and concentration (Schiavon *et al*, 1995; Dolske, 1995) and the rate of biological growth (Caneva *et al*, 1992).

The lack of a uniform weathering trend for increasing course height (see Figure 7.2 for course arrangement) when analysed by individual churches could be due to a lack of sufficient data to draw reliable statistical conclusions, and indeed this will reduce the chance of finding any relationship. By examining the total rating values for each course, by aspect and across all churches, it is possible to draw conclusions with a greater statistical validity about the affect of height on SDI values. This will be followed by analysis of the average course values for the churches, across all aspects.

When the aspect data for the churches was grouped together for analysis, a measure of the difference between individual churches was also conducted. These differences were best captured by the date of construction. This is discussed in more detail shortly.

### 7.3.1. South Facing Walls

When south facing course rating values were examined across all churches, shown below in Figure 7.35, significant differences were found between the courses<sup>59</sup>. Post-hoc analysis focused on the variance of two groups; the top two courses, and the bottom two courses.

The top two courses were compared against the bottom two because a) they both experience similar conditions as the other in their group, and b) increasing the number of values in the data set improves the statistical reliability of the analysis. Post-hoc T-test analysis of the course data shows that there was a significant difference between the top two courses (150 - 180 cm above ground level) and the bottom two courses<sup>60</sup> (0 - 60 cm above ground level). The significance between the course groups was replicated in comparisons between courses 5 and 6, and 3 and 4<sup>61</sup>. When examined as individual courses, only course 4 was significantly higher than other courses (course 5 and 6)<sup>62</sup>.

South Facing Walls						
Course	1	2	3	4	5	6
Luesdon Cross	62.38	62.75	81.50			
Lydford	63.55	66.05	64.75	74.70	63.45	
Mary Tavy	55.61	45.68	54.07	58.50	53.36	
Mary Tavy Vestry	78.20	76.60	78.15	84.30		
Moretonhampstead	63.00	56.83	57.75	71.50	34.08	58.20
Peter Tavy	62.10	66.90	60.30	64.50	70.05	
*Postbridge	49.57					
Princetown	75.61	72.82	71.31	79.75		
Shaugh Prior	54.68	45.31	40.38	46.00	41.04	44.86
Sheepstor	40.33	50.29	56.17	57.29		
Widecombe	56.00	67.40	61.30	58.30	59.20	
<b>Average</b>	<b>61.10</b>	<b>59.84</b>	<b>60.73</b>	<b>64.03</b>	<b>53.95</b>	<b>50.42</b>
* = only measured on one course level						

Table 7.13. Total average block ratings by course, south facing walls.

<sup>59</sup> ANOVA;  $F(5, 50) = 14.29$ ,  $P < 0.01$

<sup>60</sup>  $T(70) = 2.62$ ,  $p < 0.01$

<sup>61</sup>  $T(74) = 3.19$ ,  $P < 0.01$

<sup>62</sup> course 4 against course 5;  $T(10) = 1.81$ ,  $P = 0.05$ , course 4 against course 2;  $T(16) > 1$



During the initial analysis of the south facing course values, significant differences were found between the churches<sup>63</sup>. This was supported by T-tests on the courses, by church. Analysis of the 19<sup>th</sup> century churches (built post-1800) against the medieval churches (pre-1800) showed significant differences between the two groups of churches<sup>64</sup>. The higher values of the C19<sup>th</sup> churches showed they have undergone significantly less weathering than the building stone in the medieval churches.

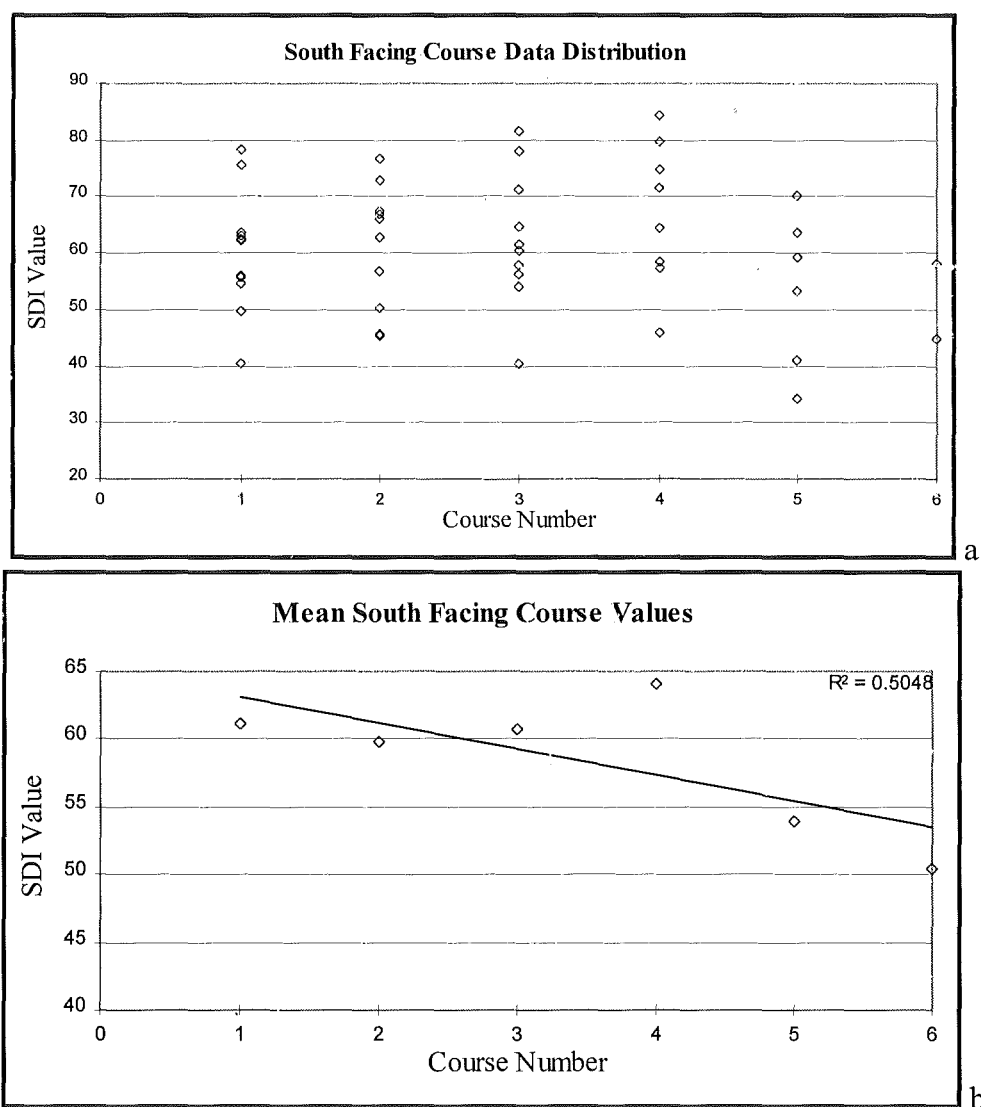


Figure 7.35a&b. Data distribution for south facing courses.

<sup>63</sup> ANOVA;  $F(9, 54) = 3.76$ ,  $P < 0.01$

<sup>64</sup> Pre-1800 churches against post-1800 churches;  $T(20) = -3.78$ ,  $P < 0.01$

Figure 7.35a&b shows the data distribution for the south facing courses, across all churches, with Figure 7.35a representing the means for the south facing courses of each church, while Figure 7.35b displays the means of the course values across all the churches. This was to produce a more reliable trendline.

Despite the high level of variability in the data (Figure 7.35a), it can be seen that the general trend of the rating values was to decrease with increasing course number (height above the ground) (Figure 7.35b). Although the validity of the trendline was compromised by the reasonably low degree of fit, the figures still indicate an SDI value decrease with increasing height.

When the south facing values from course 1 - 6 were considered, they had a mean of 59.94, the highest of the external walls, and a standard error of the mean of 1 (see Table 7.17 for exterior and interior wall averages).

Although the high mean (partly explained by lower levels of biological coverage on the south facing walls (Caneva *et al*, 1992)), suggests that building stone in a south-facing wall would weather the most slowly, the standard error of the data partially negates this.

Variations in the data set can be partially accounted for by the strong bi-modal distribution of the data, and by differences in course measuring height. Course sampling is constrained by the construction of the building under investigation, and the position of suitable measurement sites within the sample block. Also, there are variations in course and building block sizes across the churches. As a result, an average value of 30cm is used to calculate course height above ground.

Regression analysis showed a weak negative overall relationship between height above ground and rating value ( $R^2 = 0.51$ )<sup>65</sup> for the south wall, indicating that the level of weathering and stone deterioration increased with increasing height (up to the measured maximum height of around 180cm from ground level). Further examination of the data points revealed a bi-modal distribution suggesting that below course 4 (around 120 cm above ground level) the stones were somehow protected, possibly by the ground. This protection results in an increasing rating value, up to course 4 (around 120 cm above the ground), where the level of protection, and therefore the SDI values, decreased. This resulted in the south facing walls having

---

<sup>65</sup> All correlation and regression values reported at the 95% confidence limit.

the greatest levels of decrease over courses 1- 5 (~7 point decrease) of all the exterior walls.

Livingston and Baer (1988) found that tombstones measured in United States cemeteries were thinner at the top than at the bottom, where the original surface persisted. They suggested that the reduction in tombstone volume at the top was due to increased levels of atmospheric exposure, and it is likely that this process was operating on the upper courses of the south facing walls. This was supported by analyses by Hawes (1992) of wind velocities around buildings. He showed that when an air flow encountered a building, some of the air rose to pass at an increased velocity over the top of the building, while the rest formed a horizontal vortex and spiralled around both ends. The level of the vortex was determined by the height of the surrounding obstructions. This meant that while rain was thrown against the top of the building, relatively little hit the lower surfaces.

Although this model of air-flow was developed for larger, aerodynamically simpler urban buildings than the churches on Dartmoor (i.e.; concrete tower blocks), it can still be used to partially explain the decrease in the SDI rating totals for the higher course blocks.

Similarly, Delgado Rodrigues and Gil Saraiva (1985) studied wind flow around monuments, in particular a 25m building. They found that wind velocity around the tower varies with height. Of particular interest is the Atmospheric Boundary Layer, a layer of turbulence whose thickness is a function of the roughness of the surroundings. This will produce wind velocities 1.5-2 times the undisturbed flow velocities recorded higher up the building.

### **7.3.2. West Facing Walls**

Analysis of the west facing course data distribution, in Table 7.14 below, showed no significant differences between the courses when analysed as a group<sup>66</sup>. This was supported by post-hoc T-test analysis of the west facing course data, which found no significant differences between the upper two (measurements taken 120 -

---

<sup>66</sup> ANOVA;  $F(3, 30) = 1.7, P > 0.1$

150 cm above ground level) and lower (measurements taken 0 - 60 cm above ground level) two courses<sup>67</sup>.

The lack of differentiation between the courses was confirmed by post-hoc analysis of the data, which showed no significant variations between any of the individual course averages when viewed by the west aspect<sup>68</sup>.

Further ANOVA analysis of the course data showed significant differences between the churches when the west facing course data was examined by group<sup>69</sup>. This was supported by post-hoc T-test analyses, which showed that 19<sup>th</sup> century church values were significantly higher than those of the older medieval buildings<sup>70</sup>.

West Facing Walls					
Course	1	2	3	4	5
Luesdon Cross	64.88	62.69	66.25		
Lydford	55.63	55.50	50.63	54.63	47.88
Mary Tavy	55.17	52.88	39.13	59.38	40.46
Moretonhampstead	56.30	55.95	57.25	52.88	75.88
Peter Tavy	60.15	60.51	59.85	69.25	59.88
*Postbridge	66.00				
**Princetown	75.50	73.15	74.93	79.85	75.67
Shaugh Prior	41.75	37.03	40.38	44.06	50.50
Sheepstor	51.25	46.71	50.17	51.88	
Widecombe	49.63	54.96	54.13	47.54	
<b>Average</b>	<b>58.70</b>	<b>55.74</b>	<b>55.04</b>	<b>58.80</b>	<b>56.12</b>
* = only measured on one course level					
** = east measured instead of west					

Table 7.14. Total average block ratings by course, west facing walls.

The west facing mean course rating values, shown in Figure 7.36a, and the means of the raw course values across all churches, shown in Figure 7.36b, (mean; 56.81) had a lower degree of variability (standard error; 1) than the north facing walls (see Table 7.17 for details), but one that was similar to the south facing walls.

<sup>67</sup>  $T(23) < 1$

<sup>68</sup>  $T(9) < 1$

<sup>69</sup>  $F(8, 32) = 7.01, P < 0.01$

<sup>70</sup>  $T(17) = 7.37, P < 0.01$

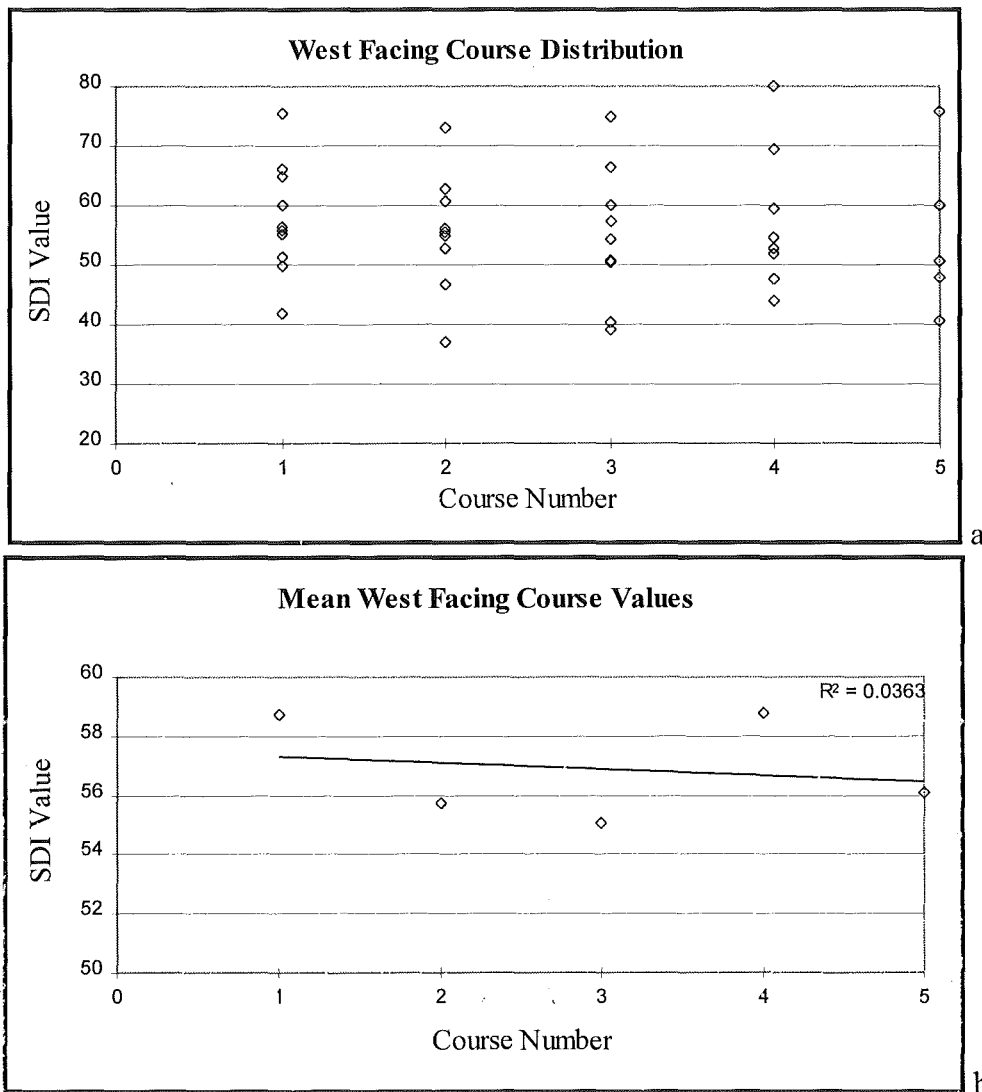


Figure 7.36a&b. Data distribution of west facing courses.

This could be explained by the position of the west facing walls. They were generally not wet enough to allow the continuous growth of lithobionts and other plants, although there was some biological growth, and they were not exposed to the thermal variations of the southern walls. This combination of factors would suggest that the micro-environment surrounding the west-facing walls was more uniform than the other walls - they were not as exposed as the south facing walls, shown by the rating drop with increasing height displayed by the southern course values, and they were not as affected by biological growth as the northern walls, promoting similar levels of weathering and a lower spread of rating values across course values.

Although there was a slight decrease (around 1 rating point) in the trendline in Figure 7.36b, this had an extremely low significance ( $R^2 = 0.04$ ). The low degree of fit for the trend line is explained by the small range in both the course and rating values, which reduces the reliability of assigning variability to any specific parameter change. This implies that variation in the data was due to natural variation in the rock, and was not the result of a relationship with increasing height.

### 7.3.3. North Facing Walls

Analysis of the north facing data by course, in Table 7.15 below, showed that there were significant differences between the courses when analysed overall<sup>71</sup>. Post-hoc T-test analysis of the data, however, showed no significant differences between the top (measurements taken 120 - 150 cm above ground level) and the bottom (measurements taken within 0 - 60 cm of ground level) two courses<sup>72</sup>.

North Facing Walls					
Course	1	2	3	4	5
Luesdon Cross	62.29	58.63	67.88		
Lydford	49.00	41.75	39.60	42.75	
Mary Tavy	44.75	50.13	53.63	66.50	59.19
Moretonhampstead	60.00	53.05	55.45	65.17	45.83
Peter Tavy	63.60	72.25	59.05	55.90	52.10
*Postbridge	67.92				
Princetown	71.82	79.97	72.47	68.39	
Shaugh Prior	36.29	38.80	36.33	32.21	
Sheepstor	57.25	35.00	37.81	40.44	20.94
Widecombe	31.58	41.08	53.07	59.25	54.46
<b>Average</b>	<b>53.22</b>	<b>54.14</b>	<b>53.39</b>	<b>53.27</b>	<b>47.51</b>
* = only measured on one course level.					

Table 7.15. Total average block ratings by course, north facing walls.

This was further supported by individual course analyses, which revealed no main effect between courses 1 and 5<sup>73</sup>. This was the same as the west facing wall distribution, but varied from the south facing walls, which showed significant

<sup>71</sup> ANOVA;  $F(3, 30) = 4.6$ ,  $P < 0.01$

<sup>72</sup>  $T(26) < 1$

<sup>73</sup>  $T(7) < 1$

differences between the top and bottom two courses (although there was no significance when courses 1 and 5 were analysed against each other).

The ANOVA analysis of the course data also showed significant differences between the churches when analysed by north facing course values<sup>74</sup>. This was supported by post-hoc T-test analyses, which showed that SDI rating values for the C19<sup>th</sup> churches (constructed post-1800) were significantly higher than the medieval (constructed pre-1800) church buildings<sup>75</sup>.

The north facing course values had a mean of 52.81, the lowest of all the measured aspects, and a standard error of 1.2 (see Table 7.17), the highest level of data variation in the study. The low mean and high variance can be explained by the high levels of biological growth that occurred on the majority of north facing walls. The presence of the biological coverage was also indicative of a continuously moist or wet location (Caneva *et al*, 1992), and this would also have an effect on the deterioration rate of the rocks.

There was approximately a five point drop in the trendline between course 1 (measurements taken within 30cm of ground level) and course 5 (around 150 cm above ground level), shown in Figure 7.37a&b, where 7.37a shows the mean north facing course values for each church, while Figure 7.37b show the mean course values across the measured churches.

Although the high levels of variability in the data reduces the statistical significance, analysis of the mean values by course, across all churches, shows a regression value between course and rating value of  $R^2 = 0.52$ . This was the highest degree of relationship between course height and SDI value of all the measured walls, but was still not significant. Like the south facing walls there was a weak inverse relationship between course number and average course rating value, with a drop of around 5 rating points over the plotted courses. It is suggested that although this appears to be function of increasing exposure with height, variations in the original condition of the ashlar, and its degree of weathering resistance will also strongly influence the SDI values.

---

<sup>74</sup> ANOVA;  $F(9, 36) = 8.35$ ,  $P < 0.01$

<sup>75</sup>  $T(20) = 6.51$ ,  $P < 0.01$

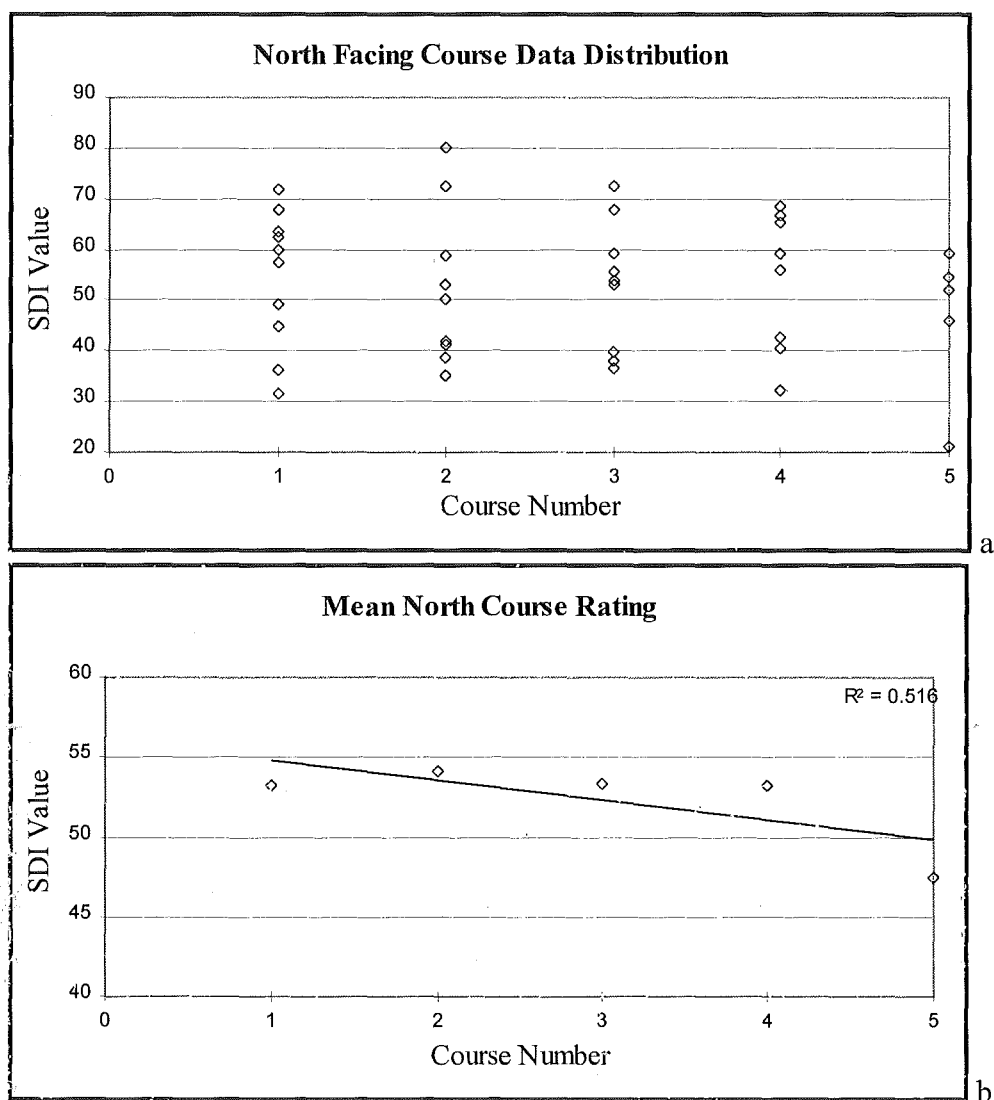


Figure 7.37a&b. Data distribution of north facing courses.

#### 7.3.4. Interior Walls

Interior church readings do not follow the standard course pattern set for the external church readings, but nevertheless it is import to examine their distribution as they can potentially be used as a baseline for examinations of the rate of change experienced by the external stones since church construction. Therefore it is important to know if there are variations in the measured interior values as a result of measurement height or date of construction, both of which could have significant implications of the baseline.

Measurements of interior building sites were usually performed on columns and other unplastered, exposed stone, which was limited in extent. As a result the



restrictions in sampling sites, measurements were taken at progressively higher position on the columns, simulating the effects of increasing height above ground with increasing course number. This allowed a degree of comparison between the interior and exterior data sets, although the interior courses had no physical dimensions as the readings were, by necessity, taken at different heights from church to church. The average values for interior course ratings are shown below in Table 7.16.

Analysis of the interior course data across the churches showed that there was a significant difference between the measurement sites<sup>76</sup>. This was not, however, supported by individual course comparisons, which revealed no significant differences between course means when compared with each other<sup>77</sup>. Comparisons between the top two courses and the bottom two courses also revealed no significant differences<sup>78</sup>, which was expected, given the protected environment of a church interior.

Interior Walls				
Course	1	2	3	4
Lydford	90.81	92.69	84.19	83.13
Mary Tavy	81.69	79.25		
Mary Tavy Vestry	96.00			
Moretonhampstead	76.83	87.33	77.75	87.42
Peter Tavy	77.85	73.20	60.50	
*Postbridge	90.92			
Shaugh Prior	87.04	85.75	84.25	
Sheepstor	81.69	94.00	89.00	
Widecombe	74.50	90.25	96.92	
<b>Average</b>	<b>84.82</b>	<b>85.43</b>	<b>80.55</b>	<b>84.96</b>
* = only measured on one course level.				

Table 7.16. Total average block ratings by course, interior walls.

The initial group analysis of church interiors showed significant differences between the values of the interiors, by church<sup>79</sup>. Post-hoc T-tests confirmed this,

<sup>76</sup> ANOVA;  $F(2, 20) = 6.33$ ,  $P < 0.01$

<sup>77</sup> course 2 against course 3;  $T(8) < 1$

<sup>78</sup>  $T(30) < 1$

<sup>79</sup> ANOVA;  $F(8, 24) = 3.23$ ,  $P < 0.01$

with 19<sup>th</sup> century church interior values significantly higher than those recorded at the medieval buildings<sup>80</sup>.

The internal values had a mean rating of 83.92, the highest average value for any wall in the study (see Table 7.17 for comparison). This figure, coupled with a standard error of 1.1, indicates that the rock used in the interior building stones was, as expected, the least weathered of all the stones in the studied churches, although there was a moderate degree of variation in the readings.

As post-construction weathering processes should not influence the performance of the interior stone in a significant fashion, it was thought that the variation in the data between churches would occur as a result of a) natural variation in rock quality prior to quarrying, and b) a rating reduction brought about as a result of the extraction, finishing and transport of the stones.

Nevertheless, it was surprising to find significant differences between the churches, given the relatively stable nature of church interiors, and it is suggested that one of causes was variation in the data from one church to another. This will be introduced not only by variations in the measurement heights, but also by differences in the internal atmosphere of the churches i.e. the presence of heating, damp courses etc., which will affect humidity and temperature, and therefore weathering rates.

The second source of variability in the interior rating values between churches of differing age could be the build up thin reaction crusts on the surfaces of the interior stones. These crusts can be formed through a variety of process, ranging from the deposition of fats and smoke from candles, to mineralogical changes of exposed surface minerals as a result of damp and condensation over the course of many centuries. The presence of the reaction crust on the surfaces of the interior stones will result in a reduction of surface strength over time, and could explain the significant variations in interior rating values between churches.

---

<sup>80</sup>  $T(2) = 3.25$ ,  $P < 0.05$

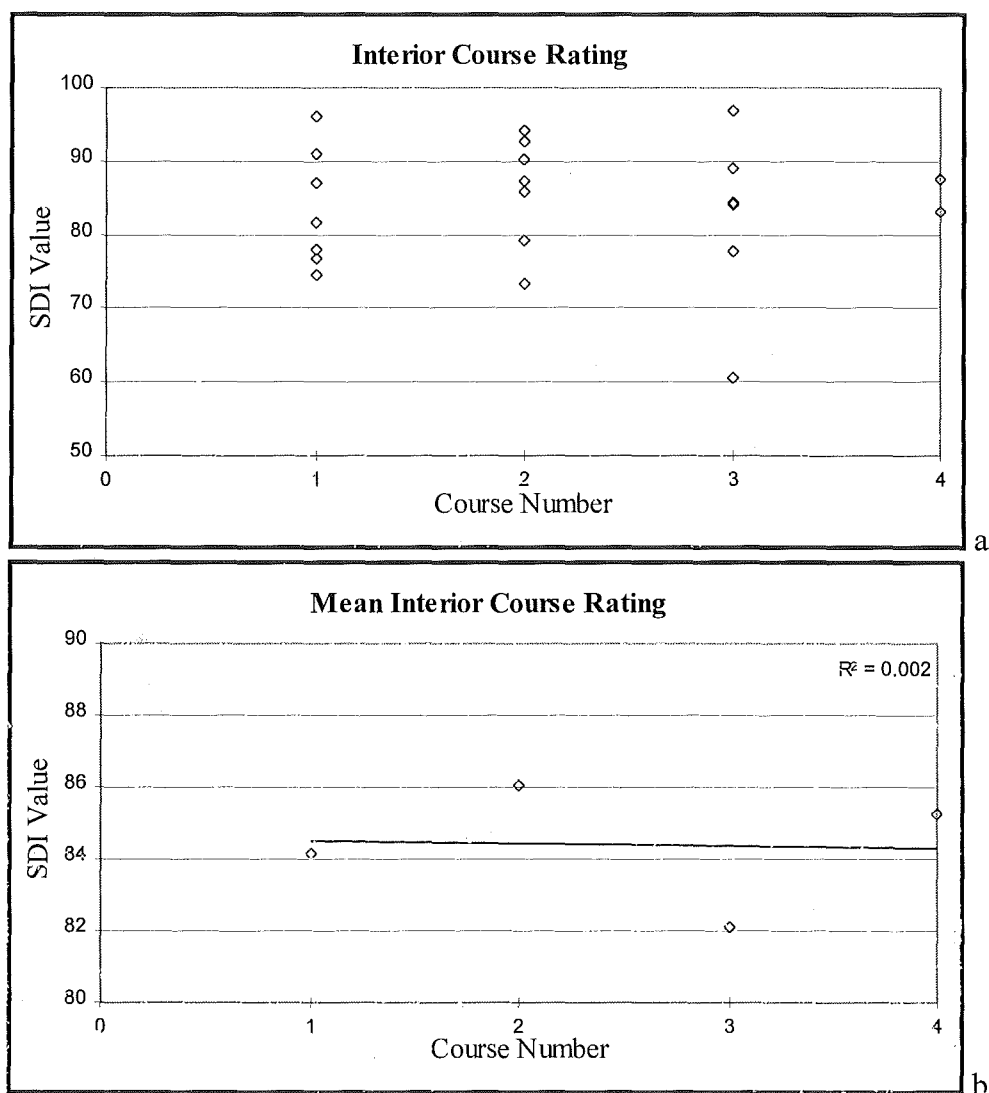


Figure 7.38a&b. Data distribution of interior courses.

Wall Aspect	Mean	Standard Error
South	59.94	1
West	56.38	1
North	52.81	1.2
Interior	83.92	1.1
Average external	56.81	0.6

Table 7.17. Exterior and interior wall averages and standard error of the mean across all churches.

To support the absence of normal atmospheric weathering processes, the trendline in Figure 7.38b showed no decrease in the mean values of the interior

courses, as a function of increasing height. The extremely low  $R^2$  ( $R^2 = 0.002$ ) value indicates the random nature of the course variation. The significant differences between the courses registered by the initial group ANOVA was likely to be due to course two, which had the highest mean of all the courses, and the least variability in the data.

### 7.3.5. Exterior Course Averages

Analysis of the exterior course averages across all aspects and all churches, with the data values shown below in Table 7.18, revealed significant differences between the course values<sup>81</sup>. Analysis by T-tests showed that although there was a significant difference between the top two courses (measurements between 150 - 180 cm above ground level) against the bottom two courses (measurements between 0 - 30 cm above ground level)<sup>82</sup>, this was not replicated for the individual courses<sup>83</sup>.

Exterior course Average						
Course	1	2	3	4	5	6
Luesdon Cross	63.18	61.35	71.88			
Lydford	56.06	54.43	51.66	57.36	55.66	
Mary Tavy	51.84	49.56	48.94	61.46	51.00	
Mary Tavy Vestry	78.20	76.60	78.15	84.30		
Moretonhampstead	59.77	55.28	56.82	63.18	51.93	58.20
Peter Tavy	61.95	66.55	59.73	63.22	60.68	
*Postbridge	61.16					
Princetown	74.31	75.31	72.90	76.00	75.67	
Shaugh Prior	44.24	40.38	39.03	40.76	45.77	47.91
Sheepstor	49.61	44.00	48.05	49.87	20.94	
Widcombe	45.74	54.48	56.17	55.03	56.83	
<b>Average</b>	<b>57.88</b>	<b>56.78</b>	<b>56.65</b>	<b>59.10</b>	<b>53.04</b>	<b>50.64</b>
* = only measured on one course level.						

Table 7.18. Total average block ratings by course, average across all aspects

The initial group analysis of the exterior average course values showed significant differences between the churches involved in the study when rated by

<sup>81</sup> ANOVA;  $F(5, 50) = 14.14$ ,  $P < 0.01$

<sup>82</sup>  $T(173) = 2.59$ ,  $P < 0.01$

<sup>83</sup> course 5 against course 4;  $T(14) = -1.28$ ,  $P > 0.1$

course<sup>84</sup>. Post-hoc T-test analysis of the average external course values, across all aspects, showed significant differences exist between the churches, with the SDI values of the C19<sup>th</sup> churches rated significantly higher than the medieval buildings<sup>85</sup>.

The average external course values had a mean of 56.81, and a standard error of 0.6 (see Table 7.17). Like the south and north facing aspects, a moderate relationship between course height and SDI rating point totals was found when the average external course values were examined ( shown in Figure 7.39a). The graph also shows that the mean for course 4 was still higher than all the other courses in the study.

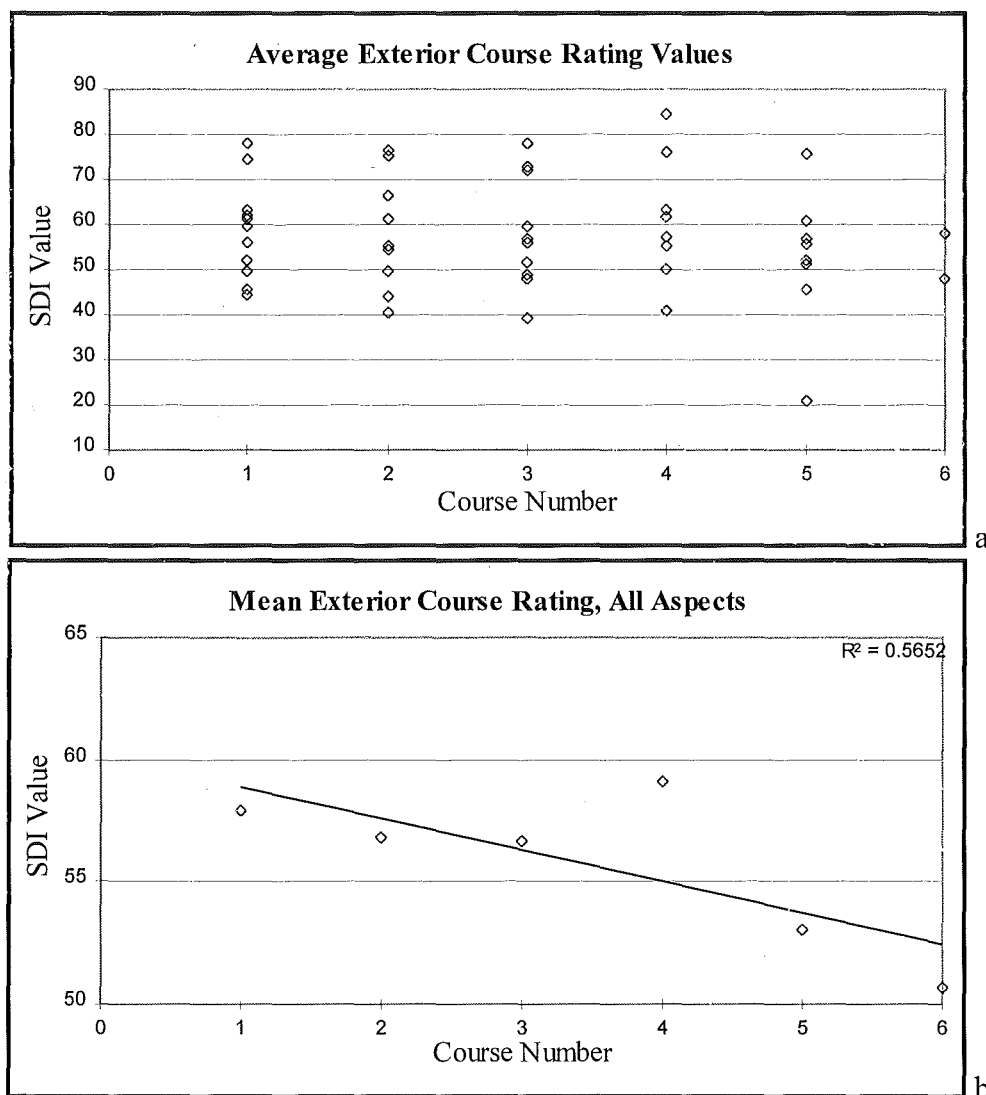


Figure 7.39a&b. Mean course values, across all aspects.

<sup>84</sup> ANOVA;  $F(9, 54) = 4.1$ ,  $P < 0.01$

<sup>85</sup>  $T(26) = 8.54$ ,  $P < 0.01$

The course value distribution is more clearly illustrated in Figure 7.39 b, which shows the average course means for the raw course values from all the measured churches, and the trendline. The trendline shows a clear decline in the average course value with increasing course number of ~6 SDI point over 6 courses, with a reasonable degree of fit ( $R^2 = 0.57$ ). This implies that there was a moderate relationship between decreasing rock quality with increasing height.

However, as found in other aspects, course four (around 120 cm above ground level) was above the fit of the trendline. This is more fully shown in Figure 7.40, which shows all three of the external aspects in comparison with each other. It is unknown whether this was a consistent function of course height across the churches as the result of changes in the degree of weathering the rock experienced, which could be explained decrease in the level of ground-water infiltration, or as a result of changes in the flow velocity of winds around the church buildings (Delgado Rodrigues and Gil Saraiva, 1985). This could increase the rate of friable particle removal from the stone surfaces, which would increase the SDI values as readings are taken from the fresher rock underneath the friable surface.

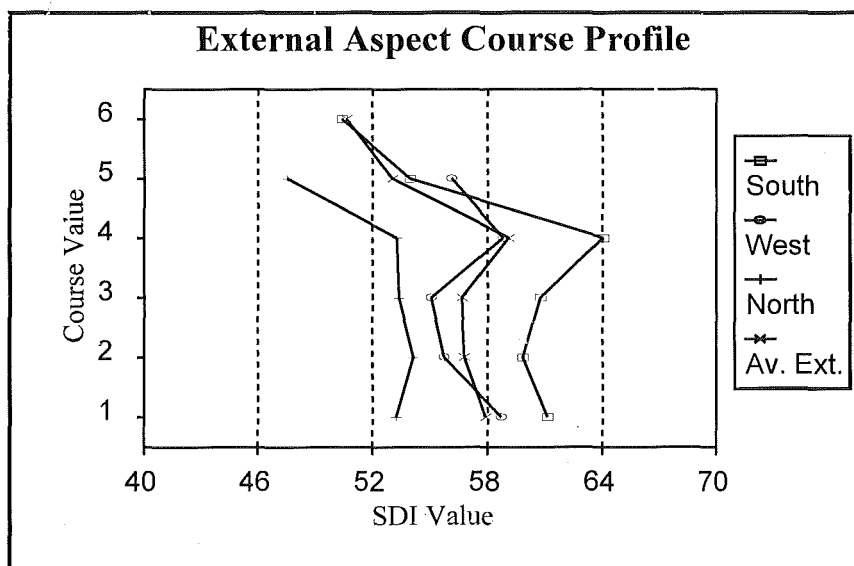


Figure 7.40. External aspect course profiles.

### 7.3.6. Medieval and 19<sup>th</sup> century Church Aspect Differences

When the churches were divided into post- and pre-1800 groups (or medieval and nineteenth century churches (Robinson and Williams, 1996)), further differences in the distribution of aspect rating points emerged. This is shown in Figure 7.41, where the mean SDI aspect values for the 19<sup>th</sup> century and medieval church groups are plotted with  $\pm 2$  standard error of the means.

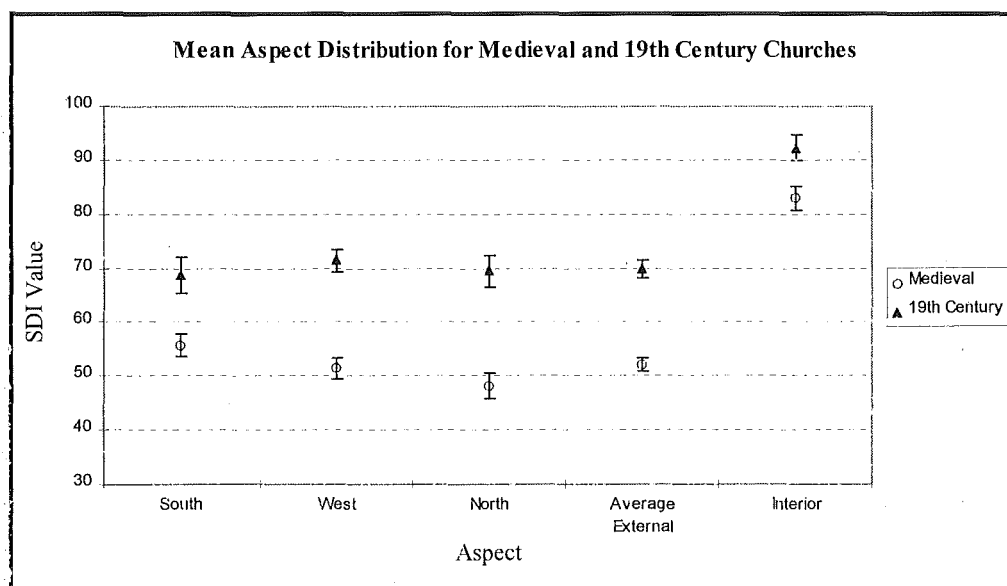


Figure 7.41. Mean aspect distribution for 19<sup>th</sup> century and medieval churches, with  $\pm 2$  standard errors of the mean.

The highest level of variability in the 19<sup>th</sup> century church data set was for the south facing walls, with a standard error of 1.64 SDI points, which was larger than the equivalent figure for the medieval churches ( $SE = 0.99$ ). This variability could be due to the unequal input of Mary Tavy Vestry, which was the most recent (built in 1895) of all the constructed churches measured in the study, and the one with the freshest rock. The vestry only had one clear aspect to measure, and so this input of high measurements could explain the larger than expected variation, which produced a standard error that was considerably higher than the nearest value (see Table 7.19).

The other aspects followed the expected order of variability, with the north showing a higher standard error than either the west or the interior values. The

interior standard error of the means was the lowest of the measured aspects, and this was explained by the homogeneity in conditions between the church interiors.

Unexpectedly, the 19<sup>th</sup> century church standard error of the mean values were higher than the equivalent medieval church group values, implying that the medieval church values are more closely distributed around their means than the more recent church quality values. The greater variance in the newer churches could be explained by the rapid alteration of granite at the start exposure as it adjusts to a new equilibrium with the ambient atmospheric conditions, a process observed during the exposure of micro-catchment unit slabs around England. Once the stone has been exposed for period of time greater than the period of adjustment required for the new conditions, the alteration rate decreases, and the building stone begin to reflect their surrounding conditions.

The average of the raw values from across all the 19<sup>th</sup> century church external values produced an average standard error value of 1.19, once again a higher degree of variability than that recorded for the medieval churches ( $SE = 1.11$ ). It is suggested that this was a typical rating variation value in 19<sup>th</sup> century churches, where the limited exposure time produces a rapid degree of alteration from the granites original state until equilibrium is reached and the rate of change decreases.

Medieval churches display a slightly different rating pattern than the 19<sup>th</sup> century churches. Variability in the data was at a similar level across the south and west aspects, while the north wall had the lowest mean and highest variability. This is most easily explained by the presence of almost total biological growth on the north aspect walls of the church towers and buildings, and the similarity in the impact of weathering processes such as freeze/thaw cycles and thermal weathering on the west and south facing walls.

When the values from all of the medieval church external aspects were examined the standard error of the mean across the external aspects for all the churches was 1.11. The higher degree of variation in the SDI rating values for the 19<sup>th</sup> century buildings, coupled with a mean external value that is 17.76 SDI points higher than the equivalent medieval church value, suggests that there is an increased weathering rate for individual stones that have recently been incorporated into the



building fabric, but that the rate of weathering decreases over time, producing a smaller amount of variance in the medieval churches.

The increased weathering levels of the medieval churches is shown in Figure 7.41, where the medieval church distribution had more of an exaggerated profile, with a greater difference between the interior and exterior values than the C19<sup>th</sup> churches. This was not unexpected, as differences between the levels of exposure and weathering the exterior walls experience are emphasised by prolonged incorporation in the building fabric. The aspect distribution and standard error of the means for the two church groups is shown below in Table 7.19.

	19 <sup>th</sup> Century		Medieval	
	Mean	Std. Error.	Mean	Std. Error.
South	68.81	1.64	55.78	0.99
West	71.45	1.09	51.44	0.98
North	69.47	1.49	48.20	1.15
Interior	92.31	0.83	83.02	0.61
Average External	69.93	1.19	52.17	1.11

Table 7.19. Aspect means and standard error of the mean for C19<sup>th</sup> and Medieval churches.

#### 7.4. AGE - RATING COMPARISONS

One of the aims of the SDI study was to relate building age with the level of weathering the church has undergone. This was achieved by plotting the SDI values of external building stones against the age of construction to give an indication of the deterioration rate. This is a valuable parameter for building conservation, as it will allow conservators to examine the rates of deterioration experienced by specific buildings in comparison to a clean, rural benchmark.

This is an area that has been consistently overlooked by the vast majority of building decay assessments, which tend to examine the interactions between air pollution and stone decay (Fassina, 1978; Fobe, 1993; Smith et al, 1993; Schiavon, 1993; Schiavon, 1996) or the petrographic impact of weathering on building stone (Fort González *et al*, 1993; La Inlesia, del Cura and Ordoñez, 1994; Fiora, Chiari and Compagnoni, 1996). Exceptions to this are Robinson and Williams (1996), who

evaluated weathering features on sandstone churches of varying ages, and Trudgill, Viles, Cooke and Inkpen (1990) who used exposed point-specific measurements from lead plugs in limestone balustrades to create a limited, linear decay rate for St. Paul's Cathedral since 1718.

In contrast, the SDI scheme avoids process- and feature-led decay evaluation, by assessing the products of the total deterioration processes that affect the building stone condition. This is achieved through the measurement of the near-surface characteristics of the building stones, without trying to account for specific decay processes that might be affecting the stone. This generic approach allows the comparison of buildings in different weathering regimes and pollution environments.

To examine the effectiveness of the SDI scheme at rating building deterioration over time, a correlation analysis between the raw values from the four measured parameters (surface strength, surface roughness, crustal coatings and discolouration) against age, and the total SDI value against age was conducted, with the correlation values shown in table 7.20.

These figures describe the degree of fit between the parameter values and building age, and show that the SDI block rating scheme is the most accurate in terms of describing the relationship between stone deterioration and building age. The high degree of fit is due to the combination of the assessment parameters to produce a measure of stone deterioration, parameters that assess each major area of the process, i.e. material strength reduction, material loss, chemically-induced discolouration and biological and pollution crust-induced deterioration.

Parameter	Correlation Value
Surface Strength	0.69
Surface Roughness	-0.49
Surface coatings	-0.30
Discolouration	-0.15
SDI Block Rating	0.74

Table 7.20. Correlation values between SDI parameters and building age.

The SDI value correlation analysis was first carried out on seven of the ten churches. These were the first buildings rated after the pilot study, and their rating

averages showed a high degree of relatedness to the age of the building ( $r = 0.8$ ).

The inclusion of three more recent churches, plus a separate vestry, (see Table 7.21 for details) did not significantly alter the positive relationship between the weathering level of the building, and its age ( $r = 0.74$ ).

Church	Age	South	West	North	Average External
Luesdon Cross	1863	68.88	64.60	62.93	65.47
Lydford	1450	66.50	52.85	43.28	55.25
Mary Tavy	1440	53.44	49.40	54.84	52.27
Mary Tavy Vestry	1895	79.31			79.31
Moretonhampstead	1418	57.55	59.65	55.90	57.56
Peter Tavy	1520	64.77	61.93	60.58	62.35
Postbridge	1868	49.57	66.00	67.92	61.74
Princetown**	1812	74.87	75.82	73.16	74.93
Shaugh Prior	1430	45.38	44.11	35.91	43.54
Sheepstor	1510	51.02	50.00	38.29	43.09
Widcombe	1500	60.44	51.56	47.89	52.91
<b>Mean Values</b>	--	<b>61.07</b>	<b>57.59</b>	<b>54.07</b>	<b>58.95</b>
Moretonhampstead uses only porphyritic block values					
** = east was measured instead of west					

Table 7.21. Church age against average external SDI values. Shaded churches were built post-1800.

External block rating totals from all aspects were used in the analysis, with mean church aspect values shown below in Table 7.21. External average values are derived from the combined raw aspect values from each church. Interior rating values are not reported as they do not reflect the actions of prolonged atmospheric exposure.

When the external church values were plotted by aspect against date of construction, it was possible to develop an estimation of the rate of decay experienced by granitic building stone incorporated in church fabrics of the Dartmoor region. This is shown below in Figure 7.42, with average course values for the south facing walls against the date of construction of the sample churches.

Two estimations of the rate of decay are shown in Figure 7.42. The first is an exponential trendline, which is designed to reflect the postulated accelerated decay building stone experiences when first incorporated into the building fabric, with a

weathering rate that decreases with time (Robinson and Williams, 1996). This higher level of initial deterioration could explain why external south aspect SDI values for the 19<sup>th</sup> century churches have a relatively low mean value of 68.8 (see table 7.19), despite their recent construction.

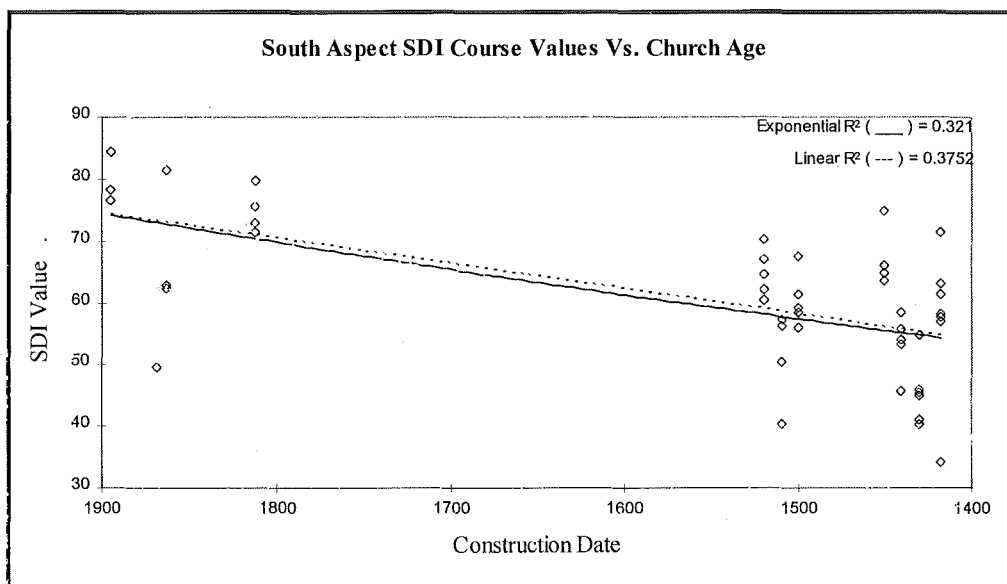


Figure 7.42. South aspect SDI deterioration rates.

The linear trendline reflects the mean deterioration rate for a regular step-wise cycle of decay, with the formation of less-resistant weathering products and a weakened near-surface area, followed by the removal of the weathering products and erosion back to the relatively fresh rock underneath. For the linear trendline, the low values of the 19<sup>th</sup> century churches could be the result of a reduction in strength and the expansion of microfracture networks as a result of extraction and finishing of the building stones. Examination of the significant differences in strength values between *in situ* type B granite from Burrator quarry and building stones from Widecombe-in-the-Moor and Sheepstor churches is shown in section 7.3.2.1.

However, it is likely that the mean weathering rate for the churches in the study is likely to be more complicated than either the linear or exponential patterns, with a high level of initial deterioration as the fresh building stone adjusts to the new ambient environmental conditions, followed by a relatively linear cycle of stepwise decay patterns. This continues until the building stone is completely weathered,

when a acceleration of the deterioration rate is likely as the stone undergoes rapid disintegration with the destruction of the crystal lattice (Helmi, 1985; Smith *et al*, 1996). This suggested pattern of decay is shown in Figure 7.43.

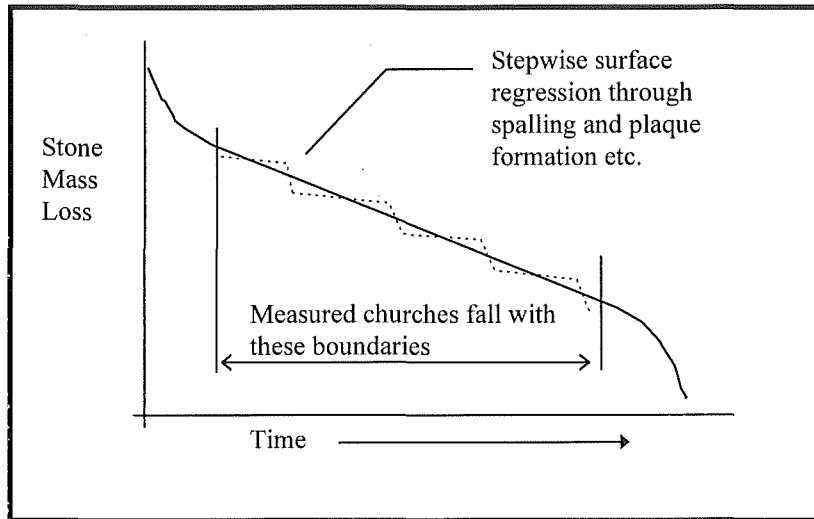


Figure 7.43. Possible weathering pattern over time.

Given the decay pattern shown above, the increased applicability of the linear fit trendline is shown by A) The very small difference between the exponential and linear trendlines when plotted in Figure 7.42, and B) The higher degree of fit for the linear trendline (exponential  $r^2 = 0.32$ , linear  $r^2 = 0.38$ ). This, coupled with the fact that the SDI scheme was used to evaluate buildings and monuments that were at least 100 years old and have therefore already undergone the increased levels of initial decay, means that the linear trendline might be more appropriate for use as a predictive device.

Both of the south aspect trendlines can be used to produce a predictive rate of decay for granitic building stone in a clean, rural area. The exponential equation (equation 7.1) is shown below, followed by the linear trendline analysis (equation 7.2).

$$y = 21.469e^{0.0007x} \quad (7.1)$$

$$y = 0.0409x - 2.9635 \quad (7.2)$$

Where  $y$  is the south aspect rating SDI value and  $x$  = the buildings date of construction. Both the trendlines can be used to predict the rate of deterioration, with the linear and exponential estimations for each of the external aspects shown in figure 7.47. Using predictive power of the trendlines, the linear estimate of stone deterioration for the south facing walls was 4.09 SDI points per hundred years, while the exponential deterioration rates for the external aspects are shown below in Table 7.23.

The deterioration rate of the external west facing walls was slightly higher than that recorded for south aspect course values, with values derived from trendlines shown in Figure 7.44.

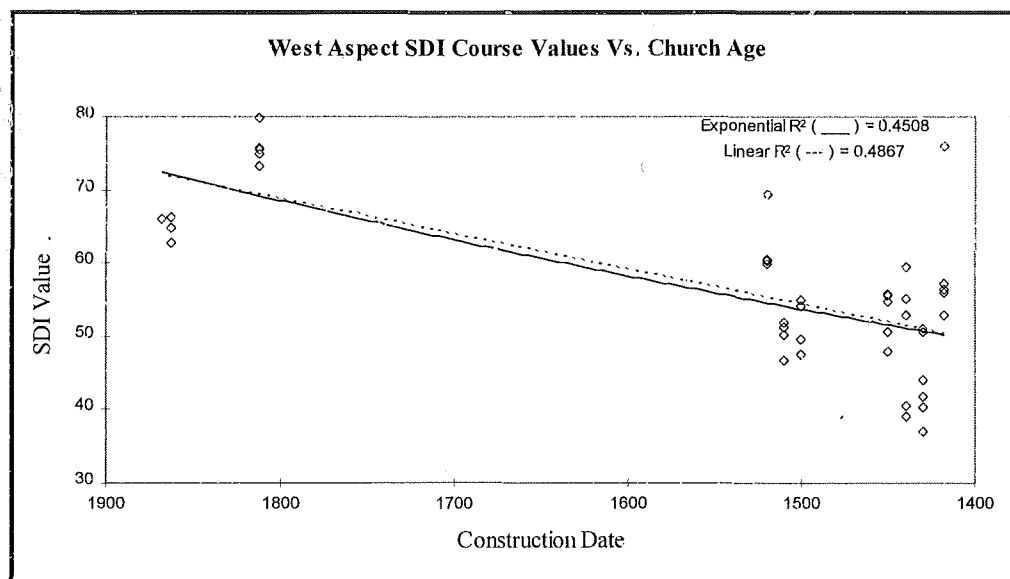


Figure 7.44. West aspect SDI deterioration rates.

These produce figures for the rate of deterioration experienced by west facing walls in the Dartmoor region, with the exponential equation (equation 7.3) and the linear analysis (equation 7.4) shown below, of 4.87 SDI points per hundred years

using the linear deterioration rate. The linear rate of deterioration was chosen over the exponential because it once again produced a higher degree of fit to the data points (linear  $r^2 = 0.49$ , exponential  $r^2 = 0.45$ ). It must be noted, however, that due to the non-linear nature of the decay rates experienced by fresh building stones as they adjust to the atmospheric conditions, this figure should not be applied to buildings less than 100 years old.

$$y = 15.823e^{0.0008x} \quad (7.3)$$

$$y = 487x - 17.197 \quad (7.4)$$

Where  $y$  is the west aspect rating SDI value and  $x$  = the buildings date of construction. The exponential deterioration rates for the west external aspects are shown below in table 7.23.

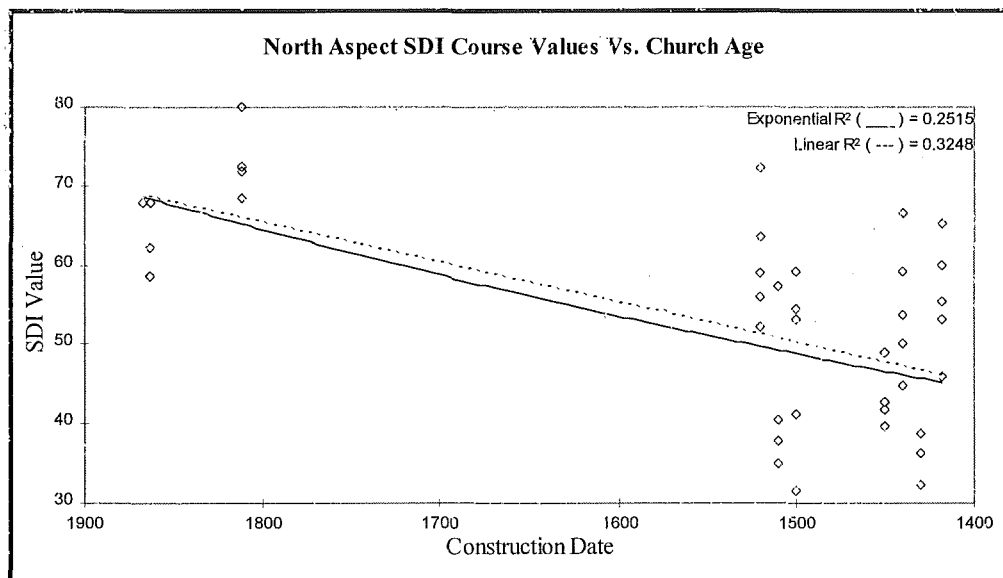


Figure 7.45. North aspect SDI deterioration rates.

The north facing walls displayed the greatest degree of weathering of all the measured aspects, and this is reflected in Figure 7.45, which shows the relationship between the north facing wall course averages and the construction date of the

sample building. The greater rate of deterioration is shown in Figure 7.47, which compares the deterioration rate estimate with those generated by the other external aspects. The north facing building stones also show that greatest degree of rock quality variation, producing the lowest degree of fit for any of the external aspects (linear  $r^2 = 0.33$ , exponential  $r^2 = 0.25$ ).

Using the trendlines generated in Figure 7.45, it is possible to determine a linear rate of deterioration for the north facing walls as 5.05 SDI points per hundred years, for buildings over 100 years old. This is generated by the linear equation (7.6), while the exponential equation (7.5) is shown below, with the results shown in Table 7.23.

$$y = 12.086e^{0.0009x} \quad (7.5)$$

$$y = 0.505x - 25.259 \quad (7.6)$$

Where  $y$  is the north aspect rating SDI value and  $x$  = the buildings date of construction. The deterioration rate derived from equation 7.6 is the highest rate of decay shown by all of the measured aspects in the study. This is likely to be caused by the high levels of biological coverage recorded on the north facing walls in comparison to the rest of the external aspects.



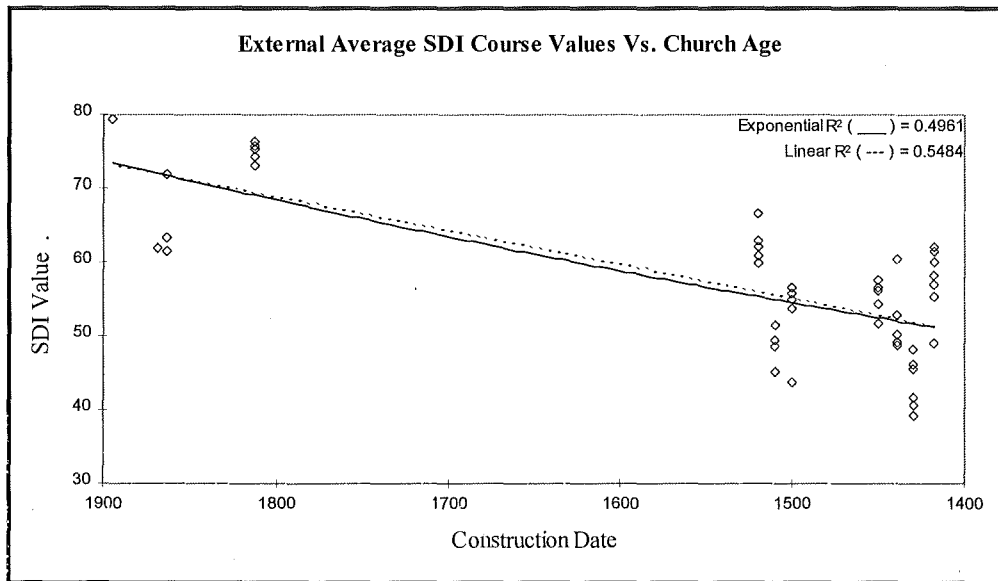


Figure 7.46. Average external SDI deterioration rates.

By studying the deterioration rates for the average external walls of the churches (with mean figures derived from block totals from each measured aspect across all churches), it is possible to derive an average linear deterioration rate for exposed building stones in the Dartmoor region of 4.59 SDI points per hundred years for buildings over 100 years old. This was obtained from the trendlines shown in Figure 7.46, which have a higher degree of fit over the individual aspect analyses (linear  $r^2 = 0.55$ , exponential  $r^2 = 0.5$ ). The exponential (7.7) and linear (7.8) deterioration equations are shown below, with the exponential deterioration rates shown in Table 7.23.

$$y = 17.469e^{0.0008x} \quad (7.7)$$

$$y = 0.0459x - 13.636 \quad (7.8)$$

Where  $y$  is the average external aspect rating SDI value and  $x$  = the buildings date of construction.

As the deterioration rate for the average external rating values is derived from values for each of the three measured aspects, it is the most important of the

estimates. This is because it can provide a generic weathering rate for granitic building stone in a clean, rural area for comparisons with urban results from future studies.

The accuracy of the predicted deterioration rates depends on the variability encountered within the data sets for the individual aspects. One measure of this is to compare the degree of fit between the trendlines for the aspects, while another method is to determine the correlation between the measured SDI values and the sample churches date of construction. These values are shown below in Table 7.22, while comparisons between the linear and exponential deterioration rates are shown in Figure 7.47.

Although the south facing walls have the lowest deterioration rate of the external aspects, the level of variation in the south aspect data was higher than that found in the west facing walls. This is demonstrated by both the lower degree of fit for the trendline, and the lower correlation value. The lower correlation value of 0.61 indicates that around 39% of variability in the south facing stone values was due to variations in weathering rates and rock quality prior to inclusion in the building fabric, and was not due to changes introduced as a result of prolonged exposure.

External Aspect	Deterioration Rate per 100 Years	R <sup>2</sup> Value		Correlation Value
		Linear	Exp.	
South	4.09	0.38	0.32	0.61
West	4.87	0.49	0.45	0.7
North	5.05	0.33	0.25	0.57
External Average	4.59	0.55	0.5	0.74

Table 7.22. Linear SDI deterioration rates between external aspects.

Age	south	west	North	Average External
1800	5.49	5.56	5.75	6.14
1700	5.12	5.13	5.26	5.67
1600	4.77	4.74	4.80	5.23
1500	4.45	4.38	4.39	4.83
1400	4.15	4.04	4.01	4.46

Table 7.23. Exponential SDI deterioration rates per century.

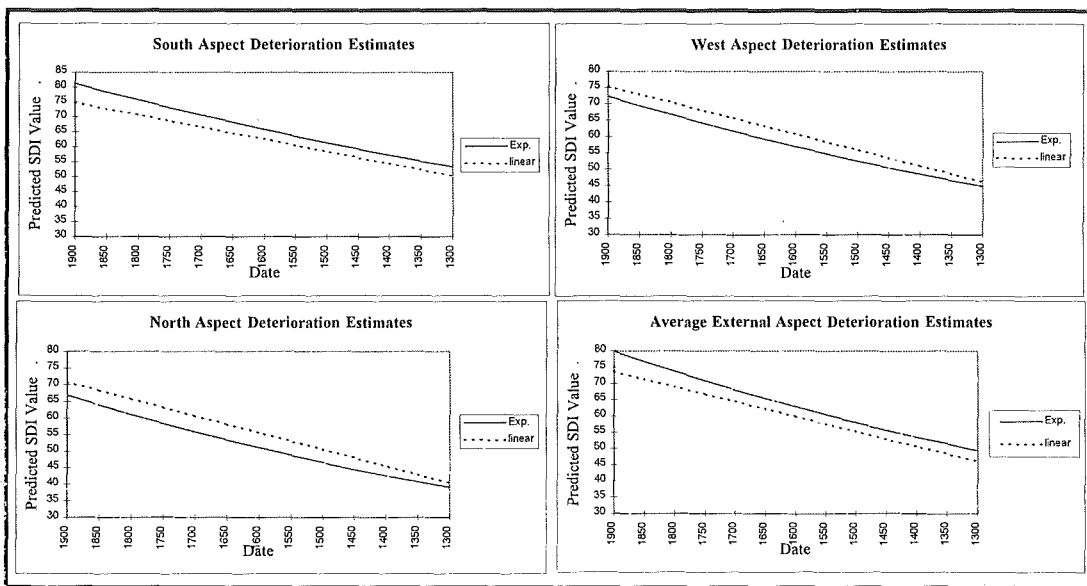


Figure 7.47. Exponential and linear deterioration estimations.

The west facing walls follow the same distribution shown at individual churches, with the median deterioration rate of the external aspects. The values derived from the west facing building stones also shows the highest degree of homogeneity of the individual aspects, with the highest degree of fit for the trendline, suggesting the most accurate individual aspect prediction. The correlation rate between west facing wall values and the construction date is also the highest of the individual aspects, with a value just less than the average external aspect correlation value. The high correlation value suggests that the majority of variation in the west aspect SDI can be explained by the prolonged stone exposure since building construction.

The most weathered of the three aspects is the north facing walls, with the lowest mean SDI values and the greatest rate of deterioration. The higher deterioration rate is most likely explained by the almost total biological coverage observed on the north facing walls. This is supported by the correlation analysis, which shows that only around 57% of the variation in north facing wall SDI values can be accounted for by increasing exposure. This suggests that the biological coverage is promoting localised decay, and therefore increasing the variation in rock

quality measured on the northern walls, although it will also have a reduced effect on the other walls..

The distribution of biological cover on Dartmoor churches was similar to the ranking of Prieto Lamas *et al* (1995), who found that lichen distribution on churches in Galicia, north-west Spain, followed the same pattern. Total lichen cover was highest on north and west facing walls, intermediate on south facing walls, and very low on east facing walls for the twenty churches they studied.

The degree of fit for the average external values is the highest of all the external analyses. This could be explained by the fact that as the external average is drawn from aspects that reflect different levels of weathering around the churches it is the most rigorous of the assessments. This is reflected with the correlation value, which indicates that 74% of the variation in the external average aspect values can be ascribed to the buildings date of construction. The rate of deterioration (4.59 SDI points per 100 years) is the suggested weathering rate of Type B granite (Floyd *et al*, 1993) in the Dartmoor region (a clean, rural site).

The deterioration rates, shown in Table 7.22, Table 7.23 and Figure 7.47 emphasise the influence of aspect, and therefore near-surface micro-environment, can have on building stone deterioration. Thermal weathering, moisture content and biological growth are all influenced by the position of the stone, and can have significant impacts on rock quality.

There are possible sources of error in these analysis, such as; a) the lack of data in the 1550 - 1750 period; b) a relatively low number of data points in the analysis; c) building stones that have come from different quarries. Although all of the measured stone (with the exception of the excluded Moretonhampstead stones) were classified as Type B (a broad group), they are likely to have different detailed petrography, and to have been extracted, worked and finished using different methods. However, the values shown in Table 7.22 estimate the relative levels of weathering the different aspects undergo with fair degree of accuracy, as shown by the high correlation value for the average external aspect values.

## 7.5. CONCLUSIONS

The SDI study was created to allow a generic assessment of building stone quality. This was achieved by measuring and combining the response of selected characteristics of the sample stones to generate a rating of the near-surface condition, opposed to a geochemical (Fort González *et al*, 1993), petrographic (Del Monte and Sabbioni, 1986) or decay feature-led (Robinson and Williams, 1996) assessment of stone condition.

To test the effectiveness of the assessment scheme, measurements were taken of the external and internal condition of 10 buildings and a monument over a wide age range from the Dartmoor area. This also allowed a quantification of the rate and pattern of decay the building stone was experiencing.

Although analyses of individual churches were carried out, and small differences in stone quality were detectable by the SDI scheme, it was found that the results were inconclusive in defining any overall trends in deterioration rates beyond the relative ordering of the rates for the different aspects.

However, when the churches and monuments were analysed collectively, deterioration trends and estimations could be made with a greater degree of statistical reliability. With orientation and placement of the building stones rated as one of the most critical constraints on the rate of deterioration, analyses focused first on the role of increasing height on rock quality, followed by the impact of aspect on stone deterioration rates over time.

Analysis of the course (height above ground) rating distribution showed a weak inverse relationship between course height (up to a measured maximum of 1.8 metres) and rating value for the south facing walls, with an SDI drop of around 7 points over the first six courses. This pattern of deterioration was repeated by the north facing walls, which had a reduction in the SDI course value of 5 points over the first five courses. The west facing walls and interior values, however, showed no relationship between SDI block values and increasing height.

It is suggested that the slight reduction in SDI values for the course values in south facing walls was the result of increased exposure, such as thermal cycling and incident rainfall, while it was combination of increasing exposure and biological action for the north walls. The west and interior walls showed no relationship with

increasing height, and therefore the majority of differences in the SDI values is likely to be due solely to variation in the original condition of the stones when the churches were first constructed. The lack of relationship between course height and SDI values suggests that the west walls were the most sheltered of the three measured external aspects.

The south facing walls had the highest mean SDI value of the external aspects, and the lowest deterioration rate, shown in Table 7.22, with a level of variability in the data set comparable to that of the west facing walls. The high mean could be the result of a combination of lower levels of biological coverage on the south facing walls (Caneva *et al*, 1992), and of the removal by rain action of less resistant reaction crusts and friable material back to fresher rock underneath.

The west facing walls produced the median aspect SDI mean and deterioration value of the individual external aspects, with a data set that contained the a similar level of variability as the south facing walls, and less than the north facing walls. The north facing walls displayed the lowest mean of the individual external aspects, and the highest rate of deterioration. North facing walls also showed the highest level of data variability, and this, it is suggested, is the result of variations in rock quality introduced by heavy biological growth on the external north facing walls.

Comparisons of the weathering rate suggest that the west walls experience a reduction in rock quality that is 6% higher than the south facing walls, while the heavily bio-colonised north facing wall deteriorate 14% faster.

Although there was little difference between exponential and linear patterns of deterioration between the external aspects, analysis of the SDI values over time suggested that there was an initial rapid adjustment period of up to 100 years for granitic stone incorporated in the building fabric as they moved to equilibrium with the ambient atmospheric conditions. It is suggested that this could be due to the removal of friable material, the establishment of lithobionts and other colonising species, and the expansion of microcrack networks within the stone as the result of chemical and physical weathering process exploiting pre-existing fracture networks.

The SDI scheme showed a clear inverse relationship between age and rock quality when applied to Type 'B' granite buildings in the Dartmoor area, with the age

of exposure accounting for around 74% of the variation in rock quality. The average deterioration rate for Type 'B' granite buildings over 100 years old in the Dartmoor area was 4.6 SDI points per hundred years.

## CHAPTER 8. Discussion and Conclusions

### 8.1. INTRODUCTION

In recent years there has been growing concern across Europe about the level of deterioration experienced by culturally significant buildings and monuments as a result of exposure to polluted urban atmospheres. This has resulted in numerous studies examining decay mechanisms and rates for calcareous stone (Jaynes and Cooke, 1986; Leysen *et al*, 1989; Inkpen *et al*, 1994) and sandstone (Fobe *et al*, 1993; Smith *et al*, 1994; Halsey *et al*, 1996; Robinson and Williams, 1996). Granite (Smith and Magee, 1990; Smith *et al*, 1993; Schiavon, 1996), however, has until recently, been under-represented in this area in comparison to other stone types, despite its significance as an important building stone.

This research programme was designed to attempt some redress of this imbalance by examining granite deterioration in two parts. The first section focused on the rate and pattern of decay experienced by fresh granite with a variety of surface finishes on exposure to selected levels of atmospheric pollution. This was conducted over a short time-scale (two years of exposure), using micro-catchment units to collect run-off from the granite slabs that were situated in two urban (London and Birmingham) and one rural (Dartmoor) area of England.

Although micro-catchment units have commonly been used for other rock types, such as limestone and sandstone (Cooper, 1986; Reddy, 1988; Halsey *et al*, 1995; O'Brien *et al*, 1995; Torfs and Van Grieken, 1996), very few studies have used granite (Sweevers and Van Grieken, 1992; Sweevers *et al*, 1995). Therefore, an enlargement of the number of granite micro-catchment unit studies will allow the potential for comparison of deterioration rates between different stone types. It will also provide information of the performance of fresh granite on exposure to atmospheric conditions. At the end of the exposure period the micro-catchment unit slabs were also examined for evidence of alteration as a result of exposure.

The second section of the study was to create a quick, simple, accurate, non-destructive and *in situ* method of building deterioration assessment. This scheme differs from other building evaluations in that it did not A) involve the destructive analysis of the stone (Sequeira Braga *et al*, 1993; La Iglesia *et al*, 1994; Sequeira



Braga *et al*, 1996); B) use process- or feature-led assessments of rock condition (Smith *et al*, 1992; Robinson and Williams, 1996).

The development of the Stone Deterioration Index allowed the rapid evaluation of the deterioration patterns of selected granitic buildings, through the use of a novel rating scheme. By measuring four stone parameters that account for the majority of changes produced by stone deterioration, the SDI produced a single generic value of near-surface rock quality. This assessment was carried out at the material scale, something that is, at present, unavailable to civil engineers (Cragg and Ingman, 1995).

The subject constructions were chosen to allow the formulation of a granitic building stone deterioration rate for a clean, rural area, a rate which could, in subsequent studies, be used as a benchmark for comparison with results from granite buildings in a polluted, urban environment.

The micro-catchment unit study was run alongside the SDI scheme for two main reasons. 1) By analysing the effect of increasing surface roughness on the micro-catchment unit slab run-off composition and the physical condition of the stone, it was intended to make some comparison of the decay patterns experienced by granite in the urban and rural environment, which could have important ramifications for the prediction of building deterioration. 2) Comparison of the rates of deterioration experienced by the urban against rural stones was intended to provide an indication of the relative impact of pollution on granite, as well as on the SDI values for churches in urban areas.

## **8.2. GRANITE EXPOSURE STUDIES**

The granite exposure studies were created as part of the research programme to evaluate the performance of granite in clean and polluted environments, by assessing the role of pollution on the rates and pattern of granite decay. This was investigated by placing selected granite samples in micro-catchment units that were situated at London, Birmingham and Dartmoor. These sites were chosen to reflect conditions found in urban and rural environments, and the mean pollution concentrations of the three sites is shown below in Table 8.1.

In addition to the microcatchment units, the primary method of investigation for pollution-induced weathering, carousel tablets were placed at each site to examine the relative importance of dry and total deposition on granite weathering rates. These will be discussed after the microcatchment unit investigations.

	London		Birmingham		Dartmoor	
	8/94 - 4/95	5/95 - 4/96	8/94 - 4/95	5/95 - 4/96	9/94 - 4/95	5/95 - 4/96
SO <sub>2</sub> (ppb)	9.3	9.7	8.3	7.5	2.2	1.8
NO <sub>x</sub> (ppb)	76.6	83.5	48	50.7	8.8 - 12.7*	
PM <sub>10</sub> (µg m <sup>-3</sup> )	26.3	32	22.6	26.6	3 - 6**	

Table 8.1. Exposure site pollution averages. \* Background NO<sub>2</sub>. Values from Newton Abbot, 1994 NO<sub>x</sub> diffusion tube survey, AEA technology. \*\* Secondary particulate matter, estimated by HARM model (QUARG, 1996).

Four microcatchment units were placed at each site; one contained a ground glass sheet to act as blank (a material that is durable (Butlin, 1991) and the most suitable to act as a control (Halsey *et al*, 1995)), while the other three contained Mountsorrel granodiorite slabs with different surface finishes (polished, cut and flame-dressed).

Analysis of the run-off collected from the microcatchment units showed that site was the most significant variable in influencing run-off concentrations. Only two (Fe<sup>++</sup> and PO<sub>3</sub><sup>-</sup>) of the eleven measured parameters failed to show any significant differences between the sites. The lack of significance for these components is explained by the low frequency and high levels of variance in the concentrations.

The significant interactions of the measured parameters across both site and finish is shown in Table 8.2. '/' indicates a significant differences between the variables, with the parameter on the left significantly higher than those listed to the right.

The majority of the other components had significant differences between all three sites. There were two exceptions; volume, where Dartmoor was significantly higher than either London or Birmingham, and pH, where London was significantly

higher than either Dartmoor or Birmingham. There were no significant differences between those two sites.

The pH distribution, with the most polluted urban site (London) producing higher pH values than either the Birmingham or rural Dartmoor sites, could be explained by the presence of 'calcium-rich clouds' around St. Paul's cathedral, a building constructed of Portland limestone. Leysen *et al* (1989) studied a limestone cathedral in Belgium and found a similar effect -  $\text{Ca}^{++}$ -rich aerosols, which can be derived from urban dust and from erosion of the building itself (Delgado and Gil Saraiva, 1985), surrounded the building and produced a higher pH and an enrichment of  $\text{Ca}^{++}$  containing particulates in comparison to standard rainwater samples from elsewhere in Europe.

	Site	Inter-finish
Volume	Dart./London & Birm.	--
pH	London/Dart. & Birm.	Birm.: cut/blank Dart.: cut & polished/blank
Conductivity	All sites	--
$\text{Cl}^-$	All sites	--
$\text{NO}_3^-$	All sites	--
$\text{PO}_3^-$	--	--
$\text{SO}_4^{2-}$	All sites	--
$\text{Al}^{3+}$	All sites	--
$\text{Ca}^{++}$	All sites	Dart.: cut/blank
$\text{Mg}^{++}$	All sites	All sites: stones higher than blank
$\text{Fe}^{++}$	--	London: flame/blank London: flame/polished

Table 8.2. Inter-site and inter-finish significant differences.

This effect had previously been noted by Roekens *et al* (1988), who suggested that the high pH (mean pH = 6.7) of bulk deposition samples from the cathedral was a function of rainwater neutralisation by the washout of  $\text{CaCO}_3$ . This is supported by Conlan and Longhurst (1993), who reported that rainwater acidity in Manchester was a function of the spatial variability of  $\text{CaCO}_3$  and its buffering activity. The neutralising action of the Belgium cathedral produced a mean pH that

was very similar to the mean site pH (6.68) for run-off samples collected from London, and this suggests that a similar process is operating at both cathedrals.

Aluminium, although showing a significant difference between the three sites, also deviated from the expected concentration distribution of the other components, where London > Birmingham > Dartmoor concentration. With aluminium, the highest concentrations were recorded by the Birmingham site run-off, with a mean run-off concentration of 138 ppm, while London had a concentration of 91 ppm and Dartmoor, 77 ppm. This result could be explained by an industrial point source near the exposure site

Run-off concentrations generated by the microcatchment units should also be affected by surface roughness. To evaluate the relative importance of surface roughness on deterioration rates, a roughness continuum was created, with polished as the smoothest finish and flame-dressed as the roughest.

This is significant because as igneous building stones weather their surface roughness increases, until a maximum level of roughness is reached and parallel surface retreat occurs (Grimm, 1983). As surface roughness increases, so does the deposition capture efficiency and the time of wetness, two factors that can strongly affect the rate of weathering. This could, therefore, result in a cycle of accelerating rates of decay for igneous building stones as roughness increases, affecting the deposition rate, which in turn results in a further increase in surface roughness. Weber (1995) has recorded that rates of aerosol deposition to a vertical surface increased with time as surface roughness increased as a result of weathering.

However, when the run-off component concentrations were analysed from the different finishes, shown in Table 8.2, few significant differences were found between them. Although some significant statistical differences were found between the means of the different populations (blank, cut, polished and flame-dressed finishes) when sites were examined as a group, these differences were not reflected in the majority of analyses between individual MCU's

Only four of the eleven parameters showed any significant effect of roughness on run-off component concentration. Three of them (pH,  $\text{Ca}^{++}$  and  $\text{Mg}^{++}$ ) showed significant differences between the blank (the level of concentration generated solely by atmospheric deposition processes) and the stone slabs

(atmospheric deposition and inputs as a result of mineral dissolution), but no significant inter-finish interaction. Only iron showed a significant difference between the stones and the blank, as well as an inter-finish interaction with the flame finish significantly higher than the polished finish at the London site. Given the lack of inter-finish interaction at the other sites, and across the other measured components, this suggests that the flame/polished interaction was of limited significance in trying to determine the role of finish in granite-derived run-off concentration.

The general paucity of significant results associated with the inter-finish examinations of concentration suggests that, in general, the role of finish-induced component change is minimal in comparison to the role of site. The lack of results could be explained by the relatively short-term exposure of the fresh granite samples. With a longer period of exposure, a more reliable data set could be constructed, allowing the determination of subtle, long-term trends engendered by finish type which is, at present, obscured by variations in the data set as the stones adjust the ambient environment.

To further examine the influence of surface roughness of the micro-catchment slabs weathering rate, a laser profileometer was used to assess the 1<sup>st</sup> order (surface variation) and 2<sup>nd</sup> order (inter-grain roughness) roughness of the slabs after exposure. These results were then compared to roughness values derived from the equivalent finish of unexposed control slabs. This was to determine if there was an increase in the finish roughness as a result of exposure.

Only the polished finish showed any significant variation between the values from the exposed and control roughness values, with the exposed polished slabs significantly rougher on both the 1<sup>st</sup> and 2<sup>nd</sup> order. None of the other finishes, shown in Figure 8.1, showed any variation from the protected control slabs.

The variation in the polished values could be explained by the finishing processes used in polishing the stones. The radial movements used to finish the stone could introduce stresses to the minerals as they are ground down. Subsequent weathering processes will result in the removal of friable minerals, so increasing the inter-mineral 2<sup>nd</sup> order roughness. Given the limited variation in roughness of the

original polished finish, the removal of weakened mineral grains will also increase the 1<sup>st</sup> order roughness, although not to as great an extent.

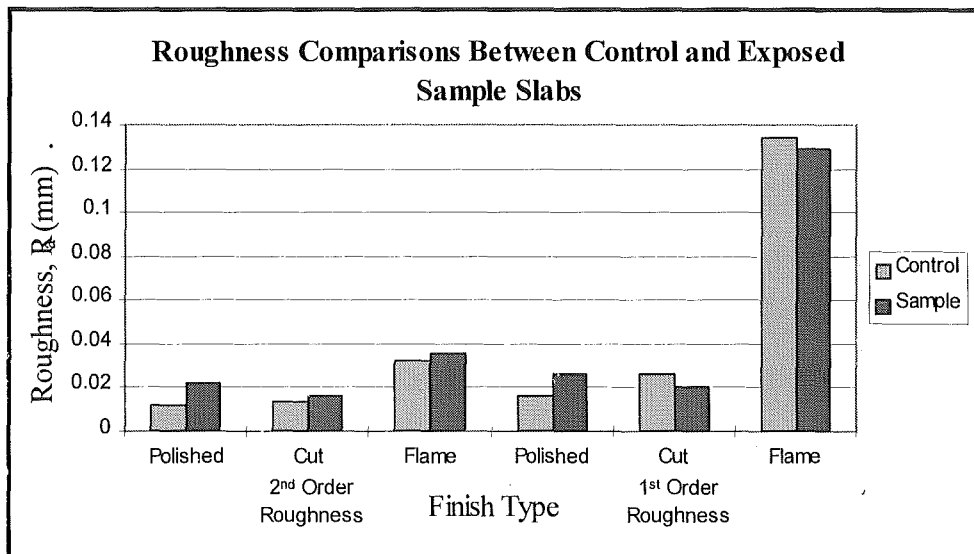


Figure 8.1. Control and exposed finish roughness variation.

Although the other finishes did not show a significant increase in roughness, this could be explained by the greater variation in the initial roughness values of the finish, a variation that could absorb any small increase in roughness as a result of exposure. Although there was a systematic, although not significant, increase in roughness in the 2<sup>nd</sup> order roughness readings, this was not repeated in the 1<sup>st</sup> order readings, where the cut and flame-dressed finishes showed a reduction in surface roughness. This is likely to be due to increased erosion of projecting peaks of the finish, which have a higher surface area/volume ratio than other areas of the stone, or due to the removal of friable particles generated by the cutting and finishing process. Either mechanism will result in a reduction in the 1<sup>st</sup> order general surface roughness of the finish.

The overall lack of variation between the roughness values of the control and exposed slabs was reflected in the lack of significant differences in the weights of the micro-catchment units slabs before and after exposure, and in SEM/EDX analysis of the London slabs. Elemental plots, mapping and visual examinations of the London sites slabs (selected because London had the highest levels of pollution for the three

sites, and was therefore the most likely to show any pollution-induced weathering effects) failed to find any evidence for mineral dissolution or leaching for a number of different depth readings.

In addition to microcatchment units, carousel tablets of three granite types (Mountsorrel granodiorite, Merrivale coarse biotite granite and Bolventor fine biotite granite) were placed at the sites. These were placed at each site in two suites; the upper suite (total deposition) and the lower suite (dry deposition). This was to assess the relative importance of variations in granitic rock composition, and the two deposition groups. Carousel tablet composition is shown in Table 4.2.

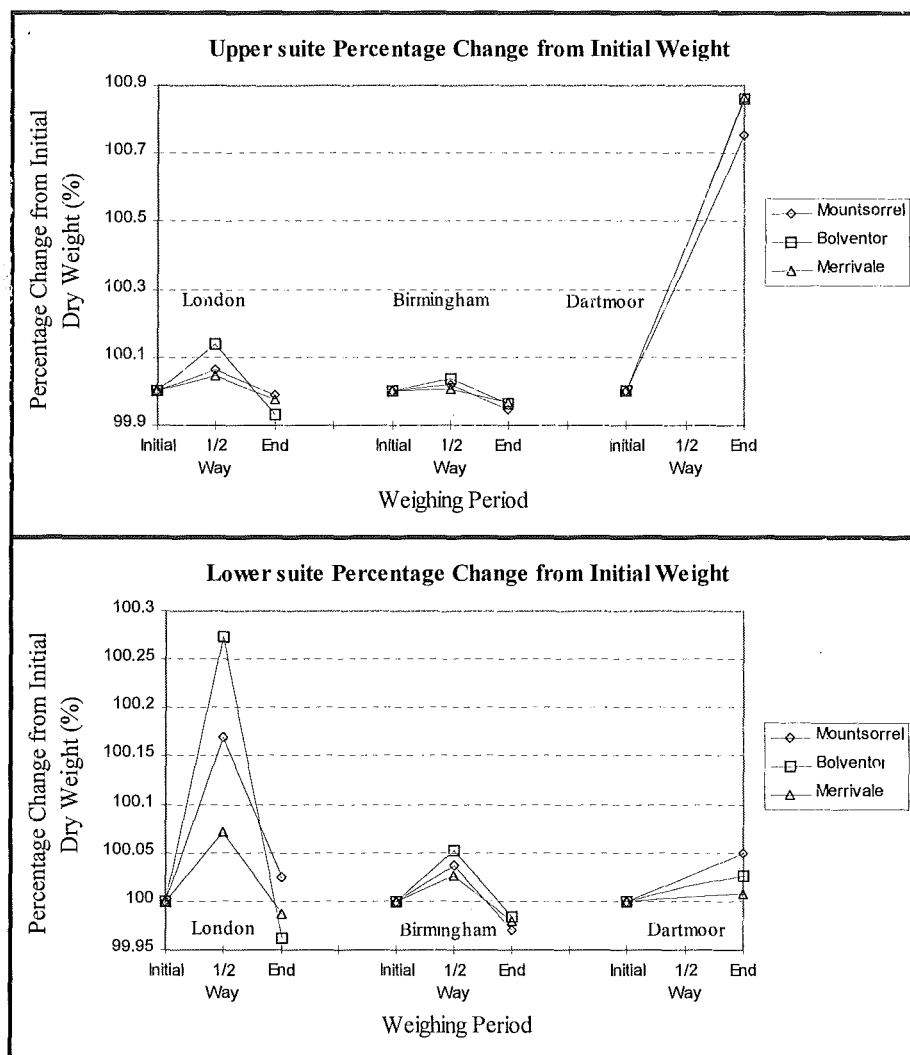


Figure 8.2. Carousel tablet weight changes, by site and suite.

Although there were significant variations between the weight change values (expressed as percentage change from initial dry weight) for the stone types located at the urban sites at the half-way weighing (45 weeks into the exposure period), only the Birmingham Mountsorrel granodiorite stones showed any significant differences from the other stone types at the end-point weighing, shown in Figure 8.2.

This suggests that stone type variation within the exposure programme had little effect on weight change values. Although the different stone types might initially display different weight change values as they moved to equilibrium, both coarse and fine grained granites showed no significant differences from each other at the end of the exposure period. The (relatively)  $\text{Ca}^{++}$ -rich Mountsorrel granodiorite showed the only variation, and was, contrary to expected results, significantly lighter than the other two stone types. This could be a function of weighing error introducing errors into the small and subtle weight changes of the stones over time.

When the role of dry and total deposition on weight change was examined, there was a clear trend across both suites at the urban sites for weight gain at the half-way point, shown in Figure 8.2. By the end of the exposure programme, however, the urban tablets had lost weight, across both suites. Although the upper suite tablets experienced less weight gain than the protected lower suite tablets, they followed the same weight change distribution. The rural site carousel tablets, however, followed a different distribution, with the only significant inter-site variation occurring between the Dartmoor and London end weight change values. Despite there being no mid-point weighing, the Dartmoor tablets showed significant weight gains by the end of the exposure period.

This suggests that the stones were moving to equilibrium with the environment throughout the exposure period, with the urban stones adjusting more rapidly than the rural stones, probably the result of increased pollution levels. It is suggested that they initially gained weight through a combination of increased surface reactions with friable fragments on the surface of the tablets, and insoluble particle deposition. Weight loss then occurred as fragments generated by the cutting of the tablets were removed.

This pattern of weight loss was different from limestone results recorded by Jaynes and Cooke (1987), who exposed tablets of Monks Park and Portland



limestone tablets at 25 sites around south east England. They found that both sheltered and exposed samples lost weight over time, and that weight loss was significantly higher in central London than in provincial centres, and both were higher than in rural areas. The weight loss patterns for tablets exposed at St. Marylebone, London, is shown in Figure 8.3.

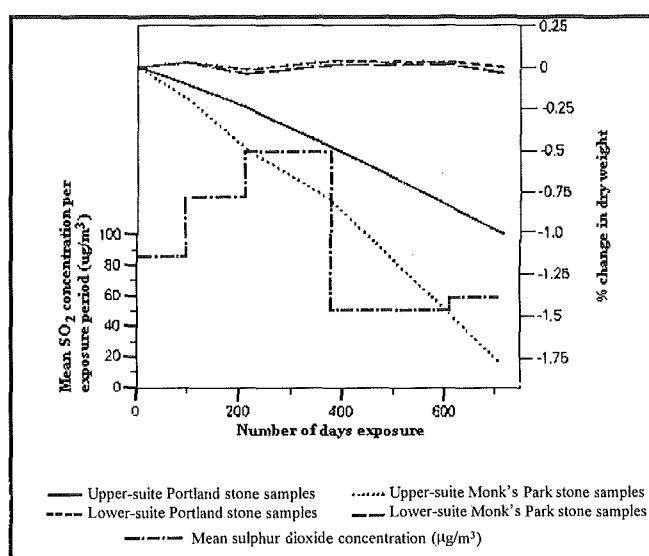


Figure 8.3. Limestone tablet weight changes at St. Marylebone.

The limestone tablet weight loss pattern differed from the granite tablets used during this exposure programme, in that not only were there significant differences in weight loss as a result of increased pollution concentration, but there were also significant differences between the sheltered and exposed tablets. Unlike the granite tablets, the limestone tablets exposed to total deposition showed a regular decrease in weight as the result of sulphation and dissolution by rainfall, and to a greater extent, while sheltered tablet weight fluctuated around zero weight loss. Jaynes and Cooke attributed the weathering of the lower-suite tablets primarily to sulphation of the limestone, with small amounts of salt action at coastal and central London sites.

The lack of results of the granite exposure programme in comparison to the limestone study is indicative of the differences in the resistance of the two rock types to weathering. Although the sheltered granite tablets did show weight gains at the 45-week measuring period, this had turned into weight loss by the end of the exposure period for five of the six tablets.

More importantly, the same pattern of weight gain, albeit to a lesser degree, was shown by the exposed, upper-suite tablets. This implies that the same processes were operating on both suites, and that therefore the role of acidic rainfall was much less significant for granite weight changes than for limestone - a function of the reduced solubility of granitic minerals, and the reduced porosity of the igneous stones.

Overall, the paucity of significant variations between the MCU run-off concentrations, slab roughness values and carousel weight change values suggest that the exposure period was not long enough for significant physical or chemical changes to occur in a resilient rock like granite, despite differences in surface finish and stone type. This was confirmed by elemental analysis of the MCU slabs, which showed no detectable changes in incremental depth composition analyses of selected minerals in exposed MCU slabs. Carousel weight change values, in particular, imply that the stone types, in both the upper and lower suites, were only just reaching equilibrium with the ambient atmospheric environment, with weight changes recorded during the exposure period symptomatic of a period of adjustment (with no clear pattern evident).

The lack of significant interactions between the run-off from the microcatchment units, and the absence of weathering alterations to the granite samples in comparison to other, less resistant rock types such as limestone (Reddy, 1988) and sandstone (Halsey *et al*, 1995) corresponds to results found by other workers, especially Sweevers *et al* (1995), who examined Leinster granite microcatchment units over a three year period. They found that material loss and ion concentrations from the granite were so small that they could only conclude that the weathering levels experienced by fresh Leinster granite after 2-3 years of exposure was negligible. This corresponds to additional work by Sweevers and Van Grieken (1992) on granite in microcatchment units who found that although there was an initial fluctuation on exposure, fresh Leinster granite then showed no appreciable leaching over the two year exposure period.

### **8.3. STONE DETERIORATION INDEX RESULTS**

The Stone Deterioration Index was created to allow a generic evaluation of

the near-surface rock quality of building stones. Building on the principles of numerous engineering rock mass rating schemes (Barton, 1974; Bieniawski, 1974; Price, 193; Anon., 1995), the SDI evaluated a number of different rock parameters to provide an estimation of near-surface rock quality. However, unlike the majority of engineering rock mass rating schemes, which are plagued by a lack of resolution on the material scale (Hencher and Martin, 1986), the SDI is designed for simple, yet comprehensive, assessment and application on the material scale, reflecting the relatively uniform nature of individual building stones. This allowed the scheme to produce an easy to apply, non-destructive, *in situ* and quantifiable measure of building stone condition, without the use of decay-feature distribution, mineralogical alteration or high-tech analytical instruments (Montoto et al, 1996).

It is the SDI scheme's focus on non-destructive, *in situ* and material grade index test evaluations for the determination of building stone quality, that distinguishes it from the previous evaluation methods. It also means it is inappropriate for direct comparisons with other existing granite rock mass rating schemes (Cragg and Ingman, 1995). Not only is there a problem with a comparison between different scales of measurement, but mass rating schemes usually require the measurement of parameters such as compressive strength (i.e. Irfan and Dearman, 1978) and slakeability (i.e. Lee and de Freitas, 1989). These procedures require the removal of samples for destructive lab-based analysis - an option unsuitable for historic building evaluation.

For this reason the SDI scheme differed from other methods of building stone evaluation, such as geochemical (Vargas *et al*, 1996) and petrographic (García-Talegón *et al*, 1996) analysis, which also required the undesirable removal of samples from the subject building, reducing their applicability to a wide range of monuments.

The scheme also differs from feature-led determinations of building decay levels (Robinson and Williams, 1996), as it combined the visual assessment of selected parameters with index testing of the sample stones. This allowed the formation of a quantifiable method for evaluating rock quality that is not significantly affected by variations in the subjective and qualitative assessment of

rock condition from worker to worker, an important aspect of rating scheme application (Bieniawski, 1989).

Using the Stone Deterioration Index, the building stone condition of ten churches and one monument from the Dartmoor region were assessed. The selected buildings were taken from a wide age range (1418 - 1895AD) and were constructed out of Type B granite - a coarse-grained megacrystic biotite granite (Floyd *et al*, 1993). Correlation analysis between building age and the raw values from individual index parameters included in the SDI scheme, and building age and the SDI block totals showed that the SDI scheme was the most accurate method for the measurement of rock quality over time. The correlation values are shown in Table 8.3.

Parameter	Correlation Value
Surface Strength	0.69
Surface Roughness	-0.49
Surface Coatings	-0.30
Discolouration	-0.15
SDI Block Rating	0.74

Table 8.3. Correlation values between building age and individual index parameters and SDI block totals.

When individual church course (height above ground) values were examined, the SDI scheme revealed that there appeared to be no consistent aspect-wide influence on rock quality with increasing height. This was supported by the collective analysis of the course values, which showed that although there was a reasonable relationship between increasing course height and decreasing rock quality for the north aspect values ( $r^2=0.52$ ) and the south facing walls ( $r^2=0.51$ ), there was no relationship for the west facing walls ( $r^2=0.04$ ).

Although process-led investigations of the stone were not conducted, it seems likely that the reduction in rock quality as shown by the north-facing walls is linked to the extremely high degree of biological coverage recorded on the north aspect building stones. The south facing wall SDI reduction with increasing course height could be the result of variations in wind speed (protection from ground roughness

and the boundary layer effect) and ground water ingress. The lack of a consistent relationship between course height and rock quality for the west facing walls suggests that it was natural variation in the rock resistance that determined the weathering levels, rather than a systematic process that affected the building stones, i.e. increasing exposure with increasing course height.

When the influence of aspect on rock quality was examined, it was found that it exerted a major influence on external SDI value distribution, with mean SDI values for the church aspects shown below in Table 8.4. The level of weathering experienced by the building stones in each wall was also indicated by the level of variation. Of the external walls, the north facing walls had the highest level of variability and lowest mean value. This implies that the variation in external rock quality was greatest in the north aspect - once again this was logically explained by the high levels of biological growth. This supports the theory that the largest impact on rating values for the external building stones was aspect.

Wall Aspect	Mean	Standard Error
South	59.94	1
West	56.38	1
North	52.81	1.2
Interior	83.92	1.1
Average external	56.81	0.6

Table 8.4. Exterior and interior wall averages and standard error of the mean across all churches.

Examination of the interior rock quality variation was also possible with the SDI scheme, a function of the index test assessment, rather than feature-led evaluations. This revealed that although, as expected, there was no relationship with course height, there was a level of variation in the SDI values on par with external south and west facing building stones, shown in Table 8.4. This was surprising, given that there is an almost total absence of weathering processes that can affect interior stones after construction. Therefore, the conclusion was that the variability shown by the south, west and internal aspects, equivalent to a standard error of the

mean of 1 - 1.1 SDI points, was introduced by natural quality variation in the granitic building stones, rather than through weathering processes.

Another function of the SDI scheme was that it allowed the assessment of the deterioration rates of granitic building stones over time. This was achieved by measuring a variety of buildings using the same construction material (granite) from a wide age range. Comparisons between the external aspects then allowed an estimation of the effect of aspect on the rates of deterioration experienced by the granitic building stones over time.

The determination of the pattern of temporal deterioration is, however, complex, with many processes operating as episodic or sporadic events that rapidly increase decay for a limited time, i.e. spalling (Livingston and Baer, 1988). This produces a weathering pattern that is characterised by periods of relative quiescence interspersed with episodes of rapid change (Smith *et al*, 1992), rather than one that is linear and uniform throughout time.

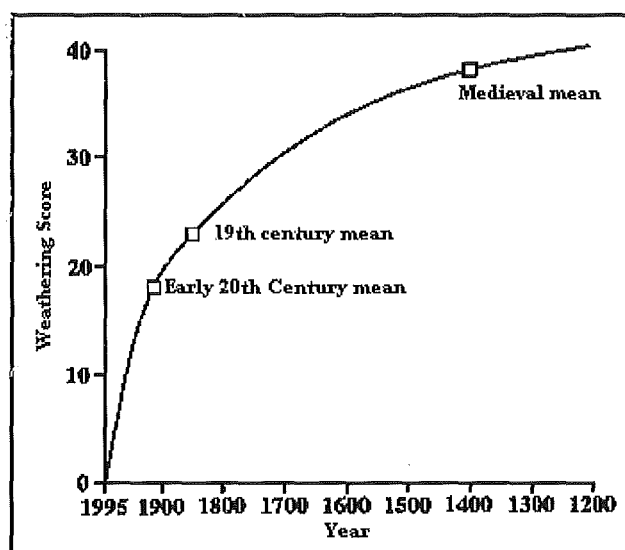


Figure 8.4. Mean weathering scores for churches of different ages (Robinson and Williams, 1996)

Robinson and Williams (1996) evaluated the rock quality of 42 sandstone buildings located in the central Weald that were constructed during a number of different age ranges, from medieval churches to twentieth century houses. Using

visual assessment to evaluate the level of weathering shown by individual stone by 'assessing the percentage area of surface that visibly displays surface weathering phenomena', Robinson and Williams constructed a deterioration pattern over time, shown in Figure 8.4.

This shows a period of rapid change as the fresh building stone undergoes weathering as it reaches equilibrium with the environmental conditions, followed by a reduction in the weathering rate possibly as a result of the formation of protective crusts over the sandstone surfaces (Robinson and Williams, 1996). There are, however, a number of problems with directly applying the interpretation of sandstone weathering patterns to granite building stones.

The first is that the mean weathering values are plotted through zero. This implies that building stones have experienced no weathering or alteration at all prior to incorporation in the building fabric, a situation that is unlikely to occur.

The second is that granite building stones do not build up protective crusts that inhibits weathering, one of the theories postulated by Robinson and Williams for the reduction in the sandstone weathering rate. Although pollution crusts can build up on granites in urban areas, these can be directly responsible for increased scaling (Smith and Magee, 1990) and an increase in the break-up of the granite surface (Schiavon *et al*, 1995; Schiavon, 1996).

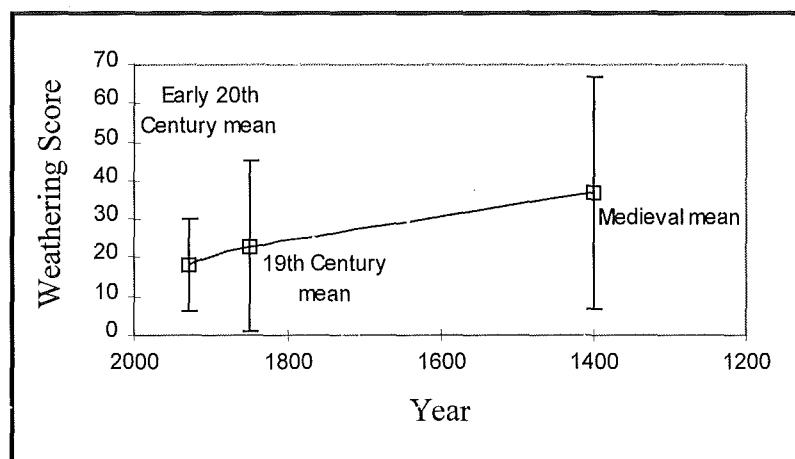


Figure 8.5. Mean sandstone building weathering scores, plus two standard deviations.

The third area of concern is the size of the standard deviation of the sample populations, shown in Figure 8.5. When the line is not forced through zero, and error bars corresponding to two standard deviations are plotted, it can be seen that the theorised rate of deterioration is much less, and that the spread of the data could be captured by a linear fit.

Although there are the problems discussed previously that are associated with a linear fit, it could provide the best deterioration estimate for the episodic/step-wise decay that characterises the middle of a stones deterioration pattern over time. There are also other limitations with the linear fit, particularly for recently constructed buildings, where decay is likely to be greater as a result of the stones moving to environmental equilibrium, or building stones at the end of their functional life, where decay is accelerated by the rapid disintegration of the stone (Smith *et al*, 1994). Therefore an estimate of the deterioration pattern for granitic building stones is shown below in Figure 8.6.

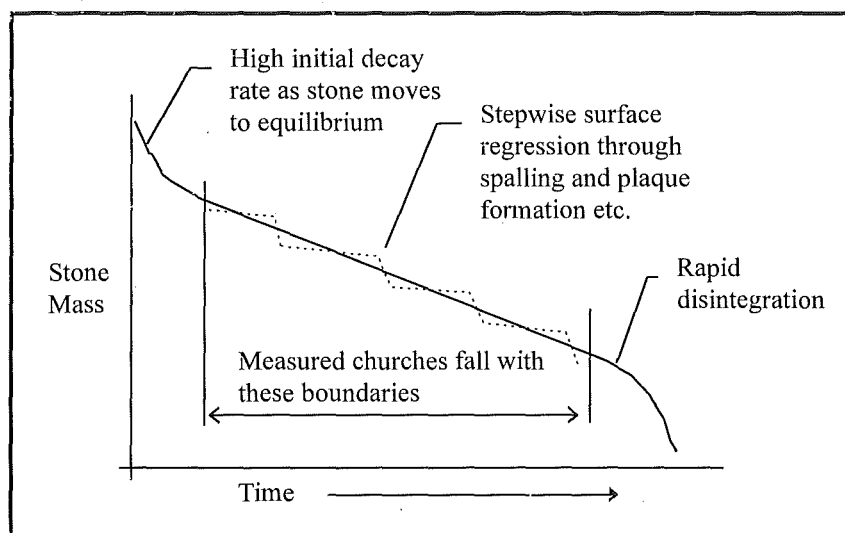


Figure 8.6. Possible weathering pattern over time.

Although it is felt that a linear expression of the deterioration rate for the external aspects of the measured Dartmoor churches is the most effective method of describing the deterioration, it is limited. Therefore an exponential fit for each aspect was also included.



The analysis of the collected aspect values for each church allowed not only the relative ranking of the aspects in terms of deterioration, but also a determination of the decay rate. This is illustrated by Table 8.5, which shows the exponential and linear deterioration rates for the individual external aspects, as well as values for the average external aspect. This is derived from a combination of each of the external aspect block values, and reflects the average level of decay experienced by the Dartmoor churches as a group.

Linear Deterioration Rate		Exponential Deterioration Rate				
Aspect	Deterioration Rate per 100 Years	Age	south	west	North	Average External
South	4.09	1800	5.49	5.56	5.75	6.14
West	4.87	1700	5.12	5.13	5.26	5.67
North	5.05	1600	4.77	4.74	4.80	5.23
Average External	4.59	1500	4.45	4.38	4.39	4.83
		1400	4.15	4.04	4.01	4.46

Table 8.5. Linear and exponential SDI deterioration rates.

Using the linear deterioration rates for comparison, the relative ranking of the external aspects was: South < West < North, with the west facing walls experiencing a reduction in near-surface rock quality that was 6% higher than the south facing walls, while the north facing walls had a deterioration rate that was 14% higher than the south. These figures emphasise the importance that near-surface micro-environments, and therefore aspect, play in the determination of building stone deterioration rates. Thermal weathering, moisture content and biological growth are all influenced by the position of the stone (Caneva *et al*, 1992), and can have significant impacts on rock quality.

Aspect	Correlation Value
South	0.61
West	0.7
North	0.57
External Average	0.74

Table 8.6. Age/aspect correlation values.

This is illustrated by the north facing walls, which had a high level of biological colonisation, and the highest rate of weathering and rock quality variation. The north facing walls also showed the lowest level of relationship between SDI values and building age in correlation analyses, shown in Table 8.6, while the external average had the highest level of relationship. This produced a clear inverse relationship between building age and rock quality, with the age of exposure accounting for around 74% of the variation in the SDI values.

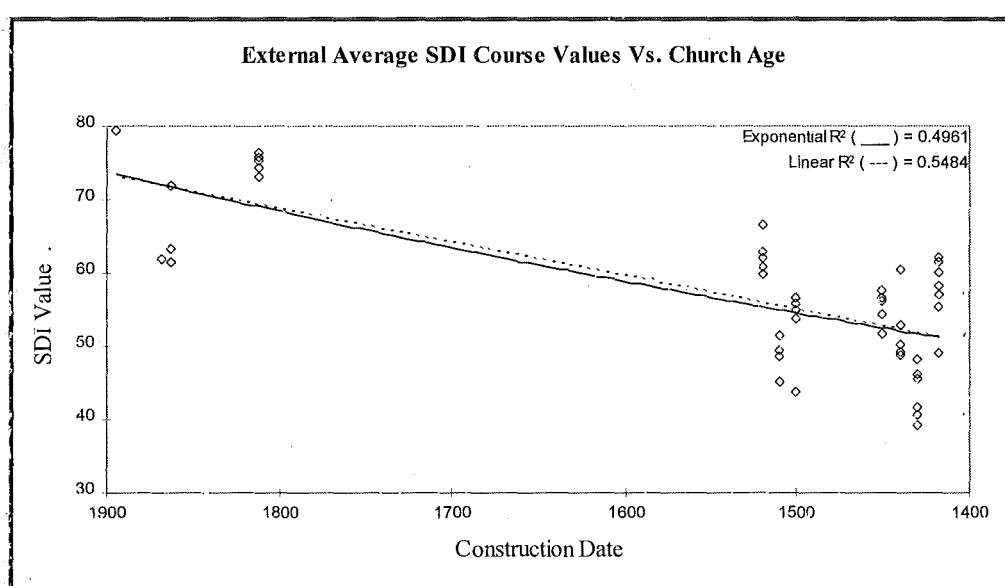


Figure 8.7. Average external SDI deterioration rates.

When the average external aspect values were examined, it was possible to create an average deterioration rate for the granite Type B building stones in the Dartmoor region, using values derived from each aspect and each church. This ensured that the decay estimate reflected the all of the conditions that acted on the building stone. The linear analysis of deterioration, shown in Table 8.5 and Figure 8.7, suggests that the average deterioration rate for the external stones of buildings over 100 years old in the Dartmoor region, an area with lower pH and a lighter pollution load than selected urban centres, was a reduction of 4.59 SDI points per hundred years of exposure ( $r^2=0.55$ ).

#### 8.4. CONCLUSIONS

The research programme explored two avenues of granite weathering. The first, a microcatchment study of the influence of surface roughness and pollution on granite weathering rates, found that site (and therefore ambient pollution concentration) was the most important parameter in determining run-off concentration, while the influence of surface roughness was insignificant over this time period.

The microcatchment unit exposure programme revealed the limitations of working with a resistant rock such as granite. There were no significant interactions between run-off concentrations derived from finishes with surface finishes, and no significant weight changes to the MCU slabs during the exposure period, or to the exposed carousel tablets. The paucity of results, and the lack of physical alteration of the granite slabs as a result of exposure, corresponds to the findings of other workers who have used microcatchment units to examine granite decay.

One area of interest, however, occurred when exposed and sheltered granite carousel samples underwent weight gains, before returning to around their original values by the end of the exposure period. It is suggested that the exposure period covered a period of adjustment as the granite samples moved to equilibrium with the ambient environmental conditions, and that a longer period of measurement would be more productive and informative as the gradual changes engendered by differences in finish and stone type would emerge.

The second area of study was the formulation of a novel, non-destructive, *in situ*, index test-based rating scheme for the evaluation of historic granitic buildings. Using the Stone Deterioration Index, ten churches and one monument from the Dartmoor region were analysed, and it was found that aspect was the most important parameter in determining the level of decay experienced by the building stones, with west facing stones deteriorating 6% faster than south facing walls, and north aspect building stones experiencing a deterioration rate that was 14% faster than the south. The high deterioration rate for the north facing walls was a product of intensive biological colonisation, which resulted in the highest level of rock quality variation and the lowest mean SDI values of the external walls

Measurements of building stones from different heights (upto 1.8 m from the ground) showed no overall relationship between rock quality and course height. Although the north and south walls showed a decrease in near-surface rock quality with increasing height, the west facing walls showed only random variation with increasing measurement height above ground.

By studying churches that had been constructed over a wide age range, it was found that there was a clear correlation between rock quality and building age (correlation = 0.74). However, there seemed to be a period of rapid adjustment of fresh building stones incorporated into the building fabric, producing a rapid level of weathering for the first 100 years of the buildings existence.

This process appears to be similar to the period of adjustment experienced by the exposure samples, although over an extended time period. It is suggested that this could be due to the removal of friable material, the establishment of lithobionts and the initiation and expansion of microfracture networks.

## **8.5. AREAS FOR FUTURE RESEARCH**

### **8.5.1. Granite Exposure Studies**

The lack of significant pollution-induced change as a result of the exposure study shows the limitations of working with resilient rock over a short time span. Granite, although it can weather significantly over the life-span of a building, did not provide enough of a response for the characterisation of physical alteration as result of pollution exposure. Indeed, results from the carousel tablets suggest that the small carousel tablets were only just reaching equilibrium with the atmospheric environment by the end of the programme, when they would start to generate results that truly reflected changes in the pollution regime around them. This period of adjustment experienced by fresh granite might be reduced or even removed by the incorporation of pre-exposed granite e.g. granite facing removed from buildings.

Part of the lack of variation may also be due to insufficient variation in the degree of surface roughness used on the exposure slabs. Although the finishes used on the MCU slabs reflected commercial stone finishes, only one of the measured components, at one of the sites, showed significant differences between the finishes.

This problem might be addressed by the use of more exaggerated roughness profiles to generate run-off, although this would reduce the applicability of the data to current building materials.

Although care was taken to place the run-off sample containers in wooden boxes out of direct sunlight, they were stored at ambient temperatures, and then transported through standard parcel/mail channels. A further development of this exposure programme would be the installation of refrigerated containers at each site, and insulated cool boxes for transport. This would ensure that the samples would be kept in the dark, and at below 4°C throughout the collection and transport period, and would result in a lower degree of chemical change in the measured run-off components.

Ultimately, however, it is the length of exposure time that is likely to be the determining factor. As granite is a resistant rock, and generally slow to weather, a longer period of data collection would be needed to gain an accurate insight into the stones performance changes. Also, a longer period of exposure, e.g. five to ten years, would allow the granite samples to move to equilibrium with the ambient environment, allowing differences in the composition and degree of surface roughness to gradually emerge. These could influence run-off characteristics to the extent that systematic differences can be recognised between them. Alternatively, artificial weathering chambers could be used, with accelerated weathering cycles, to characterise the performance of the stones and the finishes over time (Haneef *et al*, 1993), as well as the interactions of the granites with other stones types (Haneef *et al*, 1989).

### **8.5.2. Stone Deterioration Index Development**

This study of the buildings and monuments in the Dartmoor area has allowed the formation of decay rates for building over 100 years old. This age of building was chosen at the start of the project to ensure that measurable granite deterioration had occurred. However, on investigation, marked fabric deterioration of the buildings was noted, and this allowed the scope of the study to be expanded. One of the areas highlighted by the study for further investigation is the performance of new building stone, where there appears to be a period of rapid deterioration within the

first 100 years of construction as the stone moves towards equilibrium with its new environment.

Another aspect of the SDI study that could be addressed by future research is the comparison of buildings in different pollution environments, such as Dartmoor granite buildings in urban environments. Although there are problems associated with this extension of the work, i.e. buildings that are older than the onset of marked urban pollution (around 170 - 200 years ago), and aspects of an urban setting, such as vibration etc., that could stress the stone, it would allow a quantifiable estimation of the increase urban pollution has on stone decay. This is, however, dependant on the identification and measurement of a sufficient number of buildings of the same stone type, located in a similar environment to each other, that can be referenced against the Dartmoor results (a clean, rural benchmark).

The measurement of types of granite other than Type B, which would be necessary for this extension, should be possible through the SDI scheme. Although it was initially thought that the rating of granitic buildings would be limited to a particular granite species (Type B granites (Floyd *et al.*, 1993)), with specific grain-size characteristics (and therefore surface strength and roughness), a wider application of the SDI scheme may now be possible, as illustrated by Moretonhampstead church.

Moretonhampstead contained two different rock types in the tower fabric, 1) Dartmoor granite Type B; the common porphyritic biotite granite represented at each of the measured sites, and 2) Granite Type C (Floyd *et al.*, 1993), a fine-grained granite. Despite differences in the mineralogy and crystal size, the ratio of Type C external strength to internal strength values (external Type C values equal 85.46% of internal values) was very similar to that of the common Type B granite (85.84%).

This ratio parity implies that although individual rating values may vary considerably between Type B and Type C granites of the same exposure age, they reflect the same level of weathering as each other, relative to values generated by internal stones. Although there might be problems in assessing strength values and its contribution (requiring a re-grading of the strength classes) to the total SDI block score, this would allow the extension of the SDI scheme to other granitic types and buildings around the UK, providing enough comparative measurements are made.

Another facet of the SDI scheme is its modularity. As instrumental advances are made, i.e. the portable X-ray fluorescent spectrometer, for on-site chemical analysis of building stones (Stillman, 1996), these can be incorporated into the scheme, replacing the original method of measurement. Another example would be the inclusion of laser scan plots for the roughness parameter, made possible through the development of a portable and hand-held CyberScan device for roughness assessment. The development of the SDI scheme through higher instrumental power will increase the accuracy of the overall assessment.

Finally, although it was not conducted in this research programme, the SDI values for an entire wall can be plotted graphically, to show the pattern of decay that affects any given wall in an individual building. This would allow the identification of high areas of deterioration, and let restorers or conservation officers pin-point the application of water repellents (Esbet, Alonsom Diaz-Pache, Ordaz and Pérez-Ortiz, 1996), remedial techniques and consolidation measures (Delgado Rodrigues and Costa, 1996a) accordingly. This will allow the protection of the granite in aggressive environments, prolonging its useful life. However, such consolidants, although increasing the material strength of decayed materials, can introduce harmful effects to the stone, i.e. reducing water vapour permeability, and therefore should only be applied to areas that fully require the remedial techniques (Delgado Rodrigues and Costa, 1996b).

## REFERENCES

- AEA/DOE. (1995). *Air Pollution in the UK: 1993/94. Document reference number AEA/CSR1033/C*. AEA Technology: Oxford.
- Amoroso, G. G. & Fassina, V. (1983). *Stone Decay and Conservation: Pollution, Cleaning, Consolidation and Protection*. Elsevier: New York.
- Anon. (1977). The Description of Rock Masses for Engineering purposes, A Report by the Geological Society Engineering Group Working Party. *Quarterly Journal of Engineering Geology*, 10, 355-388.
- Anon. (1995). The Description and Classification of Weathered Rocks for Engineering Purposes. The Geological Society Engineering Group Working Party Report. *Quarterly Journal of Engineering Geology*, 28, 207-242.
- Arino, X. & Saiz-Jimenez, C. (1994). Granite Weathering by the Lichen *Rhizocarpon Geographicum*. In *Granite Weathering and Conservation. Proceedings of a Conference held at Trinity College, Dublin, September, 1993*, ed. E. Bell & T. P. Cooper, pp. 33-36. Trinity College, Dublin: Dir. of Buildings Office.
- Ascaso, C. & Ollacarizqueta, M. A. (1991). Structural Relations between Lichen and Carved Stonework of Silos Monastery, Burgos, Spain. *International Biodeterioration*, 27, 1-13.
- Ascaso, C., Sancho, L. G. & Rodriguez-Pascual, C. (1990). The Weathering Action of *Saxicolous* Lichens in Maritime Antarctica. *Polar Biology*, 11, 33-39.
- Ascaso, C., Vizcayno, C. & Garcia Gonzalez, M. T. (1993). Biodeterioration Produced by *Leconora Albescens* (Hoffm.) Ranth and Rostr. on the Abaci of the Silos Monastery. In *Actas Del Workshop Alteration De Granitos Y Rocas Afines Empleados Como Materiales De Construcccion. Consejo Superior De Investigacions Cientificas*, ed. E. M. Hernandez, E. M. Ballesteros & V. R. Arnav, pp. 181-185. Madrid: CSIC.
- Atkins, D. H. F. & Lee, D. S. (1995). Spatial and Temporal Variation of Rural Nitrogen Dioxide Concentrations Across the United Kingdom. *Atmospheric Environment*, 29 No. 2, 223-239.
- B.E.R.G. (1989). *The Effects of Acid Deposition on Buildings and Building Materials*. Building Effects Review Group. HMSO: London.



- Bächmann, K., Haag, I. & Roder, A. (1993). A Field Study to Determine the Chemical Content of Individual Raindrops as a Function of their Size. *Atmospheric Environment*, 27A No. 13, 1951-1958.
- Bächmann, K., Haag, I. & Steigerwald, K. (1995). Determination of Transition Metals in Size-Classified Rain Samples by Atomic Absorption Spectrometry. *Atmospheric Environment*, 29 No. 2, 175-177.
- Bächmann, K., Roder, A. & Haag, I. (1992). Determination of Anions and Cations in Individual Raindrops. *Atmospheric Environment*, 26A, No. 9, 1795-1797.
- Barker, D. S. (1983). *Igneous Rocks*. Prentice-Hall: New Jersey.
- Barton, N., Lien, R. & Lunde, J. (1974). Engineering Classification of Rock Masses for the Design of Tunnel Supports. *Rock Mechanics*, 6, 189-236.
- Baumgärtner, M., Rende, A., Bock, E. & Conrad, R. (1990). Release of Nitric Acid from Building Stones into the Atmosphere. *Atmospheric Environment*, 24B(1), 87-92.
- Bawden, R. J. & Ferguson, J. M. (1978). Trends in Materials Degradation Rates in the UK. *Proceedings of Corrosion Science and Technology. UK Corrosion, 1987. Brighton, 26-28 October*, 383-396.
- Baynes, F. J. & Dearman, W. R. (1978). The Relationship Between the Microfabric and the Engineering Properties of Weathered Granite. *Bulletin of the International Association of Engineering Geology*, 18, 191-197.
- Bell, E., Dowding, P. & Cooper, T. P. (1994). The Biodeterioration of Granite. In *Granite Weathering and Conservation. Proceedings of a Conference held at Trinity College, Dublin*, ed. E. Bell & T. P. Cooper, pp. 28-32. Dublin: The director of Building's Office, Trinity College.
- Bieniawski, Z. T. (1974). Geomechanics Classification of Rock Masses and its Application in Tunnelling. *Proceedings of the Third International Conference on Rock Mechanics*, 11a, 27-32.
- Bieniawski, Z. T. (1976). Rock Mass Classification in Rock Engineering. *Proceedings of the Symposium on Exploration for Rock Engineering, Johannesburg*, 1, 97-106.
- Bieniawski, Z. T. (1989). *Engineering Rock Mass Classifications*. Wiley and Sons: New York.

- Blyth, F. G. H. & De Freitas, M. H. (1974). *A Geology for Engineers*. (6<sup>th</sup> Ed.). Edward Arnold: London.
- Brady, N. C. (1990). *The Nature and Properties of Soils* (10<sup>th</sup> Ed.). Macmillan: New York.
- Brimblecombe, P. (1977). London Air Pollution, 1500 - 1900. *Atmospheric Environment*, 11, 1157-1162.
- Brimblecombe, P. (1986). *Air, Composition and Chemistry*. Cambridge University Press: Cambridge.
- Broch, E. & Franklin, J. A. (1972). The Point-Load Strength Test. *International Journal of Rock Mechanics and Mining Sciences*, 9, 669-697.
- Butlin, R. N. (1991). Effects of Air Pollutants on Buildings and Materials. *Proceedings of the Royal Society of Edinburgh*, 97B, 255-272.
- Camuffo, D. (1992). Acid Rain and the Deterioration of Monuments: How Old is the Phenomenon?. *Atmospheric Environment*, 26B(2), 241-247.
- Camuffo, D. (1993). Reconstructing the Climate and the Air Pollution of Rome During the Life of the Trajan Column. *Science of the Total Environment*, 128, 205-226.
- Camuffo, D. (1995). Physical Weathering of Stones. *Science of the Total Environment*, 167, 1-14.
- Camuffo, D., Bernardi, A. & Enzi, S. (1993). *Conservation of Historic Buildings, Monuments and Associated Cultural Property*. Consiglio Nazionale delle Ricerche, Istituto di Chimica e Tecnologia dei Radio-elementi.
- Camuffo, D., Bernardi, A., Enzi, S. & Vincenzi, S. (1994). Effects of Air Pollution on Historic Buildings and Monuments. Scientific Basis for Conservation: Case Studies in the Deterioration of Stone Monuments in Italy. *European Cultural Heritage Newsletter on Research*, 8, No1, 7-15.
- Caneva, G., Gori, E. & Danin, A. (1992). Incident Rainfall in Rome and its Relation to Biodeterioration of Buildings. *Atmospheric Environment*, 26B(2), 255-259.
- Casal Porto, M., Silva Hermo, B. & Delgado Rodrigues, J. (1989). Agents and Forms of Weathering in Granitic Rocks used in Monuments. In *Science, Technology and European Cultural Heritage*. *Proceedings of the European Symposium*,

- 13 - 16 June, 1989, ed. N. S. Baer, C. Sabbioni & A. I. Sors, pp. 439-442. Bologna, Italy: Butterworth - Heinmann.
- Cheng, R. J. (1983). Emissions from Electric Power Plants and their Impact on the Environment. ?? 591-598.
- Conlan, D. E. & Longhurst, J. W. S. (1993). Spatial Variability in Urban Acid Deposition, 1990: Results from the Greater Manchester Acid Deposition Survey (GMADS) Network in the UK. *Science of the Total Environment*, 128, 101-120.
- Cooke, R. U. & Smalley, I. J. (1968). Salt Weathering in Deserts. *Nature*, 220, 1226-1227.
- Cooper, T. (1993). The Effects of Air pollution on Historic Buildings and Monuments. *A Synthesis of the Research Work Carried out in the 3rd. and 4th. Environmental Research and Development Programmes and Current S.T.E.P. Programme 'Conservation of Historic Buildings, Monuments and Associated Cultural Property*. Trinity College: Dublin.
- Cooper, T. P. (1986). Saving Buildings from the Weather. *Technology Ireland*, , 32-35.
- Cooper, T. P., Dowding, P., Lewis, J. O., Mulvin, L., O'Brien, P., Olley, J. & O'Daly, G. (1989). Contribution of Calcium from Limestone and Mortar to the Decay of Granite Walling. In *Science, Technology and European Cultural Heritage. Proceedings of the European Symposium, 13 - 16 June, 1989*, ed. N. S. Baer, C. Sabbioni & A. I. Sors, pp. 456-461. Bologna, Italy: Butterworth - Heinmann.
- Cooper, T. P., Duffy, A., O'Brien, P., Bell, E. & Lyons, F. (1993). Conservation of Historic Buildings at Trinity College, Dublin. In *Actas Del Workshop Alteration De Granitos Y Rocas Afines Empleados Como Materiales De Construcccion. Consejo Superior De Investigacions Cientificas*, ed. E. M. Hernandez, E. M. Ballesteros & V. R. Arnav, pp. 59-67. Madrid: CSIC.
- Cragg, D. J. & Ingman, J. (1995). Rock Weathering Descriptions: Current Difficulties. *Quarterly Journal of Engineering Geology*, 28, 277-286.

- De La Torre, M. A., Gomez-Alarcon, G., Melgarejo, P. & Saiz-Jimenez, C. (1991). Fungi in Weathered Stone from Salamanca Cathedral, Spain. *Science of the Total Environment*, 107, 159-168.
- Dearman, W. R. & Irfan, T. Y. (1978). Assessment of the Degree of Weathering in Granite Using Petrographic and Physical Index Tests. *International Symposium on Deterioration and Protection of Stone Monuments, Paper 2.3*. UNESCO: Paris.
- Dearman, W. R., Baynes, F. J. & Irfan, T. Y. (1978). Engineering Grading of Weathered Granite. *Engineering Geology*, 12, 345-374.
- Deer, W. A., Howie, R. A. & Zussman, J. (1992). *An Introduction to Rock Forming Minerals (2nd ed.)*. Longman: Harlow.
- Deere, D. U. (1964). Technical Description of Rock Cores for Engineering Purposes. *Rock Mechanics and Engineering Geology*, 1, 16-22.
- Del Monte, M. & Sabbioni, C. (1986). Chemical and Biological Weathering of an Historical Building: Reggio Emilia Cathedral. *Science of the Total Environment*, 50, 165-182.
- Del Monte, M., Sabbioni, C. & Vittori, O. (1984). Urban Stone Sulphation and Oil - Fired Carbonaceous Particles. *Science of the Total Environment*, 36, 369-376.
- Del Monte, M., Sabbioni, C., Ventura, A. & Zappia, G. (1984). Crystal Growth from Carbonaceous Particles. *Science of the Total Environment*, 36, 247-254.
- Delgado Rodrigues, J. (1996). Summary Report Project STEP CT90-0110, Conservation of Granitic Rocks with Application to the Megalithic Monuments. In *Degradation and Conservation of Granitic Rocks in Monuments. Proceedings of the EC Workshop Held in Santiago de Compostela (Spain) on 28-30 November 1994. Protection and Conservation of the European Cultural Heritage. Report No 5*, ed. M. A. Vincente, J. Delgado-Rodrigues & J. Acevedo, pp. 161-242. Brussels: European Commission.
- Delgado-Rodrigues, J. & Costa, D. (1996a). Assessment of the Efficacy of Consolidants in Granites. In *Degradation and Conservation of Granitic Rocks in Monuments. Proceedings of the EC Workshop Held in Santiago de Compostela (Spain) on 28-30 November 1994. Protection and Conservation*

- of the European Cultural Heritage. Report No 5*, ed. M. A. Vincente, J. Delgado-Rodrigues & J. Acevedo, pp. 343-348. Brussels: European Commission.
- Delgado-Rodrigues, J. & Costa, D. (1996b). Assessment of the Harmfulness of Consolidants in Granites. In *Degradation and Conservation of Granitic Rocks in Monuments. Proceedings of the EC Workshop Held in Santiago de Compostela (Spain) on 28-30 November 1994. Protection and Conservation of the European Cultural Heritage. Report No 5*, ed. M. A. Vincente, J. Delgado-Rodrigues & J. Acevedo, pp. 349-354. Brussels: European Commission.
- Delgado Rodrigues J. & Gil Saraiva, J. A. (1985). Experimental and Theoretical Approach to the Study of the Mechanism of Wind Erosion of Stone in Monuments. In *Proc. 5th Int. Congress on the Deterioration and Conservation of Stone. Vol 1*. Pp. 167-175. Presses Polytechniques Romandes: Lusanne.
- Dibb, T. E., Hughes, D. W. & Poole, A. B. (1983). Controls of Size and Shape of Natural Armourstone. *Quarterly Journal of Engineering Geology*, 16, 31-42.
- DOE. (1991). *Digest of Environmental Protection and Water Statistics, No. 14*. HMSO: London.
- DOE. (1995a). *Digest of Environmental Statistics, No. 17*. HMSO: London.
- DOE. (1995b). *Expert Panel on Air Quality Standards - Sulphur Dioxide*. HMSO: London.
- DOE. (1996). *Digest of Environmental Statistics, No. 18*. HMSO: London.
- Dolske, D. A. (1995). Deposition of Atmospheric Pollutants to Monuments, Statues and Buildings. *Science of the Total Environment*, 167, 15-31.
- Duffy, A. P. & Perry, S. H. (1994). The Effects of Mortars on Granite Decay. In *Granite Weathering and Conservation. Proceedings of a conference held at Trinity College, Dublin. September 1993*, ed. E. Bell & T. P. Cooper, pp. 1-10. Dublin: Director of Buildings, Trinity College.
- Emerick, K. (1995). The Survey and Recording of Historic Monuments. *Quarterly Journal of Engineering Geology*, 28, 201-205.

- Erismann, J. W. & Wyers, G. P. (1993). Continuous Measurements of Surface Exchange of SO<sub>2</sub> and NH<sub>3</sub>; Implications for their Possible Interaction in the Deposition Process. *Atmospheric Environment*, 27AN13, 1937-1949.
- Esbert, R. M., Alonso, F. J., Diaz-Pache, F., Ordaz, J. & Perez-Ortiz, A. (1996). Superficial Protection of Granite Face to Saline Spray. In *Degradation and Conservation of Granitic Rocks in Monuments. Proceedings of the EC Workshop Held in Santiago de Compostela (Spain) on 28-30 November 1994. Protection and Conservation of the European Cultural Heritage. Report No 5*, ed. M. A. Vincente, J. Delgado-Rodriguez & J. Acevedo, pp. 337-342. Brussels: European Commission.
- Everitt, B. (1996). *Making Sense of Statistics in Psychology*. Oxford University Press: Oxford.
- Exley, C. S. & Stone, M. (1982). Geological Setting of the Hercynian Granites. In *Igneous Rocks of the British Isles*, ed. D. S. Sutherland. Chichester: J. Wiley and Sons.
- Exley, C. S., Stone, M. & Lee, G. J. (1982). Petrology of the Granites and Minor Intrusions. In *Igneous Rocks of the British Isles*, ed. D. S. Sutherland. Chichester: J. Wiley and Sons.
- Fassina, V. (1978). A Survey on Air pollution and Deterioration of Stonework in Venice. *Atmospheric Environment*, 12, 2205-2211.
- Fiora, L., Chiari, G. & Compagnoni, R. (1996). Granitic Rocks in the Historic Buildings of Turin (Piedmont, Italy). In *Degradation and Conservation of Granitic Rocks in Monuments. Proceedings of the EC Workshop Held in Santiago de Compostela (Spain) on 28-30 November 1994. Protection and Conservation of the European Cultural Heritage. Report No 5*, ed. M. A. Vincente, J. Delgado-Rodriguez & J. Acevedo, pp. 375-380. Brussels: European Commission.
- Floyd, P. A., Exley, C. S. & Styles, M. T. (Eds.). (1993). *Igneous Rocks of Southwest England*. Chapman and Hall: London.
- Fobe, B., Sweevers, H., Vleugels, G. & Van Grieken, R. (1993). Weathering of Miocene Ferruginous Sandstone in Ancient Buildings in North-eastern Belgium. *Science of the Total Environment*, 132, 53-70.

- Fookes, P. G., Dearman, W. R. & Franklin, J. A. (1971). Some Engineering Aspects of Rock Weathering with Field Examples from Dartmoor and elsewhere. *Quarterly Journal of Engineering Geology*, 4, 139-185.
- Fookes, P. G., Gourley, C. S. & Ohikere, C. (1988). Rock Weathering in Engineering Time. *Quarterly Journal of Engineering Geology*, 21, 33-57.
- Fort González, R., Bustillo Revuelta, M., Mingarro Martín, F. & López De Azcona, C. (1993). Weathering of Granite Rocks in the Cathedral of Toledo (Spain): Geochemical Evolution. In *Actas Del Workshop Alteration De Granitos Y Rocas Afines Empleados Como Materiales De Construcción. Consejo Superior De Investigaciones Científicas*, ed. E. M. Hernandez, E. M. Ballesteros & V. R. Arnav, pp. 155-159. Madrid: CSIC.
- Galloway, J. N. & Likens, G. E. (1981). Acid Precipitation: The Importance of Nitric Acid. *Atmospheric Environment*, 15(6), 1081-1085.
- García-Talegón, J., Molina, E. & Vicente, M. A. (1996). Behaviour of Granitic Materials under a Non-Polluted, Semiarid Climate (Avila Cathedral, Spain). In *Degradation and Conservation of Granitic Rocks in Monuments. Proceedings of the EC Workshop Held in Santiago de Compostela (Spain) on 28-30 November 1994. Protection and Conservation of the European Cultural Heritage. Report No 5*, ed. M. A. Vincente, J. Delgado-Rodrigues & J. Acevedo, pp. 61-66. Brussels: European Commission.
- Glass, G., Peckham, P. & Sanders, J. (1972). Consequences of Failure to Meet Assumptions Underlying the Fixed Effects of Analysis of Variance and Co-Variance. *Review of Educational Research*, 42, 237-288.
- Grimm, W. D. (1983). Measurements of Surface Roughness to Characterise the Degree of Deterioration of Natural Stones. In *Proceedings of the International Conference on Materials Science and Restoration. Esslingen, September*, pp. 321-324. Ingerman: Esslingen. In German.
- Hall, A. L. (1987). *Igneous Petrology*. Longman: Harlow.
- Halsey, D. P., Dews, S. J., Mitchell, D. J. & Harris, F. C. (1995). Real Time Measurements of Sandstone Deterioration: A Microcatchment Study. *Building and Environment*, 30 No3, 411-417.

- Halsey, D. P., Dews, S. J., Mitchell, D. J. & Harris, F. C. (1996). The Black Soiling of Sandstone Buildings in the West Midlands, England: Regional Variations and Decay Mechanisms. In *Processes of Urban Stone Decay*, ed. B. J. Smith & P. A. Warke, pp. 53-65. : Donhead Publishing Ltd. London.
- Hamilton, R. S., Revitt, D. M., Vincent, K. J. & Butlin, R. N. (1995). Sulphur and Nitrogen Particulate Pollutant Deposition on to Building Surfaces. *Science of the Total Environment*, 167, 57-66.
- Haneef, S. J., Johnson, J. B., Dickinson, C., Thompson, G. E. & Wood, G. C. (1992). Effect of Dry Deposition of NO<sub>x</sub> and SO<sub>2</sub> Gaseous Pollutants on the Degradation of Calcareous Building Stones . *Atmospheric Environment*, 26A(2), 2963-2974.
- Haneef, S., Dickinson, C., Johnson, J., Thompson, G. & Wood, G. (1989). Degradation of Coupled Stones by Artificial Acid Rain. In *Science, Technology and European Cultural Heritage. Proceedings of the European Symposium, 13 - 16 June, 1989*, ed. N. S. Baer, C. Sabbioni & A. I. Sors, pp. 469-474. Bologna, Italy: Butterworth - Heinmann.
- Haneef, S., Johnson, J. B., Jones, M., Thompson, G. E., Wood, G. C. & Azzaz, S. A. (1993). A Laboratory Simulation of Degradation of Leinster Granite by Dry and Wet Deposition Processes. *Corrosion Science*, 34(3), 511-524.
- Harrison, R. M. (1992). Important Air Pollutants and their Chemical Analysis. In *Pollution: Causes, Effects and Control. 2nd Ed*, ed. R. M. Harrison, pp. -. Cambridge: Royal Society of Chemistry.
- Hatch, F. H., Wells, A. K. & Wells, M. K. (1972). *Petrology of Igneous Rocks*. Allen and Unwin: London.
- Hawes, F. (1992). Weathering as a Controllable Phenomenon. In *Stone Cleaning and the Nature, Soiling and Decay Mechanisms of Stone. Proceedings of the International Conference held in Edinburgh, 14 - 16 April, 1992.*, ed. R. G. M. Webster, pp. 283-292. London: Donhead.
- Hawkes, J. R. & Dangerfield, J. (1978). The Variscan Granites of South-West England: A Progress Report. *Proceedings of the Ussher Society*, 4, 158-171.
- Hawksworth, D. L. & Rose, F. (1976). *Lichens as Pollution Monitors*. Arnold: London.



- Helmi, F. M. (1985). Deterioration of some Granite in Egypt. In *5th International Congress on Deterioration and Conservation of Stone, Lausanne, 25-27 Sept*, ed. G. Felix, pp. 421-429. Lausanne: Polytechniques Romandes Press.
- Hencher, S. R. & Martin, R. P. (1982). The Description and Classification of Weathered Rocks in Hong Kong for Engineering Purposes. In *Proceedings of the Seventh Southeast Asian Geotechnical Conference. 22-26 November, 1982, Hong Kong*, pp. 125-142.
- Hidy, G. M. & Countess, R. (1984). Combined Analysis of Air Quality and Precipitation Chemistry Data. In *Deposition Both Wet and Dry*, ed. B. B. Hicks, pp. 37-62. Butterworth. Boston
- Hoke, E. (1978). Investigations of Weathering Crusts on Salzburg Stone Monuments. *Studies in Conservation*, 23, 118-126.
- Hewell, D. C. (1992). *Statistical Methods in Psychology*. Duxbury Press: Belmont.
- Hughes, C. J. (1982). *Igneous Petrology*. Elsevier Scientific Publishing: Amsterdam.
- Hutchinson, A. J., Johnson, J. B., Thompson, G. E. & Wood, G. C. (1992). The Role of Fly-ash Particulate Material and Oxide Catalysts in Stone Degradation. *Atmospheric Environment*, 26A,15, 2795-2803.
- Inkpen, R. J., Cooke, R. U. & Viles, H. A. (1994). Processes and rates of Urban Limestone decay. In *Rock Weathering and Landform Evolution*, ed. D. A. Robinson & R. B. G. Williams, pp. 120-130. New York: J. Wiley and Sons Ltd.
- Irfan, T. Y. & Dearman, W. R. (1978a). Engineering Classification and Index Properties of a Weathered Granite. *Bulletin of the International Association of Engineering Geology*, 17, 79-90.
- Irfan, T. Y. & Dearman, W. R. (1978b). The Engineering Petrography of a Weathered Granite in Cornwall, England. *Quarterly Journal of Engineering Geology*, 11, 233-244.
- Irfan, T. Y. & Powell, G. E. (1985). Engineering Geological Investigations for Pile Foundations on a Deeply Weathered Granitic Rock in Hong Kong. *Bulletin of the International Association of Engineering Geology*, 32, 67-80.

- Irfan, T. Y. (1994). Aggregate Properties and Resources of Granitic Rocks for Use in Concrete in Hong Kong. *Quarterly Journal of Engineering Geology*, 27, 25-38.
- Irfan, T. Y. (1996). Mineralogy, Fabric Properties and Classification of Weathered Granites in Hong Kong. *Quarterly Journal of Engineering Geology*, 29, 5-35.
- Jackson, N. J., Halliday, A. N., Sheppard, S. M. F. & Mitchell, J. G. (1982). Hydrothermal Activity in the St. Just Mining District, Cornwall, England. In *Metallization Associated with Acid Magmatism*, ed. A. M. Evans, pp. 137-179. London: John Wiley and Sons Ltd.
- Jaynes, S. M. & Cooke, R. U. (1987). Stone Weathering in Southeast England. *Atmospheric Environment*, 12(7), 1601-1622.
- Judeikis, H. S. & Stewart, T. B. (1976). Laboratory Measurement of SO<sub>2</sub> Deposition Velocities on Selected Building Materials and Soils. *Atmospheric Environment*, 10, 769-776.
- Kennan, P. S. (1973). Weathered Granite at Turlough Hill Pumped Storage Scheme, County Wicklow, Ireland. *Quarterly Journal of Engineering Geology*, 6, 177-180.
- Keppel, G. (1982). *Design and Analysis: A Researchers Handbook*. Prentice Hall Inc: New Jersey.
- Kirkitsos, P. & Sikiotis, D. (1995). Deterioration of Pentelic Marble, Portland Limestone and Baumberger Sandstone in Laboratory Exposures to Gaseous Nitric Acid. *Atmospheric Environment*, 29 No. 1, 77-86.
- La Iglesia, A., Del Cura, M. A. G. & Ordoñez, S. (1994). The Physicochemical Weathering of Monumental Dolostones, Granites and Limestones; Dimension Stones of the Cathedral of Toledo (Spain). *Science of the Total Environment*, 152, 179-188.
- Lal, B. B. (1985). Weathering and Disintegration of Stone Monuments. In *5th International Congress on Deterioration and Conservation of Stone, Lausanne, 25-27 Sept*, ed. G. Felix, pp. 213-222. Lausanne: Polytechniques Romandes Press.

- Lee, S. G. & De Freitas, M. H. (1989). A Revision of the Description and Classification of Weathered Granite and its Application to Granites in Korea. *Quarterly Journal of Engineering Geology*, 22, 31-48.
- Leysen, L., Roekens, E. & Van Grieken, R. (1989). Air-Pollution-Induced Chemical Decay of a Sandy-Limestone Cathedral in Belgium. *Science of the Total Environment*, 78, 263-287.
- Lipfert, F. W. (1989). Dry Deposition Velocity as an Indicator for SO<sub>2</sub> Damage to Materials. *Journal of the Air Pollution Control Association*, 39, 446-452.
- Livingston, R. A. & Baer, N. S. (1988). The Use of Tombstones in the Investigation of the Deterioration of Stone Monuments. In *Engineering Geology of Ancient Works, Monuments and Historical Sites, Vol. 2*, ed. P. G. Marinos & G. C. Koukis, pp. 859-867. Rotterdam: Balkema.
- Livingston, R. A. (1985). The Role of Nitrogen Oxides in the Deterioration of Carbonate Stone. In *5th International Congress on Deterioration and Conservation of Stone, Lausanne, 25-27 Sept*, ed. G. Felix, pp. 509-515. Lausanne: Polytechniques Romandes Press.
- Lumb, P. (1962). The Properties of Decomposed Granite. *Geotechnique*, 12, 226-246.
- Lumb, P. (1985). Engineering Properties of Fresh Granite and Decomposed Igneous Rocks from Hong Kong. *Engineering Geology*, 19, 81-94.
- Madnawat, P. V. S., Rani, A., Sharma, M., Prasad, D. S. N. & Gupta, K. S. (1993). Role of Surface and Leached Metal Ion Catalysis in Autoxidation of Sulphur (IV) in Power Plant Flyash Suspensions. *Atmospheric Environment*, 27A No. 13, 1985-1991.
- Martin, R. P. & Hencher, S. R. (1986). Principles for Description and Classification of Weathered Rock for Engineering Purposes. In *Site Investigation Practice: Assessing BS 5930. Engineering Geology Special Publication No. 2*, ed. A. B. Hawkins, pp. 299-308. London: Geological Society.
- Martin, R. P. (1988). Use of Index Tests for Assessment of Weathered Rocks. *Proceedings of the 5th International Congress of the International Association of Engineering Geologists, Buenos Aires, Vol. 2*. A. A. Balkema: Rotterdam.

- Massey, S. (1996). Private correspondence.
- McCarroll, D. (1991). The Schmidt Hammer, Weathering and Rock Surface Roughness. *Earth Surface Processes and Landforms*, 16, 477-480.
- McGee, E. S. (1989). Biodeterioration in Stone. 88-93.
- Metcalfe, S. E., Atkins, D. H. F. & Derwent, R. G. (1989). Acid Deposition Modelling and the Interpretation of the United Kingdom Secondary Precipitation Network Data. *Atmospheric Environment*, 23 No. 9, 2033-2052.
- Montoto, M., Valdeón, L. & Esbert, R. M. (1996). Non-Destructive Tests in Stone Conservation: Tomography of the Axeitos (La Coruña, Spain) Megalith. In *Degradation and Conservation of Granitic Rocks in Monuments. Proceedings of the EC Workshop Held in Santiago de Compostela (Spain) on 28-30 November 1994. Protection and Conservation of the European Cultural Heritage. Report No 5*, ed. M. A. Vincente, J. Delgado-Rodrigues & J. Acevedo, pp. 281-287. Brussels: European Commission.
- Moorhouse, W. W. (1964). *The Study of Rocks in Thin Section*. Harper and Row: New York.
- Moye, D. G. (1955). Engineering Geology for the Snowy Mountains Scheme. *Journal of the Institution of Engineers, Australia*, 27, 287-298.
- Mulvin, L. & Lewis, J. O. (1994). Architectural Detailing, Weathering and Stone Decay. *Building and Environment*, 29 No. 1, 113-138.
- Namorado Rosa, R. & Silva, O. (1993). The Role of Water and Salts in the Alteration of Porous Rocks. In *Actas Del Workshop Alteration De Granitos Y Rocas Afines Empleados Como Materiales De Construcción. Consejo Superior De Investigaciones Científicas*, ed. E. M. Hernandez, E. M. Ballesteros & V. R. Arnav, pp. 177-179. Madrid: CSIC.
- Nord, A. G., Svardh, A. & Tronner, K. (1994). Air Pollution Levels Reflected in Deposits on Building Stone. *Atmospheric Environment*, 28, 16, 2615-2622.
- Norton, D. (1952). *An Empirical Investigation of Some of the Effects on Non-Normality and Heterogeneity of the F Distribution*. Unpublished Doctoral Dissertation. State University of Iowa: Iowa. Taken from Keppel, G. (1982). *Design and Analysis: A Researchers Handbook*.

- O'Brien, P. F., Bell, E., Orr, T. L. L. & Cooper, T. P. (1995). Stone Loss Rates at Sites Around Europe. *Science of the Total Environment*, 167, 111-121.
- O'Brien, P. F., Cooper, T. P. C. & Lyons, F. (1993). Granite Decay research in Ireland. In *Actas Del Workshop Alteration De Granitos Y Rocas Afines Empleados Como Materiales De Construcccion. Consejo Superior De Investigacions Cientificas*, ed. E. M. Hernandez, E. M. Ballesteros & V. R. Arnav, pp. 163-166. Madrid: CSIC.
- Ollier, C. D. (1969). *Weathering*. Oliver and Boyd: Edinburgh.
- Palmer, J. & Neilson, R. A. (1962). The Origin of Granite Tors on Dartmoor. *Proceedings of the Yorkshire Geological Society*, 33, 315-340.
- Price, D. G. (1993). A Suggested Method for the Classification of Rock Mass Weathering by a Rating System. *Quarterly Journal of Engineering Geology*, 26, 69-76.
- Price, D. G. (1995). Weathering and Weathering processes. *Quarterly Journal of Engineering Geology*, 28, 243-252.
- Prieto Lamas, B., Rivas Brea, M. T. & Silva Hermo, B. M. (1995). Colonisation of Lichens of Granite Churches in Galicia (Northwest Spain). *Science of the Total Environment*, 167, 343-351.
- QUARG. (1993a). *Urban Air Quality in the United Kingdom*. HMSO: London.
- QUARG. (1993b). *Diesel Vehicle Emissions and Urban Air Quality*. HMSO: London.
- QUARG. (1996). *Airborne Particulate Matter in the United Kingdom*. HMSO: London.
- Quinlan, M., O'Daly, G. & Lewis, J. O. (1994). Condition Assessment of Granite - Exterior Facades. In *Granite Weathering and Conservation. Proceedings of a Conference held at Trinity College, Dublin. September, 1993*, ed. E. Bell & T. P. Cooper, pp. 46-56. Dublin: Director of Buildings', Trinity College.
- Rainey, M. M. & Whalley, W. B. (1994). The Importance of Microfractures in Granitic Rock Breakdown with Reference to Building Stone Decay. In *Granite Weathering and Conservation. Proceedings of a Conference Held at Trinity College, Dublin, September, 1993*, ed. E. Bell & T. P. Cooper, pp. 36-45. Dublin: Director of Buildings' Office.

- Raymahashy, B. C. & Sharma, S. (1993). Decay of Building Stones: A Mineralogical Model of Konark Temple, India. *Quarterly Journal of Engineering Geology*, 26, 155-157.
- Realini, M., Negrotti, R., Appollonia, L. & Vaudan, D. (1995). Deposition of Particulate Matter on Stone Surfaces: An Experimental Verification of its Effects on Carrara Marble. *Science of the Total Environment*, 167, 67-72.
- Reddy, M. M. (1988). Acid Rain Damage to Carbonate Stone: A Quantitative Assessment Based on the Aqueous Geochemistry of Rainfall Runoff from Stone. *Earth Surface Processes and Landforms*, 13, 335-354.
- Reddy, M. M., Sherwood, S. I. & Doe, B. R. (1986). Limestone and Marble Dissolution by Acid Rain: An Onsite Weathering Experiment. In *Material Degradation by Acid Rain. ACS Symposium Series*, ed. R. Baboian, pp. 227-238. Washington: American Chemical Society.
- Ridder, T. B., Buishand, T. A., Reijnders, H. F. R., Hart, M. J. & Slannina, J. (1985). Effects of Storage on the Composition of Main Components in Rainwater Samples. *Atmospheric Environment*, 19(5), 759-762.
- Robinson, D. A. & Williams, R. B. G. (1996). An Analysis of the Weathering of Wealden Sandstone Churches. In *Processes of Urban Stone Decay. Proceedings of SWAPNET '95, Stone Weathering and Atmospheric Pollution Network Conference, held in Belfast 19-20 May 1995*, ed. B. J. Smith & P. A. Warke, pp. 133-149. London: Donhead Publishing Ltd.
- Roekens, E., Komy, Z., Leysen, L., Veny, P. & Van Grieken, R. (1988). Chemistry of precipitation near a Limestone Building. *Water, Air and Soil Pollution*, 38, 273-282.
- Sabbioni, C. & Zappia, G. (1992). Atmospheric - Derived Element Tracers on Damaged Stone. *Science of the Total Environment*, 126, 35-48.
- Sabbioni, C. (1995). Contribution of Atmospheric Deposition to the Formation of Damage Layers. *Science of the Total Environment*, 167, 49-55.
- Saunders, I. & Young, A. (1983). Rates of Surface Processes on Slopes, Slope Retreat and Denudation. *Earth Surface Processes and Landforms*, 8, 473-501.
- Schiavon, N. (1993). Microfabrics of Weathered Granite in Urban Monuments. In *Proceedings of the International Congress on the Conservation of Stone and*

- other Materials: Research-Industry-Media. Paris, June 29 - July 1, 1993*, ed. M. J. Theil, pp. 271-278. London: E. and F. Spon.
- Schiavon, N. (1996). Soiling of Urban Granite 1: Microfabrics and Mineralogical Aspects. In *Degradation and Conservation of Granitic Rocks in Monuments. Proceedings of the EC Workshop Held in Santiago de Compostela (Spain) on 28-30 November 1994. Protection and Conservation of the European Cultural Heritage. Report No 5*, ed. M. A. Vincente, J. Delgado-Rodrigues & J. Acevedo, pp. 307-312. Brussels: European Commission.
- Schiavon, N., Chiavari, G., Schiavon, G. & Fabbri, D. (1995). Nature and Decay Effects of Urban Soiling on Granitic Building Stones. *Science of the Total Environment*, 167, 87-101.
- Seaward, M. R. D. & Giacobini, C. (1988). Lichen Induced Biodeterioration of Italian Monuments, Frescoes and other Archaeological Materials. *Studia Geobotanica*, , 3-11.
- Seaward, M. R. D. & Giacobini, C. (1989). Oxalate Encrustation by the Lichen *Dirina Massiliensis* forma *Sorediata* and its Role in the Deterioration of Works of Art. In *Le Pellicole ad Ossalati. Origine e Significato Nella Conservazione Delle Opere D'art*, pp. 215-219. Milan: Centro CNR.
- Selby, M. J. (1982). *Hillslope Materials and Processes*. Oxford university Press: Oxford.
- Sequeira Braga, M. A., Alves, C., Begonha, A. & Gomes Da Silva, F. (1996). Industrial and Urban Pollution Impact in Portuguese Granitic Monuments: Comparative Study between Two Regions. In *Degradation and Conservation of Granitic Rocks in Monuments. Proceedings of the EC Workshop Held in Santiago de Compostela (Spain) on 28-30 November 1994. Protection and Conservation of the European Cultural Heritage. Report No 5*, ed. M. A. Vincente, J. Delgado-Rodrigues & J. Acevedo, pp. 127-132. Brussels: European Commission.
- Sequeira Braga, M. A., Simões Alves, C. A. & Begonha, A. (1993). Weathering of the Oporto Granite and the Deterioration of the Hospital St. Antonio: Historical Monument Built with Granitic Materials. In *Actas Del Workshop Alteration De Granitos Y Rocas Afines Empleados Como Materiales De*

- Construccion. Consejo Superior De Investigacions Cientificas*, ed. E. M. Hernandez, E. M. Ballesteros & V. R. Arnav, pp. 153-155. Madrid: CSIC.
- Sjoberg, R. (1994). Diagnosis of Weathering on Rock Carving Surfaces in Northern Bohuslan, Southwest Sweden. In *Rock Weathering and Landform Evolution*, ed. D. A. Robinson & R. B. G. Williams, pp. 223-241. New York: J. Wiley and Sons Ltd.
- Smith, B. J. & Magee, R. W. (1990). Granite Weathering in an Urban Environment: Example from Rio De Janeiro. *Singapore Journal of Tropical Geography*, 2, 143-153.
- Smith, B. J. (1996). Scale Problems in the Interpretation of Urban Stone Decay. In *Processes of Urban Stone Decay. Proceedings of SWAPNET '95, Stone Weathering and Atmospheric Pollution Network Conference, held in Belfast 19-20 May 1995*, ed. B. J. Smith & P. A. Warke, pp. 3-18. London: Donhead Publishing Ltd.
- Smith, B. J., Magee, R. W. & Whalley, W. B. (1993). Decay of Granite in a Polluted Environment: Budapest. In *Actas Del Workshop Alteration De Granitos Y Rocas Afines Empleados Como Materiales De Construccion. Consejo Superior De Investigacions Cientificas*, ed. E. M. Hernandez, E. M. Ballesteros & V. R. Arnav, pp. 159-162. Madrid: CSIC.
- Smith, B. J., Magee, R. W. & Whalley, W. B. (1994). Breakdown patterns of Quartz Sandstone in a Polluted Urban Environment, Belfast, Northern Ireland. In *Rock Weathering and Landform Evolution*, ed. D. A. Robinson & R. B. G. Williams, pp. 131-150. New York: J. Wiley and Sons Ltd.
- Smith, B. J., Whalley, W. B. & Magee, R. W. (1989). Building Stone Decay in a Clean Environment: Western Northern Island. In *Science, Technology and European Cultural heritage, Proceedings of the European Symposium, Bologna, Italy. 13 - 16 June, 1989.*, ed. N. S. Baer, C. Sabbioni & A. I. Sors, pp. 434-438. : Butterworth-Heinmann.
- Smith, B. J., Whalley, W. B. & Magee, R. W. (1992). Assessment of Building Stone Decay: A Geomorphological Approach. In *Stone Cleaning and the Nature, Soiling and Decay Mechanisms of Stone. Proceedings of the International*



- Conference held in Edinburgh, 14 - 16 April, 1992.*, ed. R. G. M. Webster, pp. 249-257. London: Donhead.
- Sorlini, C., Allievi, L., Sacchi, M. & Ferrari, A. (1982). Micro-organisms Present in Deteriorated Materials of *Palazzo della Ragione* in Milan. *International Biodeterioration Bulletin*, 18(4), 105-110.
- Steiger, M., Wolf, F. & Dannecker, W. (1993). Deposition and Enrichment of Atmospheric Pollutants on Building Stones as Determined by Field Exposure Experiments. In *Proceedings of the International Congress of Stone and other Materials: Research-Industry-Media. Paris, June 29 - July 1, 1993*, ed. M. J. Theil, pp. 35-42. Paris: E. and F. Spon.
- Stillman, C. (1996). Growth Areas: Geology and Geochemistry in Archaeology. *Geology Today*, May, 89-90.
- Sweevers, H. & Van Grieken, R. (1992). Analytical Study of the Deterioration of Sandstone, Marble and Granite. *Atmospheric Environment*, 26B(2), 159-163.
- Sweevers, H., Peeters, A. & Van Grieken, R. (1995). Weathering of Leinster Granite under Ambient Atmospheric Conditions. *Science of the Total Environment*, 167, 73-85.
- Torfs, K. & Van Grieken, R. (1996). Effect of Stone Thickness on Run-off Water Composition and Derived Damage Functions in Ambient Exposure Experiments. *Atmospheric Environment*, 30(1), 1-8.
- Trudgill, S. T., Viles, H. A., Cooke, R. U. & Inkpen, R. J. (1990). Rates of Stone Loss at St. Paul's Cathedral, London. *Atmospheric Environment*, 24B, 2, 361-363.
- Turkington, A. V. (1996). Stone Durability. In *Processes of Urban Stone Decay. Proceedings of SWAPNET '95, Stone Weathering and Atmospheric Pollution Network Conference, held in Belfast 19-20 May 1995*, ed. B. J. Smith & P. A. Warke, pp. 19-31. London: Donhead Publishing Ltd.
- Valdeón, L., Montoto, M. & Esbert, R. M. (1996). Tomography of the Axeitos Megalith (La Coruña, Spain): Practical Procedures and Instrumentation. In *Degradation and Conservation of Granitic Rocks in Monuments. Proceedings of the EC Workshop Held in Santiago de Compostela (Spain) on 28-30 November 1994. Protection and Conservation of the European*

- Cultural Heritage. Report No 5*, ed. M. A. Vincente, J. Delgado-Rodrigues & J. Acevedo, pp. 275-276. Brussels: European Commission.
- Vargas, M., Maqueda, C., Franquelo, M. L., García Talegón, J. & Pérez Rodríguez, J. L. (1996). Chemical Analysis of Granites from Quarries and Monuments. In *Degradation and Conservation of Granitic Rocks in Monuments. Proceedings of the EC Workshop Held in Santiago de Compostela (Spain) on 28-30 November 1994. Protection and Conservation of the European Cultural Heritage. Report No 5*, ed. M. A. Vincente, J. Delgado-Rodrigues & J. Acevedo, pp. 53-60. Brussels: European Commission.
- Vicente, M. A. (1996). Summary Report Project STEP CT90-0101, Granitic Materials and Historical Monuments: Study of the Factors and Mechanisms of Weathering and Application to Historical Heritage Conservation. In *Degradation and Conservation of Granitic Rocks in Monuments. Proceedings of the EC Workshop Held in Santiago de Compostela (Spain) on 28-30 November 1994. Protection and Conservation of the European Cultural Heritage. Report No 5*, ed. M. A. Vincente, J. Delgado-Rodrigues & J. Acevedo, pp. 4-44. Brussels: European Commission.
- Vicente, M. A., Garcia-Talegon, J. & Inigo, A. C. (1993). Weathering Mechanisms of Silicate Rocks in Continental Environments. In *Proceedings of the International Congress of Stone and other Materials: Research-Industry-Media. Paris, June 29 - July 1, 1993*, ed. M. J. Theil, pp. 320-327. Paris: E. and F. Spon.
- Warke, P. A. & Smith, B. J. (1994). Inheritance Effects on the Efficacy of Salt Weathering Mechanisms in Thermally Cycled Granite Blocks Under Laboratory and Field Conditions. In *Granite Weathering and Conservation. Proceedings of a Conference held at Trinity College, Dublin, September, 1993*, ed. E. Bell & T. P. Cooper, pp. 19-28. Dublin: Dir. of Buildings Office, Trinity College.
- Weber, H. & Zinsmeister, K. (1991). *Conservation of Natural Stones: Guidelines to Consolidation, Restoration and Preservation*. Expert Verlag: .
- Weber, J. (1985). Natural and Artificial Weathering of Austrian Building Stones Due to Air Pollution. In *5th International Congress on Deterioration and*

*Conservation of Stone, Lausanne, 25-27 Sept*, ed. G. Felix, pp. 527-533.

Lausanne: Polytechniques Romandes Press.

Winkler, E. E. (1987). Weathering and Weathering Rates of Natural Stone.

*Environmental Geology Water Science*, 9(2), 85-92.

Young, A. R. M. (1987). Salt as an Agent in the Development of Cavernous

Weathering. *Geology*, 15, 962-966.

Zhao, J., Broms, B. B., Zhou, Y. & Choa, V. (1994). Study of the Weathering of the Bukit Timah Granite. Part A: Review, Field Observations and Geophysical Survey. *Bulletin of the International Association of Engineering Geology*, 49, 97-106.

Zhao, J., Zhou, Y., Sun, J., Low, B. K. & Choa, V. (1995). Engineering Geology of the Bukit Timah Granite for Cavern Construction in Singapore. *Quarterly Journal of Engineering Geology*, 28, 153-162.

## Appendix

<b>A.1 London Site Correlation</b>	298
<b>A.2 Birmingham Site Correlation</b>	298
<b>A.3 Dartmoor Site Correlation</b>	299
<b>A.4 Pilot Study Strength Readings</b>	290
<b>A.5 Luesdon Cross</b>	303
<b>A.6 Lydford</b>	303
<b>A.7 Mary Tavy</b>	304
<b>A.8 Moretonhampstead</b>	305
<b>A.9 Peter Tavy</b>	306
<b>A.10 Postbridge</b>	307
<b>A.11 Princetown</b>	308
<b>A.12 Shaugh Prior</b>	308
<b>A.13 Sheepstor</b>	309
<b>A.14 Widecombe in the Moor</b>	310

## Tables

Table A.1	London correlation table	298
Table A.2	Birmingham correlation table	298
Table A.3	Dartmoor correlation table	299
Table A.4	Burrator quarry Schmidt Hammer raw values	299
Table A.5	Sheepstor church raw Schmidt Hammer values	301
Table A.6	Widecombe-in-the-Moor Schmidt Hammer raw values	302
Table A.7	Block ratings, by aspect, for Luesdon cross	303
Table A.8	Block ratings, by aspect, for Lydford	304
Table A.9	Block ratings, by aspect, for Mary Tavy church	305
Table A.10	Total block ratings for Mary Tavy Vestry	305
Table A.11	Total block rating values for Moretonhampstead church	306
Table A.12	Total block rating for Peter Tavy church	307
Table A.13	Total block rating for Postbridge church	308
Table A.14	Total block rating values for Princetown church	308
Table A.15	Average block rating values for Shaugh Prior	309
Table A.16	Average block ratings for Sheepstor church	310
Table A.17	Widecombe-in-the-moor, average block ratings	311

**A.1. London Site Correlation.**

	pH	Cl <sup>-</sup>	NO <sub>3</sub>	PO <sub>3</sub>	SO <sub>4</sub>	Al	Ca	Mg	Fe	SO <sub>2</sub>	NO <sub>x</sub>	PM <sub>10</sub>
pH	1											
Chloride	0.46	1										
Nitrate	0.14	0.42	1									
Phosphate	0.07	0.31	0.51	1								
Sulphate	0.42	0.68	0.74	0.54	1							
Al	-0.01	0.08	-0.07	0.17	0.00	1						
Ca	0.48	0.74	0.69	0.46	0.93	-0.01	1					
Mg	0.61	0.78	0.48	0.34	0.71	-0.07	0.84	1				
Fe	0.28	0.32	0.26	0.23	0.39	0.44	0.41	0.31	1			
SO <sub>2</sub>	0.33	0.29	0.01	0.05	0.25	0.13	0.29	0.29	0.26	1		
NO <sub>x</sub>	-0.38	0.31	-0.13	-0.06	0.05	0.15	0.16	0.22	0.31	0.62	1	
PM <sub>10</sub>	0.25	0.07	0.14	-0.10	0.18	0.08	0.22	0.13	0.15	0.62	0.58	1

Table A.1. London correlation table. Shaded cells are significant ( $r \geq 0.7$ ).**A.2. Birmingham Site Correlation.**

	pH	Cl <sup>-</sup>	NO <sub>3</sub>	PO <sub>3</sub>	SO <sub>4</sub>	Al	Ca	Mg	Fe	SO <sub>2</sub>	NO <sub>x</sub>	PM <sub>10</sub>
pH	1											
Chloride	0.01	1										
Nitrate	-0.08	0.54	1									
Phosphate	-0.02	0.53	0.71	1								
Sulphate	-0.04	0.69	0.80	0.94	1							
Al	-0.01	0.63	0.56	0.90	0.86	1						
Ca	-0.06	0.67	0.86	0.89	0.94	0.79	1					
Mg	-0.02	0.64	0.82	0.90	0.89	0.82	0.94	1				
Fe	-0.10	0.30	0.27	0.26	0.24	0.21	0.24	0.25	1			
SO <sub>2</sub>	0.10	0.38	0.44	0.61	0.56	0.58	0.53	0.61	0.32	1		
NO <sub>x</sub>	-0.02	0.36	0.50	0.58	0.53	0.56	0.53	0.60	0.31	0.78	1	
PM <sub>10</sub>	0.28	0.29	0.47	0.36	0.38	0.25	0.35	0.36	0.10	0.56	0.58	1

Table A.2. Birmingham correlation table. Shaded cells are significant ( $r \geq 0.7$ ).

### A.3. Dartmoor Site Correlation.

	pH	Cl <sup>-</sup>	NO <sub>3</sub>	PO <sub>3</sub>	SO <sub>4</sub>	Al	Ca	Mg	Fe	SO <sub>2</sub>
pH	1									
Chloride	0.31	1								
Nitrate	-0.14	-0.21	1							
Phosphate	0.29	0.06	0.35	1						
Sulphate	-0.06	0.06	0.85	0.39	1					
Al	0.35	0.24	0.20	0.12	0.32	1				
Ca	0.18	0.05	0.56	0.61	0.73	0.28	1			
Mg	0.29	0.54	0.42	0.45	0.70	0.41	0.83	1		
Fe	0.24	-0.01	0.02	0.03	0.06	0.36	0.10	0.10	1	
SO <sub>2</sub>	-0.11	-0.14	0.17	0.00	0.19	0.03	0.08	0.07	0.10	1

Table A.3. Dartmoor correlation table. Shaded cells are significant ( $r \geq 0.7$ ).

### A.4. Pilot Study Strength Readings.

South Aspect Face. Raw Values						
Face	Position	1	2	3	4	Average
1	1	54	54	31	38	44.25
	2	34	48	54	32	42
	3	44	60	54	57	53.75
	4	42	46	65	46	49.75
	5	34	58	58	59	52.25
	6	31	54	50	60	48.75
2	1	54	47	64	34	49.75
	2	58	60	54	67	59.75
	3	40	56	41	48	46.25
	4	54	36	63	54	51.75
	5	62	34	50	65	52.75
	6	60	59	53	54	56.5
3	1	64	60	48	58	57.5
	2	44	60	37	57	49.5
	3	58	53	40	56	51.75
	4	70	55	50	67	60.5
	5	65	48	55	35	50.75
	6	60	56	48	60	56
4	1	45	50	47	71	53.25
	2	61	54	62	71	62
	3	56	61	59	56	58
	4	50	60	52	58	55
	5	53	59	64	51	56.75
	6	58	55	51	58	55.5

Table A.4. Burrator quarry Schmidt Hammer raw values. Units measured in R<sub>%</sub>.

		South facing Wall. Raw Values					West facing Wall. Raw Values					North facing Wall. Raw Values					Interior Readings. Raw Values				
Course	Stone	1	2	3	4	Average	1	2	3	4	Average	1	2	3	4	Average	1	2	3	4	Average
1	1	12	20	18	22	18	30	21	14	36	25.25	40	42	38	32	38	20	26	32	32	27.5
	2	24	24	16	16	20	30	28	26	22	26.5	40	26	45	44	38.75	38	42	40	30	37.5
	3	22	22	20	12	19	23	25	38	20	26.5	30	46	55	39	42.5	34	36	31	28	32.25
	4	18	20	23	18	19.75	24	32	28	32	29	46	31	52	32	40.25	34	36	30	28	32
	5	28	34	28	24	28.5	22	26	30	30	27										
	6	35	24	30	26	28.75	24	20	34	30	27										
2	1	30	26	30	36	30.5	27	14	24	25	22.5	42	32	27	28	32.25	54	30	44	42	42.5
	2	28	26	30	30	28.5	26	16	24	28	23.5	56	51	38	18	40.75	40	38	50	52	45
	3	16	12	32	20	20	28	32	38	24	30.5	19	38	24	22	25.75	50	55	30	46	45.25
	4	28	15	12	25	20	20	26	30	28	26	24	26	32	28	27.5	48	48	50	40	46.5
	5	38	26	24	30	29.5	26	22	27	20	23.75										
	6	10	17	22	12	15.25	28	18	30	37	28.25										
3	1	34	36	44	36	37.5	26	18	25	16	21.25	29	28	28	23	27	22	34	38	46	35
	2	36	30	32	25	30.75	34	14	24	28	25	32	34	11	22	24.75	32	44	41	43	40
	3	24	20	28	32	26	33	20	22	26	25.25	26	25	20	28	24.75	35	26	26	42	32.25
	4	28	28	30	39	31.25	27	24	28	11	22.5	30	22	32	26	27.5	36	43	44	35	39.5
	5	26	18	28	24	24	24	26	28	25	25.75										
	6	25	30	37	30	30.5	27	22	22	21	23										
4	1	30	26	22	28	26.5	26	40	45	40	37.75	32	40	33	26	32.75					
	2	24	24	32	17	24.25	32	20	24	22	24.5	34	28	30	30	30.5					

	7	32	39	40	46	39.25															
5	1	20	33	26	30	27.25	24	16	22	22	21	28	20	31	24	25.75					
	2	28	25	30	38	30.25	28	18	28	20	23.5	20	22	14	14	17.5					
	3	32	32	32	24	30	25	22	20	26	23.25	24	26	12	26	22					
	4	33	16	21	24	23.5	28	25	24	28	26.25	42	40	24	22	32					
	5	15	30	24	25	23.5	21	25	16	28	22.5										
	6	24	18	26	18	21.5	28	25	24	32	27.25										
	7	30	32	32	14	27															

Table A.5. Sheepstor church raw Schmidt Hammer values. Units measured in R<sub>%</sub>.

	South facing Wall - Raw Values							West facing Wall - Raw Values					North facing Wall - Raw Values.					Interior				
Course	Stone	1	2	3	4	5	Average	1	2	3	4	Average	1	2	3	4	Average	1	2	3	4	Average
1	1	23.5	24.5	25	29	31.5	26.7	13	22	28	32	23.75	18	26	24	22	22.5	30.5	26	29	28.5	28.5
	2	42	31.5	28	34.5	31	33.4	28	26	20	22	24	36	24	46	28	33.5	35.5	35.5	43	38	38
	3	27.5	15.5	26	21.5	19.5	22	32	18	23	37	27.5	28	25	32	16	25.25	52	55	58	55	55
	4							13	20	18	30	20.25	15	12	27	30	21	37.5	52	46.5	45.33	45.33
	5							30	30	26	34	30	28	18	30	24	25					
	6							18	24	12	22	19	21	26	26	28	25.25					
2	1	35	40.5	31	33	38	35.5	26	24	22	36	27	20	16	36	23	23.75					
	2	27	37	26	21	31	28.4	26	41	20	33	30	19	19	30	21	22.25					
	3	17.5	39	42	32	38	33.7	13	23	33	24	23.25	29	37	31	39	34					
	4	38.5	37.5	39	40	47	40.4	18	20	23	25	21.5	36	24	17	28	26.25					
	5	25	44.5	40	47.5	40	39.4	21	16	24	14	18.75	31	29	27	44	32.75					
	6	28.5	22	26	25.5	18.5	24.1	19	22	28	24	23.25	33	33	47	14	31.75					
3	1	34	34.5	19	22	25.5	27	30	31	33	24	29.5	27	24	34	24	27.25					
	2	20.5	32.5	28	26.5	33.5	28.2	38	17	29	45	32.25	28	32	31	34	31.25					
	3	32	36	31.5	30	31.5	32.2	23	30	18	12	20.75	36	52	36	52	44					



	4	29.5	38.5	39.5	29	20.5	31.4	26	20	16	20	20.5	41	51	43	50	46.25					
	5	28	21	23	29	26	25.4	16	20	23	19	19.5	35	26	48	32	35.25					
	6							28	34	26	21	27.25	25	41	34	23	30.75					
	7												40	40	43	50	43.25					
4	1	18	33	29.5	32	31.5	28.8	20	35	27	18	25	35	34	30	30	32.25					
	2	26.5	27	33	29	33.5	29.8	2	12	16	14	11	34	28	45	34	35.25					
	3	23.5	32	26	25	33	27.9	32	22	25	20	24.75	23	34	41	41	34.75					
	4	28	26	30	38	27	29.8	14	17	12	14	14.25	32	40	38	43	38.25					
	5	36	25.5	29.5	28	30.5	29.9	20	26	33	20	24.75	45	31	41	41	39.5					
	6							26	18	35	11	22.5	26	45	32	45	37					
	7												29	38	46	46	39.75					
5	1	29.5	28	49	30	27	32.7						25	31	35	24	28.75					
	2	50	30.5	28.5	33	34	35.2						35	50	45	41	42.75					
	3	28.5	17	16.5	24.5	31.5	23.6						36	20	19	36	27.75					
	4	22.5	22	23	25	31	24.7						37	31	26	42	34					
	5	31	34	32.5	30.5	30	31.6						44	32	38	42	39					
	6												45	33	33	12	30.75					

Table A.6. Widecombe-in-the-Moor Schmidt Hammer raw values. Units measured in  $R_{\%}$ .

### A.5. Luesdon Cross.

Total Block Rating: Luesdon Cross			
Block 1	South	West	North
	70.5	69	65.25
	58.5	56.5	66.25
	66.75	61.75	59.25
	49	68	50.5
	61.5	65.75	71.5
	68	68.25	61
<b>Block 1 Average</b>	<b>62.375</b>	<b>64.875</b>	<b>62.29167</b>
Block 2			
	63.75	59.25	57
	61.5	66	62
	62.75	73.5	56.25
	63	52	59.25
<b>Block 2 Average</b>	<b>62.75</b>	<b>62.6875</b>	<b>58.625</b>
Block 5			
	72.5	79.75	73
	90.5	52.75	62.75
<b>Block 5 Average</b>	<b>81.5</b>	<b>66.25</b>	<b>67.875</b>
<b>Overall Average</b>	<b>65.6875</b>	<b>64.375</b>	<b>62</b>

Table A.7. Block ratings, by aspect, for Luesdon cross.

### A.6. Lydford.

Rating totals				
Course 1	South	West	North	Interior
	55	46.25	51.75	84.5
	60	72	54	95
	80	60	48	90.5
	53	44.25	42	93.25
	69.75		49.25	
Course 2				
	66.75	49.75	64.5	97.5
	51.5	76.25	46.25	94.5
	73.5	51.75	24.25	90.75
	79.75	44.25	28.5	88
	58.75		45.25	
Course 3				
	71.75	41	36.75	84
	47.75	43.5	37.5	79.5
	65.5	68.5	36.5	80.75
	70.25	49.5	35.25	92.5
	68.5		52	
Course 4				
	85.5	57.25	35.5	82.5
	70	46.75	49	70.25
	60	48	42.75	87.5

	73	66.5	52.5	92.25
	85		34	
<b>Course 5</b>				
	81.5	50.5		
	56.75	28.25		
	68	59.75		
	43.5	53		
	67.5			
<b>Average</b>	<b>66.5</b>	<b>52.85</b>	<b>43.275</b>	<b>87.7031</b>

Table A.8. Block ratings, by aspect, for Lydford.

**A.7. Mary Tavy.**

Total Block Rating: Mary Tavy Church				
<b>Course 1</b>	South	West	North	Interior
	67	70	71.75	80.5
	66.75	26	40	75.5
	43.75	34.25	23	77.25
	47	50.75	44.25	93.5
	54	79.25		
	62	70.75		
	48.75			
<b>Course 2</b>				
	40.75	45.5	53.5	67.25
	45.25	58.75	37.5	87.25
	56.25	54.5	54.5	83.25
	38.5	51.5	55	
	43	57.75		
	42.5	49.25		
	53.5			
<b>Course 3</b>				
	76.5	52.5	54	
	55	18.75	57.75	
	37.25	13.5	40.5	
	71	51.75	62.25	
	40.25	53.5		
	40.5	44.75		
	58			
<b>Course 4</b>				
	46.5	64	64.25	
	70.5	56.5	75.25	
	59.75	52.5	60	
	57.5	69.5		
	65	54		
	66.25	59.75		
	44			
<b>Course 5</b>				
	54.75	62.5	71	
	63	9.5	53.5	
	46	38.75	58.5	
	51.5	35.75	53.75	

	32.75	52.5		
	61.75	43.75		
	63.75			
<b>Average</b>	<b>53.4429</b>	<b>49.4</b>	<b>54.2237</b>	<b>80.6429</b>

Table A.9. Block ratings, by aspect, for Mary Tavy church.

Block Rating Totals: Mary Tavy Vestry					
	Exterior	Interior		Exterior	Interior
<b>Course 1</b>			<b>Course 3</b>		
	93.25	90.5		70.25	
	84	98.75		81.5	
	68	96		80.75	
	59.25	93.25		75.25	
	86.5	98.75		83	
		98.75			
<b>Course 2</b>			<b>Course 4</b>		
	84.5			86	
	81.25			86.75	
	79.5			80.75	
	72.5			81	
	65.25			87	
			<b>Average</b>	<b>79.3125</b>	<b>96</b>

Table A.10. Total block ratings for Mary Tavy Vestry.

**A.8. Moretonhampstead.**

Type B Block Rating Totals					Type C Block Rating Totals			
Course 1	South	West	North	Interior	South	West	North	Interior
	61.5	45.5	39	79.25		36		
	73.25	40.75	57.75	82.25				
	78.5	78.25	53.5	69				
	74	73.25	77					
	61.75	43.75	72.75					
	29							
<b>Average</b>	<b>63</b>	<b>56.3</b>	<b>60</b>	<b>76.8333</b>		<b>36</b>		
<b>Course 2</b>	39	77.25	48.25	90.75		75.5		
	68.25	59.5	47	91				
	65.5	69.75	47.5	80.25				
	60.5	36.25	59					
	56.75	37	63.5					
	51							
<b>Average</b>	<b>56.8333</b>	<b>55.95</b>	<b>53.05</b>	<b>87.3333</b>		<b>75.5</b>		
<b>Course 3</b>	60.5	58.25	38	77.25	88.75	68.75		
	56.5	51.75	51	78.75		71.25		
	68	73.25	53.25	77.25				
	74.25	45.75	52.75					
	57.75		82.25					

	29.5							
<b>Average</b>	<b>57.75</b>	<b>57.25</b>	<b>55.45</b>	<b>77.75</b>	<b>88.75</b>	<b>70</b>		
<b>Course 4</b>	71.5	42.5	77.75	84	61.75	77	53.25	
		63.25	52.75	88.75	69.5	83	80.75	
			65	89.5	76	84.5		
					86	85		
					75.25			
					89			
<b>Average</b>	<b>71.5</b>	<b>52.875</b>	<b>65.1667</b>	<b>87.4167</b>	<b>76.25</b>	<b>82.375</b>	<b>67</b>	
<b>Course 5</b>	24.25	74	27.75		82.75	69	67.75	93.25
	56	77.75	52.25		81.5	56.75	47.75	93
	22		57.5		69	79.75	22.5	88.75
					83.75	82		
					74			
					40			
<b>Average</b>	<b>34.0833</b>	<b>75.875</b>	<b>45.8333</b>		<b>71.8333</b>	<b>71.875</b>	<b>46</b>	<b>91.6667</b>
<b>Course 6</b>	78.5				86			89
	73.25				90.25			90.75
	69.75							96
	57.5							
	12							
<b>Average</b>	<b>58.2</b>				<b>88.125</b>			<b>91.9167</b>
<b>Course 7</b>	29				57.25			
	74.75				27.5			
	90.75							
	51.25							
	74							
	49							
<b>Average</b>	<b>61.4583</b>				<b>42.375</b>			
<b>Average</b>	<b>57.5455</b>	<b>58.2083</b>	<b>55.9762</b>	<b>82.3333</b>	<b>72.8382</b>	<b>72.375</b>	<b>54.4</b>	<b>91.7917</b>

Table A.11. Total block rating values for Moretonhampstead church.

**A.9. Peter Tavy.**

Total Block Rating: Peter Tavy				
Course 1	South	West	North	Interior
	47.5	44.25	59.75	78.5
	65	65.5	78.5	87.5
	70.5	64.75	50	75
	67	53.5	70.25	71.25
	60.5	72.75	59.5	77
<b>Course 2</b>				
	61.75	69.75	77	76.75
	71.25	59.5	66	66.5
	70.75	57	68.75	77.5
	71.25	52.3	75.5	79.75
	59.5	64	74	65.5
<b>Course 3</b>				
	59.5	39.25	75	64.75
	53.75	78.5	50.75	68.75
	53	37.75	47.75	61

	69.75	70.5	58.75	50.75
	65.5	73.25	63	57.25
<b>Course 4</b>				
	66.25	68.75	58.25	
	69.75	73.75	59.5	
	64.25	66.75	51.25	
	67	67.75	49.75	
	55.25		60.75	
<b>Course 5</b>				
	75	56.25	52	
	66	60.25	51.5	
	65	63	61.75	
	80.25	60	44	
	64		51.25	
<b>Average</b>	<b>64.77</b>	<b>61.6978</b>	<b>60.58</b>	<b>70.5167</b>

Table A.12. Total block rating for Peter Tavy church.

**A.10. Postbridge.**

Block Total Rating: Postbridge Church				
	North	West	South	Interior
	63.75	75.25	48.5	95
	71.25	59.75	50.25	95
	75	68.25	35.5	89
	85	61.75	44	79.75
	62.75	63.75	33	88.25
	60.75	67	55.25	96.25
	62	89.5	51.25	85
	90	66.25	43.5	96.75
	73	70	50	95
	73.25	70.5	42.75	87
	62.25	67.25	30.5	92.25
	73.5	75.75	46	92.5
	70	59.75	45	96.25
	39.5	75.5	47	96
	63	55.25	69.25	80
	58.5	50.75	59.5	90.75
	80	66.75	70.5	
	67.25	73	70.5	
	80.25	54		
	50.75	54.5		
	64.5	61.5		
<b>Average</b>	<b>67.9167</b>	<b>66</b>	<b>49.5694</b>	<b>90.9219</b>

Table A.13. Summary of the parameter values for Postbridge church.

**A.11. Princetown**

Block Rating Totals: Princetown Church							
Section 1	South	East	North	Section 4	South	East	North
	62	79.5	74		76	85.5	75.75
	73.25	81.5	63.25		74.75	86	70.75
	88.75	78	83		79.75	79.5	92
	73	70.5	58		76.25	84.75	62.5
	70.75	74	73.25		86	83	57.25
	75.75	86.25	84.5		85.75	78.25	52
	85.75	63	66.75			71.75	68.5
		71.25				71.5	
Section 2						85.75	
	62.5	85	72.25			72.5	
	64.25	77.25	69.5	Section 5			
	67.75	78	120.5			77	
	76.5	55	74.75			86.75	
	74.5	73	82.5			83.25	
	81.25	67.25	72			72.75	
	83	73.5	68.25			80.5	
		65.5	80			53.75	
		79.75		Average	74.5714	75.8465	73.3666
		77.25					
Section 3							
	57.5	69.25	67.25				
	77.5	71.5	58.75				
	75	79.25	86				
	73	80.5	70.5				
	72.25	84.75	75.25				
	70.5	70.75	74.75				
	62	76	80.25				
	82.75	80.25	67				
		69.25					
		67.75					

Table A.14. Total block rating values for Princetown church.

**A.12. Shaugh Prior**

Block Rating Totals: Shaugh Prior				
Course 1	South	West	North	Interior
	34.5	40	45	88
	68.75	43.5	39.5	87.25
	55.25		45	84.5
	50.75		30.25	90.5
	53.5		30	85.5
	56.5		28	86.5
	63.5			
Course 2				
	51	40.75	39.5	93.25
	56	35.5	38.25	89
	51.25	39.5	27.75	75
	24.25	43.25	51.5	
	62.75	37	37	
	47.75	52.5		
	28	29		

	41.5	18.75		
<b>Course 3</b>				
	42.75	28	30.75	91.5
	39.5	24.5	33	77.5
	27.75	41.25	45	83.75
	37.5	46	41.5	
	49.25	48	34.25	
	49.5	44.25	33.5	
	35	41.75		
	41.75	49.25		
<b>Course 4</b>				
	59	45	39.25	
	49.5	39.25	26	
	43.5	43.75	32	
	41.5	46.5	34.75	
	49.5	36.25	25.75	
	36.5	34.75	35.5	
	52.5	53		
	36	54		
<b>Course 5</b>				
	49.75	47		
	37	41.5		
	48.25	43.75		
	46.75	44.75		
	23.75	62.25		
	33	51.75		
	48.75	50.75		
		62.25		
<b>Course 6</b>				
	30.75	54		
	53.75	58.75		
	33.25	58.75		
	43.5	53.5		
	56	53		
	53.75	43.5		
	43	37		
		49.25		
<b>Average</b>	<b>45.2778</b>	<b>44.4524</b>	<b>35.7826</b>	<b>86.0208</b>

Table A.15. Average block rating values for Shaugh Prior.

**A.13. Sheepstor**

Rating Totals: Sheepstor Church				
Course 1	South	West	North	Interior
	44.25	55	56.75	81.25
	31	57	51.25	83
	29.5	40.5	63.75	79
	31.5	64.25	57.25	83.5
	52.5	46.5		
	53.25	44.25		
<b>Course 2</b>				



	71.75	45	39.25	95
	65.75	42	46.25	100
	41	58.25	25.75	92.25
	29.75	51	28.75	88.75
	51.5	35		
	42	49		
<b>Course 3</b>				
	68.25	38.5	21.75	90
	64.25	57	40.25	97.5
	55.25	47.75	48.5	75
	57.5	52	40.75	93.5
	42.75	53		
	49	52.75		
<b>Course 4</b>				
	39.5	73.25	50.75	
	39.5	58	41	
	74.5	27.25	36.5	
	60.5	48.25	33.5	
	62.5	51.25		
	53	53.25		
	71.5			
<b>Course 5</b>				
			24	
			7	
			19	
			33.75	
<b>Average</b>	<b>51.27</b>	<b>50</b>	<b>38.2875</b>	<b>88.2292</b>

Table A.16. Average block ratings for Sheepstor church.

**A.14. Widecombe in the Moor.**

Rating Totals: Widecombe-in-the-moor church				
<b>Course 1</b>	South	West	North	Interior
	49.5	48	30.5	77.25
	68	51.25	36.25	71.75
	50.5	59.25	35	
		39.5	18.75	
		59.75	24.25	
		40	44.75	
<b>Course 2</b>				
	55.5	70.25	35	87.5
	54.75	65.75	37.75	93
	70.75	54.75	56	
	79	45.25	40.5	
	77	40	39.25	
		53.75	38	
<b>Course 3</b>				
	42.25	59.5	41.75	98.75
	62.75	71	57	96.25
	78.75	40	58.5	95.75
	69	41.75	70.25	

	53.75	55.5	42.5	
		57	46	
			55.5	
<b>Course 4</b>				
	46.25	61	72	
	64	26.75	52	
	65.5	61	56	
	63.25	36.25	58.75	
	52.5	56.75	66.5	
		43.5	50.25	
<b>Course 5</b>				
	63.25		56.75	
	64.75		69.25	
	43		40	
	59.5		53.25	
	65.5		62.5	
			45	
<b>Average</b>	<b>60.8261</b>	<b>51.5625</b>	<b>48.0565</b>	<b>88.6071</b>

Table A.17. Widecombe-in-the-moor, average block ratings.

## Glossary of Terms

**Hydrothermal Alteration:** After final consolidation of magma, high-temperature  $H_2O$  is released into surrounding country rock, and can produce dramatic physical and compositional changes, leading to minerals such as Kaolinite.

**Megacrystic:** Also called porphyritic, this denotes large mineral crystals, often feldspar, set within smaller-grained rock matrix i.e. Type B granite - a coarse-grained megacrystic biotite granite.

**Metasomatism:** Changes introduced to existing rock when volatile elements, or 'fugitive constituents', of an intrusive magmatic mass pass through the country rock, resulting in the formation of rocks closely resembling those formed by the crystallisation of magma.

**Microfractures:** These are cracks that can form inter-, intra-, and trans-granular microfracture networks throughout the stone body, and can be the result of micro-dilation features formed with the removal of confining pressure, or volume alteration of individual minerals within the stone matrix.

**Pneumatolysis:** After final consolidation of magma, fugitive gaseous constituents are released. These can escape through joints and fissures into surrounding country rock, producing compositional changes such as greisening and tourmalinization, where minerals are selectively replaced with reaction products.

**Q:** Formulated by Barton *et al* in 1974 the Rock Mass Quality scheme (*Q*) measured tunnel stability by assessing six parameters, and it could be used to estimate rock mass quality from heavy squeezing-ground to sound unjointed rock.

**Rock Mass Rating (RMR).** Devised by Bieniawski in 1974, the RMR uses the measurement of 6 parameters to rate rock quality, with results referenced against a class rating table to provide a figure of unsupported tunnel stand-up time. However, since it's formulation, the RMR has also been applied to slopes, foundations and mining problems.

**Rock Quality Designation (RQD):** A simple index for the evaluation of rock core and *in situ* rock exposure quality, the RQD is the sum of intact core lengths  $\geq 100\text{mm}$  as a percentage of the total length drilled.

**Schmidt Hammer:** The Schmidt hammer was designed for *in situ* testing of the surface hardness of concrete, and it does this by recording the distance of rebound of a spring-loaded mass for a given force.

**Slake Durability Test:** An engineering geology method for testing weathered rock samples. Samples are placed in a rotating mesh drum that is partially immersed in water. The drum is rotated 200 times in ten minutes, with the Slake durability index

defined as the ratio of dry fragments that survived the test to the original dry weight of the sample.

**Xenoliths:** Fragments of rock generally derived from surrounding country rock during the intrusion of igneous rock that is incorporated into the invading rock body. Although initially distinct, with prolonged heating and exposure to magmatic fluids xenoliths will lose their separate characteristics and merge with the enveloping rock.

**X-Ray Diffraction (XRD):** An analysis technique which bombards a powdered, crystalline sample with X-rays, and builds up a characteristic profile based on the degree of refraction each ray undergo as it passes through the sample. This will produce a plot that will allow the determination of the chemical species within the sample.